NOVEL GROUP 4, 9, 10, AND 12 COMPLEXES OF INDENYL-DERIVED YLIDES

by

KOUROSH PURDAVAIE

A thesis submitted to the Department of Chemistry

In conformity with the requirements for

the degree of Doctor of Philosophy

Queen's University

Kingston, Ontario, Canada

(May, 2015)

Abstract

The coordination chemistry of the phosphonium-1-indenylide (PHIN) ligand methyldiphenylphosphonium-1-indenylide (1-$C_9H_6PMePh_2$, **I**) has been studied, and a new phosphonium-1-indenylide (PHIN) ligand methyldiphenylphosphonium-4,7-dimethyl-1-indenylide (4,7-dimethyl-1-$C_9H_4PMePh_2$, **II**) has prepared and characterized by NMR spectroscopy, elemental analysis and X-ray crystallography. The zwitterionic structure of methyldiphenylphosphonium-4,7-dimethyl-1-indenylide **II** is isoelectronic with the cyclopentadienyl ligand and one can anticipate interesting coordination chemistry.

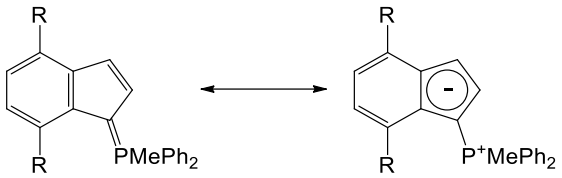

I: R = H
II: R = CH_3

$[Ir(COD)][BF_4]$ and $[Rh(COD)][BF_4]$ were prepared by reactions of silver tetrafluoroborate, $AgBF_4$, with $[Ir(COD)Cl]_2$ and $[Rh(COD)Cl]_2$ and by reacting the resulting $[Ir(COD)][BF_4]$ and $[Rh(COD)][BF_4]$ with **I** and **II**. The resulting planar chiral iridium(I) and rhodium(I) complexes $[Ir(\eta^4\text{-}C_8H_{12})(\eta^5\text{-}\mathbf{I})]BF_4$ (**III**), $[Ir(\eta^4\text{-}C_8H_{12})(\eta^5\text{-}\mathbf{II})]BF_4$ (**IV**), $[Rh(\eta^4\text{-}C_8H_{12})(\eta^5\text{-}\mathbf{I})]BF_4$ (**V**), and $[Rh(\eta^4\text{-}C_8H_{12})(\eta^5\text{-}\mathbf{II})]BF_4$ (**VI**) were synthesized as pairs of enantiomers depending on which face of five-membered rings coordinates to the metal centers. The iridium and rhodium complexes have been characterized by extensive NMR spectroscopy, high resolution mass spectrometry and elemental analyses. Hydrogenation of $[Rh(\eta^4\text{-}C_8H_{12})(\eta^5\text{-}\mathbf{I})]BF_4$ (**V**) and the oxidative

addition of methyl iodide and benzyl chloride to all the new complexes **III-VI** were attempted. Coordination of **I** to a variety of metals in Groups IV, IX, X, and XII, was attempted.

Acknowledgements

I am grateful to the God for the good health and wellbeing that were necessary to complete this thesis.

This thesis is dedicated to the memory of my dear father, Mehdi Purdavaie, who passed away recently. I miss him every day, but I am glad to know he saw this process through to its completion, offering the great support to make it possible, as well as plenty of unforgettable good memories and friendly encouragement. I feel that my father is looking at this work from the Heaven.

I would like to express my sincere gratitude to my supervisor, Dr. Michael C. Baird for all his patient guidance, encouragement and advice throughout this thesis process and the time I was his research student at the Chemistry Department at Queen's University.

I would also place on record, my appreciation for all my students in CHEM 211, 282 and 397, and Dr. Henryka Tilk, Dr. Jason Vlahakis, and Lyndsay Hull for their constant guidance and advice through my teaching assistantship. I would like to thank all faculty members and staff of the Chemistry Department, and the past and present members in the Baird group for all their support and friendship.

A very special thanks goes out to Dr. F. Nasiri, Dr. B. Alasti, Dr. F. Nikpour, Dr. F. Sauriol, Dr. G. Schatte, Dr. M. Mohseni, Dr. J. Wang, Dr. S. Mohebbi, B. Bailey, B. Poles, who directly or indirectly, have helped and supported me through this journey.

My greatest appreciation from the bottom of my heart goes out to my lovely wife, Sahar, who has been with me all these years and has made them the best years of my life. I wish to express my unqualified thanks to her. I could never have accomplished this

dissertation without her love, support, patience and understanding. Words cannot express how much I love you. The last word of acknowledgement I have saved for my dear mother, sister, brother-in-law, and nephew. My mom was always there cheering me up and stood by me through the good and bad times. Her pure love, support, encouragement and companionship have continually excited me to progress.

Statement of Originality

(Required only for Division IV Ph.D.)

I hereby certify that all of the work described within this thesis is the original work of the author. Any published (or unpublished) ideas and/or techniques from the work of others are fully acknowledged in accordance with the standard referencing practices.

(Kourosh Purdavaie)

(May, 2015)

Table of Contents

List of Figures

List of Tables

List of Abbreviations

bp	Boiling point
br	Broad
Bu	Butyl
°C	Degree Celsius
d	Doublet (NMR), day
δ	Chemical shift
η	Hapticity
COD	1,5-Cyclooctadiene
COSY	Correlation Spectroscopy
^{13}C NMR	Carbon NMR
Cp	Cyclopentadienyl (η^5-C_5H_5)
Cp*	Pentamethylcyclopentadienyl (η^5-C_5Me_5)
DMAD	Dimethylacetylenedicarboxylate
DME	Dimethyl ethylene glycol
DMSO	Dimethyl sulfoxide
Et	Ethyl
dppb	$Ph_2P(CH_2)_4PPh_2$
dppe	$Ph_2P(CH_2)_2PPh_2$
dppm	$Ph_2PCH_2PPh_2$
dppp	1,3-Bis(diphenylphosphino)propane
ESI-MS	Electrospray Ionization Mass Spectroscopy
Et	Ethyl

g	Gram
h	Hour
HMBC	Heteronuclear multiple bond coherence
^{1}H NMR	Proton NMR
HR-MS	High resolution mass spectrometry
HR-EMS	High resolution electrospray mass spectrometry
HSQC	Heteronuclear single quantum coherence
Hz	Hertz
i	Iso
J	Coupling constant
IR	Infrared
m	Multiplet
m	Meta
Me	Methyl
mg	Milligram
min	Minute
mmol	Millimoles
mL	Milliliter
nbd	Norbornadiene
n-Bu	*n*-Butyl
NMR	Nuclear Magnetic Resonance
NOESY	Nuclear overhauser effect spectroscopy
n-Pr	*n*-Propyl

o	Ortho
p	Para
Ph	Phenyl
^{31}P NMR	Phosphorus NMR
ppm	Parts per million
Pr	Propyl
R	Alkyl substituent
s	Singlet
t	Triplet
t	Tert
THF	Tetrahydrofuran (C_4H_8O)
Trityl	Triphenylmethyl

Chapter 1 : Introduction

1.1 Ramirez Ylide

Synthesis of triphenylphosphonium cyclopentadienylide was reported first by Ramirez and Levy in 1956.[1] It was found that the triphenylphosphonium cyclopentadienylide, henceforth the Ramirez ylide, does not react with dilute aqueous of alcoholic potassium hydroxide and does not absorb hydrogen in benzene solution using Pt_2O catalyst. This ylide also does not react with ketones, such as cyclohexanone, unlike typical ylides, even at high temperatures (Wittig reaction to synthesize olefins), and thus this ylide is unusually inert. This unusual stability of triphenylphosphonium cyclopentadienylide was attributed to the electron delocalization implied by zwitterionic resonance structure shown in Figure 1, consistent with the relatively high dipole moment of 7.0 D.[2,3] The zwitterionic resonance structure of the triphenylphosphonium cyclopentadienylide is thus isoelectronic with the cyclopentadienyl (Cp) anion.

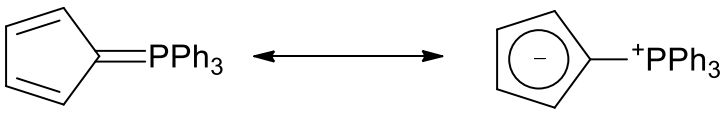

Figure 1. Resonance structures of the Ramirez ylide.

The high degree of conjugation of the triphenylphosphonium cyclopentadienylide was in evidence by the ultraviolet absorption spectrum of the triphenylphosphonium cyclopentadienylide.[4-7]

The structure of triphenylphosphonium cyclopentadienylide was determined from an X-ray crystallographic investigation.[8] In this report, the amount of double or single

bond character of the P-C bond was investigated from the P-C bond length. The X-ray crystallographic analysis revealed the extensive delocalization of the π electron density triphenylphosphonium cyclopentadienylide, which showed a lengthened P-C_5H_4 bond, somewhere between a single and a double bond. It was found that the P-C(Ph) distances, average 1.806 Å, considerably longer than the ylide phosphorus-carbon bond, P-C(Cp ring) = 1.718 Å. The shortest ylide P-C bond lengths are 1.648 Å for $Ph_3P=C=C=O$[9] and 1.631 Å for $Ph_3P=C=PPh_3$[10]. Ammon *et al.* found *inter alia* that the average C(Ph)-P-C(Cp) (111.4°) is larger than the average C(Ph)-P-C(Ph) (107.5°).[8] Triphenylphosphonium methylide, $Ph_3P=CH_2$, is the best example of an ylidic compound with a considerable amount of P=C character. The P-C bond length in the $Ph_3P=CH_2$ (1.66 Å)[11] revealed that even the bond character in the $Ph_3P=CH_2$ is not a pure P=C(sp^2) bond, but the $Ph_3P=CH_2$ seems to be the most ideal compound for the P=C(sp^2). By comparing the bond length of P-C in the $Ph_3P=CH_2$ (1.66 Å)[11], the typical bond lengths of P-(C)Ph (1.78 Å), and the P-C(Cp) bond in the Ramirez ylide with the bond length of P-C(Cp) = 1.718 Å[8], one would assume that the P-C(Cp) bond in the Ramirez ylide falls between a single and double bond. In the ^{13}C NMR spectrum of triphenylphosphonium cyclopentadienylide, the ylide carbon exhibited an unusually high field chemical shift and a P-C(ylide) coupling constant typical of an aliphatic carbon-phosphorus bond, apparently supporting the importance of the zwitterionic resonance structure of triphenylphosphonium cyclopentadienylide.[12]

In the field of coordination chemistry, the cyclopentadienyl (Cp) anion has attracted a lot of attention for a long period of time. Therefore, the zwitterionic resonance structure of triphenylphosphonium cyclopentadienylide, which is isoelectronic with the

Cp anion, was expected to be ubiquitous in organometallic chemistry. The Ramirez ylide with different steric and electronic properties compare with the Cp anion was expected to show a lot of interesting chemistry. The Ramirez ylide was therefore investigated by various research groups in the 1970s to 1980s.

1.1.1 The Ramirez Ylide Preparation

The reaction sequence shown in Figure 2 was followed to synthesize the Ramirez ylide, triphenylphosphonium cyclopentadienylide. Bromination of cyclopentadiene gave 1,3-dibromocyclopentene which was reacted with two equivalents of triphenylphosphine. The diphosphonium salt produced was deprotonated twice to form the phosphonium cyclopentadieylide by reaction with two equivalents of sodium hydroxide (NaOH). In this synthesis, none of the intermediates was isolated. During the deprotonation of the C_5 ring, two steps occurred. First, one equivalent of phosphine was replaced by one equivalent of bromide. Second, the second equivalent of NaOH deprotonated the C_5 ring to afford the Ramirez ylide. This methodology afforded the Ramirez ylide in 41% yield.[1]

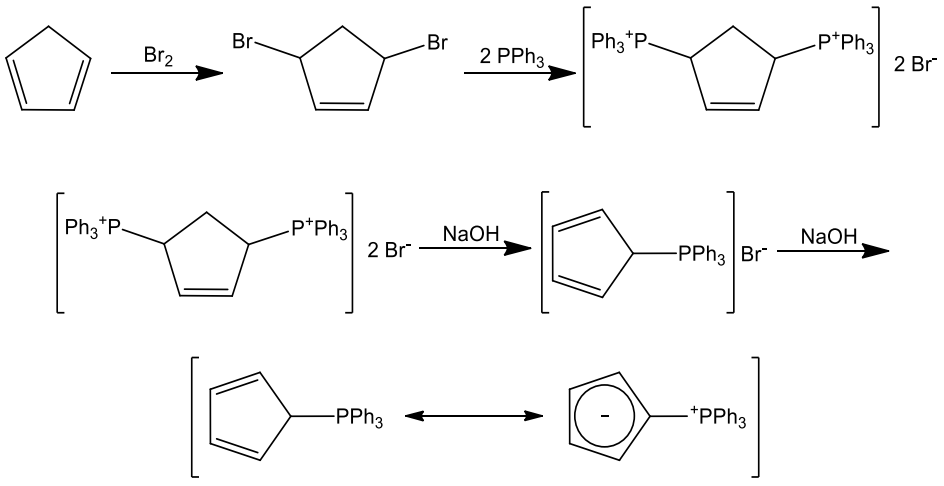

Figure 2. Synthesis of the Ramirez ylide, triphenylphosphonium cyclopentadienylide.

The reaction of diazocyclopentadienes with phosphines failed to synthesize triphenylphosphonium cyclopentadienylide by Ramirez (Figure 3).[6]

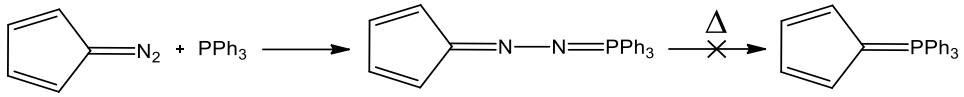

Figure 3. Attempted synthesis of $CpPPh_3$ using diazocyclopentadiene.

Ramirez did not attempt to synthesize other derivatives in order to extend his method, and attempts to develop this synthetic route to other phosphines have generally resulted in the formation of black, insoluble tars which were probably polymeric materials.[13] However, the tri-*n*-propyl derivative of phosphonium cyclopentadienylide, $CpP(n\text{-}Pr)_3$, was the only reported phosphonium cyclopentadienylide with low yield.[14]

1.1.2 Preparation of C_5 Ring Substituted Triphenylphosphonium Cyclopentadienylides

A triphenylphosphonium-1,2,3,4-tetraphenylcyclopentadienylide derivative of $C_5H_4PPh_3$ was prepared by Freeman *et al.* (Figure 4).[15]

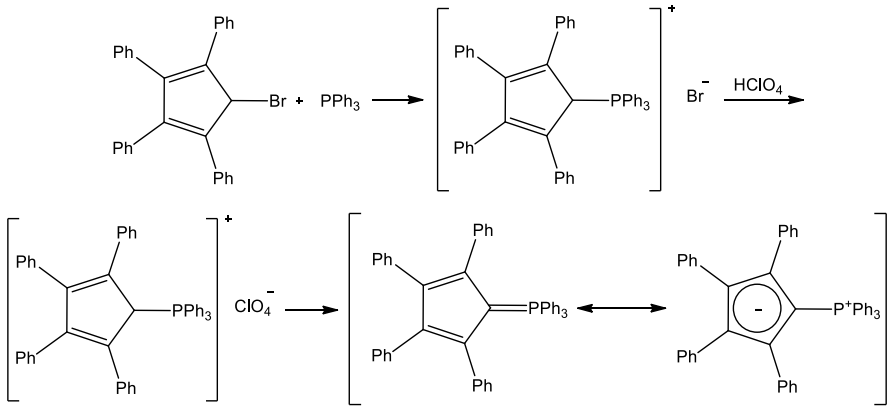

Figure 4. The preparation of $(C_5Ph_4)PPh_3$.

In this reaction, 5-bromo-1,2,3,4-tetraphenylcyclopentadiene was treated with PPh_3 to form the phosphonium bromide. The bromide was exchanged with ClO_4^- to yield the perchlorate salt which was deprotonated with NaOH in the next step to afford the ylide in high yield. The bulky substitutuents on bromocyclopentadiene result in it being more stable than non-substituted bromocyclopentadiene. The same group developed a synthetic method to prepare the triphenylphosphonium-2,3,4-triphenylcyclopentadienylide.[16]

Freeman *et al.* reported the synthesis of substituted ylide from substituted diazocyclopentadienes (Figure 5).[17,18]

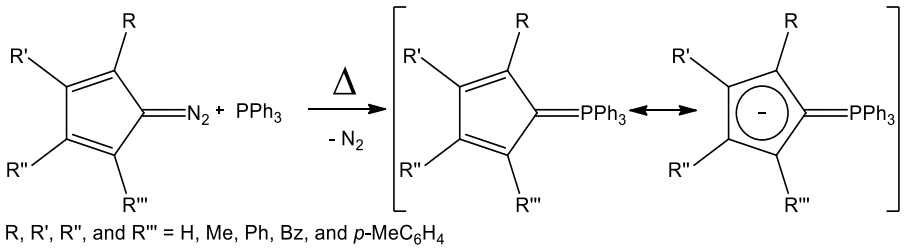

Figure 5. The syntheses of ylides using substituted diazocyclopentadienes.

The diazo-cyclopentadienes and triphenylphosphine were ground together and then N_2 was released after heating the reaction mixture (150-160°C). Yields were varied from 26% to 68% depending on the diazo-cyclopentadienes used.

1.1.3 The Mathey Preparation of Phosphonium Cyclopentadienylides

Methyldiphenyl phosphonium cyclopentadienylide was synthesized by Mathey in 1975.[19] The Mathey synthetic route starts with the reaction of cyclopentadienylthallium, CpTl, with chlorodiphenylphosphine, PPh_2Cl, to synthesize

cyclopentadienyldiphenylphosphine, followed by reaction *in situ* with MeI to methylate cyclopentadienyldiphenylphosphine to form the phosphonium iodide which was deprotonated by *n*-butyllithium, in the final step (Figure 6). The yield of the final step was reported to be 70% by Mathey. The methyldiphenyl phosphonium cyclopentadienylide prepared by Mathey was not fully characterized. Rudie *et al.* also synthesized cyclopentadienyltriphenylphosphine by using NaCp instead of using TlCp.[20]

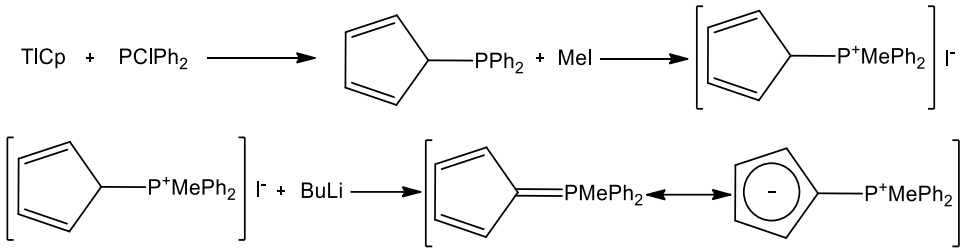

Figure 6. The Mathey preparation of $C_5H_4PMePh_2$.

There are two challenges to the general use of the Mathey method for the synthesis of phosphonium cyclopentadienylides. First, it utilizes one of the very few commercially available chlorodisubstituted phosphines. Second, phosphines of the type $CpPR_2$ are generally not stable at room temperature, probably because of Diels-Alder dimerization, and must be converted into phosphonium salts, immediately.[21]

The Mathey procedure was later investigated further by Brownie *et al.*, who used the Mathey procedure, to develop a reliable synthetic method with the full spectroscopic and crystallographic characterization of methyldiphenylphosphonium cyclopentadienylide.[22] In the same paper by Brownie *et al.*, the structure of methyldiphenyl phosphonium cyclopentadienylide ($C_5H_4PMePh_2$) was compared with

the Ramirez ylide ($C_5H_4PPh_3$), and the electronic structure of $C_5H_4PMePh_2$ was also studied by using DFT calculations. While one could assume that new phosphonium cyclopentadienylides can be synthesized by using alkyl halides other than MeI, this possibility was unfortunately not assessed.

1.1.4 Preparation of Phosphonium Cyclopentadienylides with Different Substituents on Phosphorus

Four novel Cp substituted phosphonium cyclopentadienylides with different alkyl groups on phosphorus, $(Me)_4C_5PMePh_2$, $(Me)_4C_5PMe_3$, (t-Bu)$C_5H_3PMePh_2$, and (t-Bu)$C_5H_3PMe_3$ were synthesized by Sundermeyer *et al.*, in 2012 (Figure 7).[23]

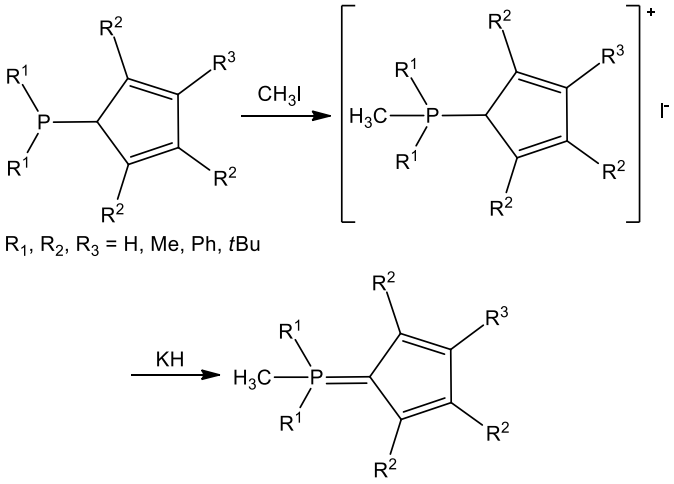

Figure 7. Syntheses of Cp substituted phosphonium cyclopentadienylides with different substituents on phosphorus.

In this synthetic route, dialkylphosphino cyclopentadienes were chosen as the starting materials and methylation of these dialkylphosphino cyclopentadienes with MeI formed the corresponding phosphonium salts. Deprotonation of the resultant

phosphonium salts by potassium hydride afforded the desired phosphonium cyclopentadienylides. All the four novel synthesized phosphonium cyclopentadienylides were fully characterized by NMR, IR, ESI MS, and elemental analyses. Two phosphonium cyclopentadienylides, $(CH_3)_4C_5PMePh_2$, and $(CH_3)_4C_5PMe_3$, were also crystallized and characterized by X-ray crystallography.

In 2013, Sundermeyer *et al*. reported the syntheses of a di-*t*-butylmethylphosphonium cyclopentadienylide, $C_5H_4P(t\text{-}Bu)_2Me$, along with other previously reported phosphonium cyclopentadienylides (Figure 8).[24]

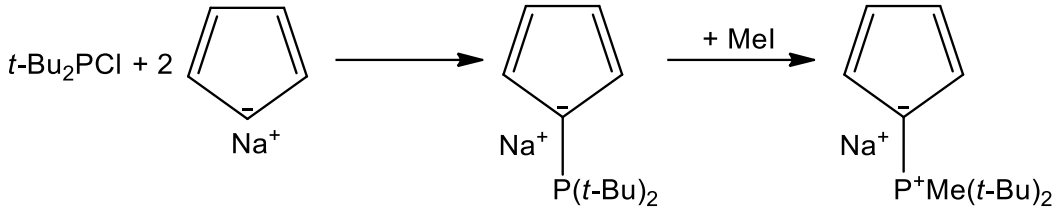

Figure 8. Synthesis of $C_5H_4P(t\text{-}Bu)_2Me$.

In this method, two equivalents of CpNa were reacted with one equivalent of *t*-Bu_2PCl, followed by methylation with MeI to afford the desired phosphonium cyclopentadienylide, $C_5H_4P(t\text{-}Bu)_2Me$, in a 48% yield. It was discovered that methylation could not occur in a reaction of *in situ* produced $C_5H_5P(t\text{-}Bu)_2$ with MeI due to the presence of high steric bulk around the phosphorus atom. However it was found that deprotonated phosphine can react smoothly with MeI to afford the desired phosphonium cyclopentadienylide, $C_5H_4P(t\text{-}Bu)_2Me$. The proposed mechanism as shown in Figure 9 involves the first equivalent of cyclopentadienyl anion attack to phosphorus atom of $(t\text{-}Bu)_2PCl$ to form $C_5H_5P(t\text{-}Bu)_2Me$, followed by deprotonation with the second equivalent of cyclopentadienyl anion to yield the final product, $C_5H_4P(t\text{-}Bu)_2Me$.

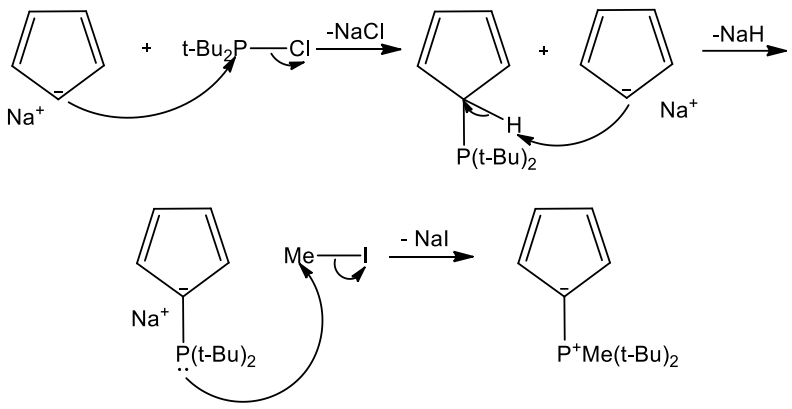

Figure 9. Proposed mechanism for synthesis of $C_5H_4PMe(t\text{-}Bu)_2$.

In 2014, Sundermeyer *et al*. reported the synthesis of a new phosphonium cyclopentadienylide, tri-*n*-butylphosphonium cyclopentadienylide, $C_5H_4P(n\text{-}Bu)_3$,[25] via the two different methods A (shown in Figure 10), and B (shown in Figure 11). The final product, $C_5H_4P(t\text{-}Bu)_2Me$, was fully characterized by NMR, IR, and ESI MS.

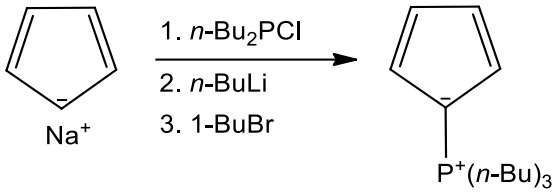

Figure 10. Synthesis of tri-*n*-butylphosphonium cyclopentadienylide (Method A).

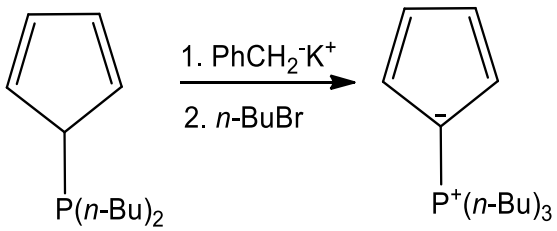

Figure 11. Synthesis of tri-*n*-butylphosphonium cyclopentadienylide (Method B).

The mechanism in Method A begins with nucleophilic attack of Cp anion to the phosphorus atom of *n*-BuPCl, followed by deprotonation with *n*-BuLi, and addition of 1-BuBr (Figure 12).

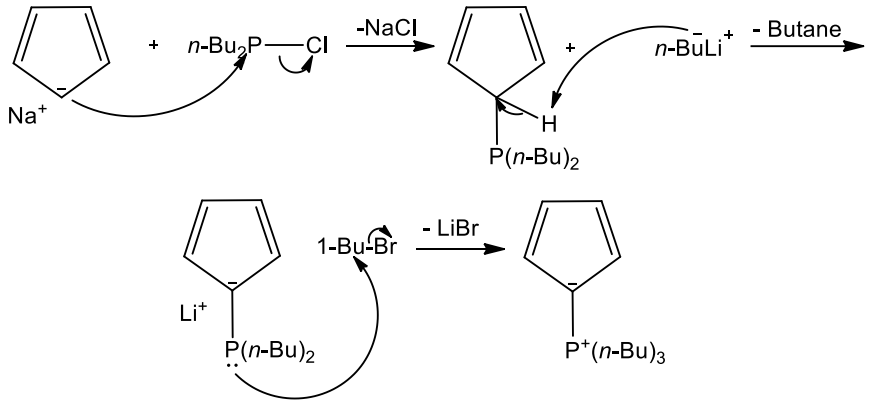

Figure 12. Mechanism of the synthesis of tri-*n*-butylphosphonium cyclopentadienylide (Method A).

The mechanism in Method B involves deprotonation of the allylic C-H of $C_5H_5P(n\text{-Bu})_2$, followed by addition of *n*-BuBr to $[C_5H_4P(n\text{-Bu})_2]K$ (Figure 13).

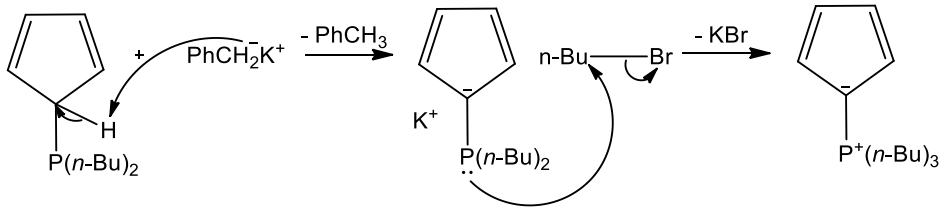

Figure 13. Mechanism of the synthesis of tri-butylphophonium cyclopentadienylide (Method B).

1.1.5 Coordination Chemistry of the Ramirez Ylide to Transition Metals

Although it was anticipated that coordination of the Ramirez ylide to a wide range of metal centers would be possible and that comparisons with similar complexes

containing neutral arene and aromatic Cp anion ligands would be interesting, very little research of this type was carried out over the next 20 or 30 years.[13] However, in view of the large variety of the Ramirez ylide derivatives now available, containing different substituents at both phosphorus and the C_5 ring, it became possible to tune the electronic and the steric parameters of these ligand systems. Since the coordination chemistry of Ramirez-type ylides is a vast area of research,[13] only the relevant group 4, 6 and 9 metal complexes will be discussed in detail.

The first report on the coordination of group 4 metals to a phosphonium cyclopentadienylide ligand was published by Holy *et al*. in 1977.[26] Their synthetic route involved reaction of the Ramirez ylide with the group 4 metal halides as shown in Figure 14.

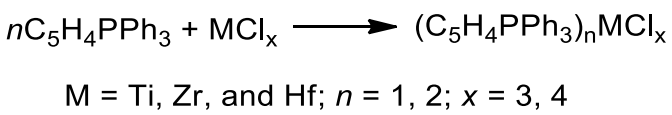

Figure 14. The syntheses of the group 4 metal complexes of the Ramirez ylide.

In this method, the ylide was dissolved in THF and the metal halide was added to the solution to afford the product within a few minutes; petroleum ether or diethyl ethyl ether were then added to the solutions to precipitate the products. A tan precipitate was formed with $TiCl_4$, and the product was identified by IR and ^1H NMR spectroscopy as $[(\eta^5\text{-}C_5H_4PPh_3)_2TiCl_2]Cl_2$ although X-ray quality crystals were not obtained for X-ray analysis. In this report, the ^1H NMR spectra of the Ramirez ylide and $[(\eta^5\text{-}C_5H_4PPh_3)_2TiCl_2]Cl_2$ were compared and it was found out that the protons of the C_5 ring shifted downfield from δ 6.30-6.65 to δ 7.9 on complexation. By using a similar

procedure, and apparent Ti(III) complex of the Ramirez ylide was formed as a light beige solid and was identified as $(C_5H_4PPh_3)TiCl_3.4H_2O$. All attempts to synthesize a Ti(II) complex were unsuccessful. Both complexes were reported to be very sensitive to air and to decompose in a few minutes after exposing to air. Similar reactions were attempted with $ZrCl_4$ and $HfCl_4$, but the rather insoluble products could not be purified and were not characterized satisfactorily.

In 2000, Shin *et al*. reported the syntheses of phosphonium-bridge ansa-metallocene complexes, $[(Me_2P(C_5Me_4)_2)ZrCl_2]^+$ and $[(Me_2P(C_5Me_4)_2)HfCl_2]^+$ from the reactions of $[Me_2P(C_5Me_4)_2]Li_2I$ with $ZrCl_4$ and $HfCl_4$, respectively.[27] This synthetic method involves, the reaction of tetramethylcyclopentadiene with *n*-BuLi, followed by the addition of $MePCl_2$. All volatile components were removed by vacuum, the residue was extracted with pentane and MeI was added to the resultant filtrate to afford $[Me_2P(C_5Me_4H)_2]I$ as a white solid product. The reaction of *n*-BuLi with $[Me_2P(C_5Me_4H)_2]I$, followed by the addition $ZrCl_4$ or $HfCl_4$ gave $[(Me_2P(C_5Me_4)_2)ZrCl_2][I]$ and $[(Me_2P(C_5Me_4)_2)HfCl_2][I]$, respectively (Figure 15). Both products were characterized by X-ray crystallography. The bond lengths of P-C_5Me_4 for the zirconium complex, $[(Me_2P(C_5Me_4)_2)ZrCl_2][I]$, and the hafnium complex, $[(Me_2P(C_5Me_4)_2)HfCl_2][I]$, were 1.80 Å, and 1.79 Å, respectively. These bond lengths of P-C_5Me_4 in the zirconium and hafnium complexes were notably longer than in other complexes of the Ramirez ylide, 1.75 Å in $(\eta^5\text{-}C_5H_4PPh_3)Cr(CO)_3$,[28] 1.76 Å in $(\eta^5\text{-}C_5H_4PMePh_2)Cr(CO)_3$,[22] 1.76 Å in $(\eta^5\text{-}C_5H_4PMePh_2)Mo(CO)_3$,[22] 1.77 Å in $(\eta^5\text{-}C_5H_4PMePh_2)W(CO)_3$,[22] $[(C_6H_5CH_2PPh_2(\eta^5\text{-}C_5H_4))Fe(\eta^5\text{-}C_5H_5)][Cl]$,[29] $[(\eta^5\text{-}$

$C_5H_4PPh_3Co(CO)_2][Co(CO)_4]$,[30,31] 1.76 Å in $[(\eta^5\text{-}C_5H_4PPh_3Rh(1,5\text{-}COD)][BPh_4]$,[32] and 1.78 Å in $(\eta^5\text{-}C_5H_4PPh_3Pd(C_4(CO_2Me)_4$.[33]

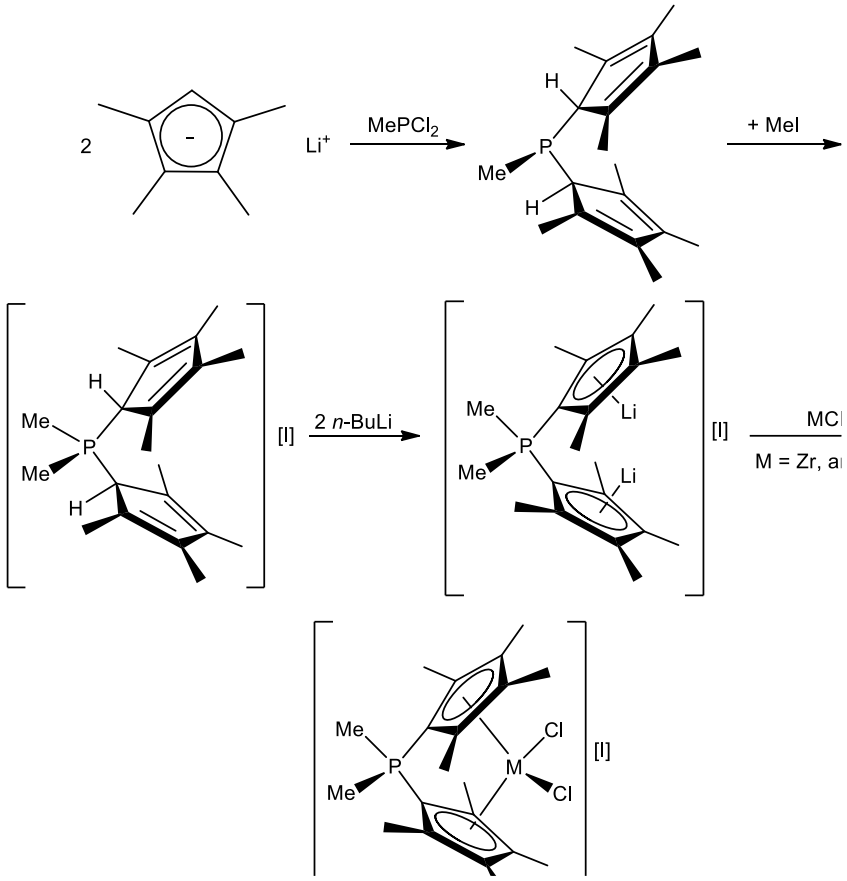

Figure 15. Syntheses of the ansa-zirconocene and ansa-hafnocene-like complexes of the phosphonium bridge pentamethylcyclopentadienyl ligand.

The dichlorozirconocene complex was further reacted with MeMgI to form the dimethyl analogue, followed by reaction with CO to afford an acyl complex by inserting CO into one of the metal-alkyl bonds (Figure 16).

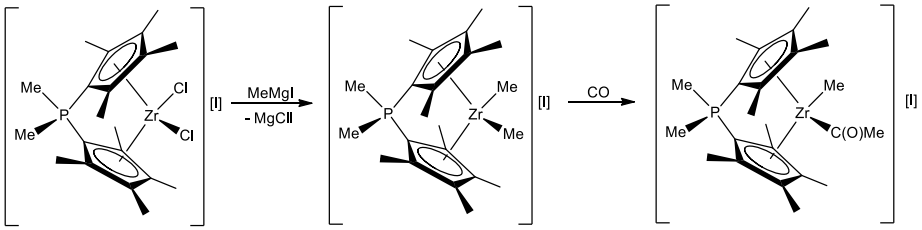

Figure 16. The methylation and carbonylation reactions of $[(Me_2P(C_5Me_4)_2)ZrCl_2][I]$.

The coordination chemistry of the phosphonium cyclopentadienylide ligand with group 6 metals has been extensively investigated. Wilkinson *et al.* noted that the electronic structure of the zwitterionic resonance structure of the Ramirez ylide is isoelectronic with benzene, and were the first to anticipate that the Ramirez ylide might coordinate to group 6 metals as does benzene to form $(\eta^5\text{-}C_5H_4PPh_3)M(CO)_3$ (M = Cr, Mo, W).[34] The Ramirez ylide was indeed found to form such complexes, which were characterized by ^{1}H NMR and IR spectroscopy.[34,35] The chemistry and reactivity of these complexes were also investigated, later.[36,37]

Kotz *et al.* synthesized these complexes by refluxing excesses of the metal hexacarbonyls, $Cr(CO)_6$ and $Mo(CO)_6$, in diglyme with $C_5H_4PPh_3$, the tungsten analogue by reaction of excess of $W(CO)_3(CH_3CN)_3$ with $C_5H_4PPh_3$ at 110 °C (Figure 17).[35]

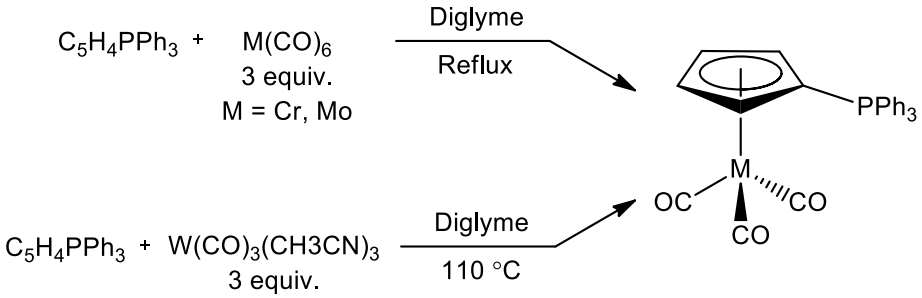

Figure 17. The syntheses of the group 6 tricarbonyl complexes of $C_5H_4PPh_3$.

Kotz *et al.* characterized the complexes by IR and ^{1}H NMR spectroscopy, and discovered that the protons on the C_5 ring were all shifted upfield noticeably on coordination. The ^{13}C NMR spectra of $(\eta^5\text{-}C_5H_4PPh_3)M(CO)_3$ (M = Cr, Mo), were studied, later.[38] In related work, Cashman *et al.* synthesized tricarbonylmolybdenum triphenylphosphonium tetraphenylcyclopentadienylide, $(\eta^5\text{-}C_5Ph_4PPh_3)Mo(CO)_3$, by using the same procedure reported by Kotz[35] except that refluxing THF was used as the solvent.[37]

In 2007, Brownie *et al.* synthesized $C_5Ph_4PMePh_2$ by using the Mathey method,[19] and coordinated this ligand to Cr, Mo, and W by following the previous published method by Kotz[35] to form the group 6 complexes of methyldiphenylphosphonium cyclopentadienylide, $(\eta^5\text{-}C_5H_4PMePh_2)M(CO)_3$, (M = Cr, Mo, and W) as shown in Figure 18.[22]

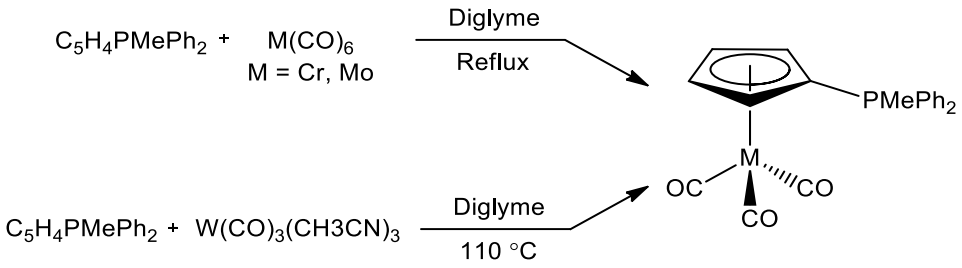

Figure 18. Syntheses of $(C_5H_4PMePh_2)M(CO)_3$, M = Cr, Mo, W.

All three complexes were characterized by IR and NMR spectroscopy, elemental analyses and X-ray crystallography. The ligand $C_5H_4PMePh_2$ had advantages compared with the Ramirez ylide since the methyl group gave a valuable NMR ‘’handle’’ for characterization. The ^{1}H NMR data for $(\eta^5\text{-}C_5H_4PMePh_2)M(CO)_3$ (M = Cr, Mo, W) revealed that all the C_5 protons in these complexes shifted upfield relative to the free

ligand, while the ^{1}H NMR resonances of the P-Me group shifted downfield. Similar changes were earlier reported for the group 6 complexes of $CpPPh_3$, (η^5-$C_5H_4PPh_3$)$M(CO)_3$ (M = Cr, Mo, and W), by Kotz.[35] The ^{31}P resonance of the free ligand shifted downfield on coordination, while the carbon atoms of the C_5 ring became more shielded.

The structure of the chromium tricarbonyl complex (η^5-$C_5H_4PMePh_2$)$Cr(CO)_3$ is shown in Figure 19 and it was found that all three complexes (η^5-$C_5H_4PMePh_2$)$M(CO)_3$ (M = Cr, Mo, and W) were isomorphic.

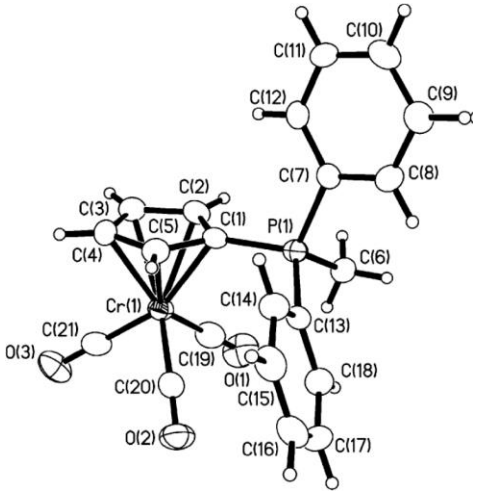

Figure 19. Molecular structure of (η^5-$C_5H_4PMePh_2$)$Cr(CO)_3$.

The X-ray crystallographic studies showed that all three complexes assume the piano-stool-type structures shown in Figure 19, thus confirming that the $C_5H_4PMePh_2$ ligand is coordinated in an η^5 fashion in all the three complexes. The C_5H_4 ring bond lengths were elongated considerably in all three complexes compared with the free ligand, and the C_5 ring bond angles were ~108 °C as expected for a regular pentagon. The X-ray crystallography data also showed that the P-C(1) bond lengths of the all three

complexes were increased relative to the free ligand. This increase in the P-C(1) bond length provided evidence for an increase in the contribution of zwitterionic character of the phosphonium cyclopentadienylide ligand in the complexes.

Two ν(CO) at 1915 and 1812 cm^{-1} were observed in the IR spectrum of (η^5-$C_5H_4PMePh_2$)$Cr(CO)_3$, and were compared with similar data for the two isoelectronic complexes (η^6-C_6H_6)$Cr(CO)_3$ with ν(CO) at 1971 and 1892 cm^{-1}, and [(η^5-C_5H_5)$Cr(CO)_3$]$^-$ with ν(CO) at 1895 and 1778 cm^{-1}. Thus the electron donating properties of the ylide were deduced to be less than that of the cyclopentadienyl anion but much greater than that of benzene. Brownie *et al.* later also studied the oxidation of Cr(η^5-$C_5H_4PMePh_2$).[39]

The first group 9 metal complex of a phosphonium cyclopentadienylide was synthesized by Holy *et al.* in 1978.[31] The synthesis of [(η^5-$C_5H_4PPh_3$)$Co(CO)_2$]$^+$[$Co(CO)_4$]$^-$ was reported, made by the reaction of dicobalt octacarbonyl with the Ramirez ylide in a 65% yield (Figure 20).

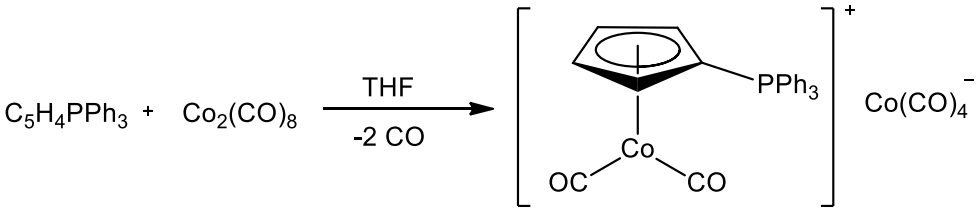

Figure 20. The synthesis of [(η^5-$C_5H_4PPh_3$)$Co(CO)_2$][$Co(CO)_4$].

The structure of [(η^5-$C_5H_4PPh_3$)$Co(CO)_2$]$^+$[$Co(CO)_4$]$^-$ was confirmed by X-ray crystallography and showed that the C_5 ring is bound in an η^5 manner.[30,31] The C_5H_4 ring bond length was elongated slightly in this complex compared with the free ligand, and the P-C(1) bond length was 1.77 Å compared with 1.72 Å in the free ligand. This increase in

the P-C(1) bond length thus provided further evidence for an increase in the contribution of the zwitterionic character of the phosphonium cyclopentadienylide ligand in [(η^5-$C_5H_4PPh_3$)$Co(CO)_2$]$^+$[$Co(CO)_4$]$^-$.

A cobalt(III) complex of $C_5H_4PEt_3$, [(η^5-$C_5H_4PEt_3$)$CoH(PEt_3)_2$][BF_4]$_2$, was synthesized by the reaction of [(η^5-$C_5H_5Co(PEt_3)_2$][BF_4] with silver tetrafluoroborate, $AgBF_4$, followed by the addition of triethylphosphine, PEt_3, unexpectedly, in 1982 (Figure 21).[40]

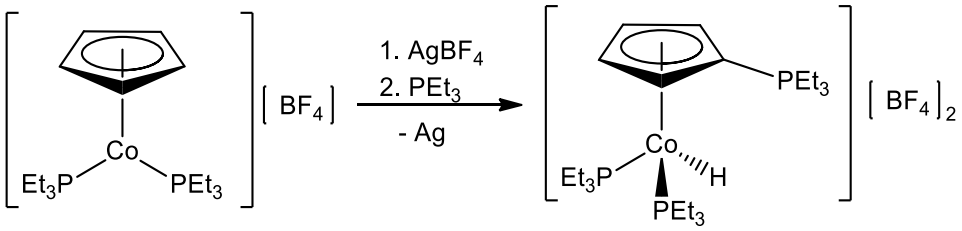

Figure 21. The synthesis of [$Cp(PEt_3)CoH(PEt_3)_2$][BF_4]$_2$.

The product, [(η^5-$C_5H_4(PEt_3)CoH(PEt_3)_2$][$BF_4$], was synthesized in a 88% yield, and its identity was confirmed by ^{1}H NMR spectroscopy and elemental analyses. In the suggested mechanism, the mechanism of formation of the product, [(η^5-$C_5H_4CoH(PEt_3)_2$][BF_4]$_2$, was thought to involve oxidation of [$CpCo(PEt_3)_2$][BF_4] by $AgBF_4$ to form [$CpCo(PEt_3)_2$][BF_4]$_2$, the addition of PEt_3 to [$CpCo(PEt_3)_2$][BF_4]$_2$ to form [($CpPEt_3$)$Co(PEt_3)_2$][BF_4]$_2$, followed by loss of a proton from ring and attack on the cobalt center (Figure 22).

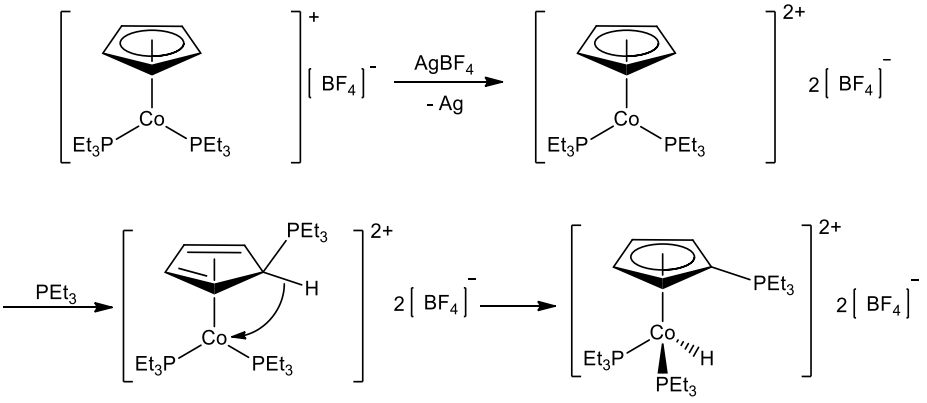

Figure 22. Proposed mechanism of synthesis of $[(\eta^5\text{-}C_5H_4PEt)CoH(PEt_3)_2][BF_4]_2$.

The first rhodium complexes of the Ramirez ylide were reported by Tresoldi *et al.* in 1981 along with other rhodium complexes.[41] In this report, a set of rhodium complexes of the Ramirez ylide, $[Rh(C_5H_4PPh_3)(CO)_2][PF_6]$, $[Rh(C_5H_4PPh_3)(1,5\text{-}COD)][PF_6]$ (COD = cyclooctadiene), and $[Rh(C_5H_4PPh_3)(nbd)][PF_6]$ (nbd = norbornadiene), was prepared by reactions of $[Rh(CO)_2Cl]_2$, $[Rh(1,5\text{-}COD)_2Cl]_2$, and $[Rh(nbd)_2Cl]_2$, with $AgPF_6$ followed by the addition of $C_5H_4PPh_3$, respectively (Figure 23).

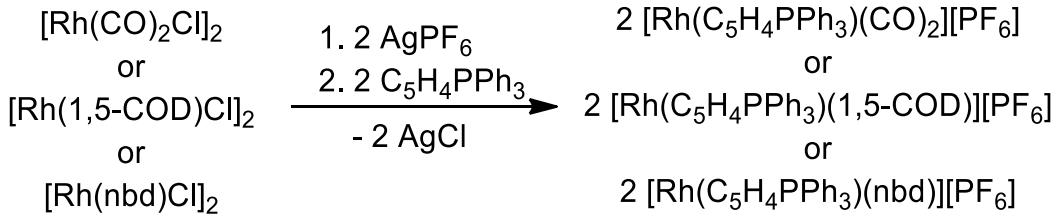

Figure 23. Syntheses of rhodium complexes of the Ramirez ylide.

It was found that the Ramirez ylide is too poor a nucleophile to cleave the chloro bridges of the starting materials, $[Rh(CO)_2Cl]_2$, $[Rh(1,5\text{-}COD)_2Cl]_2$, and $[Rh(nbd)_2Cl]_2$. All of the new complexes, $[Rh(C_5H_4PPh_3)(CO)_2][PF_6]$, $[Rh(C_5H_4PPh_3)(1,5\text{-}COD)][PF_6]$,

and $[Rh(C_5H_4PPh_3)(nbd)][PF_6]$ were soluble in acetone and DMSO, slightly soluble in CH_2Cl_2, and MeOH but insoluble in non-polar solvents such as benzene. The products were characterized by ^1H and ^{13}C NMR and IR spectroscopy, and it was found that the Ramirez ylide is not a good electron donating ligand compared with Cp anion because the IR spectrum of $[Rh(C_5H_4PPh_3)(CO)_2][PF_6]$ exhibited carbonyl stretches at higher frequencies than $[Rh(C_5H_5)(CO)_2][PF_6]$. The same group reported the crystal structure of $[Rh(C_5H_4PPh_3)(CO)_2]^+$ with BPh_4^- as the counteranion and found that the C_5 ring is bound in an η^5 manner to the rhodium center.[32] The Rh-C_5 and P-C_5 distances were reported 2.26 Å and 1.76 Å, respectively.

The reactions of $[Rh(C_5H_4PPh_3)(CO)_2][PF_6]$ with $[AsPh_4][Cl]$, TlCp, PPh_3, and diphosphines such as $Ph_2P(CH_2)_nPPh_2$ (n = 1 (dppm), 2 (dppe), and 4 (dppb)) were studied to investigate the substitution chemistry of $[Rh(C_5H_4PPh_3)(CO)_2][PF_6]$ as shown in Figure 24.[41] It was found that PPh_3 was displaced in the reactions of $[Rh(C_5H_4PPh_3)(CO)_2][PF_6]$ with $[AsPh_4][Cl]$, and TlCp to from $[Rh(CO)_2Cl_2][AsPh_4]$, and $RhCp(CO)_2$, respectively. In contrast, the reaction of $[Rh(C_5H_4PPh_3)(CO)_2][PF_6]$ with PPh_3 showed that $C_5H_4PPh_3$ was not displaced by PPh_3; one of CO ligands was displaced instead, and $[RhPPh_3(C_5H_4PPh_3)(CO)][PF_6]$ was formed. A more detailed investigation on the mechanism and kinetics of the latter substitution reaction was reported by Reck and Basolo, and this study revealed that the PPh_3 was displaced by CO ~100 times faster than in $[Rh(C_5H_5)(CO)_2][PF_6]$.[42]

Substitution reactions of dppm, dppe, and dppb with $[Rh(C_5H_4PPh_3)(CO)_2][PF_6]$ were also examined by Tresoldi *et al.* in 1981.[41] It was found that dppm and dppb formed phosphine-bridged complexes $[Rh(C_5H_4PPh_3)(CO)(\mu\text{-dppm})Rh(C_5H_4PPh_3)(CO)][PF_6]_2$

and $[Rh(C_5H_4PPh_3)(CO)(\mu\text{-dppb})Rh(C_5H_4PPh_3)(CO)][PF_6]_2$. It was also found that both CO and PPh_3 ligands were displaced with dppe in the substitution reaction of $[Rh(C_5H_4PPh_3)(CO)_2][PF_6]$ and dppe to afford $[Rh(dppe)_2][PF_6]$.

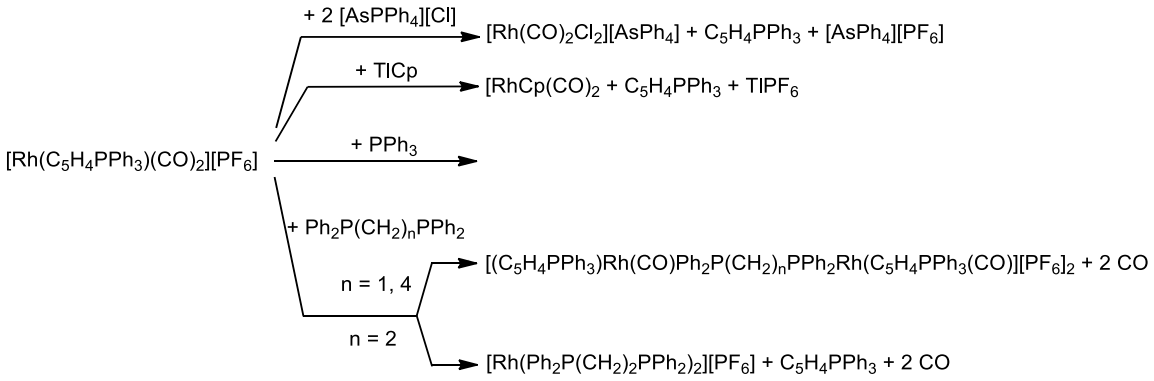

Figure 24. Substitution reactions of $[Rh(C_5H_4PPh_3)(CO)_2][PF_6]$.

A sandwich complex, $[Rh(Cp^*)(C_5H_4PPh_3)][PF_6]_2$ (Cp^* = pentamethylcyclopentadienyl), was synthesized in a 78% yield from the reaction of $[Rh(Cp^*)(acetone)_3][PF_6]_2$ with $C_5H_4PPh_3$, and was characterized by elemental analyses and ^1H and ^{13}C NMR spectroscopy (Figure 25).

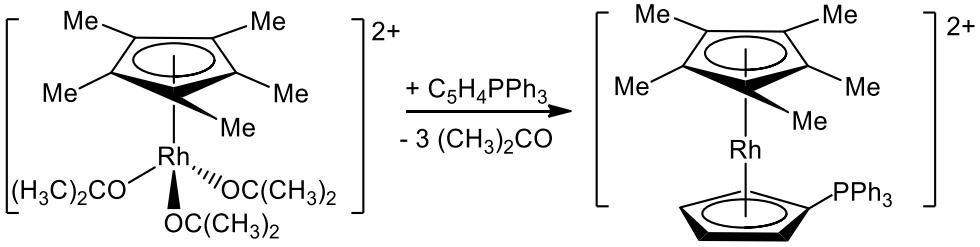

Figure 25. The synthesis of $[Rh(Cp^*)(C_5H_4PPh_3)][PF_6]_2$.

An investigation was carried out to examine the catalytic activities of a variety of η^5-CpRh complexes for the cyclotrimerization of acetylenes.[43] In this report, a variety of

η^5-CpRh complexes such as $[Rh(C_5H_4PPh_3)(CO)_2][PF_6]$, η^5-$CpRh(CO)_2$, and η^5-$Cp^*Rh(CO)_2$ were studied for the cyclotrimerization of dimethylacetylenedicarboxylate (DMAD) and hex-3-yne to find out if there is any difference in the catalytic activities among these complexes. It was found that $[Rh(C_5H_4PPh_3)(CO)_2][PF_6]$ exhibited the lowest catalytic activity, the rates of cyclotrimerization of DMAD varying in the order $[Rh(C_5H_4PPh_3)(CO)_2][PF_6] < \eta^5$-$CpRh(CO)_2 < \eta^5$-$Cp^*Rh(CO)_2$.

1.1.6 The Ramirez Ylide Limitations

In this section, some drawbacks of the Ramirez ylide will be discussed. These difficulties have limited the utilization of this class of ligand in the development of its coordination chemistry. First, the lack of a general synthesis for $CpPPh_3$ and its analogues narrowed the preparation of a variety of these ligands and resulted in publishing just a few reports on the syntheses of metal complexes of this ligand. Second, in the Mathey synthetic method, a chloro-disubstituted phosphine is required; these are expensive, and few are commercially available. Third, in the Mathey synthetic method, compounds of the type $CpPR_2$ are intermediates and these are unstable at room temperature and need to be converted immediately to the corresponding phosphonium salts, probably because of Diels-Alder dimerization. All of these factors have limited development of the coordination chemistry of this class of ligand, as of now.

The coordination chemistry of this class of ligand has focused mostly on the Ramirez ylide and many of these studies have not resulted in the preparation of well characterized products. For instance, while complexes of the group 4 metals, titanium, zirconium and hafnium, have been studied, the complexes obtained could not be

characterized by elemental analyses and the X-ray crystallography due to combustion problems and poor solubilities.[26] Purification and complete characterization of the synthesized phosphonium cyclopentadienylide complexes have thus often been difficult to achieve.

1.2 Preparation of Phosphonium Fluorenylides

Pinck and Hilbert reported the first synthesis of triphenylphosphonium fluorenylide, in 1947,[44] almost a decade before the synthesis of Ramirez ylide[1] in 1956. The synthetic route involves the addition of triphenylphosphine to 9-bromofluorene to give the corresponding phosphonium salt followed by deprotonation of the phosphonium salt with aqueous ammonia to afford the ylide, triphenylphosphonium fluorenylide (Figure 26).[44]

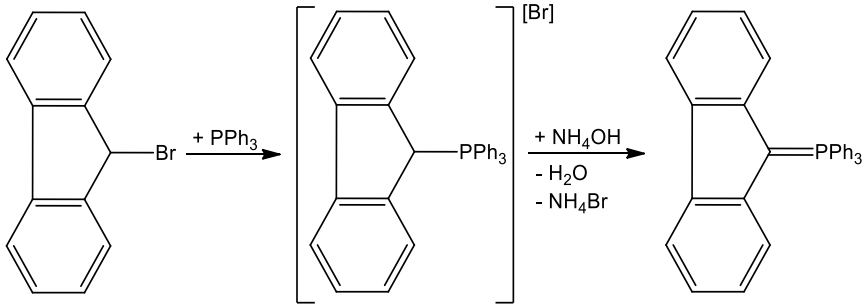

Figure 26. Synthesis of triphenylphosphonium fluorenylide.

A variety of derivatives of phosphonium fluorenylide were synthesized by using the same synthetic route reported by Pinck and Hilbert,[44] with different substituents on the aryl and phosphorus atom, in 1966.[45] Holy[46] and Schmidbaur[47] reported the syntheses of different phosphonium fluorenylides and phosphonium fluorenyl bis-ylides (Figure 27).

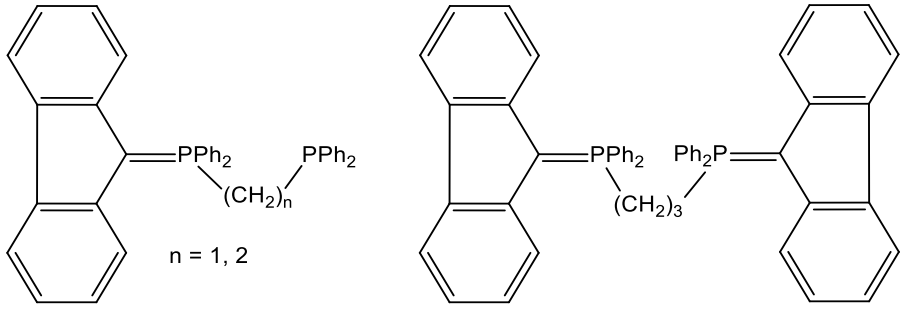

Figure 27. Phosphonium fluorenylide and phosphonium fluorenyl bis-ylides.

The synthetic route involves the addition of 9-bromofluorene to the diphosphines to give the monophosphonium bromide salts, followed by deprotonation to afford the desired compounds.

The nucleophilicity of a phosphine decreases on the formation of a nearby phosphonium center and the effect decreases as the number of intervening CH_2 groups increases. Thus the monophosphonium salt was the only product in the case of dppm, while the diphosphonium salt formed in small amounts along with the monophosphonium salt in 73% yield when dppe (n = 2) was used. It was also reported that by shortening the reaction times and adding excess diphosphine, formation of the diphosphonium salt was minimized by almost 20% when dppe was used.

In the case of 1,3-bis(diphenylphosphino)propane (dppp), (n = 3), the reaction of dppp with 9-bromofluorene always formed the diphosphonium salt as the major product under all reaction conditions, and this made the isolation of pure monophosphonium salt and subsequently the mono-ylide impossible. Using dppp in the reaction with 9-bromofluorene, followed by deprotonation with Na_2CO_3, the propylene bridged bis-ylide was obtained in 85% yield.

1.2.1 Coordination Chemistry of Phosphonium Fluorenylides

A report on the coordination of fluorenyl derived ylide with metal was published by Holy *et al*. in 1982.[46] Reactions of fluorenyl derived ylide shown in Figure 28 with $Cr(CO)_6$ and $W(CO)_3(CH_3CN)_3$ afforded the group 6 complexes.

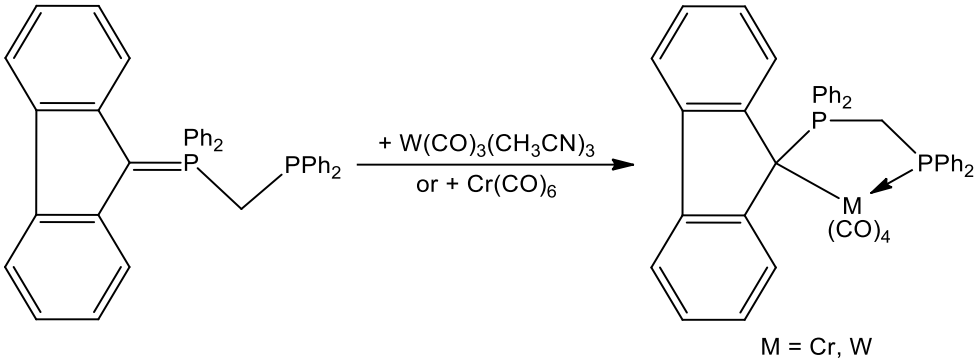

Figure 28. The syntheses of group 6 fluorenyl derived ylide.

These complexes were characterized by IR and NMR spectroscopy. The IR spectrum of tungsten complex showed four CO stretching bands. The ^{31}P NMR spectrum was used for further investigation on the suggested structure for tungsten complex. It was found that the chemical shifts of two phosphorus atoms of tungsten complex were notably shifted downfield compare to the free ligand. In the case of the chromium system, the reaction afforded two products which were separated by chromatography. One product was shown by IR, NMR and MS data to have the same structure suggested for the tungsten complex, while the other exhibited three CO stretching bands in the IR spectrum. There was not much change in the chemical shifts of phosphorus atoms in the second product compared with the free ligand, and the suggested structure is shown in Figure 29.

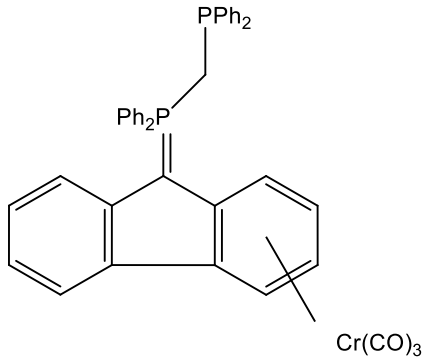

Figure 29. Suggested structure for one of the chromium complexes.

Reactions of the fluorenyl phosphonium ylide when n = 1 with $Pd(PPh_3)_2Cl_2$, $Pt(PPh_3)_2Cl_2$, $Cr(CO)_6$ and $W(CO)_3(CH_3CN)_3$ were studied by Holy *et al*.[46] The structures proposed for the Pd, and Pt complexes, shown in Figure 30, are supported by IR and ^1H and ^{31}P NMR data. The two phosphorus resonances of the palladium complex appeared as an AB quartet with J = 59.0 Hz, similar to the ^{31}P NMR spectral data for the chromium and tungsten complexes. In the case of the platinum complex, the two phosphorus resonances appeared as an AB quartet with J = 45.8 Hz.

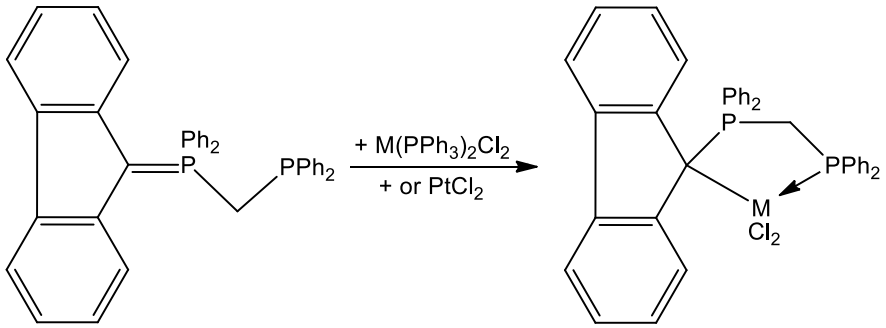

Figure 30. Syntheses of palladium and platinum complexes of the fluorenyl ylide.

This work was also extended to the coordination of palladium to the ethylene bridged chelating fluorenyl phosphonium ylide (Figure 27, n = 2), and the palladium complex shown in Figure 31 was obtained.[46]

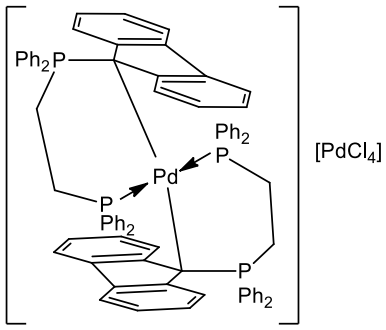

Figure 31. The palladium complex of the ethylene bridge fluorenyl ylide.

The IR spectrum of this complex exhibited one Pd-Cl stretching band at 325 cm^{-1}, which is observed in K_2PdCl_4 and this confirms the presence of $PdCl_4^-$ in the complex.

Coordination of the propylene bridged chelating fluorenyl phosphonium ylide (Figure 27, n = 3) to Me_3PAuCl was reported, and the resultant gold complex was characterized by the IR, ^1H and ^{13}C NMR spectroscopy (Figure 32).[46] The IR spectrum of the gold complex did not exhibit an absorption for the Au-Cl stretching mode, and the ^{31}P NMR spectrum showed just one singlet peak at δ 32.29 although no ^1H NMR data were reported.

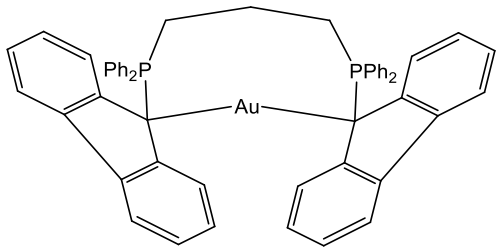

Figure 32. Suggested structure for the gold complex of the propylene bridged fluorenyl phosphonium ylide.

1.3 Phosphonium Indenylides (PHINs)

Ito *et al.* synthesized triphenyphosphonium indenylide, $C_9H_6PPh_3$, in 1966, but gave very little information concerning synthetic procedures or characterization.[48] One year later, Crofts and Williamson[49] reported the synthesis of triphenyphosphonium indenylide and this will be discussed later in this chapter in detail with the synthetic method in **1.3.1**. Triphenyphosphonium indenylide is the indenyl analogue of the Ramirez ylide, and it was anticipated to also show interesting coordination chemistry like the Ramirez ylide. Although the zwitterionic resonance structure of the triphenylphosphonium cyclopentadienylide is aromatic and isoelectronic with the cyclopentadienyl (Cp) anion, like the Ramirez ylide, the coordination chemistry of this class of ligands has not received a lot of attention.

Rufanov *et al.* reported the syntheses of two phosphonium 1-indenylides, 1-$C_9H_6(CH_2Ph)Ph_2$ and 1-$C_9H_6(CH_2C_6F_5)Ph_2$, in 2004,[50] but their possible coordinating properties were not investigated. Only after several years did the Baird lab initiate research on the syntheses, characterization, and coordination chemistry of phosphonium 1-indenylides (PHIN ligands).

1.3.1 Preparation of $C_9H_6PPh_3$ (PHIN) from 1-bromoindene

It was anticipated that 1-bromoindene would be a suitable candidate to synthesize PHIN ligands. Buu-Hoï reported the synthesis of 1-bromoindene, in a low yield, via reaction of indene with N-bromosuccinimide, in 1944.[51] Croft and Williamson reinvestigated the synthesis of 1-bromoindene in 1967, and used it to synthesize triphenyphosphonium indenylide, $C_9H_6PPh_3$.[49] Their synthetic method involved the

addition of bromine to freshly distilled indene to form 1,2-bromoindene, followed by the addition of 2,6-lutidine to 1,2 bromoindene to produce 1-bromoindene. There followed the addition of PPh_3 to form $C_9H_7PPh_3$, and the deprotonation of $C_9H_7PPh_3$ with NH_3 to give triphenylphosphonium indenylide, $C_9H_6PPh_3$ (Figure 33).

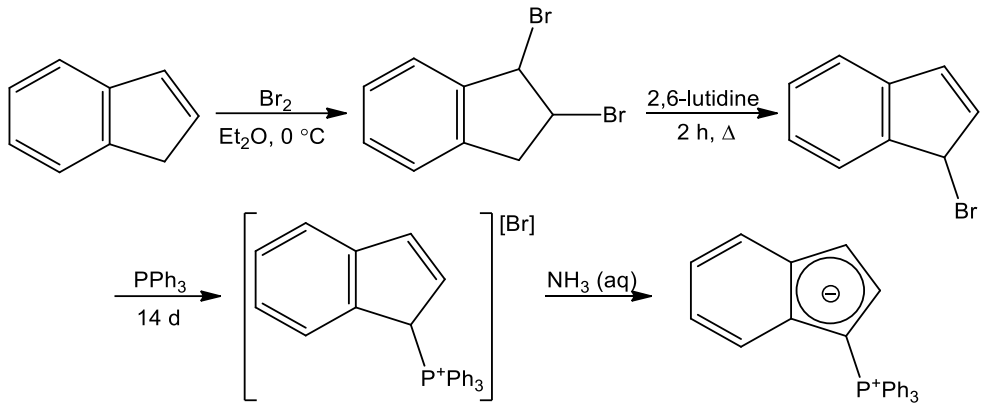

Figure 33. Synthesis of triphenylphosphonium indenylide.

In 1980, Woell *et al.* suggested that the elimination of hydrogen bromide should result in the formation of 3-bromoindene.[52]

Improvements on the synthesis of 1-bromoindene were necessary to increase the efficiency of this synthesis with higher percent yield, and C-Si bond cleavage by electrophiles was found to be a good starting point to achieve a more efficient synthetic route to synthesize 1-bromoindene.[52,53] 1-Bromoindene was prepared by deprotonation of indene by *n*-BuLi followed by addition of trimethylchlorosilane to afford 1-trimethylsilylindene and addition of dioxane dibromide to yield a pale yellow liquid in 86% yield (Figure 34).[53]

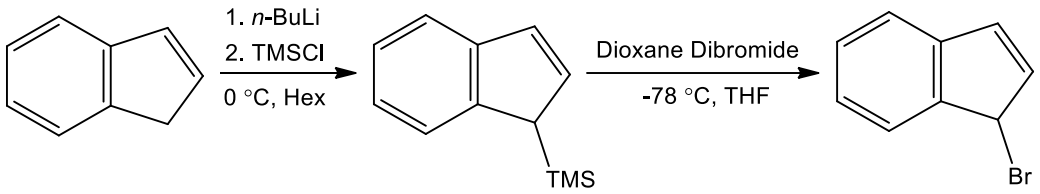

Figure 34. Synthesis of 1-bromoindene from dioxane dibromide.

In 2010, Fowler *et al.* reported the syntheses of triphenylphosphonium-1-indenylide, 1-$C_9H_6PPh_3$, methyldiphenylphosphonium-1-indenylide, 1-$C_9H_6PMePh_2$ (**I**), and dimethylphenylphosphonium-1-indenylide, 1-$C_9H_6PMe_2Ph$ (Figure 35).[54]

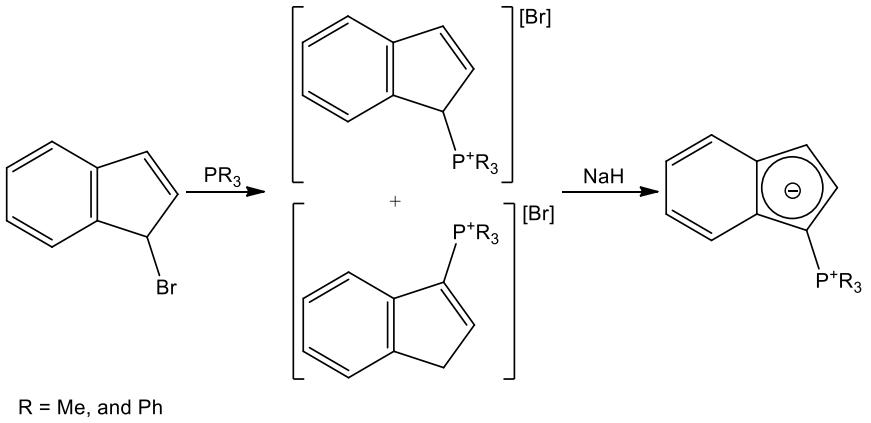

Figure 35. Syntheses of PHIN ligands from 1-bromoindene.

In this report, two new PHIN ligands, 1-$C_9H_6PPh_3$, and 1-$C_9H_6PMe_2Ph$, and one previously reported PHIN, 1-$C_9H_6PMePh_2$ (**I**),[55] were synthesized using 1-bromoindene prepared as in the previous reported paper.[53] Reaction of 1-bromoindene with the phosphines afforded the corresponding salts, and deprotonation with NaH produced the desired PHINs, 1-$C_9H_6PPh_3$, 1-$C_9H_6PMePh_2$ (**I**), and 1-$C_9H_6PMe_2Ph$, in 65%, 85%, and 94% yields, respectively. All these three PHIN ligands, were characterized by ^{1}H, ^{13}C, and ^{31}P NMR spectroscopy, elemental analyses, and X-ray crystallography.

1.3.2 Preparation of PHIN from 1-$C_9H_7PPh_2$

In 2004, Rufanov *et al.* synthesized two phosphonium 1-indenylides, 1-$C_9H_6(CH_2Ph)Ph_2$ and 1-$C_9H_6(CH_2C_6F_5)Ph_2$, from 1-$C_9H_7PPh_2$ (Figure 36).[50] The precursor, 1-$C_9H_7PPh_2$, was synthesized from the reaction of indene with *n*-BuLi (Figure 36).[56] In this synthetic route, 1-$C_9H_7PPh_2$ reacted with RBr (R = CH_2Ph or $CH_2C_6F_5$) to form the phosphonium salts, followed by deprotonation by NaH, to afford 1-$C_9H_6(CH_2Ph)Ph_2$ and 1-$C_9H_6(CH_2C_6F_5)Ph_2$ in 79% and 78%, respectively. Both phosphonium 1-indenylides were characterized by ^1H, ^{13}C and ^{31}P NMR spectroscopy, EI MS and elemental analyses, while 1-$C_9H_6(CH_2Ph)Ph_2$ was also characterized by X-ray crystallography.

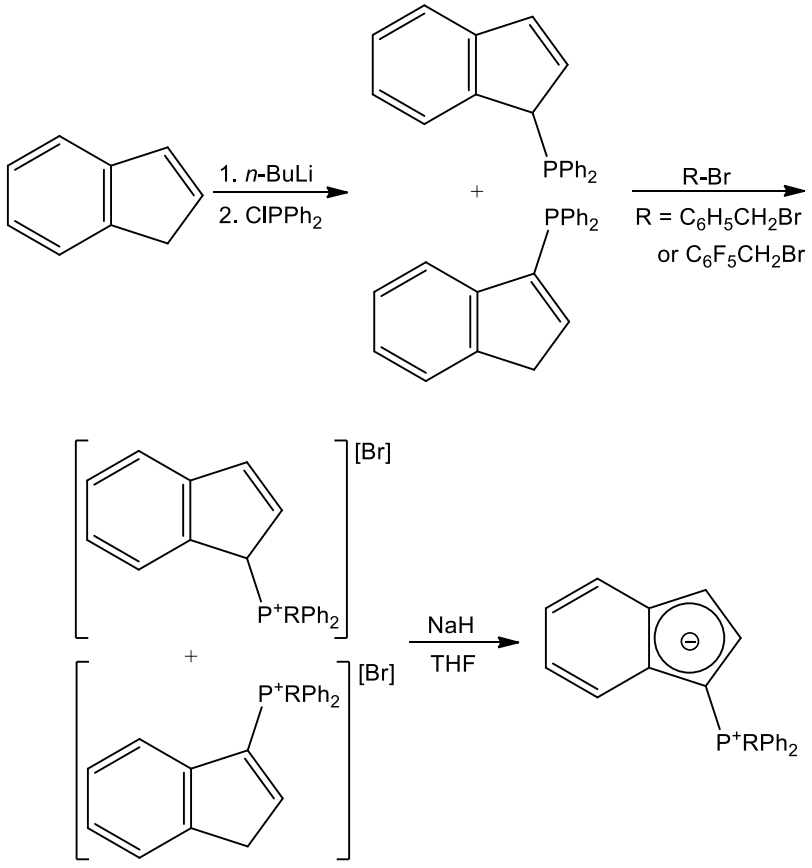

Figure 36. Syntheses of $C_9H_6P(CH_2Ph)Ph_2$ and $C_9H_6P(CH_2C_6F_5)Ph_2$.

Brownie *et al.* synthesized $C_9H_6PMePh_2$ (**I**) in 87% yield by the reaction of 1-$C_9H_7PPh_2$ with MeI to form a mixture of two regioisomers of the phosphonium salt, $[C_9H_7PMePh_2]I$, followed by deprotonation with NaH (Figure **37**).[55] The compound was characterized by ^{1}H, ^{13}C, and ^{31}P NMR spectroscopy, elemental analyses, and X-ray crystallography. The synthesis of $C_9H_6PMePh_2$ (**I**) is more efficient compared with the synthesis of $C_5H_4PMePh_2$ because 1-$C_9H_7PPh_2$ does not undergo Diels-Alder dimerization and thus does not need to be used immediately in the case of $C_5H_4PPh_2$. Moreover, a higher yield was obtained after deprotonation of two phosphonium salts compare with $C_5H_4PMePh_2$.

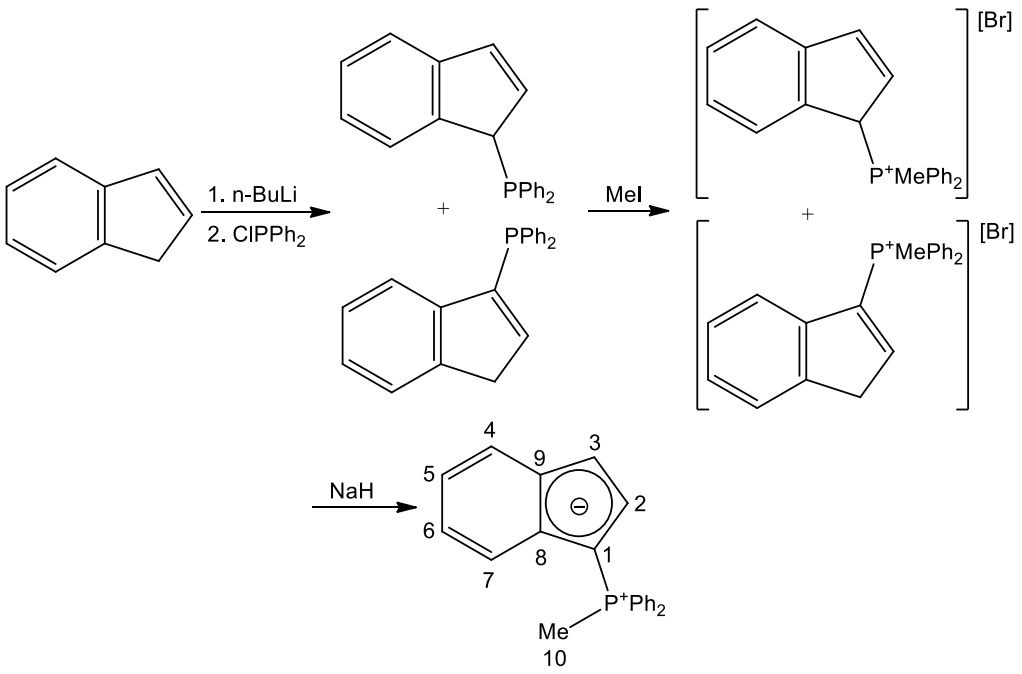

Figure 37. Synthesis of $C_9H_6PMePh_2$ (**I**).

The ^{1}H and ^{13}C NMR chemical shifts and coupling constants of 1-$C_9H_6PMePh_2$ (**I**), 1-$C_9H_6P(CH_2Ph)Ph_2$[50] and 1-$C_9H_6P(CH_2C_6F_5)Ph_2$[50] are very similar. For 1-$C_9H_6PMePh_2$ (**I**), the chemical shift of C(1) in the ^{13}C NMR spectrum appeared as

doublet at δ 66.1, shifted downfield in comparison with those of $C_9H_6P(CH_2Ph)Ph_2$ (δ 59.9),[50] and 1-$C_9H_6P(CH_2C_6F_5)Ph_2$ (δ 62.2),[50] but shifted upfield in comparison with $C_5H_4PMePh_2$ (δ 79.2).[22] The ^{31}P NMR spectrum of 1-$C_9H_6PMePh_2$ (**I**) (δ 5.69) is shifted upfield in comparison with $C_5H_4PMePh_2$ (δ 7.95).[22]

X-ray crystallography was used to confirm the structures of 1-$C_9H_6PMePh_2$ (**I**), and $Cr(\eta^5$-**I**$)(CO)_3$. The P-C(1) bond lengths of cyclopentadienyl type ylides provides an estimation of the bond character and the contribution of each resonance structure to the overall bonding situation. The P-C(1) bond length, 1.711 Å, in 1-$C_9H_6PMePh_2$ (**I**) was shorter than the similar Cp derived ylide, $C_5H_4PMePh_2$ (1.727 Å average),[22] and shorter than that observed for the same bond in the Ramirez ylide (1.718 Å average).[8] It is also shorter than the P-C(1) bond of 1-$C_9H_6P(CH_2Ph)Ph_2$, which is 1.733 Å.[50] The shortening of the P-C(1) bond indicates that this bond in 1-$C_9H_6PMePh_2$ (**I**) has potentially more double bond character than that of the Cp derived ylides. The P-C(1) bond is significantly shorter than that the P-Ph bonds in 1-$C_9H_6PMePh_2$ (**I**). The C_5 ring bonds of 1-$C_9H_6PMePh_2$ (**I**) are, on average, longer than the C_5 ring bonds of $C_5H_4PMePh_2$[22] and $C_5H_4PPh_3$.[8] The similarity in the C-C lengths in the C_5 ring provided evidence of delocalization of the π bond electron density.

1.3.3 Phosphonium Indenylides in Organometallic Chemistry

PHIN ligands are potentially very interesting, but their coordination chemistry is largely unexplored. The similar electronic structure of PHINs to Cp anion and electron donating abilities intermediate between Cp anion and neutral arene are two key important features of PHINs in the field of coordination chemistry. In **1.3.4**, coordination of PHIN

to chromium, as the first reported complex of PHIN,[55] will be discussed in detail to prove the two mentioned important features of PHINs. Many papers and reviews are reported on arene[57-59] and Cp[60-66] complexes and their catalytic applications, and PHIN complexes are expected to exhibit the same coordination chemistry and a wide range of catalytic activities.

Moreover, PHINs are planar pro-chiral ligands and form planar-chiral complexes upon coordination with metal centers (Figure 38). In **1.3.4**, more details of the synthesis and characterization of chiral chromium PHIN complex will be presented. The formation of these chiral complexes raise the possibility of applications in enantioselective catalysis since the chirality exists very close to the metal.

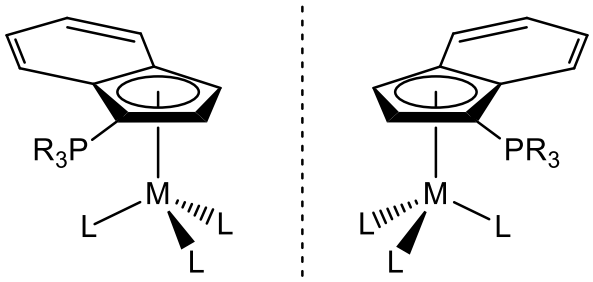

Figure 38. Chiral complexes of PHIN ligands.

1.3.4 Coordination of Phosphonium Indenylides to Cr and Ru

The PHIN ligand 1-$C_9H_6PMePh_2$ (**I**) was refluxed in diglyme with an excess of $Cr(CO)_6$ to afford a new chromium complex of PHIN, $Cr(\eta^5$-**I**$)(CO)_3$ (Figure 39).[55]

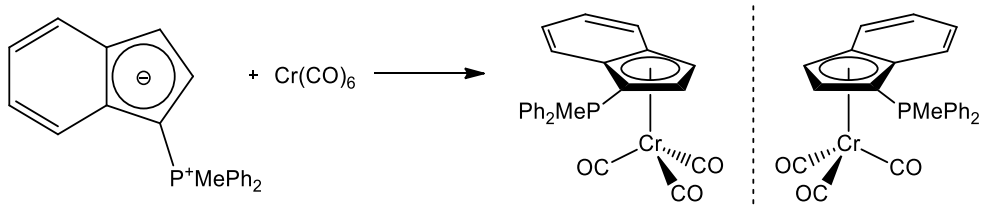

Figure 39. Synthesis of $Cr(\eta^5$-**I**$)(CO)_3$.

The product, $Cr(\eta^5$-**I**$)(CO)_3$, was characterized by IR, ^1H, ^{13}C, and ^{31}P NMR spectroscopy, elemental analyses, and X-ray crystallography. The IR spectrum of $Cr(\eta^5$-**I**$)(CO)_3$ exhibited carbonyl stretches at 1916 (s), 1816 (s), and 1820 (sh) cm^{-1}, very similar to those of $Cr(\eta^5\text{-}C_5H_4PMePh_2)(CO)_3$,[22,39] and $Cr(\eta^5\text{-}C_5H_4PPh_3)(CO)_3$[35] and showing that the electron donating properties of 1-$C_9H_6PMePh_2$ (**I**) are very similar to those of $\eta^5\text{-}C_5H_4PMePh_2$, and $\eta^5\text{-}C_5H_4PPh_3$. In the ^1H NMR spectrum of $Cr(\eta^5$-**I**$)(CO)_3$, the two protons of C_5 ring were shifted upfield in comparison with the free ligand, as was the case with $Cr(\eta^5\text{-}C_5H_4PMePh_2)(CO)_3$.[22] No significant changes were observed for the four protons of the C_6 ring, but a downfield shift was seen for the P-Me resonance of $Cr(\eta^5$-**I**$)(CO)_3$ in comparison with the free ligand, from δ 2.48 to 2.88.

The ^{13}C NMR spectrum showed that the ylidic carbon of $Cr(\eta^5$-**I**$)(CO)_3$ is more shielded than in 1-$C_9H_6PMePh_2$ (**I**). The same change was observed in the ^{13}C NMR spectrum for the ylidic carbon of $Cr(\eta^5\text{-}C_5H_4PMePh_2)(CO)_3$ compare to $\eta^5\text{-}C_5H_4PMePh_2$ with smaller degree.[22] All the carbons of C_5 ring were shielded in $Cr(\eta^5$-**I**$)(CO)_3$ compared to 1-$C_9H_6PMePh_2$ (**I**). The most interesting feature of the ^{13}C NMR spectrum is the presence of the diastereotopic phenyl groups. Two sets of peaks for these carbons with identical coupling constants, $J_{P\text{-}C}$, were easily distinguishable. The ^{31}P NMR spectrum of $Cr(\eta^5$-**I**$)(CO)_3$ appeared at lower field (δ 19.84) than that of free ligand, 1-

$C_9H_6PMePh_2$ (**I**) (δ 5.69). In the ^{31}P NMR spectra of $Cr(\eta^5\text{-}C_5H_4PMePh_2)(CO)_3$ and $C_5H_4PMePh_2$, the same change in chemical shifts were reported.[22]

X-ray crystallography was used to confirm the structures of 1-$C_9H_6PMePh_2$ (**I**), and $Cr(\eta^5\text{-}\mathbf{I})(CO)_3$ (Figure 40).

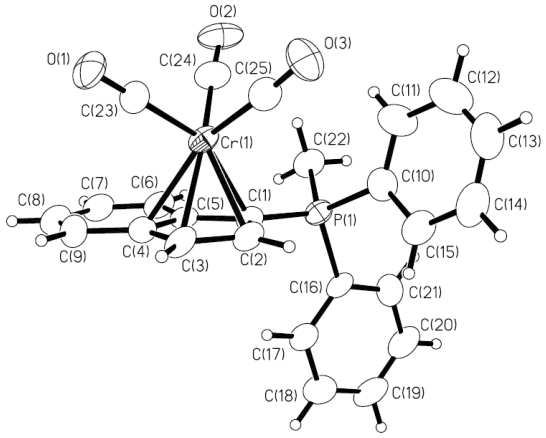

Figure 40. The molecular structure of $Cr(\eta^5\text{-}\mathbf{I})CO_3$.

The P-C(1) bond length in $Cr(\eta^5\text{-}\mathbf{I})(CO)_3$ (1.75 Å) is very similar to those of $Cr(\eta^5\text{-}C_5H_4PMePh_2)(CO)_3$ (1.76 Å) [22] and $Cr(\eta^5\text{-}C_5H_4PPh_3)(CO)_3$ (1.75 Å average).[35] The P-C(1) bond length changed on coordination to the $-Cr(CO)_3$ fragment. The P-C(1) bond length is elongated in $Cr(\eta^5\text{-}\mathbf{I})(CO)_3$ compared to that of 1-$C_9H_6PMePh_2$ (**I**) and the increase of this bond length is indicative of a greater contribution of the zwitterionic resonance structure of the ligand upon coordination, indicating a greater degree of aromaticity.

Three novel PHIN complexes of ruthenium, $[Ru(\eta^5\text{-}C_5H_5)(\eta^5\text{-}1\text{-}C_9H_6PPh_3)]PF_6$, $[Ru(\eta^5\text{-}C_5H_5)(\eta^5\text{-}\mathbf{I})]PF_6$ and $[Ru(\eta^5\text{-}C_5H_5)(\eta^5\text{-}\mathbf{I})]PF_6$, were reported in 2011 (Figure 41).[54]

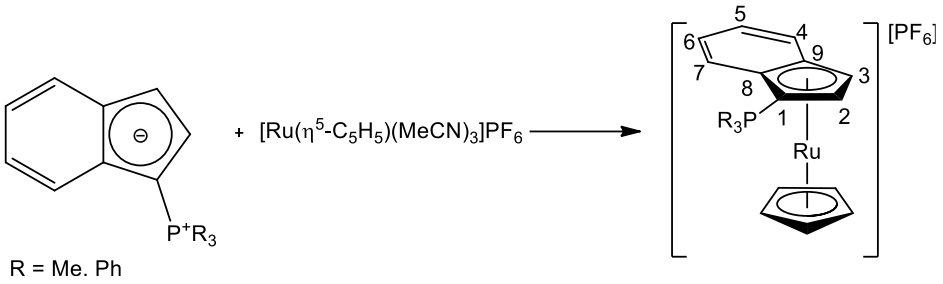

Figure 41. Syntheses of PHIN complexes of ruthenium.

It had previously been reported by Slugovc[67] and Trost[68] that the acetonitrile ligands of the complex $[Ru(Cp)(MeCN)_3]^+$ are readily substituted by aromatic ligands, and it was thought that novel PHIN complexes of ruthenium may form by the substitution reaction of PHINs and $[Ru(\eta^5\text{-}C_5H_5)(MeCN)_3]PF_6$. Three PHINs were reacted with $[Ru(\eta^5\text{-}C_5H_5)(MeCN)_3]PF_6$ and, after a few minutes stirring, the corresponding PHIN complexes were prepared.[54] All were characterized by ^1H, ^{13}C, and ^{31}P NMR spectroscopy, ES mass spectrometry, X-ray crystallography and DFT calculations.

The ^1H NMR spectra of all the three PHIN complexes of ruthenium showed upfield shifts for H(2) and H(3) compared with the chemical shifts of the related uncomplexed PHINs, as was the case for $Cr(\eta^5\text{-}\mathbf{I})(CO)_3$[55] and for the protons of the C_5 ring H(2,5) and H(3,4) in $M(\eta^5\text{-}C_5H_4PMePh_2)(CO)_3$ (M = Cr, Mo, W). Very small changes in chemical shifts of the H(5)-H(8) and protons of the phenyl groups were observed, but the chemical shifts of the protons of the $\eta^5\text{-}C_5H_5$ group shifted downfield upon coordination from δ 4.29 in $[Ru(\eta^5\text{-}C_5H_5)(MeCN)_3]PF_6$ to δ 4.53 in $[Ru(\eta^5\text{-}C_5H_5)(\eta^5\text{-}1\text{-}C_9H_6PPh_3)]PF_6$, δ 4.45 in $[Ru(\eta^5\text{-}C_5H_5)(\eta^5\text{-}\mathbf{I})]PF_6$ and δ 4.55 in $[Ru(\eta^5\text{-}C_5H_5)(\eta^5\text{-}\mathbf{I})]PF_6$.

As a result of coordination of these three planar-prochiral PHIN ligands to ruthenium, enantiomeric pairs of each should be prepared (Figure 42). Thus the ^{1}H NMR spectrum of $[Ru(\eta^5\text{-}C_5H_5)(\eta^5\text{-}\mathbf{I})]PF_6$ exhibited resonances of two the diastereotopic methyl groups on the phosphorus atom with identical coupling constants ($^{2}J_{P\text{-}H}$ = 13.2 Hz).

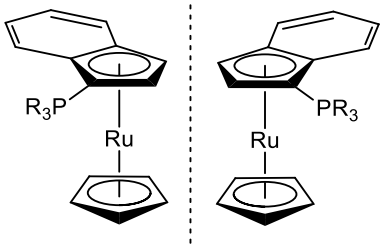

Figure 42. Two enantiomeric pairs of PHIN complexes of ruthenium.

The ^{13}C NMR spectra of all three PHIN complexes of ruthenium showed that the ylidic carbon in the complexes were more shielded than in the related uncomplexed PHINs. All the carbons of the C_5 rings were shielded in all three PHIN complexes of ruthenium compared to their related ligands; the same trends were observed for $Cr(\eta^5\text{-}\mathbf{I})(CO)_3$.[55] The most interesting features of the ^{13}C NMR spectra were the presence of resonances of the diastereotopic methyl groups of $[Ru(\eta^5\text{-}C_5H_5)(\eta^5\text{-}\mathbf{I})]PF_6$, and the presence of resonances of the diastereotopic phenyl groups of $[Ru(\eta^5\text{-}C_5H_5)(\eta^5\text{-}\mathbf{I})]PF_6$. The ^{31}P NMR resonances of all the three PHIN complexes shifted to lower field (δ 24.3 in $[Ru(\eta^5\text{-}C_5H_5)(\eta^5\text{-}1\text{-}C_9H_6PPh_3)]PF_6$, δ 23.3 in $[Ru(\eta^5\text{-}C_5H_5)(\eta^5\text{-}\mathbf{I})]PF_6$, δ 22.4 in $[Ru(\eta^5\text{-}C_5H_5)(\eta^5\text{-}\mathbf{I})]PF_6$) than that of the related uncomplexed PHINs (δ 10.39 in $1\text{-}C_9H_6PPh_3$, δ 5.69 in $1\text{-}C_9H_6PMePh_2$ (**I**), δ 1.78 in $1\text{-}C_9H_6PMe_2Ph$).

X-ray crystallography was used to confirm the structures of these three ruthenium complexes. The molecular structure of $[Ru(\eta^5\text{-}C_5H_5)(\eta^5\text{-}1\text{-}C_9H_6PPh_3)]PF_6$ is shown in Figure 43 as an example.

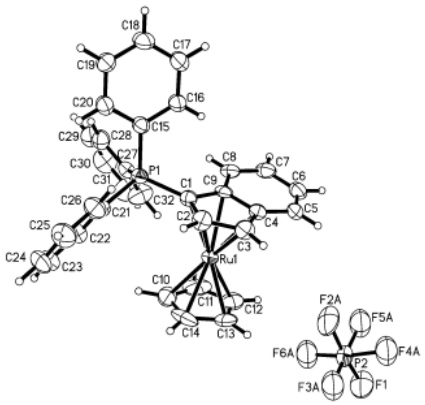

Figure 43. Molecular structure of $[Ru(\eta^5\text{-}C_5H_5)(\eta^5\text{-}1\text{-}C_9H_6PPh_3)]PF_6$.

The X-ray data showed sandwich structures for all three PHIN complexes of ruthenium, with the C_5 rings being almost eclipsed. The P-C(1) bonds in all three PHIN complexes were shorter than the average P-Ph bond length, and all of the bonds of the C_5 rings of PHINs elongated upon coordination compared with uncoordinated PHINs. The P-C(1) bond length in $[Ru(\eta^5\text{-}C_5H_5)(\eta^5\text{-}1\text{-}C_9H_6PPh_3)]PF_6$ (1.768 Å) was longer than those of $[Ru(\eta^5\text{-}C_5H_5)(\eta^5\text{-}\mathbf{I})]PF_6$ (1.763 Å) and $[Ru(\eta^5\text{-}C_5H_5)(\eta^5\text{-}1\text{-}C_9H_6PMe_2Ph)]PF_6$ (1.761 Å). This increase in the P-C(1) bond length of $[Ru(\eta^5\text{-}C_5H_5)(\eta^5\text{-}1\text{-}C_9H_6PPh_3)]PF_6$ is indicative of a greater contribution of the zwitterionic resonance structure of the ligand upon coordination, indicating a greater degree of aromaticity compared with the other two analogous complexes. The P-C(1) bond lengths in all three PHIN complexes of ruthenium (~1.76 Å) were very similar to those of $Cr(\eta^5\text{-}\mathbf{I})(CO)_3$ (1.75 Å),[55] $Cr(\eta^5\text{-}C_5H_4PMePh_2)(CO)_3$ (1.76 Å),[22] and $Cr(\eta^5\text{-}C_5H_4PPh_3)(CO)_3$ (1.75 Å average).[35] The P-

C(1) bonds were elongated in all of the PHIN complexes compared to those of the related PHIN ligands and the increase of this bond length is indicative of a greater contribution of the zwitterionic resonance structure of the ligand upon coordination. Interestingly, it was found that the Ru-C(1), Ru-C(2), and Ru-C(3) bond lengths in all three PHIN complexes were similar and only slightly longer than the averages of the Ru-C_5H_5 bonds. On the other hand, the Ru-C(4) and Ru-C(9) bond length in all three PHIN complexes were also similar but notably longer than the averages of the Ru-C_5H_5 bond lengths. As a result, it was found that the C_5 ylidic rings relative to the corresponding C_5 rings are angled away, 5.63, 6.90, and 4.94°, respectively, in [Ru(η^5-C_5H_5)(η^5-1-$C_9H_6PPh_3$)]PF_6, [Ru(η^5-C_5H_5)(η^5-**I**)]PF_6 and [Ru(η^5-C_5H_5)(η^5-1-$C_9H_6PMe_2Ph$)]PF_6). The bond angles in the C_5 ylidic rings in all three PHIN complexes of ruthenium are reported as ~108° which is expected for a regular pentagon.

These trends are all very similar to those observed previously for Cr(η^5-**I**)$(CO)_3$,[55] and Cr(η^5-$C_5H_4PMePh_2$)$(CO)_3$.[22]

1.3.5 Coordination of Phosphonium Indenylides to Group IV, and IX Metals

Because there is no report on the synthesis of PHIN complexes of group 4, and 9, we will discuss below research which has been done to synthesize analogous arene complexes.

1.4 Coordination of arene to Group IV

Solari *et al.* reported the coordination of hexamethylbenzene (C_6Me_6) to titanium.[69] Their synthetic method involved the addition of hexamethylbenzene to excess $TiCl_4$ or the addition of 2-butyne to $TiCl_4$ to afford $[(\eta^6\text{-}C_6Me_6)TiCl_3][Ti_2Cl_9]$ (Figure 44). The X-ray structure of $[(\eta^6\text{-}C_6Me_6)TiCl_3][Ti_2Cl_9]$ was also obtained as shown in Figure 45.[69,70]

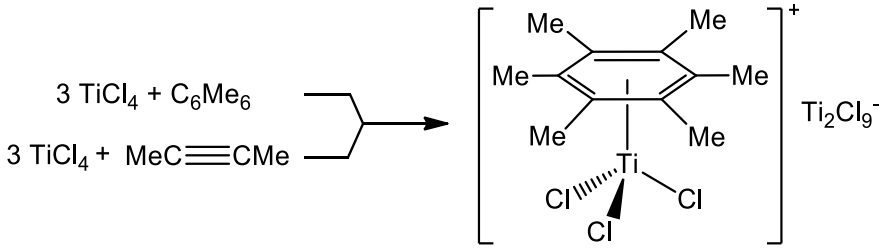

Figure 44. Synthesis of $[(\eta^6\text{-}C_6Me_6)TiCl_3][Ti_2Cl_9]$.

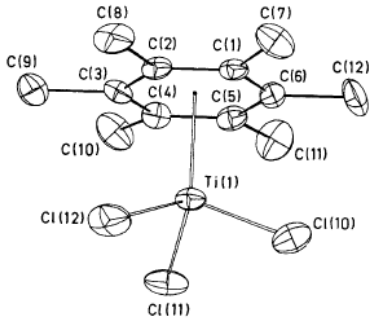

Figure 45. Molecular structure of $[\eta^6\text{-}C_6Me_6)TiCl_3]^+$.

The syntheses of analogous $[(\eta^6\text{-arene})TiX_3][AlX_4]$ (X = Cl, Br) were accomplished by using a halide abstractor, $AlCl_3$. The reaction of $AlCl_3$, TiX_4 (X = Cl, Br), and 1,3,5-$Me_3C_6H_3$, or 1,2,4,5-$Me_4C_6H_2$ afforded $[(\eta^6\text{-}1,3,5\text{-}Me_3C_6H_3)TiX_3][AlX_4]$ (X = Cl, Br), or $[(\eta^6\text{-}1,2,4,5\text{-}Me_4C_6H_2)TiCl_3][AlCl_4]$, respectively (Figure 46).[71]

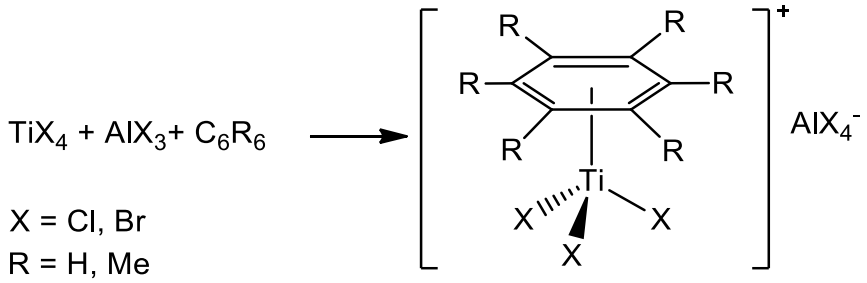

Figure 46. Syntheses of [(η^6-arene)TiX_3][AlX_4].

In the same paper, arene displacement from [(η^6-C_6Me_6)$TiCl_3$][$AlCl_4$] was also studied with THF or TlCp, and it was found that the arene ligand in [(η^6-C_6Me_6)$TiCl_3$][$AlCl_4$] was readily replaced by Lewis bases such as THF or the Cp anion. Similar reactions of [(η^6-C_6Me_6)$TiCl_3$][$AlCl_4$] and [(η^6-C_6Me_6)$TiCl_3$][$AlCl_4$] with TlCp afforded $CpTiCl_3$.[71] Using $GaCl_3$ as a chloride abstractor in the reaction of $TiCl_4$ and 1,2,4,5-$C_6Me_4H_2$ similarly afforded [(η^6-1,2,4,5-$C_6Me_4H_2$)$TiCl_3$][$GaCl_4$].[72]

Syntheses of arene complexes of zirconium using $ZrCl_4$ is challenging due to the poor solubility of $ZrCl_4$, but Solari *et al.* reported the coordination of C_6Me_6 to $ZrCl_4$ in 1,2-$Cl_2C_6H_4$ to synthesize $Zr(\eta^6$-$C_6Me_6)Cl_2(\mu$-$Cl)_3ZrCl_3$.[73] In the same paper, it was reported that the reaction of $C_6Me_4H_2$ with $ZrCl_4$ gave $Zr(\eta^6$-$C_6Me_4H_2)Cl_2(\mu$-$Cl)_3ZrCl_3$. The structure of $Zr(\eta^6$-$C_6Me_6)Cl_2(\mu$-$Cl)_3ZrCl_3$ was confirmed by X-ray crystallography as shown in Figure 47.

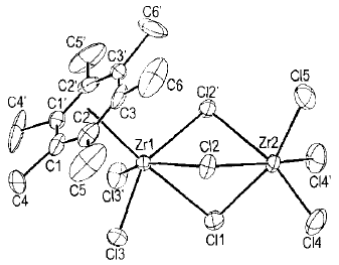

Figure 47. Molecular structure of (η^6-C_6Me_6)$ZrCl_2(\mu$-$Cl_3)ZrCl_3$.

Synthesis of $Zr(\eta^6\text{-}C_6Me_6)Cl_2(\mu\text{-}Cl)_3ZrCl_3$ was accomplished by the reaction of $ZrCl_4(THF)_2$ with C_6Me_6 in the presence of chloride abstractor, $AlCl_3$, or by the reaction of $ZrCl_4$ with C_6Me_6 in benzene (Figure 48).[72]

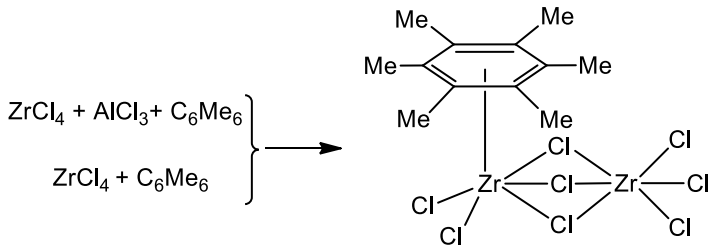

Figure 48. Synthesis of $Zr(\eta^6\text{-}C_6Me_6)Cl_2(\mu\text{-}Cl)_3ZrCl_3$.

1.5 Coordination of Arene Ligands to Group IX Metals

$[Rh(\eta^6\text{-arene})(PPh_3)_2][BAr^f_4]$ ($BAr^f_4 = B[C_6H_3(CF_3)\text{-}3,5)_2]_4$; arene = benzene or toluene) was prepared by the reaction of $[(Ph_3P)_2Rh(\mu\text{-}Cl)]_2$ with arene (benzene or toluene) in the presence of a chloride abstractor, $NaBAr^f_4 = Na[B[C_6H_3(CF_3)\text{-}3,5)_2]_4]$ (Figure 49).[74] The synthesis of $[Rh(\eta^6\text{-arene})(PPh_3)_2]^+$ was previously reported, in 2002.[75,76]

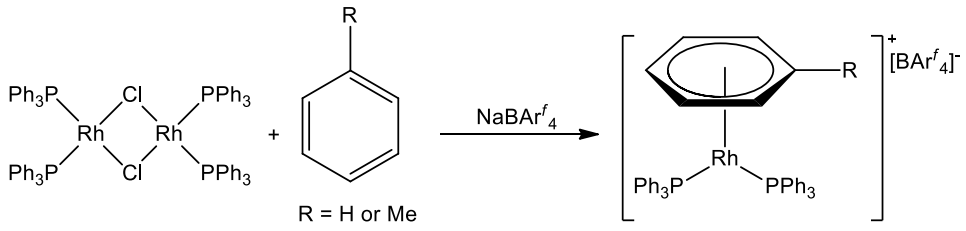

Figure 49. Synthesis of $[(\eta^6\text{-arene})Rh(PPh_3)_2][BAr^f_4]$, arene = benzene, or toluene.

Complexes of the type $[Rh(\eta^6\text{-arene})(PPh_3)_2][BAr^f_4]$, (arene = benzene, or toluene) were characterized by IR, ^1H, ^{13}C, ^{19}F, and ^{31}P NMR spectroscopy, elemental

analyses, and X-ray crystallography. Crystal structures of these complexes are shown in Figure 50.

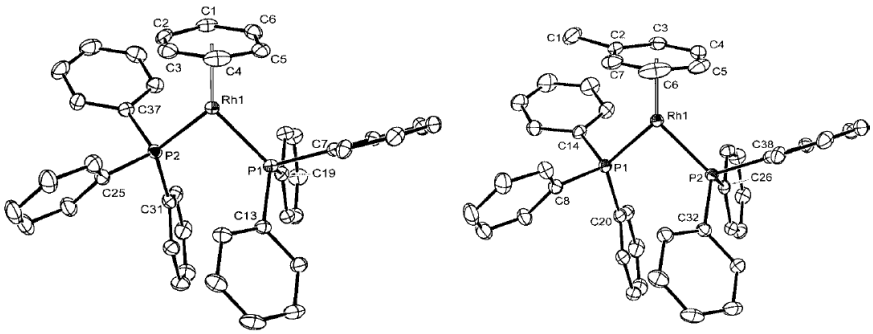

Figure 50. Molecular structures of $[Rh(\eta^6\text{-arene})(PPh_3)_2][BAr^f_4]$, arene = benzene, or toluene.

More recently, a variety of $[Rh(\eta^6\text{-arene})(P(i\text{-}Bu)_3)_2][BAr^f_4]$ (arene = benzene, *t*-Bu-benzene, naphthalene, anthracene, pyrene, triphenylene, coronene) were synthesized by the substitution reaction of $[Rh(\eta^6\text{-}C_6H_5F)(Pi\text{-}Bu_3)_2][BAr^f_4]$ with different arenes.[77]

1.6. Research Aims

In the Baird lab, Brownie *et al.* synthesized $C_5H_4PMePh_2$, and coordinated this ligand to the $Cr(CO)_3$, $Mo(CO)_3$, and $W(CO)_3$ groups to form the group 6 complexes $(\eta^5\text{-}C_5H_4PMePh_2)M(CO)_3$ (M = Cr, Mo, and W).[22] Later, in 2008, Brownie *et al.* synthesized $C_9H_6PMePh_2$ (**I**), and coordinated this planar pro-chiral ligand to the $Cr(CO)_3$ group to form the planar chiral chromium complex of methyldiphenylphosphonium indenylide, $Cr(\eta^5\text{-}\mathbf{I})(CO)_3$.[55] In 2011, Fowler *et al.* synthesized two novel ligands of this class, dimethyldiphenylphosphonium indenylide ($1\text{-}C_9H_6PMe_2Ph$), and triphenylphosphonium indenylide ($1\text{-}C_9H_6PPh_3$), along with methyldiphenylphosphonium indenylide (1-

$C_9H_6PMePh_2$, **I**), and coordinated these ligands to form the ruthenium complexes of $[Ru(\eta^5\text{-}C_5H_5)(\eta^5\text{-}1\text{-}C_9H_6PMe_2Ph)]PF_6$, $[Ru(\eta^5\text{-}C_5H_5)(\eta^5\text{-}1\text{-}C_9H_6PPh_3)]PF_6$, and $[Ru(\eta^5\text{-}C_5H_5)(\eta^5\text{-}1\text{-}\mathbf{I})]PF_6$.[54] To extend this field of research, the study of coordination chemistry of **I** to group 4, 9, 10, and 12, along with the synthesis of another novel PHIN ligand, 4,7-dimethyl-1-$C_9H_4PMePh_2$ (**II**), and its coordination chemistry were considered in this work.

To explain our motivation on the coordination of **I** to group 4, it is worth to mention that since Karl Ziegler and Giulio Natta won the chemistry Nobel Prize in the field of catalytic olefin polymerization in 1963, much work has been done to synthesize new, highly active catalysts. Applications of organometallic complexes as catalysts for α-olefin polymerization developed dramatically in the past 30 years, group 4 (Ti, Zr, Hf) metallocenes being the most important metals investigated. There has been a substantial amount of research on the development of dicyclopentadienyl (metallocene) complexes of the group 4 metals and the development of their uses as olefin polymerization initiators; however, there is less research on the monocyclopentadienyl (non-metallocene) compounds of the group 4 metals. The fact that the chemistry of a catalyst system can often be tailored via subtle changes in the steric and/or electronic properties of the ligands, means that there are more potential research area to work on. For this reason, we began our investigation to synthesize a novel series of phosphonium cyclopentadienylide ligands and, more recently, of zwitterionic phosphonium 1-indenylides of type **I** which should result in interesting new chemistry and study its coordination chemistry to group 4 metals. The aim of this part of our research is to synthesize the above-mentioned phosphonium-1-indenylide ligand **I**, a planar pro-chiral ligand, and to coordinate this

ligand to a titanium center, and study the catalytic properties of the resulting planar chiral complex. This class of phosphonium 1-indenylide compounds is expected to coordinate in an η^5 manner, similar to the cyclopentadienylide derivatives, and since the ligand (**I**) is planar pro-chiral, indenylide complexes would exhibit planar chirality. There are a few reports, which will be discussed below, that we have used as a guideline. The titanium coordination to $CpPPh_3$ to form a sandwich complex, $[CpPPh_3)_2TiCl_2]Cl_2$, was previously reported by using two-fold excess of $CpPPh_3$, in 1977,[26] and the coordination of C_6Me_6 to $TiCl_4$ was also reported to synthesize $[(\eta^6\text{-}C_6Me_6)TiCl_3][Ti_2Cl_9]$ by using a four-fold excess of $TiCl_4$, in 1994.[70] These methods could be adapted in this part of our research as **I** is expected to donate six electrons to titanium as do $CpPPh_3$ and C_6Me_6, to form the group 4 complexes of **I**. This thesis this describes a study of group 4 coordination complexes of **I** with titanium and zirconium by using $TiCl_4$, $TiCl_4(THF)_2$, and Cp^*ZrMe_3 as starting materials in conjunction with various chloride/methyl abstractors, such as $AlCl_3$, $[Ph_3C][B(C_6F_5)_4]$, and $GaCl_3$. Use of an excess of **I** in reaction with $TiCl_4$ and $TiCl_4(THF)_2$ were previously attempted unsuccessfully in the Baird lab.[78-80] Using more concentrated solution of $TiCl_4$ (~eleven-fold excess) in reaction with **I** at different temperatures was anticipated to force this coordination successfully to form $[(\eta^5\text{-}\mathbf{I})TiCl_3][Ti_2Cl_9]$. Another method that was anticipated to promote this coordination was the use of different chloride abstractors, such as $AlCl_3$,[80] $[Ph_3C][B(C_6F_5)_4]$, and $GaCl_3$, and it was anticipated that creating a vacant site on titanium after chloride abstraction would result in the formation of the cationic species $[(\eta^5\text{-}\mathbf{I})TiCl_3]^+$. Coordination of **I** to zirconium was also anticipated to occur by the reaction of Cp^*ZrMe_3, $[Ph_3C][B(C_6F_5)_4]$, and **I** to prepare $[Cp^*ZrMe_2(\eta^5\text{-}\mathbf{I})][B(C_6F_5)_4]$.

In the field of group 9 coordination complexes of **I**, it is important to mention that the use of metal complexes as catalysts for the synthesis of organic compounds has been a vast area of research for a long time, because these compounds constitute a great proportion of many products including, drugs, plastics, petrochemicals, food, explosives, and paints. Asymmetric hydrogenation is one of the most efficient methods to prepare valuable chiral organic compounds with ketones, iminies, olefins, and aromatic compounds being the most common prochiral substrates.[81-84] Indeed this field of research was awarded a Noble Prize, in 2001.[81-84] Rhodium and iridium complexes are among the most promising catalysts in the field of transition metal-catalyzed asymmetric hydrogenation,[81-85] and we therefore decided to study rhodium and iridium complexes of **I** and **II** and their catalytic properties. Coordination of **I** and **II** to group these metals was effected using several starting materials, such as $[(PPh_3)_2Rh(\mu\text{-}Cl)]_2$, $[Ir(COD)Cl]_2$, and $[Rh(COD)Cl]_2$, along with different chloride abstractors, such as $AgBF_4$, $AgNO_3$, or $[Ph_3C][B(C_6F_5)_4]$ to synthesize $[Ir(\eta^4\text{-}C_8H_{12})(\mathbf{I}\text{-}\mathbf{II})]^+$, $[Rh(\eta^4\text{-}C_8H_{12})(\mathbf{I}\text{-}\mathbf{II})]^+$, or $[(\eta^5\text{-}\mathbf{I})Rh(PPh_3)_2]^+$. Another consideration in coordination to group rhodium was first the synthesis of $[(\eta^6\text{-toluene})Rh(PPh_3)_2]^+$ by following a previously reported method,[74] and then react it with **I** to form $[(\eta^5\text{-}\mathbf{I})Rh(PPh_3)_2]$. It was anticipated that this method might result in the formation of $[(\eta^5\text{-}\mathbf{I})Rh(PPh_3)_2]$, as **I** is a better electron donor ligand than toluene, and this replacement seemed to occur to afford the desired product.

It is also important to notice that the chiral discrimination of this type of complexes will be enhanced by using **II** as ligand, as the presence of two methyl groups at position 4 and 7 may play an important role in terms of steric effects and the resultant complexes could be potentially used as enantioselective catalysis in reactions such as

alkene hydrogenation. Reaction of the group 9 complexes toward hydrogen (H_2), methyl iodide (MeI), and benzyl chloride ($PhCH_2Cl$) are investigated in this work, as well.

Coordination of **I** to group 12 was also considered by using HgX_2 (X = Br, or Cl), because the coordination of $CpPPh_3$ to HgX_2 (X = Cl, Br and I) was previously reported to prepare $[(CpPPh_3)HgX_2]_2$.[86,87] Similarly, it was anticipated that the reaction of **I** and HgX_2 (X = Br, or Cl) would form $[(\eta^1\text{-}\mathbf{I})HgX_2]_2$. The coordination of **I** to group 10 was considered, because the only report on the coordination of this class of ligand to our knowledge was published, in 1981, to synthesize $[Ni(CpPPh_3)_2][PF_6]_2$ and not much study was carried out in this field of research.[88] Coordination of **I** to $NiBr_2$(DME) was anticipated to occur, because DME is a labile ligand and can possibly be replaced by **I**.

Chapter 2 : Experimental

2.1 General Considerations

All syntheses were carried out under a dry, deoxygenated argon atmosphere using standard Schlenk line techniques. Argon was deoxygenated by passage through a heated column of BASF copper catalyst, and then dried by passing through a column of 4A molecular sieves. Glassware was allowed to dry in an oven at 160 °C for at least 24 h prior to use in order to evaporate adsorbed water from the surface. Handling and storage of air-sensitive organometallic compounds was done using Schlenk techniques and an MBraun Labmaster glove box. NMR spectra were recorded using Bruker AV300, AV400, AV500, and AV600 spectrometers, all ^{1}H and ^{13}C NMR spectra being referenced to carbons or residual protons present in the deuterated solvents with respect to TMS at δ 0. ^{31}P NMR spectra were referenced to external 85% H_3PO_4. Elemental analyses were conducted by Canadian Microanalytical Service Ltd., Delta, BC.

Anhydrous dichloromethane, tetrahydrofuran, diethyl ether, hexanes and toluene were purchased from Aldrich in 18 L reservoirs packaged under nitrogen, and were dried by passing through columns of activated alumina (Innovative Technology Solvent Purification System). The THF, Et_2O and CH_2Cl_2 acquired in this way were subsequently stored over 4 Å molecular sieves which were activated by drying in a vacuum oven at 250 °C for at least 24 h. NMR solvents were purchased from Cambridge Isotope Laboratories or Aldrich and were degassed by bubbling argon and dried by storage over activated 4 Å molecular sieves. All other reagents were obtained from Aldrich, Strem Chemicals, Johnson Matthey or Pressure Chemical and used as received.

2.2 X-ray Crystallography

X-ray crystal structure determinations were performed by Dr. Ruiyao Wang and revised by Dr. Gabriele Schatte at Queen's University. Crystals were mounted on a glass fiber with grease and cooled to -93 °C in a stream of nitrogen gas controlled with Cryostream Controller 700. Data collections were performed on a Bruker SMART APEX II X-ray diffractometer with graphite-monochromated Mo K_α radiation (λ = 0.71073 Å) operating at 50 kV and 30 mA over 2θ ranges of 4.38 ~ 51.98º. No significant decay was observed during the data collections. Data were processed on a PC using the Bruker AXS Crystal Structure Analysis Package.[89] Neutral atom scattering factors were taken from Cromer and Waber.[90]

2.3 General Synthesis of PHINs

The general procedure to synthesize PHINs involved the reaction of indene with *n*-butyllithium and PPh_2Cl to afford diphenylphosphino-1-indene followed by the addition of MeI to form phosphonium salt which was deprotonated with NaH (See Section **3.1.1**, Figure 51).[55]

2.3.1 Synthesis of 4,7-dimethyl indene[91,92]

In a Schlenk flask with a dropping funnel, 200 mL of methanol were added to 19.6 g of finely cut sodium metal (855 mmol) drop-wise. After 24 h stirring, the mixture was cooled to 0°C and 33.9 g (513 mmol) of freshly distilled cyclopentadiene with 39.0 g (342 mmol) of 2,5-hexandione were added to the reaction mixture drop-wise. After 2 h stirring, 100 mL of water and 200 mL of diethyl ether were added to the reaction mixture.

The organic layer was separated, washed with brine, and then dried with anhydrous magnesium sulfate. Diethyl ether was pumped off under reduced pressure and the product was isolated by simple distillation as a bright yellow oil (bp. 65 °C, 0.1 mbar). Yield 41.4 g (84%). ^{1}H NMR ($CDCl_3$): δ 2.51, and 2.61 (s, 6 H, H(10) and (H11)), 3.44 (br dd, 2 H, (H1)), 6.73 (br dt, 1 H, (H2)), 7.10 (m, 1 H, (H3), 7.13-7.21 (m, 2 H, (H5) and (H6)). NMR analysis may be found in **3.1.2**.

2.3.2 Syntheses of the two isomers of (diphenylphosphino)-4,7-dimethyl-1-indene[93]

A solution of 4,7-dimethylindene (6.00 mL, 41.5 mmol) was treated with *n*-BuLi (16.6 mL, 41.5 mmol) in 200 mL diethyl ether at −78 °C and stirred for 24 h at room temperature, PPh_2Cl (7.70 mL, 41.5 mmol) at −78 °C was added and stirred for 24 h at room temperature and the slurry yellow solution was filtered through Celite to obtain a yellow solution of 1-$C_9H_5PPh_2$ as a mixture of isomers (12.0 g, 88% yield). ^{31}P NMR (CD_2Cl_2): δ −16.5 (isomer **A**), −5.7 (isomer **B**). X-ray quality crystals were obtained by slow evaporation of CH_2Cl_2. NMR data may be found in **3.1.3**.

2.3.3 Syntheses of the two regioisomers of the phosphonium salts, (methyldiphenylphosphonium)-4,7-dimethyl-1-indene iodide

A white, air-sensitive precipitate of (4,7-dimethyl-1-$C_9H_5PMePh_2$)I, (methyl diphenylphosphonium)-4,7-dimethyl-1-indene iodide, was prepared by stirring a solution of 4,7-dimethyl-1-$C_9H_5PPh_2$ (14.5 g, 0.04 mmol) and MeI (2.80 mL, 0.05 mmol) in 150 mL of THF at room temperature for 48 h. The resulting white precipitate was filtered

under argon, washed with 50 mL of hexanes and dried under reduced pressure. Yield 17.5 g (84%). ^{1}H NMR (CD_2Cl_2): δ 1.71 and 2.27 (s, H(10) and H(11) of isomer **B**), 1.88 and 2.37 (s, H(10) and H(11) of isomer **A**), 2.49 (d, P*CH*$_3$, of isomer **B**, $^{2}J_{P\text{-}H}$ = 13.0 Hz), 3.02 (d, P*CH*$_3$ of isomer **A**, $^{2}J_{P\text{-}H}$ = 13.1 Hz), 3.74 (br s, H(3) of isomer **A**), 6.42 (br t, H(3) of isomer **B**), 6.60-7.51 (m, olefinic), 7.51-8.15 (m, Ph, possibly olefinic). ^{31}P NMR (CD_2Cl_2): δ 16.1 (isomer **A**), 22.9 (isomer **B**). Anal. Found for $C_{24}H_{24}PI$: C, 60.89; H, 5.03. Calcd: C, 61.29; H, 5.14. NMR analysis may be found in **3.1.4**.

2.3.4 Synthesis of PHINs 1-$C_9H_6PMePh_2$ (I) and 4,7-dimethyl-1-$C_9H_4PMePh_2$ (II)

1-$C_9H_6PMePh_2$ **(I)** was prepared as described by a published method.[55] A solution of indene was treated with *n*-BuLi in diethyl ether at −78 °C and the solution was stirred for 24 h at room temperature. PPh_2Cl was added to the solution at −78 °C, and the solution was stirred for 24 h at room temperature to give a yellow slurry. The resulting mixture was filtered through Celite to obtain a yellow solution of 1-$C_9H_5PPh_2$ as a mixture of two regioisomers. A white, air-sensitive precipitate of (methyl diphenylphosphonium)-1-indene iodide was prepared by stirring a solution of 1-$C_9H_5PPh_2$ and MeI in THF at room temperature for 48 h, and was collected by filtration, washed with THF and dried under reduced pressure. A mixture of the iodide and NaH in THF was then stirred at room temperature for 48 h, and the resulting green solution was filtered through Celite. The solvent was removed under reduced pressure to give green, air-sensitive **I** (85% yield). ^{1}H NMR (CD_2Cl_2): δ 2.48 (d, 3 H, $^{2}J_{H\text{-}P}$ = 13.0 Hz, P*CH*$_3$), 6.50 (t, 1 H, $^{3}J_{H\text{-}H} = J_{H\text{-}P}$ = 4.4 Hz, H(3)), 6.71 (m, 2 H, H(2) and H(5)), 6.84 (t, 1 H, $^{3}J_{H\text{-}H}$

= 7.2 Hz, H(6)), 6.97 (d, 1 H, $^{3}J_{H-H}$ = 7.8 Hz, H(7)), 7.40-7.80 (m, 11 H, (H(4), and Ph). ^{31}P NMR (CD_2Cl_2): δ 5.88. NMR data may be found in **3.1.1**.

To synthesize 4,7-dimethyl-1-$C_9H_4PMePh_2$ **(II)**, a mixture of (4,7-dimethyl-1-$C_9H_5PMePh_2$)I (8.00 g, 17.0 mmol) and NaH (0.73 g, 30.4 mmol) in 100 mL of THF was stirred at room temperature for 48 h. The green solution was then filtered through Celite, and the solvent was removed under reduced pressure to give the green, and air-sensitive of **II**. Yield 4.95 g (85.0%). X-ray quality crystals and analytically pure material were obtained by slow evaporation of a concentrated CH_2Cl_2 solution. ^{1}H NMR (CD_2Cl_2): δ 1.99 (s, 3 H, H(11)), 2.48 (s, 3 H, H(10)), 2.52 (d, 3 H, $^{2}J_{H-P}$ = 12.8 Hz, P*CH*$_3$), 6.46 (t, 1 H, $^{3}J_{H-H}$ = J_{H-P} = 4.5 Hz, (H(3)), 6.51 (d, 1 H, $^{3}J_{H-H}$ = 6.9 Hz, H(6)), 6.55 (t, 1 H, $^{3}J_{H-H}$ = J_{H-P} = 5.4 Hz, (H2)), 6.60 (d, 1 H, $^{3}J_{H-H}$ = 6.9 Hz, H(5)), 7.50-7.56 (m, 4 H, Ph), 7.60-7.70 (m, 6 H, Ph). ^{13}C NMR (CD_2Cl_2): δ 17.11 (d, $^{1}J_{P-C}$ = 63.4 Hz, P*CH*$_3$), 19.50 (s, C(10)), 23.70 (s, C(11)), 67.46 (d, $^{1}J_{P-C}$ = 116.3 Hz, C(1)), 104.53 (d, $^{3}J_{P-C}$ = 15.8 Hz, C(3)), 118.47 (s, C(5)), 120.36 (s, C(6)), 124.23 (s, C(7)), 126.95 (d, $^{3}J_{P-C}$ = 2.2 Hz, C(4)), 128.51 (d, $^{2}J_{P-C}$ = 16.9 Hz, C(2)), 129.64 (d, $^{3}J_{P-C}$ = 12.1 Hz, Ph), 130.06 (d, $^{1}J_{P-C}$ = 87.7 Hz, Ph), 133.01 (d, $^{2}J_{P-C}$ = 9.9 Hz, Ph), 133.06 (d, $^{4}J_{P-C}$ = 3.3 Hz, Ph), 134.18 (d, $^{3}J_{P-C}$ = 13.5 Hz, C(8)), 139.06 (d, $^{3}J_{P-C}$ = 15.4 Hz, C(9)). ^{31}P NMR (CD_2Cl_2): δ 6.64. Anal. Found for $C_{24}H_{23}P$: C, 84.49; H, 6.94. Calcd: C, 84.18; H, 6.77. X-ray quality crystals were obtained by the slow evaporation of CH_2Cl_2. NMR analysis may be found in **3.1.5**.

2.4 Synthesis of Group IX Precursors

2.4.1 Synthesis of $[Ir(COD)Cl]_2$[94]

1,5-Cyclooctadiene (12.0 mL, 0.10 mol), 95% ethanol (68.0 mL), water (34.0 mL), and iridium(III)chloride (4.00 g, 0.01 mmol) were added into a 250 mL Schlenk flask and refluxed for 24 h as the orange solid product precipitated. The mixture was cooled to the room temperature and di-μ-chloro-bis(1,5-cyclooctadiene)diiridium(I) was collected by filtration, washed with ice-cold methanol to remove the residual unreacted 1,5-cyclooctadiene, and then dried under reduced pressure at 70 °C for 24 h under reduced pressure. Yield 3.00 g (72%). ^{1}H NMR (CD_2Cl_2): δ 1.54 (m, 8 H, -CH*H*), 2.24 (m, 8 H, -C*H*H), 4.23 (br s, 8 H, =*CH*). This synthesis was also repeated in isopropanol instead of methanol, and produced the same result.[95] The literature values of di-μ-chloro-bis(1,5-cyclooctadiene)diiridium(I) were reported by Crabtree *et al.*[96] as ^{1}H NMR ($CDCl_3$): δ 4.3 (C*H*=C*H*) and by Choudhury *et al.*[97] as ^{1}H NMR (DMSO-d_6): δ 1.65-1.77 (m, 8 H, CH_2), 2.18-2.33 (m, 8 H, -CH_2), 3.97 (br, s, 4 H, =C*H*), 4.11 (br, s, 4 H, =C*H*). The literature values of di-μ-bromido-bis(1,5-cyclooctadiene)diiridium(I) were reported by Nagata *et al.*[98] as ^{1}H NMR ($CDCl_3$): δ 1.40-1.50 (m, 8 H, CH*H*), 2.20-2.24 (m, 8 H, -C*H*H), 4.35 (m, 8 H, =C*H*).

2.4.2 Synthesis of $[(PPh_3)_2Rh(\mu\text{-}Cl)]_2$[99]

A solution containing $RhCl(PPh_3)_3$ (5.40 g, 5.84 mmol) in 150 mL toluene was refluxed for 2.5 h after which the solution was cooled and salmon-pink crystals of $[(PPh_3)_2Rh(\mu\text{-}Cl)]_2$ precipitated. The collected crystals were washed with 60.0 mL of

toluene and then dried under reduced pressure at 70 °C for 24 h to yield [$(PPh_3)_2Rh(\mu\text{-}Cl)]_2$. Yield 4.90 g (62%). ^{31}P NMR (CD_2Cl_2): δ 52.6 (d, $J_{Rh\text{-}P}$ = 196.0 Hz).

2.5 Synthesis of Group IV Precursors

2.5.1 Synthesis of $TiCl_4(THF)_2$[100]

$TiCl_4$ (3.00 mL, 0.03 mol) was dissolved in CH_2Cl_2 (50.0 mL) and THF (13.0 mL, 0.16 mol) was added drop-wise to give a yellow slurry. Bright yellow crystals were obtained by the addition of 50 mL of hexanes, and the solution was filtered to obtain yellow crystals. The yellow crystals were washed with 20 mL hexanes to afford $TiCl_4(THF)_2$. Yield 9.40 g (93.8%).

2.5.2 Synthesis of (pentamethylcyclopentadienyl)zirconium trimethyl, Cp*$ZrMe_3$[101]

A Schlenk flask was charged with Cp*$ZrCl_3$ (2.00 g, 6.00 mmol) and 65.0 mL diethyl ether. To this was added drop-wise portion of CH_3MgBr (3.00 M) (6.90 mL, 20.7 mmol) in diethyl ether at −78 °C. After stirring for 4 h at −78 °C and 2 h at room temperature, a brown slurry was obtained which filtered to give a dark brown solid. The dark brown solid was washed with 60 mL hexanes and then dried under reduced pressure. Yield 1.40 g (85.0%). ^1H NMR (C_6D_6): δ 0.27 (s, 9 H, $Zr(CH_3)_3$), 1.78 (s, 15 H, $C_5(CH_3)_5$).

2.6 Coordination of PHINs to Iridium and Rhodium Using $[Ir(COD)Cl]_2$ and $[Rh(COD)Cl]_2$

2.6.1 Reaction of $C_9H_6PMePh_2$ (I) and $[Ir(COD)Cl]_2$

A solution containing of $[IrCl(C_8H_{12})]_2$ (0.08 g, 0.12 mmol) and **I** (0.04 g, 0.12 mmol) in 0.60 mL CH_2Cl_2 was stirred for 1 min in a vial to give a deep dark red solution. The solvent was then removed under reduced pressure to give a dark red oily mixture and NMR spectra were obtained. ^{1}H NMR (CD_2Cl_2): δ 0.70-2.30 (m, COD *CH*$_2$), 3.01 (d, 3 H, $^2J_{H-P}$ = 13.2 Hz, P*CH*$_3$), 3.39 and 3.87 (m, COD =*CH*), 5.70 (br t, 1 H, H(2)), 6.12 (br t, 1 H, H(3)), 6.74 (d, 1 H, $^3J_{H-H}$ = 8.6 Hz, H(7)), 7.07 (t, 1 H, $^3J_{H-H}$ = 7.9 Hz, H(6)), 7.21 (t, 1 H, $^3J_{H-H}$ = 7.2 Hz, H(5)), 7.51 (d, 1 H, $^3J_{H-H}$ = 8.4 Hz, H(4)), 7.60-7.90 (m, 10 H, Ph). ^{13}C NMR (CD_2Cl_2): δ 13.0 (d, $^1J_{P-C}$ = 61.3 Hz, P*CH*$_3$), 32.43, 32.87 and 33.61 (3s, COD *CH*$_2$), 55.30 and 58.51 (2s, COD =*CH*), 60.92 (d, $^1J_{P-C}$ = 101.8 Hz, C(1)), 80.98 (d, $^3J_{P-C}$ = 9.6 Hz, C(3)), 89.52 (d, $^2J_{P-C}$ = 13.8 Hz, C(2)), 107.51 (d, $^2J_{P-C}$ = 11.0 Hz, C(8) or C(9)), 113.42 (d, $^3J_{P-C}$ = 9.3 Hz, C(8) or C(9)), 119.90 (s, C(7)), 120.58 (d, $^1J_{P-C}$ = 90.2 Hz, *ipso*-C), 120.74 (d, $^1J_{P-C}$ = 88.3_Hz, *ipso*-C), 123.69 (s, C(4)), 126.28 (s, C(5)), 128.05 (s, C(6)), 130.7 (d, $^3J_{P-C} \approx$ 13.5 Hz, *o*-Ph, or *m*-Ph), 130.8 (d, $^3J_{P-C} \approx$ 13.5 Hz, *o*-Ph, or *m*-Ph), 133.26 (d, $^2J_{P-C}$ = 10.9 Hz, *o*-Ph, or *m*-Ph), 133.51 (d, $^2J_{P-C}$ = 11.0 Hz, *o*-Ph, or *m*-Ph), 135.43 (d, $^4J_{P-C} \approx$ 2.5 Hz, *p*-Ph), 135.55 (d, $^4J_{P-C} \approx$ 2.5 Hz, *p*-Ph). ^{31}P NMR (CD_2Cl_2): δ 18.2. HR-EMS: observed: 615.17870 $[M]^+$, calculated: 615.17871. NMR analysis may be found in **3.2.1**.

2.6.2 Synthesis of [Ir(COD)(η^5-I)]BF_4 (III)

A mixture of $[Ir(COD)Cl]_2$ (0.16 g, 0.23 mmol) and $AgBF_4$ (0.09 g, 0.47 mmol) in 15 mL THF was stirred for 45 min. The resulting dark brown solution was then filtered through Celite and a solution of 0.15 g (0.47 mmol) **I** in 10 mL of THF was added. The resulting solution was stirred for 4 h, and the deep dark brown slurry was filtered to obtain a dark brown solution. The solvent was removed under reduced pressure to give [Ir(COD)(η^5-**I**)]BF_4 as a dark brown solid. Yield 0.19 g (58%). ^{1}H NMR (CD_2Cl_2): δ 1.58-2.0 (m, COD *CH*$_2$), 2.85 (d, 3 H, $^2J_{H-P}$ = 13.3 Hz, P*CH*$_3$), 3.39 and 3.89 (m, COD =*CH*), 5.54 (t, 1 H, $^3J_{H-H}$ = $^3J_{H-P}$ = 2.8 Hz, H(2)), 6.08 (br t, 1 H, $^3J_{H-H}$ = $^4J_{H-P}$ = 4.8 Hz, H(3)), 6.75 (d, 1 H, $^3J_{H-H}$ = 8.7 Hz, H(7)), 7.11 (t, 1 H, $^3J_{H-H}$ = 8.3 Hz, H(6)), 7.24 (t, 1 H, $^3J_{H-H}$ = 7.4 Hz, H(5)), 7.53 (d, 1 H, $^3J_{H-H}$ = 8.5 Hz, H(4)), 7.68-7.73 (m, 8 H, *o,m*-Ph), 7.82-7.85 (m, 2 H, *p*-Ph). ^{13}C NMR (CD_2Cl_2): δ 11.97 (d, $^1J_{P-C}$ = 62.5 Hz, P*CH*$_3$), 32.92 and 33.56 (2s, COD *CH*$_2$), 55.43 and 58.59 (2s, COD =*CH*), 60.76 (d, $^1J_{P-C}$ = 102.1 Hz, C(1)), 80.94 (d, $^3J_{P-C}$ = 9.6 Hz, C(3)), 89.30 (d, $^2J_{P-C}$ = 14.0 Hz, C(2)), 107.65 (d, $^2J_{P-C}$ = 11.3 Hz, C(8) or C(9)), 113.42 (d, $^3J_{P-C}$ = 9.4 Hz, C(8) or C(9)), 119.76 (s, C(7)), 120.47 (d, $^1J_{P-C}$ = 90.6 Hz, *ipso*-C), 120.55 (d, $^1J_{P-C}$ = 88.8 Hz, *ipso*-C), 123.74 (s, C(4)), 126.44 (s, C(5)), 128.24 (s, C(6)), 130.7 (d, $^3J_{P-C} \approx 12.9$ Hz, *o*-Ph or *m*-Ph), 130.8 (d, $^3J_{P-C} \approx 13.4$ Hz, *o*-Ph or *m*-Ph), 133.15 (d, $^2J_{P-C}$ = 11.1 Hz, *o*-Ph or *m*-Ph), 133.31 (d, $^2J_{P-C}$ = 11.2 Hz, *o*-Ph or *m*-Ph), 135.78 (d, $^4J_{P-C}$ = 3.0 Hz, *p*-Ph), 135.83 (d, $^4J_{P-C}$ = 2.8 Hz, *p*-Ph). ^{31}P NMR (CD_2Cl_2): δ 16.98. Anal. Found for $IrC_{30}H_{31}PBF_4$: C, 51.68; H, 4.70. Calcd: C, 51.36; H, 4.45. HR-EMS: observed: 615.18164 $[M]^+$, calculated: 615.17871. NMR analysis may be found in **3.2.3**.

2.6.3 Synthesis of [Ir(COD)(η^5-II)]BF_4 (IV)

A mixture of $[Ir(COD)Cl]_2$ (0.16 g, 0.23 mmol) and $AgBF_4$ (0.09 g, 0.47 mmol) in 15 mL THF was stirred for 45 min. The resulting orange solution was then filtered through Celite, and a solution of **II** (0.16 g, 0.47 mmol) in 10 mL THF was added. The resulting solution was stirred for 4 h, and the deep dark orange slurry was filtered to obtain a dark orange solution. The solvent was removed under reduced pressure to give [Ir(COD)(η^5-**II**)]BF_4 as a dark orange solid. Yield 0.19 g (59%). ^{1}H NMR (CD_2Cl_2): δ 1.54-2.1 (m, COD *CH*$_2$), 1.97 (s, 3 H, H(11)), 2.49 (s, 3 H, H(10)), 3.07 (d, 3 H, $^2J_{H-P}$ = 13.1 Hz, P*CH*$_3$), 3.39 and 3.81 (m, COD =*CH*), 4.77 (t, 1 H, $^3J_{H-H}$ = $^3J_{H-P}$ = 3.5 Hz, H(2)), 6.08 (t, 1 H, $^3J_{H-H}$ = $^4J_{H-P}$ = 2.3 Hz, H(3)), 6.82 (d, 1 H, $^3J_{H-H}$ = 6.9 Hz, H(6)), 6.92 (t, 1 H, $^3J_{H-H}$ = 7.0 Hz, H(5)), 7.64-7.76 (m, 8 H, *o*,*m*-Ph), 7.76-7.89 (m, 2 H, *p*-Ph). ^{13}C NMR (CD_2Cl_2): δ 16.9 (d, $^1J_{P-C}$ = 63.8 Hz, P*CH*$_3$), 18.84 (s, C(10)), 23.21 (s, C(11)), 33.27 and 33.99 (2s, COD *CH*$_2$), 54.00 and 59.29 (2s, COD =*CH*), 61.34 (d, $^1J_{P-C}$ = 100.1 Hz, C(1)), 81.27 (d, $^3J_{P-C}$ = 10.5 Hz, C(3)), 91.36 (d, $^2J_{P-C}$ = 15.6 Hz, C(2)), 104.37 (d, $^2J_{P-C}$ = 10.1 Hz, C(8) or C(9)), 114.5 (d, $^3J_{P-C}$ = 9.3 Hz, C(8) or C(9)), 122.00 (d, $^1J_{P-C}$ = 91.6 Hz, *ipso*-C), 122.21 (d, $^1J_{P-C}$ = 87.9 Hz, *ipso*-C), 125.64 (s, C(5)), 127.65 (s, C(7)), 129.2 (s, C(6)), 130.90 (s, C(4)), 130.74 (d, $^3J_{P-C}$ = 12.6 Hz, *o*-Ph or *m*-Ph), 131.08 (d, $^3J_{P-C}$ = 12.9 Hz, *o*-Ph, or *m*-Ph), 133.0 (d, $^3J_{P-C}$ = 10.7 Hz, *o*-Ph or *m*-Ph), 133.2 (d, $^2J_{P-C}$ = 10.1 Hz, *o*-Ph or *m*-Ph), 135.61 (d, $^4J_{P-C}$ = 2.9 Hz, *p*-Ph), 135.74 (d, $^4J_{P-C}$ = 3.1 Hz, *p*-Ph). ^{31}P NMR (CD_2Cl_2): δ 17.59. Anal. Found for $IrC_{32}H_{35}PBF_4$: C, 53.64; H, 5.63. Calcd: C, 52.67; H, 4.84. HR-EMS: observed: 643.20770 $[M]^+$, calculated: 643.21001. NMR analysis may be found in **3.2.5**.

2.6.4 Synthesis of [Rh(COD)(η^5-I)]BF_4 (V)

A mixture of $[Rh(COD)Cl]_2$ (0.12 g, 0.23 mmol) and $AgBF_4$ (0.09 g, 0.47 mmol) in 15 mL THF was stirred for 45 min. The resulting yellow solution was then filtered, a solution of **I** (0.15 g, 0.47 mmol) in 20 mL THF was added and the resulting solution was stirred for 4 h. The resulting dark green slurry was filtered to obtain a dark green solution, and the solvent was removed under reduced pressure to give [Rh(COD)(η^5-**I**)]BF_4 as a dark green solid. Yield 0.15 g (51%). ^{1}H NMR (CD_2Cl_2): δ 1.70-2.05 (m, COD *CH_2*), 2.80 (d, 3 H, $^2J_{H-P}$ = 13.5 Hz, P*CH_3*), 3.70 and 4.19 (m, COD =*CH*), 5.67 (t, $^3J_{H-H}$ = $^4J_{H-P}$ = 2.5 Hz, H(3)), 5.94 (t, 1 H, $^3J_{H-H}$ = $^3J_{H-P}$ = 2.5 Hz, H(2)), 6.84 (d, 1 H, $^3J_{H-H}$ = 8.5 Hz, H(7)), 7.17 (t, 1 H, $^3J_{H-H}$ = 7.5 Hz, H(6)), 7.27 (t, 1 H, $^3J_{H-H}$ = 7.3 Hz, H(5)), 7.64 (d, 1 H, $^3J_{H-H}$ = 7.1 Hz, H(4)), 7.65-7.86 (m, 8 H, *o,m,p*-Ph). ^{13}C NMR (CD_2Cl_2): δ 11.47 (d, $^1J_{P-C}$ = 61.3 Hz, P*CH_3*), 30.85 and 32.38 (2s, COD *CH_2*), 65.94 (dd, $^1J_{P-C}$ = 100.0 Hz, J_{Rh-C} = 5.1 Hz C(1)), 71.96 (d, J_{Rh-C} = 13.7 Hz, COD =*CH*) and 74.58 (d, J_{Rh-C} = 13.5 Hz, COD =*CH*), 83.28 (dd, $^3J_{P-C}$ = 10.7 Hz, J_{Rh-C} = 4.1 Hz, C(3)), 100.39 (dd, $^2J_{P-C}$ = 14.1 Hz, J_{Rh-C} = 4.6 Hz, C(2)), 113.94 (br d, $^2J_{P-C}$ = 11.5 Hz, J_{Rh-C} < 1 Hz, C(8) or C(9)), 117.85 (br d, $^3J_{P-C}$ = 9.4 Hz, J_{Rh-C} < 1 Hz, C(8) or C(9)), 118.20 (s, C(7)), 121.00 (d, $^1J_{P-C}$ = 88.7 Hz, *ipso*-C), 121.21 (d, $^1J_{P-C}$ = 91.0 Hz, *ipso*-C), 122.92 (s, C(4)), 124.99 (s, C(5)), 127.07 (s, C(6)), 130.75 (d, $^3J_{P-C}$ = 12.8 Hz, *o*-Ph or *m*-Ph), 130.88 (d, $^3J_{P-C}$ = 12.8 Hz, *o*-Ph or *m*-Ph), 133.09 (d, $^2J_{P-C}$ = 5.2 Hz, *o*-Ph or *m*-Ph), 130.00 (d, $^2J_{P-C}$ = 4.8 Hz, *o*-Ph or *m*-Ph), 135.6 (m, $^4J_{P-C}$ < 1.0 Hz, *p*-Ph). ^{31}P NMR (CD_2Cl_2): δ 17.15. Anal. Found for $RhC_{30}H_{31}PBF_4$: C, 58.66; H, 5.25. Calcd: C, 58.85; H, 5.10. HR-EMS: observed: 525.1233 $[M]^+$, calculated: 525.1213. NMR analysis may be found in **3.2.4**.

2.6.5 Synthesis of [Rh(COD)(η^5-II)]BF_4 (VI)

A mixture of $[Rh(COD)Cl]_2$ (0.23 g, 0.47 mmol) and $AgBF_4$ (0.18 g, 0.94 mmol) in 15 mL THF was stirred for 45 min. The resulting yellow solution was then filtered, a solution of **II** (0.15 g, 0.94 mmol) in 25 mL THF was added and the resulting solution was stirred for 4 h. The resulting dark red solution was filtered to obtain a deep dark red solution, and the solvent was removed under reduced pressure to give [Rh(COD)(η^5-**I**)]BF_4 as a red solid. Yield 0.33 g (55%). ^{1}H NMR (CD_2Cl_2): δ 1.53-1.87 (m, COD *CH*$_2$), 1.99 (s, 3 H), 2.52 (s, 3 H), 3.02 (d, 3 H, $^2J_{H-P}$ = 13.0 Hz, P*CH*$_3$), 3.39 and 4.18 (m, COD =*CH*), 5.09 (t, 1 H, $^3J_{H-H}$ = $^3J_{H-P}$ = 4.5 Hz, H(2)), 5.74 (t, $^3J_{H-H}$ = $^4J_{H-P}$ = 2.7 Hz, H(3)), 6.87 (d, 1 H, $^3J_{H-H}$ = 7.1 Hz, H(6)), 6.93 (d, 1 H, $^3J_{H-H}$ = 7.0 Hz, H(5)), 7.56-7.68 (m, 8 H, *o*,*m*-Ph), 7.79-7.87 (m, 2 H, *p*-Ph). ^{13}C NMR (CD_2Cl_2): δ 16.2 (d, $^1J_{P-C}$ = 63.1 Hz, P*CH*$_3$), 19.11 (s, C(10)), 23.17 (s, C(11)), 31.04 and 33.00 (2s, COD *CH*$_2$), 66.91 (dd, $^1J_{P-C}$ = 99.3 Hz, J_{Rh-C} = 4.9 Hz C(1)), 70.17 (d, J_{Rh-C} = 14.1 Hz, COD =*CH*) and 75.68 (d, J_{Rh-C} = 13.8 Hz, COD =*CH*), 83.51 (dd, $^3J_{P-C}$ = 11.5 Hz, J_{Rh-C} = 3.7 Hz, C(3)), 101.80 (dd, $^2J_{P-C}$ = 15.6 Hz, J_{Rh-C} = 4.0 Hz, C(2)), 110.43 (br dd, C(8) or C(9)), 118.12 (dd, $^4J_{P-C}$ = 9.6 Hz, J_{Rh-C} = 1.5 Hz, C(8) or C(9)), 122.80 (d, $^1J_{P-C}$ = 92.2 Hz, *ipso*-C), 122.90 (d, $^1J_{P-C}$ = 88.1 Hz, *ipso*-C), 124.5 (s, C(5)), 126.08 (s, C(7)), 128.7 (s, C(6)), 130.78 (s, C(4)), 130.64 (d, $^3J_{P-C}$ = 12.9 Hz, *o*-Ph or *m*-Ph), 131.02 (d, $^3J_{P-C}$ = 12.8 Hz, *o*-Ph or *m*-Ph), 132.8 (d, $^2J_{P-C}$ = 10.6 Hz, *o*-Ph or *m*-Ph), 133.1 (d, $^2J_{P-C}$ = 10.3 Hz, *o*-Ph or *m*-Ph), 135.42 (d, $^4J_{P-C}$ = 2.8 Hz, *p*-Ph), 135.56 (d, $^4J_{P-C}$ = 2.8 Hz, *p*-Ph). ^{31}P NMR (CD_2Cl_2): δ 17.68. Anal. Found for $RhC_{32}H_{35}PBF_4$: C, 60.40; H, 5.72. Calcd: C, 60.02; H, 5.51. HR-EMS: observed: 553.1547 $[M]^+$, calculated: 553.1526. NMR analysis may be found in **3.2.6**.

2.7 Attempted Oxidative Addition to [M(η^4-C_8H_{12})(η^5-PHIN)]BF_4 (M = Ir, Rh)

2.7.1 Attempted Oxidative Addition of MeI to III on an NMR Scale

Compound **III**, MeI and 0.5 mL CD_2Cl_2 were added to a NMR tube, shaken for 5 min and ^1H and ^{31}P NMR spectra were taken. No changes were observed. ^1H NMR (CD_2Cl_2): δ 1.58-2.0 (m, COD *CH_2*), 2.0 (s, unknown), 2.16 (s, *CH_3*I), 2.3 (s, unknown), 2.86 (d, $^2J_{P\text{-}H}$ = 13.3 Hz, P*CH_3*), 3.39 and 3.88 (m, COD =*CH*), 5.57 (t, $^3J_{H\text{-}H} = J_{H\text{-}P}$ = 2.8 Hz, H(2)), 6.08 (br t, H(3)), 6.75 (d, $^3J_{H\text{-}H}$ = 8.7 Hz, H(7)), 7.10 (t, $^3J_{H\text{-}H}$ = 7.95 Hz, H(6)), 7.24 (t, $^3J_{H\text{-}H}$ = 7.1 Hz, H(5)), 7.52 (d, $^3J_{H\text{-}H}$ = 8.40 Hz, H(4)), 7.60-7.75 (m, *o*-Ph and *m*-Ph), 7.78-7.88 (m, *p*-Ph). ^{31}P NMR (CD_2Cl_2): δ 17.05. This sample gave X-ray quality crystals after 8 d in the NMR tube; see Section **3.3** for details. NMR analysis may be found in **3.3**.

2.7.2 Attempted Oxidative Addition of MeI to V on an NMR Scale

Compound **V**, MeI and 0.5 mL CD_2Cl_2 were added to a NMR tube, shaken for 5 min and ^1H and ^{31}P NMR spectra were taken. Little change in the ^1H and ^{31}P NMR spectra were observed. ^1H NMR (CD_2Cl_2): δ 1.53-2.05 (m, COD *CH_2*), 2.0 (s, unknown), 2.16 (s, *CH_3*I), 2.3 (s, unknown), 2.81 (d, $^2J_{P\text{-}H}$ = 13.2 Hz, P*CH_3*), 3.39 (d, $^2J_{P\text{-}H}$ = 5.6 Hz, unknown), 3.69 and 4.18 (m, COD =*CH*), 5.64 (t, $^3J_{H\text{-}H} = J_{H\text{-}P}$ = 2.6 Hz, (H3)), 5.95 (t, $^3J_{H\text{-}H} = J_{H\text{-}P}$ = 3.15 Hz, H(2)), 6.82 (d, $^3J_{H\text{-}H}$ = 8.5 Hz, H(7)), 7.16 (t, $^3J_{H\text{-}H}$ = 7.4 Hz, H(6)), 7.26 (t, $^3J_{H\text{-}H}$ = 7.3 Hz, H(5)), 7.62 (br d, H(4)), 7.64-7.86 (m, Ph). ^{31}P NMR (CD_2Cl_2): δ 17.22. NMR analysis may be found in **3.3**.

2.7.3 Attempted Oxidative Addition of MeI to VI on an NMR Scale

Compound **VI**, MeI and 0.5 mL CD_2Cl_2 were added to a NMR tube, shaken for 5 min and ^1H and ^{31}P NMR spectra were taken. Little change in the ^1H and ^{31}P NMR were observed. ^1H NMR (CD_2Cl_2): δ 1.53-1.87 and 2.06 - 2.17 (m, COD *CH₂*), 1.99 (s, H(11)), 2.0 (s, unknown), 2.16 (s, *CH₃*I), 2.3 (s, unknown), 2.52 (s, H(10)), 3.02 (d, $^2J_{H-P}$ = 13.0 Hz, P*CH₃*), 3.38 and 4.18 (m, COD =*CH*), 5.09 (t, $^3J_{H-H} = J_{H-P}$ = 4.25 Hz, H(2)), 5.73 (t, $^3J_{H-H} = J_{H-P}$ = 2.9 Hz, H(3)), 6.87 (d, $^3J_{H-H}$ = 7.1 Hz, H(6)), 6.93 (d, $^3J_{H-H}$ = 7.1 Hz, H(5)), 7.55-7.62 (2 br d, *o*-Ph), 7.62-7.77 (2 br t, *m*-Ph), 7.77-7.88 (2 br t, *p*-Ph). ^{31}P NMR (CD_2Cl_2): δ 17.68. NMR analysis may be found in **3.3**.

2.7.4 Attempted Oxidative Addition of $PhCH_2Cl$ to III on an NMR Scale

Compound **III**, $PhCH_2Cl$ and 0.5 mL CD_2Cl_2 were added to a NMR tube, shaken for 5 min and ^1H and ^{31}P NMR spectra were taken. Little change in the ^1H and ^{31}P NMR were observed. ^1H NMR (CD_2Cl_2): δ 1.51-2.11 (m, COD *CH₂*), 2.85 (d, $^2J_{H-P}$ = 13.3 Hz, P*CH₃*), 3.42 and 3.91 (m, COD =*CH*), 4.47 (s, unknown), 4.62 (s, Ph*CH₂*Cl), 4.78 (s, unknown), 5.54 (t, $J_{H-H} = J_{H-P}$ = 2.9 Hz, H(2), 6.08 (br t, H(3)), 6.76 (d, $^3J_{H-H}$ = 8.7 Hz, H(7)), 7.12 (t, $^3J_{H-H}$ = 7.7 Hz, H(6)), 7.27 (t, $^3J_{H-H}$ = 6.85 Hz, H(5)), 7.30-7.47 (m, *Ph*CH_2Cl), 7.50-7.60 (2 br d, H(4)), 7.66-7.76 (m, *o*-Ph and *m*-Ph of Ph_2MeP), 7.80-7.90 (m, *p*-Ph of Ph_2MeP). ^{31}P NMR (CD_2Cl_2): δ 16.99. NMR analysis may be found in **3.3**.

2.7.5 Attempted Oxidative Addition of $PhCH_2Cl$ to VI in NMR Scale

Compound **VI**, $PhCH_2Cl$ and 0.5 mL CD_2Cl_2 were added to a NMR tube, shaken for 5 min and ^1H and ^{31}P NMR spectra were taken. Little change in the ^1H and ^{31}P NMR

were observed. ^{1}H NMR (CD_2Cl_2): δ 0.70-1.96 and 2.06-2.20 (m, COD *CH_2*), 2.00 (s, H(11)), 2.54 (s, H(10)), 3.02 (d, $^{2}J_{H-P}$ = 13.0 Hz, P*CH_3*), 3.41 and 4.19 (m, COD =*CH*), 4.47 (s, unknown), 4.62 (s, Ph*CH_2*Cl), 4.77 (s, unknown), 5.10 (t, $^{3}J_{H-H} = J_{H-P}$ = 4.15 Hz, H(2)), 5.74 (t, $^{3}J_{H-H} = J_{H-P}$ = 2.9 Hz, H(3)), 6.89 (d, $^{3}J_{H-H}$ = 7.1 Hz, H(6)), 6.95 (d, $^{3}J_{H-H}$ = 7.1 Hz, H(5)), 7.29-7.47 (m, *Ph*CH_2Cl), 7.52-7.88 (m, -PMe*Ph_2*). ^{31}P NMR (CD_2Cl_2): δ 17.69. NMR analysis may be found in **3.3**.

2.7.6 Attempted Oxidative Addition of $PhCH_2Cl$ to V in Benzene

A Schlenk flask was charged with **V** (0.04 g, 0.06 mmol), a 5 fold excess of $PhCH_2Cl$ (0.04 mL, 0.30 mmol), and 10 mL benzene. The mixture was refluxed for 2 h, the volatiles were pumped off under reduced pressure, and an oily green mixture was obtained. ^{1}H NMR (CD_2Cl_2): δ 1.60-2.10 (m, COD C*H_2*), 2.76 (d, $^{2}J_{H-P}$ = 13.2 Hz, P*CH_3*), 3.70 and 4.19 (m, COD =C*H*), 4.61 (s, Ph*CH_2*Cl), 5.65 (br t, H(3)), 5.92 (br t, H(2)), 6.82 (d, $^{3}J_{H-H}$ = 8.22 Hz, H(7)), 7.17 (t, $^{3}J_{H-H}$ = 7.8 Hz, H(6)), 7.27 (t, $^{3}J_{H-H}$ = 7.6 Hz, H(5)), 7.60 (br d, H(4)), 7.63-7.90 (m, Ph). ^{31}P NMR (CD_2Cl_2): δ 17.13. NMR analysis may be found in **3.3**.

2.8 Attempted Reaction of H_2 and III or V

2.8.1 Attempted Reaction of H_2 and V at 1 bar Pressure

Compound **V** was dissolved in CH_2Cl_2 and H_2 gas was bubbled through the solution for 24 h at room temperature; no color change was observed. The solvent was pumped off to give a green solid. ^{1}H NMR (CD_2Cl_2): δ 1.70-2.07 (m, COD *CH_2*), 2.79 (d, $^{2}J_{H-P}$ = 13.25 Hz, P*CH_3*), 3.70 and 4.19 (m, COD =*CH*), 5.66 (br t, H(3)), 5.93 (br t,

H(2)), 6.82 (d, $^{3}J_{H\text{-}H}$ = 8.4 Hz, H(7)), 7.17 (t, $^{3}J_{H\text{-}H}$ = 7.9 Hz, H(6)), 7.27 (t, $^{3}J_{H\text{-}H}$ = 7.4 Hz, H(5)), 7.61 (br d, H(4)), 7.63-7.90 (m, Ph). ^{31}P NMR (CD_2Cl_2): δ 17.13. Discussion may be found in **3.4**.

2.8.2 Attempted Reaction of H_2 and V at 10 bar Pressure

Compound **V** was dissolved in EtOH, and the solution was placed in a 30 mL Parr reactor which was flushed with H_2 and then maintained at 10 bar H_2 for 24 h at room temperature. The solvent was then pumped off to give a dark brown solid. A ^{1}H NMR spectrum exhibited broad peaks at δ 0.86 (br peak), 1.26 (br peak), 2.33 (br peak), 2.80 (br d), 3.65 (br peak), 3.88 (br peak), 5.31 (br peak), 6.48 (br peak), 6.96 (br peak), 7.25 (br peak), 7.43 (br peak), 7.72 (br peak), but the ^{31}P NMR spectrum showed two singlet peaks at δ 13.08 and 25.74. This reaction was repeated with the reaction time reduced to 5 h 30 min; the ^{1}H NMR spectrum again showed broad peaks at δ 1.19 (br peak), 1.26 (br peak), 2.43 (br d), 3.67 (br peak), 4.94 (br t), 6.79 (br d), 7.13 (br t), 7.21 (br d), 7.31 (br t), 7.49-7.83 (m), but the ^{31}P NMR spectrum showed a singlet peak at δ 25.62. This reaction was also repeated with the reaction time of 1 h, and produced the same ^{1}H and ^{31}P NMR spectra as the reaction with 5 h 30 min. This reaction was repeated in MeCN over 1 d, but the result was unsatisfactory. Discussion may be found in **3.4**.

2.8.3 Attempted Reaction of H_2 and III at 10 bar Pressure

Compound **III** was dissolved in EtOH, and the solution was placed in a 30 mL Parr reactor which was flushed with H_2 and then maintained at 10 bar H_2 for 24 h at room temperature. The solvent was pumped off to give a dark brown solid, and ^{1}H and ^{31}P

NMR spectra were run. The former exhibited the same broad peaks as above, while the ^{31}P NMR spectrum showed a singlet peak at δ 25.63. Discussion may be found in **3.4**.

2.9 Attempted Coordination of PHIN to $[RhCl(PPh_3)_2]_2$

2.9.1 Attempted Synthesis of $[(\eta^6\text{-toluene})Rh(PPh_3)_2][NO_3]$

A mixture of $[(PPh_3)_2Rh(\mu\text{-}Cl)]_2$ (0.16 g, 0.12 mmol), $AgNO_3$ (0.04 g, 0.23 mmol) and toluene (7.13 mL, 67.3 mmol) in CH_2Cl_2 (40 mL) were added to a Schlenk flask and stirred for 24 h. A slurry brown solution was obtained which was filtered to give a brown solution, and the volatiles were removed under reduced pressure to yield an oily dark brown product. ^1H NMR (CD_2Cl_2): δ 0.87 (m), 1.27 (br s), 2.34 (s, Ph*CH*$_3$), 7.12-7.82 (Ph). ^{31}P NMR (CD_2Cl_2): δ 28.45 (s), 30.70 (d, $J_{Rh\text{-}P}$ = 126.6 Hz), 44.69 (d, $J_{Rh\text{-}P}$ = 158.0 Hz). NMR analysis may be found in **3.5**.

2.9.2 Attempted Synthesis of $[(\eta^6\text{-toluene})Rh(PPh_3)_2][NO_3]$ Using an Acetonitrile Solution of $AgNO_3$

Silver nitrate (0.04 g, 0.23 mmol) was dissolved in 5 mL acetonitrile and added to a Schlenk flask containing $[(PPh_3)_2Rh(\mu\text{-}Cl)]_2$ (0.16 g, 0.12 mmol) and toluene (7.13 mL, 67.3 mmol) in CH_2Cl_2 (40 mL) and the mixture was stirred for 15 h. An orange slurry was obtained and filtered to give a light orange solution from which the volatiles were removed under reduced pressure to yield a dark orange oily product. ^1H NMR (CD_2Cl_2): δ 0.87 (m), 1.27 (br s), 2.00 (s, *CH*$_3$CN), 2.34 (s, Ph*CH*$_3$), 7.05-7.90 (Ph). ^{31}P NMR (CD_2Cl_2): δ 28.48 (s), 30.70 (d, $J_{Rh\text{-}P}$ = 126.9 Hz). NMR analysis may be found in **3.5**.

2.9.3 Attempted Synthesis of [(η^6-toluene)Rh(PPh_3)$_2$][$B(C_6F_5)_4$]

A mixture of $[(PPh_3)_2Rh(\mu\text{-}Cl)]_2$ (0.16 g, 0.12 mmol), $[Ph_3C][B(C_6F_5)_4]$ (0.22 g, 0.23 mmol) and toluene (7.13 mL, 67.3 mmol) in CH_2Cl_2 (40 mL) were added to a Schlenk flask and stirred for 5 h. The solvent volume was reduced to 15 mL the reaction flask was placed in a freezer and maintained at –30 °C overnight, at which point the volatiles were removed under reduced pressure to afford a dark brown, oily mixture. This reaction was repeated without cooling to –30 °C overnight and produced the same result. ^{1}H NMR (CD_2Cl_2): δ 2.22 (s, *CH*$_3$ of coordinated toluene), 2.34 (s, *CH*$_3$ of non-coordinated toluene), 5.28 (d, $^3J_{H\text{-}H}$ = 6.4 Hz, *o*-Ph of η^6-$C_6H_5CH_3$), 5.61 (t, $^3J_{H\text{-}H}$ = 6.4 Hz, *m*-Ph of η^6-$C_6H_5CH_3$), 6.69 (t, $^3J_{H\text{-}H}$ = 6.1 Hz, *p*-Ph of η^6-$C_6H_5CH_3$), 7.04-7.61 (m, P*Ph*$_3$), 7.66 (d, $^3J_{H\text{-}H}$ = 7.14 Hz, *o*-C*H* of $[Ph_3C][B(C_6F_5)_4]$), 7.88 (t, $^3J_{H\text{-}H}$ = 7.59 Hz, *m*-Ph of $[Ph_3C][B(C_6F_5)_4]$), 8.27 (t, $^3J_{H\text{-}H}$ = 6.18 Hz, *p*-Ph of $[Ph_3C][B(C_6F_5)_4]$). ^{31}P NMR (CD_2Cl_2): δ 44.91 (d, $J_{Rh\text{-}P}$ = 206.4 Hz). NMR analysis may be found in **3.5**.

To separate trityl chloride (triphenylmethyl chloride, Ph_3CCl) from the final reaction mixture, the oily dark brown mixture was dissolved in 10 mL CH_2Cl_2, 150 mL hexanes was added and CH_2Cl_2 was pumped off and the mixture was filtered. A green solid was filtered off to give a yellow filtrate, and the solvent was removed from this under reduced pressure to give a yellow solid. ^{1}H NMR (CD_2Cl_2): δ 1.27 (br s), 2.88 (br s), 7.07-7.90 (m). No peak was detected in a ^{31}P NMR spectrum.

An NMR sample was also made of the green solid. ^{1}H NMR (CD_2Cl_2): δ 0.80-0.93 (m), 0.97 (d, J = 6.54 Hz), 1.27 (br s), 2.22 (s, *CH*$_3$ of coordinated toluene), 2.34 (s), 3.31 (s), 5.08 (t, J = 6.1 Hz), 5.27 (d, J = 6.8 Hz), 5.46 (d, J = 6.5 Hz), 5.61 (t, $^3J_{H\text{-}H}$ = 6.5 Hz), 6.69 (t, J = 6.2 Hz), 6.80-8.50 (m, aromatic C*H* of PPh_3). ^{31}P NMR (CD_2Cl_2): δ

42.74 (d, J_{Rh-P} = 205.6 Hz), 44.90 (d, J_{Rh-P} = 206.6 Hz). The green solid was redissolved in 10 mL CH_2Cl_2, 20 mL diethyl ether and decolorizing carbon were added, and the mixture was filtered through a short Celite column under an inert atmosphere. The volatiles were then removed under reduced pressure to give a dark brown, oily product. ^{1}H NMR (CD_2Cl_2): δ 1.14 (t, $^3J_{H-H}$ = 7.0 Hz, C*H*$_3$ of diethyl ether), 2.21 (br s), 2.33 (br s), 3.49 (q, $^3J_{H-H}$ = 7.0 Hz, C*H*$_2$ of diethyl ether), 3.70 (br peak), 5.04 (d, J = 6.0 Hz), 5.39 (t, J = 6.2 Hz), 5.54 (br peak), 6.12 (br t), 6.32 (br d), 6.85-8.00 (m). ^{31}P NMR (CD_2Cl_2): δ 8.70 (s), 43.60 (d, J_{Rh-P} = 205.8 Hz), 44.92 (d, J_{Rh-P} = 206.3 Hz).

The oily dark brown mixture was redissolved in 10 mL diethyl ether and the solution was passed through a short silica-gel column under inert atmosphere with hexanes as eluent. Volatiles were removed from the resulting dark solution under reduced pressure and a brown substance was obtained. ^{1}H NMR (CD_2Cl_2): δ 0.88 (br t, *CH*$_3$ of residual hexanes), 0.98 (d, J = 6.6 Hz), 1.28 (m, *CH*$_2$ of residual hexanes), 5.56 (br peak), 7.00-8.00 (m). No phosphorus was detected in a ^{31}P NMR spectrum.

After collecting the dark brown mixture from the column, the eluent was changed to diethyl ether to collect a second brown fraction, and the solvent was removed under reduced pressure to give a brown solid. ^{1}H NMR (CD_2Cl_2): δ 0.88 (br t, *CH*$_3$ of residual hexanes), 0.98 (d, J = 6.6 Hz), 1.15 (t, $^3J_{H-H}$ = 6.84 Hz, C*H*$_3$ of diethyl ether), 1.27 (m, *CH*$_2$ of residual hexanes), 3.44 (q, $^3J_{H-H}$ = 7.0 Hz, C*H*$_2$ of diethyl ether), 5.04 (d, J = 6.3 Hz), 5.39 (t, J = 7.41 Hz), 6.85-8.00 (m). ^{31}P NMR (CD_2Cl_2): δ 43.60 (d, J_{Rh-P} = 205.9 Hz).

2.9.4 Reaction Between Impure [(η^6-toluene)$Rh(PPh_3)_2$][$B(C_6F_5)_4$] and I

A Schlenk flask was charged with the impure [(η^6-toluene)$Rh(PPh_3)_2$][$B(C_6F_5)_4$] (~0.5 g, ~0.36 mmol), excess of **I** (0.17 g, 0.52 mmol) and 50 mL CH_2Cl_2. The reaction mixture was refluxed for 2 h, and the solvent was removed under reduced pressure to give a dark green solid which was found to be soluble in methanol, acetonitrile, and acetone. ^{31}P NMR (CD_2Cl_2): δ 11.48 (s), 15.76 (s), 24.45 (s), 51.37 (d, J_{Rh-P} = 196.1 Hz). NMR analysis may be found in **3.5**.

2.9.4.1 Synthesis of Chromium(III) Acetylacetonate $Cr(acac)_3$[102]

A 250 mL rounded bottom flask was charged with chromium(III) chloride (2.70 g, 0.01 mol), urea (20.0 g, 0.33 mol), acetylacetone (6.00 g, 0.06 mol) and 100 mL distilled water. The mixture was refluxed for 14 h to give a purple solid which was collected. Yield 28.0 g (80%).

2.9.5 NMR Studies of the Products of Reactions Between [(η^6-toluene)$Rh(PPh_3)_2$][$B(C_6F_5)_4$] and I

2.9.5.1 ^{31}P NMR Studies of the Product of Reaction Between Impure [(η^6-toluene)$Rh(PPh_3)_2$][$B(C_6F_5)_4$] and I Using $Cr(acac)_3$

A sample of the product (~0.04 g, ~0.03 mmol) of the reaction between impure [(η^6-toluene)$Rh(PPh_3)_2$][$B(C_6F_5)_4$] and **I**, described above in Section **2.9.4**, was mixed with three different amounts of $Cr(acac)_3$ (0.15, 0.30, and 0.45 mmol) and ^{31}P NMR spectra were run. NMR analysis may be found in **3.5**.

2.9.6 Attempted Synthesis of $[(\eta^5\text{-I})Rh(PPh_3)_2][B(C_6F_5)_4]$

A solution of $[(PPh_3)_2Rh(\mu\text{-Cl})]_2$ (0.31 g, 0.23 mmol) and $[Ph_3C][B(C_6F_5)_4]$ (0.43 g, 0.47 mmol) in 10 mL CH_2Cl_2 was added drop-wise over 10 min to a solution of **I** (0.15 g, 0.47 mmol) in 10 mL CH_2Cl_2 in a Schlenk flask. The mixture was stirred for 1 h, and the solvent was removed under reduced pressure to afford a dark green solid. ^{1}H NMR (CD_2Cl_2): δ 0.86 (br peak), 2.23 (d, $J_{H\text{-}P}$ = 12.7 Hz), 2.34 (br peak), 2.68 (d, $J_{H\text{-}P}$ = 13.0 Hz), 2.80 (br peak), 3.86 (br peak), 5.00 (br peak), 5.10 (br peak), 5.63 (br peak), 6.11 (br peak), 6.60 (br peak), 6.70 (br peak), 6.85-8.00 (m). ^{31}P NMR (CD_2Cl_2): δ 12.00 (s), 25.53 (s), 52.58 (d, $J_{Rh\text{-}P}$ = 196.7 Hz). NMR analysis may be found in **3.5**.

2.9.7 Synthesis of $[(\eta^5\text{-I})Rh(PPh_3)_2][BF_4]$

A Schlenk flask was charged with $[(PPh_3)_2Rh(\mu\text{-Cl})]_2$ (0.16 g, 0.12 mmol), $AgBF_4$ (0.05 g, 0.23 mmol), and 15 mL CH_2Cl_2, and the mixture was stirred for 24 h and filtered. The filtrate was cooled to −78 °C and a solution of **I** (0.07 g, 0.23 mmol) in 10 mL CH_2Cl_2 was added. The resulting mixture was stirred for 48 h at −78 °C to give a dark brown solution from which the solvent was removed under reduced pressure to give a brown oily mixture. Yield 0.20 g (83%). ^{13}P NMR experiments at room and low temperature, −50, −60, and −75 °C were carried out. At room temperature, ^{31}P NMR (CD_2Cl_2): δ 11.97 (s), 15.85 (s), 24.66 (s), 27.47 (br s), 51.46 (d, $J_{Rh\text{-}P}$ = 196.5 Hz). At −75 °C, ^{31}P NMR (CD_2Cl_2): δ 11.9 (s), 15.83 (s), 25.24 (s), 28.67 (br s), 41.87 (dd, $^2J_{P\text{-}P}$ = 47.0 Hz, $J_{Rh\text{-}P}$ = 201.11 Hz), 51.20 (d, $J_{Rh\text{-}P}$ = 189.86 Hz), 54.45 (dd, $^2J_{P\text{-}P}$ = 47.0 Hz, $J_{Rh\text{-}P}$ = 228.38 Hz). ^{13}P NMR at −50, −60 were the same as the ^{13}P NMR at −75 °C, but the peaks at 41.87 and 54.45 were not sharp as they were in the ^{13}P NMR at −75 °C. HR-

EMS: observed: 941.2067 $[M]^+$, calculated: 941.2097. NMR analysis may be found in **3.5**.

2.10 Attempted Oxidative Additions to $[(\eta^5\text{-I})Rh(PPh_3)_2][BF_4]$

2.10.1 Attempted Oxidative Addition of MeI to $[(\eta^5\text{-I})Rh(PPh_3)_2][BF_4]$ on an NMR scale

$[(\eta^5\text{-}\mathbf{I})Rh(PPh_3)_2][BF_4]$, MeI and 0.5 mL CD_2Cl_2 were added to a NMR tube and the mixture was shaken for 5 min. ^{1}H NMR (CD_2Cl_2): δ 2.00 (s), 2.16 (s, *CH*$_3$I), 2.31 (s), 2.49 (d, $J_{H\text{-}P}$ = 13.1 Hz, P*CH*$_3$), 2.80 (br peak), 2.90 (m), 3.00 (br peak), 3.40 (br peak), 3.89 (br peak), 3.54 (d, J = 13.9), 3.59 (br peak), 3.89 (br peak), 4.73 (br peak), 5.83 (br peak), 5.87 (br peak), 6.17 (br peak), 6.46 (br peak), 6.57-8.10 (br peak). ^{31}P NMR (CD_2Cl_2): δ 4.62 (s), 8.23 (s), 9.32 (s), 12.05 (s), 20.30 (d, J = 9.22 Hz), 20.61 (s), 21.11 (s), 21.30 (s), 22.32 (s), 22.82 (s), 24.99 (s), 26.98 (s), 39.13 (d, J = 9.4 Hz), 39.90 (d, J = 9.5 Hz). Discussion may be found in **3.6**.

2.11 Attempted the reaction of H_2 to $[(\eta^5\text{-I})Rh(PPh_3)_2][BF_4]$

$[(\eta^5\text{-}\mathbf{I})Rh(PPh_3)_2][BF_4]$ was dissolved in CH_2Cl_2 and H_2 gas was bubbled for 48 h at room temperature. Discussion may be found in **3.6**.

2.12 Coordination of PHIN to $TiCl_4$

2.12.1 Attempted Coordination of I to $TiCl_4$ (1:4 ratio) in Dichloromethane at Room Temperature[80]

Coordination of **I** to $TiCl_4$ on an NMR scale using a four-fold excess of $TiCl_4$ was attempted in a glove box under nitrogen. To a solution of 0.02 g **I** (0.06 mmol) in 0.70 mL dry CD_2Cl_2 in a vial was added 0.03 mL (0.25 mmol) of $TiCl_4$. The solution was mixed and transferred to a dry NMR tube. ^1H and ^{31}P NMR spectra were obtained for comparison with the ^1H and ^{31}P NMR data of **I**. ^1H NMR (CD_2Cl_2): δ 3.08 (d, $^2J_{H-P}$ = 13.2 Hz, P*CH*$_3$), 7.29 (t, $^3J_{H-H}$ = $^3J_{H-P}$ = 4.0 Hz, H(2)), 7.41 (d, $^3J_{H-H}$ = 8.5 Hz, H(7)), 7.66 and 7.71 (2m, *o*-Ph), 7.71 (m, H(5)), 7.74 (m, H(6)), 7.77 and 7.80 (2m, *m*-Ph), 7.84 (br t, H(3)), 7.92 and 7.95 (2m, *p*-Ph), 8.07 (d, $^3J_{H-H}$ = 8.1 Hz, H(4)). ^{13}C NMR (CD_2Cl_2): δ 11.00 (P*CH*$_3$), 102.20 (C(1)), 116.70 (*ipso*-C), 121.00 (C(3)), 124.80 (C(7)), 128.60 (C(2)), 128.70 (C(4)), 131.40 (C(5)), 131.40 and 131.5 (*o*-Ph), 132.10 (C(8)), 132.80 (C(9)), 133.0 (C(6)), 133.10 and 133.2 (*m*-Ph), 136.90 (*p*-Ph). ^{31}P NMR (CD_2Cl_2): δ 11.67, 11.83, and 14.21.

Coordination of **I** to $TiCl_4$ in a Schlenk flask using a four-fold excess of $TiCl_4$ was also attempted. To a solution of **I** (0.20 g, 0.64 mmol) in 10 mL of dry CH_2Cl_2, $TiCl_4$ (0.27 mL, 2.46 mmol) was added slowly. The solution was stirred under argon for 10 minutes to afford a deep red, opaque solution from which the volatiles were removed under reduced pressure to give a deep red, toffee-like solid. An NMR sample was made, and produced the same result as the reaction on an NMR scale. NMR analysis may be found in **3.7**.

2.12.2 Attempted coordination of I to $TiCl_4$ (1:11 ratio) in Dichloromethane at Room Temperature

A mixture of **I** (0.30 g, 0.95 mmol) and $TiCl_4$ (1.15 mL, 10.5 mmol) in 10 mL of CH_2Cl_2 in a reaction flask turned dark red immediately on mixing. The reaction mixture was stirred for 5 d at room temperature, and the color was staying dark red, and the volatiles were removed under reduced pressure to give a brown solid. An NMR sample was made, and ^1H and ^{31}P NMR spectra (See Appendix, Figure A 75 and A 76) were obtained, but the final products were not fully characterized due to the formation of several products. ^1H NMR (CD_2Cl_2): δ 2.55-3.15 (several d, P*CH*$_3$), 3.91 (br peak), 4.87 (br peak), 6.80-8.00 (m), 8.07 (br d). ^{31}P NMR (CD_2Cl_2): δ 12.82, 13.13, 15.18, and 24.01. NMR analysis may be found in **3.7**.

2.12.3 Attempted Coordination of I to $TiCl_4$ (1:11 ratio) in Dichloromethane at Low Temperature

A solution of **I** (0.30 g, 0.95 mmol) in 10 mL of CH_2Cl_2 was cooled to −78 °C and $TiCl_4$ (1.15 mL, 10.5 mmol) was added to the reaction flask. After 48 h stirring at −78 °C, the reaction mixture was in dark green color. On stirring for a further 24 h at room temperature, the color turned to deep dark brown, and the volatiles were then removed under reduced pressure to give a brown solid. An NMR sample was made, and ^1H and ^{31}P NMR spectra (See Appendix, Figure A 77 and A 78) were obtained. ^1H NMR (CD_2Cl_2): δ 2.00-3.15 (several d, P*CH*$_3$), 3.92 (br peak), 4.91 (br peak), 6.45 (br peak), 6.82 (br peak), 6.85 (br d), 6.89 (br d), 6.99 (br d), 7.03-7.95 (m). ^{31}P NMR (CD_2Cl_2): δ 11.81, 12.07, 12.16, and 24.08. ^1H NMR spectrum depicted several doublet peaks at δ 2.00-3.15 with

~13.0 Hz coupling constant, characteristic for PMe group. The formation of several products was confirmed by observing several peaks in the ^{31}P NMR spectrum. 2D NMR spectra were obtained and analyzed, but none of these products was fully characterized due to the formation of several products. NMR analysis may be found in **3.7**.

2.12.4 Attempted Solvent Free Coordination of I to $TiCl_4$ at Room Temperature

A mixture of **I** (0.34 g, 1.08 mmol) and $TiCl_4$ (2.50 mL, 22.8 mmol) was stirred for 5 d at room temperature and unreacted $TiCl_4$ was then removed under reduced pressure to afford a red solid. An NMR sample was made, and ^{1}H and ^{31}P NMR spectra (See Appendix, Figure A 81 and A 82) were obtained, but the final products were not fully characterized due to the formation of several products. ^{1}H NMR (CD_2Cl_2): δ 2.06-3.15 (several d, P*CH*$_3$), 3.91 (br peak), 4.88 (br peak), 6.80-8.15 (m). ^{31}P NMR (CD_2Cl_2): δ 11.53, 11.69, 11.72, 12.00, 14.04, and 22.87. Discussion may be found in **3.7**.

2.12.5 Attempted Coordination of I to $TiCl_4$ by Refluxing

A solution of **I** (0.30 g, 0.95 mmol) and $TiCl_4$ (1.15 mL, 10.5 mmol) in 10 mL of CH_2Cl_2 was refluxed for 3 h. The volatiles were removed under reduced pressure to give a dark red oily product. An NMR sample was made, and ^{1}H and ^{31}P NMR spectra were obtained (See Appendix, Figure A 79 and A 80). ^{1}H NMR (CD_2Cl_2): δ 2.64 (d, $^2J_{H\text{-}P}$ = 13.2 Hz, P*CH*$_3$), 2.78 (d, $^2J_{H\text{-}P}$ = 13.1 Hz, P*CH*$_3$), 3.08 (d, $^2J_{H\text{-}P}$ = 13.2 Hz, P*CH*$_3$), 3.92 (br peak), 4.86 (br peak), 6.80-7.86 (m), 7.92 (br t), 8.06 (br d). ^{31}P NMR (CD_2Cl_2): δ 12.80 (br peak), and 15.17. ^{1}H NMR spectrum depicted three doublet peaks at δ 2.64, 2.78, and 3.08, indicating that three products were formed. The final products were not fully

characterized due to the formation of several products. NMR analysis may be found in **3.7**.

2.12.6 Attempted Coordination of I to $TiCl_4$ Using $[Ph_3CB][(C_6F_5)_4]$

A solution of $TiCl_4$ (0.04 mL, 0.32 mmol), **I** (0.10 g, 0.32 mmol) and $[Ph_3C][B(C_6F_5)_4]$ (0.30 g, 0.32 mmol) in 20.0 mL CH_2Cl_2 was stirred for 30 min to give a dark brown slurry which was filtered. The volatiles were then removed under reduced pressure to afford an oily dark red mixture. An NMR sample was made, and ^1H and ^{31}P NMR spectra (See Appendix, Figure A 83 and A 84) were obtained. ^1H NMR (CD_2Cl_2): δ 2.34 (d, $^2J_{H\text{-}P}$ = 13.3 Hz, P*CH*$_3$), 2.59 (d, $^2J_{H\text{-}P}$ = 13.3 Hz, P*CH*$_3$), 2.71 (2 br d, 2 P*CH*$_3$), 3.03 (d, $^2J_{H\text{-}P}$ = 13.3 Hz, P*CH*$_3$), 3.86 (br peak), 4.50 (br peak), 4.76 (d, J = 14.8 Hz), 6.40-7.60 (m), 7.67 (br d, possibly *o*-Ph of $[Ph_3C][B(C_6F_5)_4]$), 7.88 (t, J = 7.93 Hz, possibly *m*-Ph of $[Ph_3C][B(C_6F_5)_4]$), 8.27 (t, J = 7.5 Hz, possibly *p*-Ph of $[Ph_3C][B(C_6F_5)_4]$). ^{31}P NMR (CD_2Cl_2): δ 12.02, 12.63, 12.84 and 15.17. ^1H NMR spectrum depicted several P-Me doublets, indicating the formation of several products. ^{31}P NMR spectrum showed several peaks, and the final products were not fully characterized due to the formation of several products. Discussion may be found in **3.7**.

2.12.7 Attempted Synthesis of $[(\eta^5\text{-I})TiCl_3][GaCl_4]$ in Toluene

A mixture of $TiCl_4$ (0.22 mL, 2.00 mmol), **I** (0.68 g, 2.20 mmol), $GaCl_3$ (0.37 g, 2.10 mmol) and 20 mL toluene turned dark red immediately. A dark red slurry was formed after 4 h stirring at 60 °C, and the volatiles were removed under reduced pressure to afford a dark red solid. An NMR sample was made, and ^1H and ^{31}P NMR spectra (See

Appendix, Figure A 85 and A 86) were obtained. ^{1}H NMR (CD_2Cl_2): δ 2.66 (d, $^{2}J_{H-P}$ = 13.3 Hz, P*CH*$_3$), 2.78 (2 br d, 2 P*CH*$_3$), 3.09 (d, $^{2}J_{H-P}$ = 13.3 Hz, P*CH*$_3$), 3.40 (br peak), 4.87 (br peak), 6.80-8.10 (m). ^{31}P NMR (CD_2Cl_2): δ 12.75, and 15.24. Observing several P-Me doublets at δ 2.60-3.15 in the ^{1}H NMR spectrum, and several peaks in the ^{31}P NMR spectrum indicated the formation of several products. The products were not fully characterized due to the formation of several products. Discussion may be found in **3.7**.

2.12.8 Attempted Synthesis of [(η^5-I)TiCl$_3$][GaCl$_4$] in Dichloromethane

A mixture of $TiCl_4$ (0.22 mL, 2.00 mmol), **I** (0.68 g, 2.20 mmol), $GaCl_3$ (0.37 g, 2.10 mmol) and 30 mL CH_2Cl_2 turned dark red immediately and remained dark red after 4 h stirring at room temperature. The volatiles were removed under reduced pressure to afford a dark red solid. An NMR sample was made, and ^{1}H and ^{31}P NMR experiments were run. ^{1}H NMR (CD_2Cl_2): δ 2.65 (br peak), 2.78 (br peak), 3.09 (br peak), 3.89 (br peak), 4.86 (br peak), 6.60-8.20 (m). ^{31}P NMR (CD_2Cl_2): δ 12.68, 12.79, and 15.24. The final products were not fully characterized due to the formation of several products and peak broadening in the ^{1}H NMR spectrum. Discussion may be found in **3.7**.

2.12.9 Attempted Synthesis of [(η^5-I)TiCl$_3$][AlCl$_4$][80]

A mixture of **I** (0.20 g, 0.64 mmol) and $AlCl_3$ (0.09 g, 0.67 mmol) in 10 mL of dry CH_2Cl_2 was stirred as $TiCl_4$ (0.07 mL, 0.64 mmol) was added slowly through the septum. The solution was stirred under argon for 10 minutes to yield a deep red, opaque solution, and the volatiles were removed under reduced pressure to yield a deep red, toffee-like solid. An NMR sample was made, and mass spectrometry and ^{1}H and ^{31}P

NMR experiments were run, but the final product was not fully characterized due to the formation of several products. Discussion may be found in **3.7**.

2.12.10 Attempted Coordination of I to $TiCl_4(THF)_2$ Using $AgNO_3$[78]

A solution of $AgNO_3$ (0.05 g, 0.29 mmol) in 25.0 mL dry acetonitrile was added drop-wise to a solution of **I** (0.08 g, 0.24 mmol) in 50 mL of dry acetonitrile. A chunky greenish-grey precipitate formed on mixing, and the liquid supernatant was transferred over 30 min into a solution of $TiCl_4(THF)_2$ (0.10 g, 0.29 mmol) in 50 mL of dry acetonitrile. The volatiles were removed under reduced pressure and 25 mg of fine red powder was isolated. ^1H and ^{31}P NMR of this product were taken (See Appendix, Figure A 87 and A 88), but the final product was not fully characterized. The greenish-grey precipitate was isolated and washed with acetonitrile, in which it redissolved. Investigations into this by-product were not pursued. Discussion may be found in **3.7**.

In the second attempt, a solution of **I** (0.08 g, 0.24 mmol) in 25 mL of dry, degassed acetonitrile was cannulated into a solution of $TiCl_4(THF)_2$ (0.10 g, 0.29 mmol) in 25 mL of dry, degassed acetonitrile and the reaction mixture was stirred. A red color developed as the addition continued, but the solution ultimately turned yellow. The resulting yellow solution was stirred a few minutes and turned orange color, at which point it was cooled to 0 ^oC as it turned yellow. A solution of $AgNO_3$ (0.05 g, 0.29 mmol) was then added drop-wise over 30 min to give a yellow solution and a white precipitate. The stirred reaction mixture was warmed to room temperature and filtered, and the volatiles were removed under reduced pressure to give 18.0 mg of a yellow solid (13.0% yield). Both ^1H and ^{31}P NMR spectra of the compound were taken (See Appendix, Figure

A 89 and A 90), but the final product was not fully characterized. Discussion may be found in **3.7**.

2.12.11 Attempted Coordination of I to $TiCl_4(THF)_2$ (1:4 ratio) in Dichloromethane[78]

A solution of $TiCl_4(THF)_2$ (0.21 g, 0.64 mmol) in the minimum amount of CH_2Cl_2 was added drop-wise to a solution of **I** (0.05 g, 0.16 mmol) in the minimum amount of mL CH_2Cl_2 to give, temporarily, a dark red color but ultimately an orange solution. The volume was reduced 10 mL under reduced pressure and the solution was placed in a freezer at −30 ºC for 2 d as a yellow solid formed. The orange supernatant was transferred via syringe into an empty flask and placed back in the freezer overnight. The following day a ^{31}P NMR spectrum was taken of the supernatant, which can be viewed in Appendix, Figure A 91. The yellow precipitate from the original flask was filtered off and dried under reduced pressure for 5 h and a ^{1}H NMR spectrum was taken. The yellow precipitate could not be the desired product, as ^{1}H NMR spectrum depicted no peaks in the aromatic region. By analyzing the ^{31}P NMR spectrum of supernatant, it was deduced that phosphonuim salts were formed due to the presence of two peaks at δ ~13 and ~25. Discussion may be found in **3.7**.

2.12.12 Attempted Coordination of I to $TiCl_4(THF)_2$ (1:4 ratio) in THF[78]

The same procedure as identified in 2.11.12 was completed, however, THF was used in place of CH_2Cl_2. Additionally, the flask containing **I** was dropped into that containing $TiCl_4(THF)_2$ instead of the opposite as completed in 2.11.12. A dark brown

solution was formed on complete addition of the ylide-containing solution, and the reaction was left to stir for 30 minutes. Finally, the reaction was placed in the freezer overnight, and the next morning, a yellow precipitate had formed on the bottom of the flask covered by a brown solution. A small amount of the brown supernatant was cannulated into a Schlenk flask and put under vacuum overnight. The remaining supernatant was cannulated into an empty flask and placed back in the freezer. ^{1}H and ^{31}P NMR spectra were taken of the supernatant the following day, and a ^{31}P NMR spectrum was taken of the vacuum dried product. By analyzing the ^{31}P NMR spectrum of supernatant, it was deduced that phosphonuim salts were formed due to the presence of two peaks at δ ~13 and ~25. Discussion may be found in **3.7**.

2.13 Coordination of PHIN to Zirconium Centre

Coordination of **I** to $ZrCl_4$ was attempted previously in the Baird lab, and it was unsuccessful, possibly due to the high acidity of $ZrCl_4$. It was anticipated that the coordination of **I** to Cp^*ZrMe_3 occur because of lower acidity of Cp^*ZrMe_3 compare with $ZrCl_4$.

2.13.1 Attempted Coordination of I to Cp^*ZrMe_3

A Schlenk flask was charged with Cp^*ZrMe_3 (0.11 g, 0.40 mmol), **I (**0.13 g, 0.40 mmol), and 40 mL CH_2Cl_2. A portion of $[Ph_3C][B(C_6F_5)_4]$ (0.37 g, 0.40 mmol) in 20 mL CH_2Cl_2 was added drop-wise over 10 min to the reaction flask. A dark brown was obtained after 15 min stirring which was taken under reduced pressure to afford dark brown solid and an NMR sample was made (^{1}H and ^{31}P NMR, Figure 127 and 128). ^{1}H

NMR (CD_2Cl_2): δ –1.69 (s), –0.46 (s), 1.27 (m), 1.36 (br t), 1.67 (br s), 2.10 (several d, P*CH*$_3$), 2.31 (d, $^2J_{H-P}$ = 13.3 Hz, P*CH*$_3$), 2.94 (d, $^2J_{H-P}$ = 13.3 Hz, P*CH*$_3$), 3.96 (m), 5.61 (br peak), 6.57 (br peak), 6.80-7.74 (m), 7.80 (br t). ^{31}P NMR (CD_2Cl_2): δ 11.98, and 17.82. The ^{1}H NMR spectrum depicted two peaks at δ –1.65 and –0.41 which could be assigned for two methyl groups on zirconium. The dark brown solid was dissolved in CH_2Cl_2 and passed through a frit and an NMR sample was made which gave the identical ^{1}H and ^{31}P NMR spectra before filtration. The dark brown solid was dissolved in CH_2Cl_2 and passed through a short silica gel column to give an oily dark brown mixture. An NMR sample was made, and ^{1}H and ^{31}P NMR experiments were run, but the desired product was not identified due to the absence of the two singlet peaks in the negative region. Discussion may be found in **3.7**.

2.14 Coordination of PHIN to $NiBr_2$(dimethyl ethylene glycol) or $NiBr_2$(DME)

It was anticipated that the reaction of PHIN with $NiBr_2$(DME) will result in displacement of DME with PHIN ligand, so the reaction of **I** with $NiBr_2$(DME) was attempted.

2.14.1 Solubility Tests of $NiBr_2$(DME)

Solubility of $NiBr_2$(DME) was tested in THF, CH_2Cl_2, chloroform, diethyl ether, toluene, and chlorobenzene, and none of these solvents dissolved $NiBr_2$(DME). Ethanol dissolved $NiBr_2$(DME) after 15 min stirring, and gave a yellow solution. Acetonitrile dissolved $NiBr_2$(DME) partially, and gave a clear green solution.

2.14.2 Attempted Coordination of I to $NiBr_2$(DME) in Dichloromathane

A mixture of **I** (0.15 g, 0.47 mmol), and $NiBr_2$(DME) (0.14 g, 0.47 mmol) in CH_2Cl_2 (20 mL) were added to a Schlenk flask. The reaction mixture turned to a slurry dark green color, immediately, and stirred for 12 h to give a slurry dark brown solution. The slurry dark brown solution was filtered, and the filtrate was taken under reduced pressure to afford an oily dark brown mixture. An NMR sample was made, and ^{1}H and ^{31}P NMR spectra were obtained (See Appendix, Figure A 95 and A 96). ^{1}H NMR (CD_2Cl_2): δ 2.49 (d, $^{2}J_{H-P}$ = 13.0 Hz, P*CH*$_3$), 3.33 (s, O*Me*), 3.49 (s, *CH*$_2$OMe), 4.72 (br s), 6.48 (br t), 6.70 (br peak), 6.82 (t, $^{3}J_{H-H}$ = 7.2 Hz), 6.95 (d, $^{3}J_{H-H}$ = 7.8 Hz), 7.05-8.50 (m), 9.05 (br peak), 10.19 (br peak). ^{31}P NMR (CD_2Cl_2): δ 5.91 (s, *P*Me), 11.11, 13.23, and 26.37. ^{1}H NMR spectrum showed PMe doublet at δ 2.49 with 13.0 Hz coupling constant, indicating the presence of **I**. ^{31}P NMR spectrum depicted several peaks along with phosphorus chemical shift of **I**, indicating the formation of several products. None of the products were fully characterized. This reaction was also repeated with 2 and 5 d stirring which resulted in consuming all the added **I**. An NMR sample was made from the attempted coordination after 5 d, and ^{1}H and ^{31}P NMR spectra were obtained (See Appendix, Figure A 97 and A 98). ^{1}H NMR (CD_2Cl_2): δ 3.13 (br d, P*CH*$_3$), 3.35 (s, O*CH*$_3$), 3.51 (s, *CH*$_2$OCH$_3$), 4.48 (br peak), 6.40-8.80 (m), 9.33 (br peak). ^{31}P NMR (CD_2Cl_2): δ 11.25, 13.44, and 26.30. ^{31}P NMR spectrum depicted three singlet peaks at δ 11.25, 13.44, and 26.30, and the two singlet peaks at δ 13.44, and 26.30 could be possibly due to the formation of two phosphonium salts. The other singlet peak at δ 11.25 in ^{31}P

NMR spectrum remained unidentified due to the formation of several compounds. Discussion may be found in **3.8**.

2.14.3 Attempted Coordination of I to $NiBr_2$(DME) in Toluene

Compound **I** (0.07 g, 0.23 mmol) and 15 mL toluene were added to a Schlenk flask and heated up to 100°C, and a dark green suspension was obtained. $NiBr_2$(DME) (0.14 g, 0.46 mmol) was added to the Schlenk flask under a strong flow of Ar. The reaction mixture was heated up to 30 °C for 2 h to give a pale yellow solution on top and a dark brown solid on the bottom of the reaction flask. The dark brown solid was washed with toluene, and the solid was taken under reduced pressure to afford a dark brown solid. An NMR sample was made, and ^{1}H and ^{31}P NMR spectra (See Appendix, Figure A 99 and A 100) were obtained. ^{1}H NMR (CD_2Cl_2): δ 2.34 (s, PhCH_3), 3.37 (s, OCH_3), 3.54 (s, CH_2OCH_3), 4.21 (m), 4.42 (br peak), 6.80-8.60 (m), 9.34 (br peak). ^{31}P NMR (CD_2Cl_2): δ 11.44, and 25.46. The final products were not fully characterized due to the peak broadening in the ^{1}H NMR spectrum. The top clear pale yellow solution was transferred to another Schlenk flask and the solvent was removed under reduced pressure to afford a pale yellow solid (almost white solid). An NMR sample was made, and ^{1}H and ^{31}P NMR experiments were run, and this fraction was identified as **I** due to the presence of a singlet peak at δ 5.91 in the ^{31}P NMR spectrum. Discussion may be found in **3.8**.

2.14.4 Attempted Coordination of I to $NiBr_2$(DME) in Chlorobenzene

Compound **I** (0.07 g, 0.23 mmol) and 15 mL chlorobenzene were added to a Schlenk flask, and $NiBr_2$(DME) (0.14 g, 0.46 mmol) was added to the Schlenk flask

under a strong flow of Ar. The reaction mixture turned to a slurry brown, immediately, and stirred for 3 h without changing color. The reaction mixture was refluxed for 3 h, cooled to room temperature, stirred for 12 h, and a slurry brown solution was observed. Stirring was stopped, a dark green solid was precipitated, and the dark brown supernatant was syringed out to another Schlenk flask which was taken under reduced pressure to afford a dark brown solid. NMR samples were made from both fractions, and ^{1}H and ^{31}P NMR experiments were run. ^{1}H and ^{31}P NMR spectra of the supernatant in CD_2Cl_2 (See Appendix, Figure A 101 and A 102) and DMSO-d_6 were obtained, as well as, the dark green solid in DMSO-d_6. ^{1}H NMR (CD_2Cl_2): δ 2.48 (br s, Ph*CH*$_3$), 4.77 (br peak), 5.60 (br peak), 6.26-9.52 (m), 9.14 (br peak), 10.30 (br peak). ^{31}P NMR (CD_2Cl_2): δ 5.92 (*P*Me), 10.01, 13.60 (br peak) and 26.51. In the ^{1}H and ^{31}P NMR spectra of dark brown solid in DMSO-d_6, two phosphonium salts, and unreacted **I** were identified. ^{31}P NMR spectra depicted singlet peaks at δ 7.3, 10.7, 14.48, 26.68, and 28.68. Peaks at δ 14.48 and 26.68 assigned for the two phosphonium salts, and peak at δ 7.3 assigned for the unreacted **I**. The other two peaks in ^{31}P NMR spectrum at δ 10.7 and 28.68 remained unknown. ^{1}H and ^{31}P NMR spectra of the dark green solid in DMSO-d_6 revealed that this fraction is **I**. Discussion may be found in **3.8**.

2.15 Coordination of I to $HgCl_2$ and $HgBr_2$

It was anticipated that the reaction of HgX_2 and PHIN will form [(η^5-PHIN)HgX_2]$_2$, so the reaction of **I** with $HgCl_2$, and $HgBr_2$ were attempted.

2.15.1 Attempted Coordination of I to $HgCl_2$

Compound **I** (0.30 g, 0.95 mmol), $HgCl_2$ (0.26 g, 0.95 mmol), and 60 mL THF were added to a Schlenk flask. The reaction mixture turned to a slurry brown, immediately, and stirred for 10 min without changing color. The reaction mixture was filtered, a green solid and a dark purple filtrate were obtained. An NMR sample was made from the green solid, and ^{1}H and ^{31}P NMR spectra (See Appendix, Figure A 103 and A 104) were obtained. ^{1}H NMR (CD_2Cl_2): δ 1.82 (m, *CH_2* of residual THF), 2.87 (m, possibly several P*CH_3*), 3.68 (m, *CH_3* of residual THF), 3.91 (br peak), 5.44 (br peak), 6.80-8.00 (m). ^{31}P NMR (CD_2Cl_2): δ 11.58, and 13.17. ^{1}H NMR spectrum depicted broad peaks, and the ^{31}P NMR spectrum showed two singlet peaks at δ 10.53 and 11.93, indicating the presence of two compounds. The filtrate was taken under reduced pressure to afford a dark purple solid. After adding CD_2Cl_2 to the dark purple solid for making an NMR sample, some white precipitate was formed and the amount of it increased by passing time. The dark purple solid was then dissolved in dichoromethane to precipitate the white product, and a white solid with a dark green filtrate were obtained after filtration. The white product was insoluble in CH_2Cl_2 and soluble in DMSO. An NMR sample was made from the dark green filtrate, and ^{1}H and ^{31}P NMR experiments were run. The ^{31}P NMR spectrum showed at least thirteen different peaks, and it was impossible to identify the desired product due to the formation of several compounds. An NMR sample was made from the white solid in DMSO-d_6, and ^{1}H and ^{31}P NMR spectra (See Appendix, Figure A 105 and A 106) were obtained. ^{1}H NMR (DMSO-d_6): δ 2.76 (d, $^{2}J_{H\text{-}P}$ = 13.7 Hz, P*CH_3*), 3.00 (d, $^{2}J_{H\text{-}P}$ = 14.2 Hz, P*CH_3*), 3.33 (br peak), 6.01 (br t), 6.70 (m), 6.83 (m), 6.92 (br d, J = 7.5 Hz), 7.06 (m), 7.15 (br d), 7.24 (br t, J = 7.00 Hz), 7.48

(br d), 7.55-7.95 (m), 8.02 (br d). ^{31}P NMR (DMSO-d_6): δ 8.74 (br s), and 12.19. The ^{1}H NMR spectrum (See Appendix, Figure A 105) showed two doublet peaks at δ 2.76 and 3.00. The ^{31}P NMR spectrum (See Appendix, Figure A 106) depicted two singlet peaks at δ 8.74 and 12.19, indicating the presence of two compounds. None of these products was fully characterized due to the presence of two different products. Discussion may be found in **3.9**.

2.15.2 Attempted Coordination of I to $HgBr_2$

Compound **I** (0.3 g, 0.95 mmol), $HgBr_2$ (0.34 g, 0.95 mmol), and 60 mL THF were added to a Schlenk flask. The reaction mixture turned to a dark red solution, immediately, and stirred for 30 min without changing color. The reaction mixture was taken under reduced pressure to afford a green solid. An NMR sample of the green solid was made in CD_2Cl_2. The green solid was dissolved in 10 mL CH_2Cl_2 to give a dark red solution, and 40 mL hexanes was added to the dark solution which resulted in precipitating a green solid. An NMR sample was made from the green solid which was almost identical with ^{1}H and ^{31}P NMR spectra obtained before this purification step. The ^{1}H and ^{31}P NMR spectra may be found in Appendix, Figure A 107 and A 108. ^{1}H NMR (CD_2Cl_2): δ 1.82 (m, *CH_2* of residual THF), 2.87 (m, possibly several P*CH_3*), 3.68 (m, *CH_3* of residual THF), 3.91 (br peak), 5.58 (br peak), 6.80-7.08 (m), 7.17 (br t), 7.26 (br t), 7.38 (br t), 7.49 (br d), 7.50-8.00 (m). ^{31}P NMR (CD_2Cl_2): δ 10.83 (br s), 12.92, and 24.46. The ^{31}P NMR spectrum (See Appendix, Figure A 108) did not contain **I**, indicating that it had been consumed, but three products were formed. None of these products was

fully characterized due to the formation of several products. Discussion may be found in **3.9**.

Chapter 3 : Results and Discussion

3.1 Synthesis of PHIN ligands

Investigation of the coordination chemistry of the phosphonium cyclopentadienylides showed a very slow progress for many years because of the lack of general synthetic methodologies. In order to develop this field of research further and to explore the coordination chemistry of this class of ligand, the Baird lab began a study to synthesize novel phosphonium cyclopentadienylides and phosphonium indenylides through either improving the previously reported methodologies or by developing new synthetic routes. Using the reactions of haloalkanes and phosphines, followed by deprotonation of the resulting phosphonium salts with strong bases, to synthesize phosphonium ylides resulted in very useful methodologies.

The synthesis of 1-bromoindene was reported for the first time in 1944, but the approach suffered from very low and variable yields and the final product was poorly characterized.[51] In 1967, Crofts *et al.* synthesized 1-bromoindene in 24% yield from the reaction of indene and bromine to yield 1,2-dibromoindane, followed by the addition of 2,6-lutidine.[49] The cleavage of the C-Si bond of 1-trimethylsilylindene with dioxane dibromide at −78 °C in an inert atmosphere and in darkness was attempted to prepare 1-bromoindene with a relatively high yield (86%), and the final product was characterized, properly.[52,53] Fowler, in his Queen's University Ph.D thesis, describes generally unsuccessful experiments with a variety of brominating agents such as N-bromosuccinimide, bromoform, Br_2, and 1,2-dibromomethane,[103] and he eventually settled on dibromotetrachloroethane as a brominating agent which afforded 1-

bromoindene in good yield and in greater purity than obtained using dioxane dibromide and trimethylsilyl indene.[103]

In this thesis, the general method used for the synthesis of PHIN ligand **I** or its 4,7-dimethyl analogue involved a method very similar to that used previously,[19,22,39,55] deprotonation of indene or 4,7-dimethylindene to give the corresponding indenyl anions followed by reaction with PPh_2Cl to give the corresponding phosphine. The latter was then methylated with MeI, followed by deprotonation with NaH to give the desired PHIN ligand.

3.1.1 Synthesis of 1-$C_9H_6PMePh_2$ (I)

The synthesis of 1-$C_9H_6PMePh_2$ **(I)** is outlined in the Experimental Section and proceeded as in Figure 51.

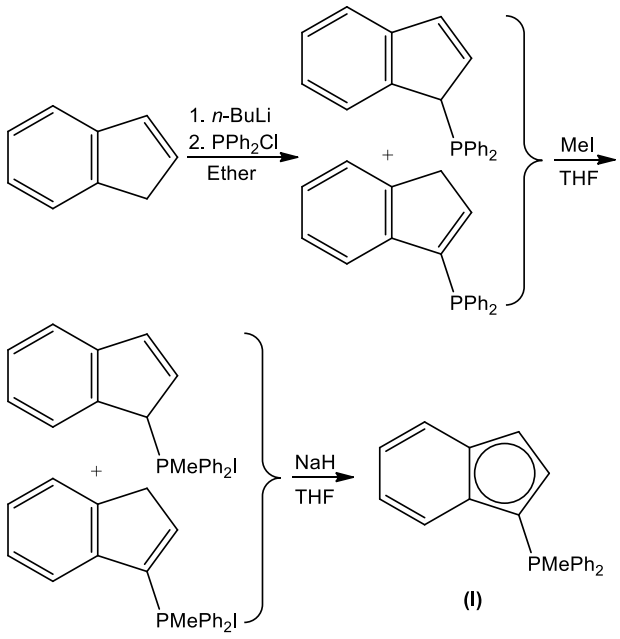

Figure 51. Synthesis of 1-$C_9H_6PMePh_2$ (**I**).

The ^{1}H and ^{31}P NMR spectra of 1-$C_9H_6PMePh_2$ (**I**) were very similar to those reported previously.[54,55] The ^{1}H NMR spectrum of **I** is shown in Figure 52. The ^{1}H and ^{13}C NMR data of **I** can be found in Table 1. [55]

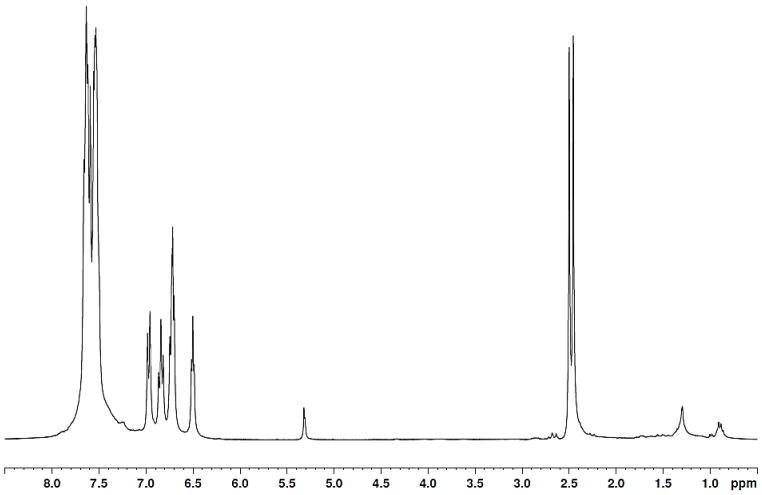

Figure 52. ^{1}H NMR spectrum of (**I**) in CD_2Cl_2.

Table 1. ^{1}H and ^{13}C NMR data for (**I**)

Position	δ (^{1}H)	δ (^{13}C)
1	-	66.14 (d, $^{1}J_{P-C}$ = 120.8)
2	6.74 (t, $J_{H-H} = J_{P-H}$ = 4.5)	126.30 (d, $^{2}J_{P-C}$ = 17.6)
3	6.64 (t, $J_{H-H} = J_{P-H}$ = 4.2)	105.00 (d, $^{3}J_{P-C}$ = 15.4)
4	7.7 (hidden)	120.82 (s)
5	6.97 (t, J_{H-H} = 7.2)	117.28 (s)
6	6.84 (t, J_{H-H} = 6.8)	117.91 (s)
7	7.04 (d, J_{H-H} = 7.9)	117.36 (s)
8[a]	-	137.79 (d, $^{2}J_{P-C}$ = 15.4)
9[a]	-	135.42 (d, $^{3}J_{P-C}$ = 14.3)
P-Me	2.50 (d, J_{H-H} = 12.6)	12.97 (d, $^{1}J_{P-C}$ = 62.6)
ipso-C	-	127.13 (d, $^{1}J_{P-C}$ = 87.8)
o-H, C[b]	7.52 – 7.55 (m)	132.68 (d, $^{2}J_{P-C}$ = 11.0)
m-H, C[b]	7.63-7.67 (m)	129.45 (d, $^{3}J_{P-C}$ = 12.1)
p-H, C	7.53 – 7.67 (m)	132.93 (d, $^{4}J_{P-C}$ = 3.3)

a. ^{13}C assignments of the C(8) and C(9) resonances may be reversed.

b. ^{13}C assignments of the *o*- and *m*-C resonances may be reversed.

3.1.2 Synthesis of 4,7-dimethylindene

Erker *et al.* reported a synthetic route to the synthesis of 4,7-dimethyl-indene via treatment of 2,5-hexandione with cyclopentadiene in methanol in the presence of sodium methoxide at ambient temperature (Figure 53).[92]

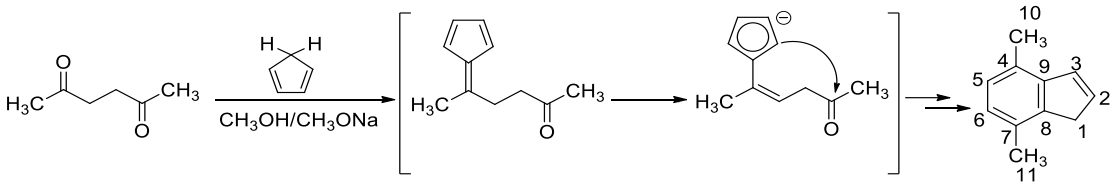

Figure 53. Synthesis of 4,7-dimethylindene.

As described in **2.3.1**, 2,5-hexandione was treated with freshly distilled cyclopentadiene in methanol in the presence of sodium methoxide at room temperature to afford 4,7-dimethylindene. A dark brown mixture was obtained, by liquid-liquid extraction using diethyl ether and water. 4,7-dimethylindene was isolated as a light yellow oil with high yield (84%), by simple distillation of the dark brown mixture.

The ^{1}H NMR spectrum is shown in Figure 54. The two singlet peaks at δ 2.51 and 2.61 were assigned for the methyl groups at positions 10 and 11, the broad peak at δ 3.44 to the two protons at position 1. The proton at position 2 appeared as a multiplet at δ 6.72, the proton at position 3 as a multiplet at δ 7.10 and the protons at positions 5 and 6 as a multiplet at δ 7.14-7.21.

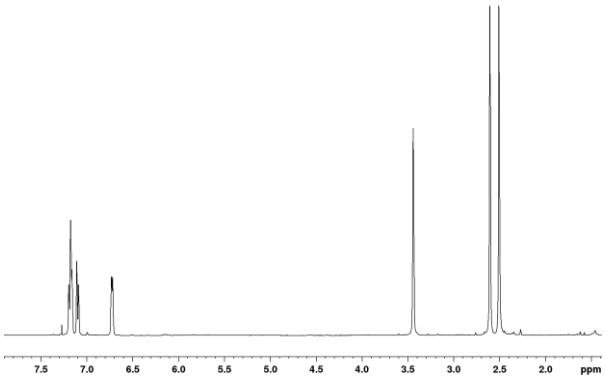

Figure 54. ^{1}H NMR spectrum of 4,7-dimethylindene in $CDCl_3$.

3.1.3 Syntheses of the two regioisomers of 4,7-dimethyl-1-$C_9H_5PPh_2$[93]

Fallis *et al.*[56] and Rufanov *et al.*[50] have earlier prepared (diphenylphosphino)-1-indene (1-$C_9H_5PPh_2$) and Curnow *et al.*[93] have earlier prepared (diphenylphosphino)-4,7-dimethyl-indene (4,7-dimethyl-1-$C_9H_5PPh_2$). The latter was characterized previously by ^{1}H, ^{13}C, and ^{31}P NMR spectroscopy, EI MS, and HR-MS,[93] but the crystal structure was not reported.[93] As described in **2.3.2**, 4,7-dimethylindene was deprotonated by *n*-butyllithium and the corresponding indenyl anion was treated with PPh_2Cl to afford a yellow solution of the two isomers of (diphenylphosphino)-4,7-dimethylindene (4,7-dimethyl-1-$C_9H_5PPh_2$) after filtration through a short Celite column (Figure 55).

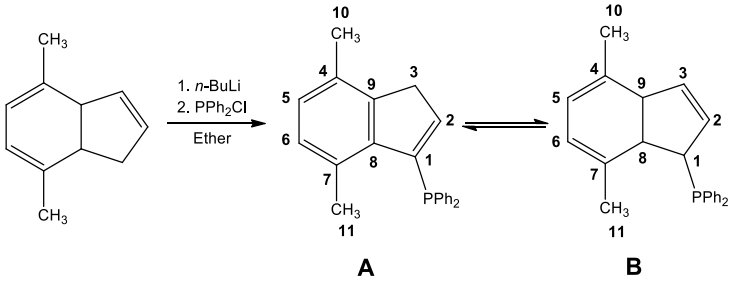

Figure 55. Synthesis of 4,7-dimethyl-1-$C_9H_5PPh_2$.

The ^{1}H NMR spectrum is shown in Figure 56. The two methyl groups at position 10 and 11 were readily identified as two singlet peaks at δ 2.32 and 2.75. A ^{31}P NMR spectrum (See Appendix, Figure A 1) exhibited two singlet peaks at δ −16.5 (isomer **A**) and −5.7 (isomer **B**). It was found that the ratio of the two regioisomers, isomer **A** and isomer **B**, varies randomly from batch to batch.

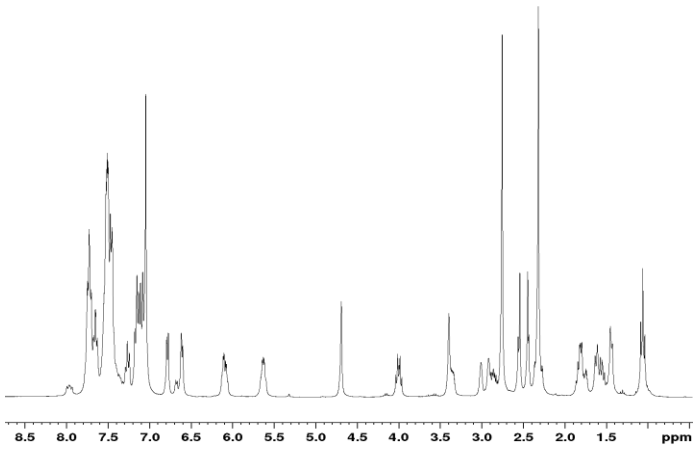

Figure 56. ^{1}H NMR spectrum of 4,7-dimethyl-1-$C_9H_5PPh_2$ in CD_2Cl_2.

One of the regioisomers, isomer **A**, was crystallized by slow evaporation of solvent, diethyl ether, from a mixture of two regioisomers and the structure is shown in Figure 57, important bond lengths and angles in Table 2 (refer to Figure 57 for the numbering system).

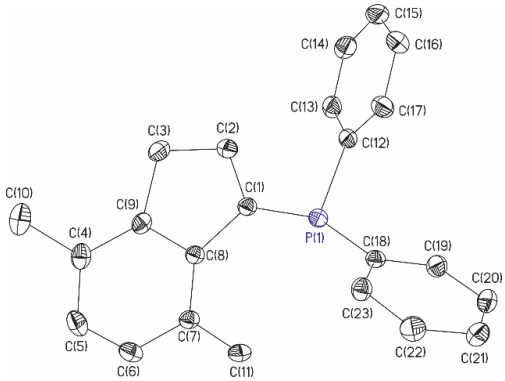

Figure 57. Molecular structure of 4,7-dimethyl-1-$C_9H_5PPh_2$.

Table 2. Selected bond lengths and angles of isomer **A** of (diphenylphosphino)-4,7-dimethyl-1-indene

Bond	Bond Length (Å)	Bond Angle	Bond Angle (°)
P(1)-C(1)	1.8301(17)	C(2)-C(1)-C(8)	107.76(14)
P(1)-C(12)	1.8358(17)	C(2)-C(1)-P(1)	124.55(13)
P(1)-C(18)	1.8294(17)	C(8)-C(1)-P(1)	127.37(11)
C(1)-C(2)	1.347(2)	C(3)-C(2)-C(1)	112.59(15)
C(1)-C(8)	1.487(2)	C(2)-C(3)-C(9)	102.55(13)
C(2)-C(3)	1.488(2)	C(5)-C(4)-C(9)	116.68(15)
C(3)-C(9)	1.498(2)	C(4)-C(5)-C(6)	121.14(17)
C(4)-C(5)	1.390(2)	C(7)-C(6)-C(5)	122.76(16)
C(4)-C(9)	1.385(2)	C(6)-C(7)-C(8)	116.77(15)
C(4)-C(10)	1.502(2)	C(7)-C(8)-C(9)	119.71(15)
C(5)-C(6)	1.386(3)	C(7)-C(8)-C(1)	132.55(15)
C(6)-C(7)	1.393(2)	C(9)-C(8)-C(1)	107.74(13)
C(7)-C(8)	1.403(2)	C(4)-C(9)-C(3)	127.72(15)
C(7)-C(11)	1.507(2)	C(4)-C(9)-C(8)	122.93(15)
C(8)-C(9)	1.410(2)	C(3)-C(9)-C(8)	109.34(14)

The P(1)-C(1) bond length of 1.8301(17) Å is shorter than the P(1)-Ph bond lengths (1.8326(17) Å). The C(1)-C(2) bond length (1.347(2) Å) is indicative of a double bound, and it was found that this bond length is the shortest bond length in the C_5 ring. The average of bond angles in C_5 ring is 107.99(74)°, as expected in a regular pentagon. The C-C bonds of the C_6 ring are all quite similar, varying between 1.386(3) and 1.410(2) Å. The average of bond angles in the C_6 ring is 119.99(99)°, which is expected from a hexagon. The bond length average of the C_6 ring (1.3947 Å) is considerably shorter than the one of C_5 ring (1.4462 Å). The C(4)-C(9) bond length is shorter than the one of C(4)-C(5), and the (4)-C(5) bond length is longer than the one of C(5)-C(6). The C(5)-C(6) bond length is shorter than the one of C(6)-C(7), and the C(6)-C(7) is shorter than the one of C(7)-C(8). The C(7)-C(8) is shorter than the one of C(8)-C(9).

3.1.4 Syntheses of the Phosphonium Salt (4,7-dimethyl-1-$C_9H_5PMePh_2$)I

As described in **2.3.3**, a white, air-sensitive precipitate of (4,7-dimethyl-1-$C_9H_5PMePh_2$)I was prepared by reacting a solution of (diphenylphosphino)-4,7-dimethyl-indene with MeI (Figure 58).

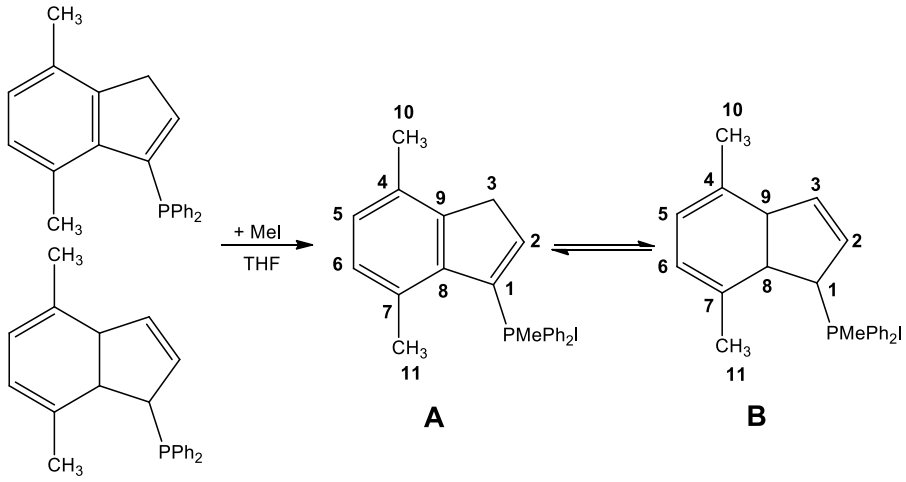

Figure 58. Syntheses of two regioisomers **A** and **B** of (4,7-dimethyl-1-$C_9H_5PMePh_2$)I.

As expected, ^{1}H NMR (Figure 59) and ^{31}P NMR (Figure 60) spectra showed that the (4,7-dimethyl-1-$C_9H_5PMePh_2$)I obtained was a mixture of regioisomers. Two singlet methyl resonances at positions 10 and 11 of isomer **B** were readily identified at δ 1.71 and 2.27. In a ^{1}H-^{31}P HMBC spectrum (Figure 61), both of these methyl resonances exhibited correlations with the ^{31}P resonance at δ 22.9 of isomer **B**. Two singlet methyl resonances of positions 10 and 11 of isomer **A** were also identified at δ 1.88 and 2.37 and, in a ^{1}H-^{31}P HMBC spectrum (Figure 61), both exhibited correlations with the ^{31}P resonance at δ 16.1 of isomer **A**. In the ^{1}H NMR spectrum, two methyl doublet resonances were observed at δ 2.49 (isomer **B**), and 3.02 (isomer **A**) with $^2J_{H\text{-}P}$ ~13.0 Hz, characteristic of a -PMe group. In view of the complexity of the ^{1}H NMR spectrum and extensive overlap, further assignments were not attempted.

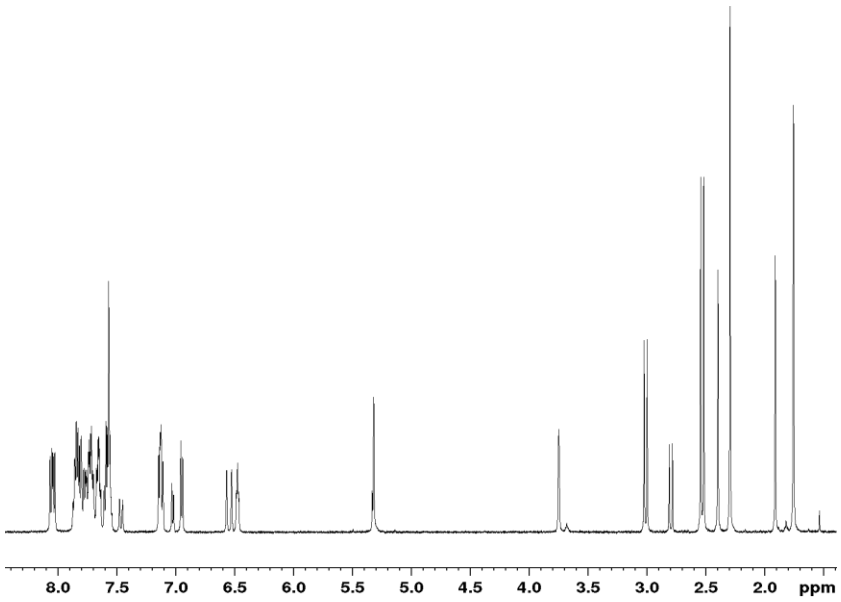

Figure 59. ^{1}H NMR spectrum of (4,7-dimethyl-$C_9H_5PMePh_2$)I in CD_2Cl_2.

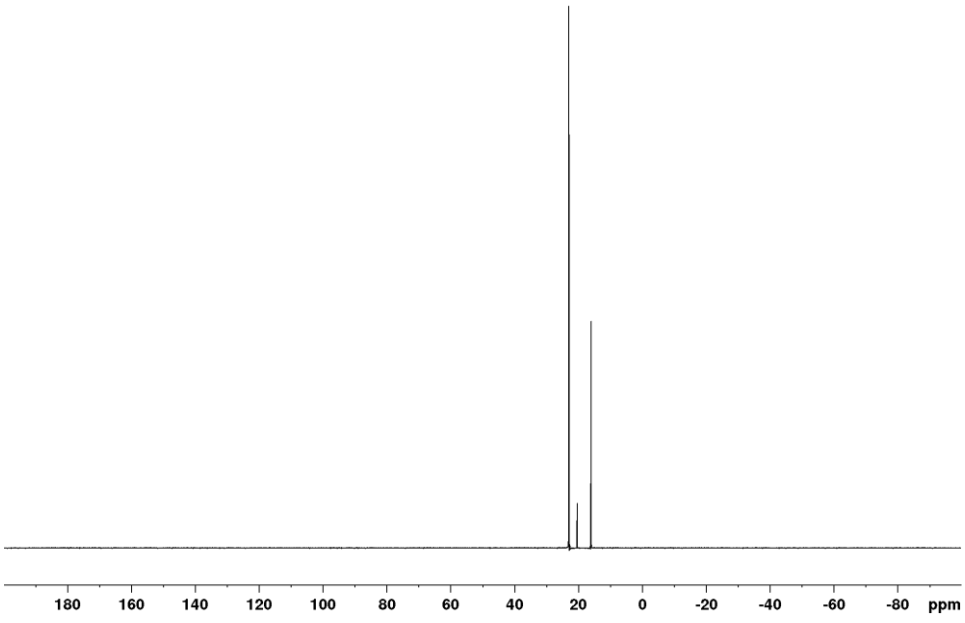

Figure 60. ^{31}P NMR spectrum of (4,7-dimethyl-$C_9H_5PMePh_2$)I in CD_2Cl_2.

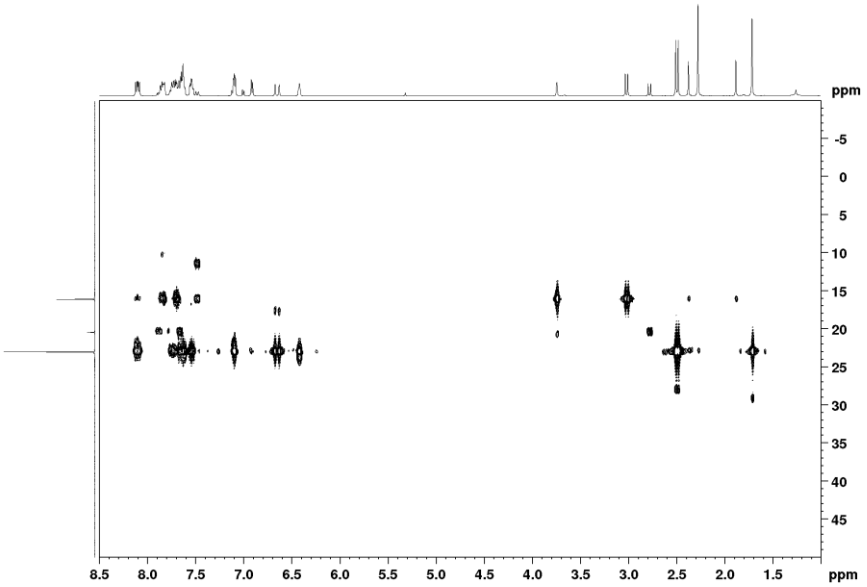

Figure 61. ^{1}H-^{31}P HMBC spectrum of (4,7-dimethyl-$C_9H_5PMePh_2$)I in CD_2Cl_2.

3.1.5 Synthesis of 4,7-dimethyl-1-$C_9H_4PMePh_2$ (II)

As described in **2.3.4**, 4,7-dimethyl-1-$C_9H_5PMePPh_2$ was readily deprotonated with an excess of NaH in THF to afford 4,7-dimethyl-1-$C_9H_4PMePPh_2$ (**II**) as a green, air-sensitive compound (Figure 62). A ^{1}H NMR spectrum of **II** is shown in Figure 63, and ^{1}H and ^{13}C NMR data can be found in Table 3.

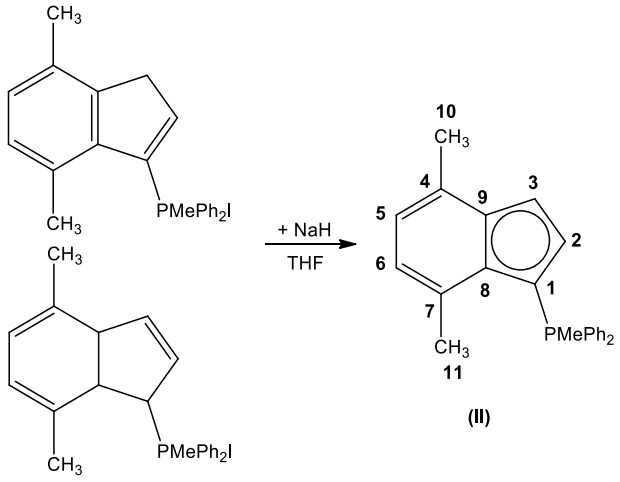

Figure 62. Synthesis of 4,7-dimethyl-1-$C_9H_4PMePh_2$ (**II**), showing numbering scheme.

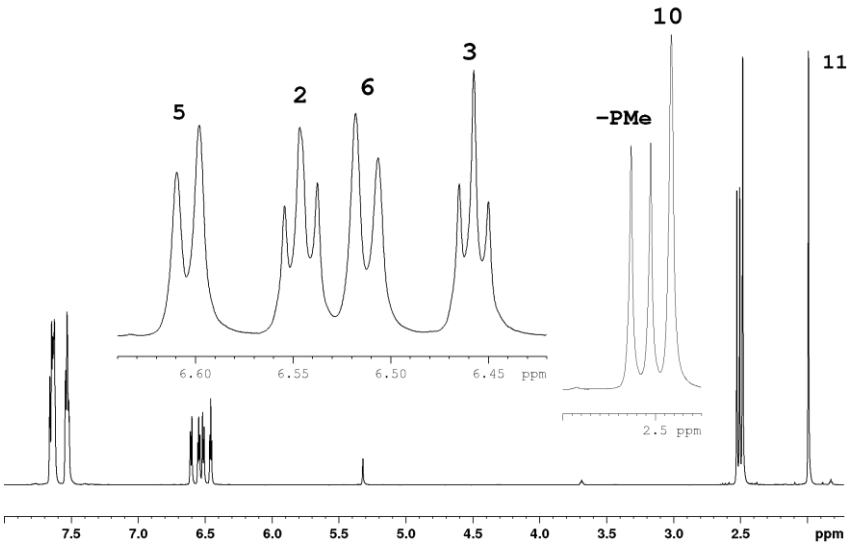

Figure 63. ^{1}H NMR spectrum of 4,7-dimethyl-1-$C_9H_4PMePh_2$ (**II**) in CD_2Cl_2.

Table 3. ^{1}H and ^{13}C NMR data of (**II**)

Position	δ (^{1}H)	δ (^{13}C)
1	-	67.46 (d, $^{1}J_{P-C}$ = 116.3)
2	6.55 (t, $J_{H-H} = J_{P-H}$ = 5.4)	128.51 (d, $^{2}J_{P-C}$ = 16.9)
3	6.46 (t, $J_{H-H} = J_{P-H}$ = 4.5)	104.53 (d, $^{3}J_{P-C}$ = 15.8)
4	-	126.95 (d, $^{3}J_{P-C}$ = 2.2)
5	6.60 (d, $^{3}J_{H-H}$ = 6.9)	118.47 (s)
6	6.51 (d, $^{3}J_{H-H}$ = 6.9)	120.36 (s)
7	-	124.23 (s)
8	-	134.18 (d, $^{3}J_{P-C}$ = 13.5)
9	-	139.06 (d, $^{3}J_{P-C}$ = 15.4)
10	2.48 (s)	19.50 (s)
11	1.99 (s)	23.70 (s)
P-Me	2.52 (d, $^{2}J_{P-H}$ = 12.8)	17.11 (d, $^{1}J_{P-C}$ = 63.4)
ipso-C	-	130.06 (d, $^{1}J_{P-C}$ = 87.7)
o-H, C	7.55 – 7.52 (m)	133.01 (d, $^{2}J_{P-C}$ = 9.9)
m-H, C	7.66 – 7.63 (m)	129.64 (d, $^{3}J_{P-C}$ = 12.1)
p-H, C	7.66 – 7.63 (m)	133.06 (d, $^{4}J_{P-C}$ = 3.3)

In the ^{1}H NMR spectrum of **II** (Figure 63), the -PMe resonance appears as a doublet at δ 2.52 ($^{3}J_{H-P}$ = 12.8 Hz); the value of $^{3}J_{H-P}$ is very similar to those reported for $CpPMePh_2$[22] and 1-$C_9H_5PR_3$ (R = Me, and Ph).[22] In the NOESY spectrum of **II** (Figure 64), a NOESY through space correlation between the doublet at δ 2.52 (P-Me) and a triplet at δ 6.55 was used to assign the latter to H(2). In the COSY spectrum (Figure 65), a COSY correlation between this triplet at δ 6.55 (H(2)) and the triplet at δ 6.46 was used to assign the latter to H(3). Similarly a NOESY correlation between the H(3) resonance at δ 6.46 and the methyl resonance at δ 2.28 permitted assignment of the latter to the methyl group at position 4. A NOESY correlation between the methyl resonance at δ 2.48 and the doublet at δ 6.60 was used to assign the latter to H(5), and assigning the methyl resonance at δ 2.48 resulted in assigning the singlet at δ 1.99 to the methyl group at position 7. The latter resonance exhibited just one NOESY correlation, with a proton at δ 6.51 which is assigned to H(6). ^{13}C NMR, HMBC, and HSQC spectra used for ^{13}C assignments may be found in Appendix, Figures A 2-A 4. By assigning all the protons and with the aid of HSQC and HMBC experiments all the carbons of **II** were assigned.

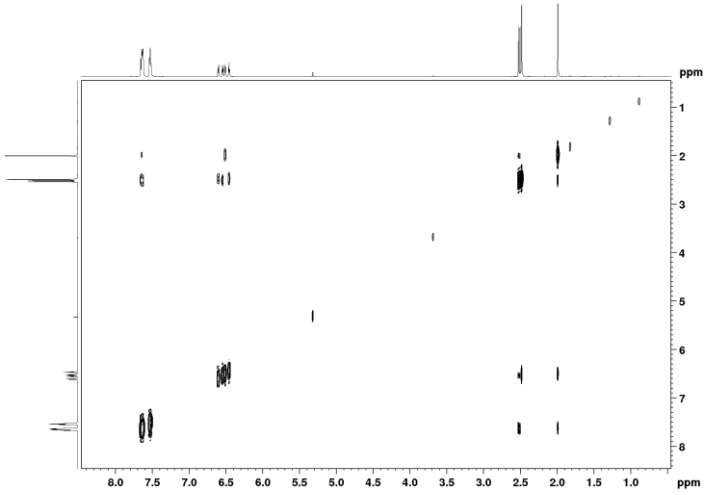

Figure 64. NOESY spectrum of 4,7-dimethyl-1-$C_9H_4PMePh_2$ (**II**) in CD_2Cl_2.

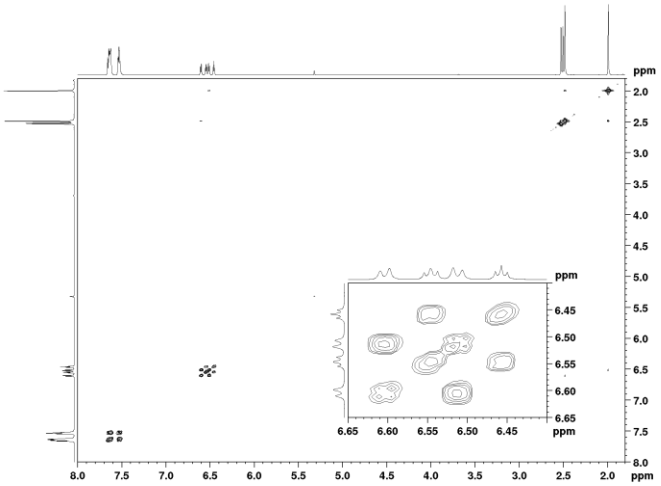

Figure 65. COSY spectrum of 4,7-dimethyl-1-$C_9H_4PMePh_2$ (**II**) in CD_2Cl_2.

The ^1H and ^{13}C chemical shifts and coupling constants of 4,7-dimethyl-1-$C_9H_4PMePh_2$ (**II**) are very similar to those of the analogous PHINs, 1-$C_9H_6P(CH_2Ph)Ph_2$,[50] 1-$C_9H_6P(CH_2C_6F_5)Ph_2$,[50] 1-$C_9H_6PMePh_2$ (**I**),[54,55] 1-$C_9H_6PMe_2Ph$,[54] and 1-$C_9H_6PPh_3$.[54] The ^{13}C chemical shift of the C(1) resonance of 4,7-dimethyl-1-$C_9H_4PMePh_2$ (**II**) (δ 67.46) is slightly downfield of those of 1-$C_9H_6P(CH_2Ph)Ph_2$ (δ 59.9),[50] $C_9H_6P(CH_2C_6F_5)Ph_2$ (δ 62.2),[50] 1-$C_9H_6PMePh_2$ (**I**) (δ 66.14),[54,55] 1-$C_9H_6PMe_2Ph$ (δ 66.69)[54] and 1-$C_9H_6PPh_3$ (δ 66.52)[54] but 11 ppm upfield than the C(1) resonance of $C_5H_4PMePh_2$ (δ 79.2).[22,39] The chemical shift of the ylidic carbon resonance of 4,7-dimethyl-1-$C_9H_4PMePh_2$ (**II**) is ~18.9 ppm upfield of that of the related resonance of 1-diphenylphosphinoind-2-ene (δ 48.6),[56] and the phosphorus carbon coupling constant in 4,7-dimethyl-1-$C_9H_4PMePh_2$ (**II**) (116.3 Hz) is significantly higher than that of 1-diphenylphosphinoind-2-ene (33.5)[56] which is consistent with previously reported PHIN ligands, 1-$C_9H_6P(CH_2Ph)Ph_2$,[50] 1-$C_9H_6P(CH_2C_6F_5)Ph_2$,[50] 1-$C_9H_6PMePh_2$ (**I**),[54,55] 1-$C_9H_6PMe_2Ph$[54] and 1-$C_9H_6PPh_3$.[54]

The ^{31}P chemical shift of 4,7-dimethyl-1-$C_9H_4PMePh_2$ (**II**) is δ 6.63 (See Appendix, Figure A 5), and is less shielded than the ^{31}P chemical shifts of 1-$C_9H_6PMePh_2$ (**I**) (δ 5.69),[54,55] and 1-$C_9H_6PMe_2Ph$ (δ 1.78)[54] but slightly more shielded than the ^{31}P chemical shifts of 1-$C_9H_6PPh_3$ (δ 10.39)[54] and $C_5H_4PMePh_2$ (δ 7.95).[22,39] The elemental analysis of **II** is in excellent agreement with calculated values. X-ray quality crystals of **II** were obtained by slow evaporation of solvent CH_2Cl_2, and the structure is shown in Figure 66 and important bond lengths in Table 4.

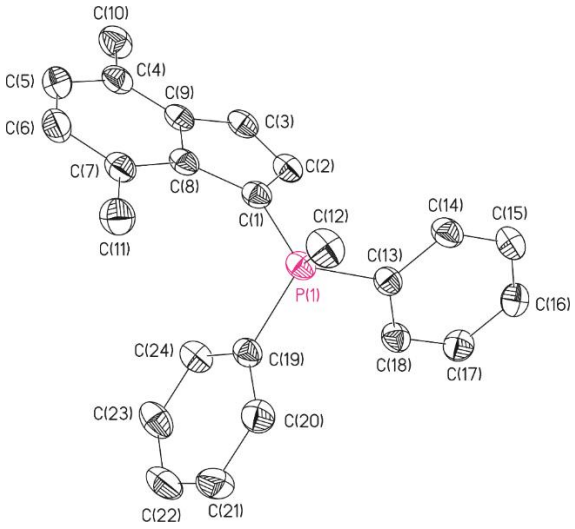

Figure 66. Molecular structure of 4,7-dimethyl-$C_9H_4PMePh_2$ (**II**).

The X-ray crystal structure showed that the P-C_9H_4 bond length of **II** is 1.7282(12) Å, significantly shorter than the corresponding P-Ph bonds. The latter average of 1.807 Å falls within the typical range for C-Ph single bonds in phenyl phosphonium ylides. On the other hand, the P-C_9H_6 bond length of **II** is significantly longer than the P=CH_2 bond in $Ph_3P=CH_2$ (1.66 Å).[11] The P=CH_2 bond is a typical example of a non-

resonance-stabilized ylide, and its P=CH_2 bond is believed to contain considerable double-bond character.[11]

Table 4. Selected bond lengths and angles of (**II**)

Bond	Bond Length (Å)	Bond Angle	Bond Angle (°)
P(1)-C(1)	1.7285(12)	C(2)-C(1)-C(8)	106.68(10)
P(1)-C(12)	1.8024(12)	C(2)-C(1)-P(1)	120.43(9)
P(1)-C(13)	1.8034(11)	C(8)-C(1)-P(1)	132.29(9)
P(1)-C(19)	1.8099(11)	C(3)-C(2)-C(1)	110.04(10)
C(1)-C(2)	1.4380(15)	C(2)-C(3)-C(9)	108.36(10)
C(1)-C(8)	1.4477(16)	C(5)-C(4)-C(9)	117.70(11)
C(2)-C(3)	1.3692(17)	C(4)-C(5)-C(6)	121.20(12)
C(3)-C(9)	1.4265(16)	C(7)-C(6)-C(5)	122.90(11)
C(4)-C(5)	1.3809(18)	C(6)-C(7)-C(8)	117.54(11)
C(4)-C(9)	1.4100(17)	C(7)-C(8)-C(9)	119.21(11)
C(4)-C(10)	1.5074(18)	C(7)-C(8)-C(1)	134.37(11)
C(5)-C(6)	1.3998(19)	C(9)-C(8)-C(1)	106.42(10)
C(6)-C(7)	1.3840(18)	C(4)-C(9)-C(3)	130.06(11)
C(7)-C(8)	1.4200(16)	C(4)-C(9)-C(8)	121.43(11)
C(7)-C(11)	1.5068(17)	C(3)-C(9)-C(8)	108.49(10)
C(8)-C(9)	1.4385(16)		

As a result, the P-C_9H_4 bond length of **II** is consistent with significant contribution from both the uncharged and the zwitterionic resonance structures **IIa** and **IIb** in Figure 67**.**

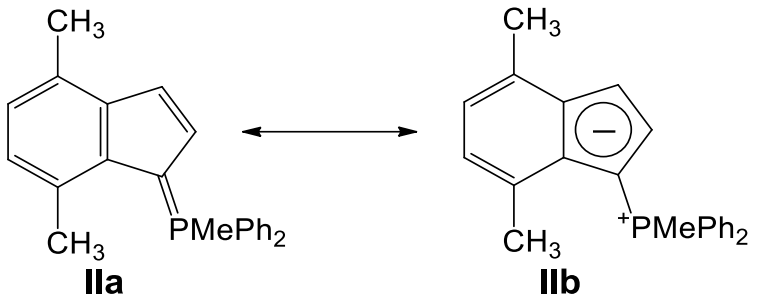

Figure 67. Resonance structure of 4,7-dimethyl-1-$C_9H_4PMePh_2$ (**II**).

3.2 Coordination of PHINs to Iridium and Rhodium Using $[M(COD)Cl]_2$ M = Ir, Rh

3.2.1 Reaction of $[Ir(COD)Cl]_2$ and I

The reaction of $[Ir(COD)Cl]_2$ with **I** in CH_2Cl_2 at room temperature was attempted, as described in **2.6.1**, and a reaction as in Equation 1 was anticipated.

$$[Ir(COD)Cl]_2 + \mathbf{I} \rightarrow [Ir(\eta^4\text{-}C_8H_{12})(\eta^5\text{-}\mathbf{I})]Cl \qquad (1)$$

The above reaction was carried out on an NMR scale in the glove box, a solution of $[Ir(COD)Cl]_2$ in CH_2Cl_2 and **I** being stirred for 1 min in a vial to give a deep dark red solution for which an NMR spectrum was run. As can be seen in Figure 68, the ^1H NMR spectrum of the product of reaction between $[Ir(COD)Cl]_2$ and **I** exhibited resonances of coordinated COD at δ 3.39 and 3.87 (=CH) and 0.70-2.3 (CH_2) in addition to an obvious 3H P-Me doublet at δ 3.01 (J_{PH} 13.2 Hz), apparent 1H PHIN ring resonances at δ 5.70, 6.12, 6.74, 7.07, 7.21 and 7.51, phenyl resonances at 7.60-7.90, COD vinyl resonances at δ 3.39 and 3.87 (the latter apparently exchange broadened; ratio of intensities ~5:1), and COD methylene resonances at δ 0.7-2.3.

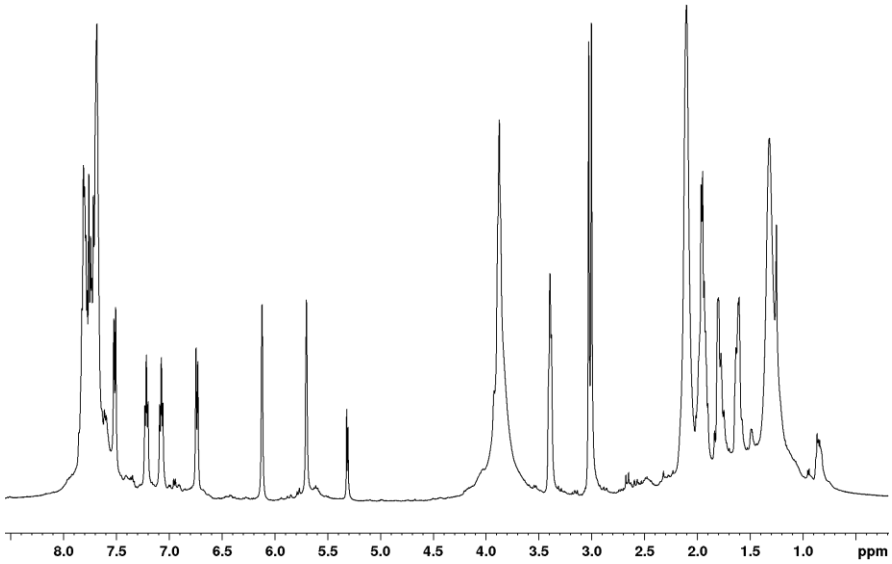

Figure 68. ^{1}H NMR spectrum of the product of reaction between $[Ir(COD)Cl]_2$ and (**I**) at room temperature in CD_2Cl_2.

A NOESY spectrum of this compound (Figure 69) indicated considerable exchange, which will be discussed below. ^{1}H and ^{13}C NMR assignments may be found in Table 5, and ^{13}C, ^{31}P, HMBC, and HSQC spectra may be found in the Appendix, Figures A 6-A 9. By assigning all the protons and with the aid of HSQC and HMBC experiments all the carbons of product of reaction between $[Ir(COD)Cl]_2$ and **I** were assigned.

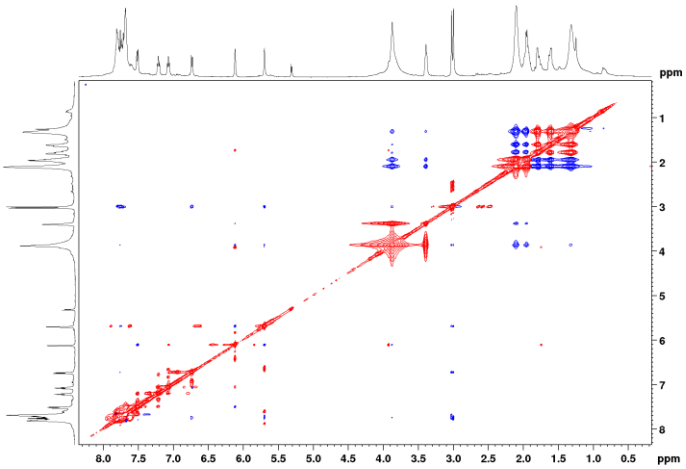

Figure 69. NOESY spectrum of the product of reaction between $[Ir(COD)Cl]_2$ and (**I**) in CD_2Cl_2.

Table 5. ^{1}H and ^{13}C NMR data for the product of reaction between $[Ir(COD)Cl]_2$ and (**I**)

Position	δ (^{1}H)	δ (^{13}C)
1	-	60.92 (d, $^{1}J_{P-C}$ = 101.8)
2	5.70 (br t)	89.52 (d, $^{2}J_{P-C}$ = 13.8)
3	6.12 (br t)	80.98 (d, $^{3}J_{P-C}$ = 9.6)
4	7.51 (d, J_{H-H} = 8.4)	123.69 (s)
5	7.21 (t, J_{H-H} = 7.2)	126.28 (s)
6	7.07 (t, J_{H-H} = 7.9)	128.05 (s)
7	6.74 (d, J_{H-H} = 8.6)	119.90 (s)
8[a]	-	107.51 (d, $^{2}J_{P-C}$ = 11.0)
9[a]	-	113.42 (d, $^{3}J_{P-C}$ = 9.3)
P-Me	3.01 (d, J_{H-P} = 13.2)	13.0 (d, $^{1}J_{P-C}$ = 61.3)
ipso-C	-	120.58 (d, $^{1}J_{P-C}$ = 90.2), 120.74 (d, $^{1}J_{P-C}$ = 88.3)
o-H, C[b]	7.6 – 7.9 (m)	133.26 (d, $^{2}J_{P-C}$ = 10.9), 133.51 (d, $^{2}J_{P-C}$ = 11.0)
m-H, C[b]	7.6 – 7.9 (m)	130.8 (d, $^{3}J_{P-C} \approx 13.5$), 130.7 (d, $^{3}J_{P-C} \approx 13.5$)
p-H, C	7.6 – 7.9 (m)	135.43 (d, $^{4}J_{P-C} \approx 2.5$), 135.55 (d, $^{4}J_{P-C} \approx 2.5$)
COD =CH	3.39 (m), 3.87 (m)	55.30 (s), 58.51 (s), ~60 (br)
COD CH_2	0.70 – 2.30 (m)	32.43 (s), 32.87 (s), 33.61 (s)

a. ^{13}C assignments of the C(8) and C(9) resonances may be reversed.

b. ^{13}C assignments of the *o*- and *m*-C resonances may be reversed.

The olefinic proton resonances of the cyclooctadiene are readily identified as they appear as two multiplets at δ 3.39 and 3.87 at room temperature while those of the CH_2 protons of the cyclooctadiene appear as multiplets at δ 0.7-2.3. The P-Me resonance appears as a doublet at δ 3.01 (J_{H-P} = 13.0 Hz), which is consistent with previous reported coupling constant values.[54,55] In the NOESY spectrum (Figure 69), a correlation between the P-Me resonance at δ 3.01 and a broad triplet at δ 5.70 is used to assign this peak to H(2), while in the COSY spectrum (Figure 70), a correlation between the latter resonance and the broad triplet at δ 6.12 is used to assign the latter peak to H(3). In the NOESY spectrum, a correlation between the resonance of H(3) and a doublet at δ 7.51 is used to assign the latter peak to H(4), while in the COSY spectrum, a correlation between this doublet of H(4) and a triplet at δ 7.21 is used to assign the latter resonance to H(5). Similar consideration of the COSY and NOESY data result in assignments of resonances at δ 7.07 and 6.74 to H(6) and H(7), respectively, conclusions which are confirmed by a correlation in the NOESY spectrum between the -PMe and H(7) resonances. The NOESY spectrum exhibited correlations between the COD olefinic resonances at δ 3.39 and δ 3.87 and between the resonances of H(2), H(3), H(4), and H(7) with the COD CH_2 resonances. ^{13}C NMR, HSQC and HMBC spectra were used for the ^{13}C assignments, while the ^{31}P NMR spectrum exhibited a single peak at δ 18.2. This is shifted 12.5 ppm downfield relative to free **I**, akin to formerly reported chromium phosphonium indenylide, and ruthenium phosphonium indenylide complexes.[54,55]

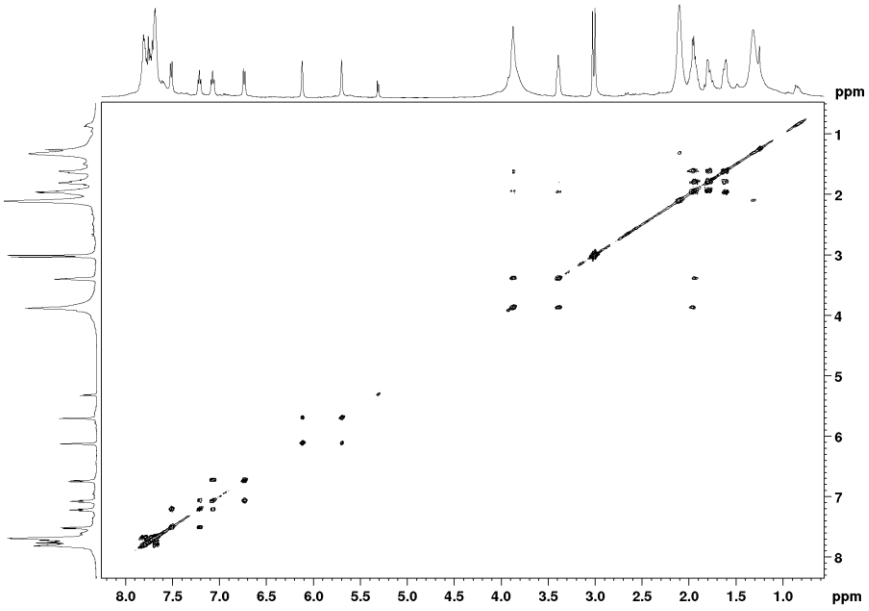

Figure 70. COSY spectrum of the product of reaction between $[Ir(COD)Cl]_2$ and (**I**) in CD_2Cl_2.

The four olefinic protons of cyclooctadiene are equivalent in $[Ir(\eta^4\text{-}C_8H_{12})Cl]_2$ and appeared in ^1H NMR spectrum (See Appendix, Figure A 10) at δ 4.23, but the olefinic protons of cyclooctadiene became inequivalent and shifted upfield upon coordination. It is difficult to compare the chemical shifts of CH_2 protons of cyclooctadiene in coordinated cyclooctadiene with non-coordinated cyclooctadiene because of the broadening of these peaks. Upon coordination of **I** to Ir, protons H(2) and H(3) shifted upfield and all carbons of the C_5 ring also shifted upfield. All carbons of the C_6 ring are shifted downfield, but there is no constant shielding or deshielding trend in chemical shifts of all protons of the C_6 ring as H(4), and H(7) shifted upfield, but H(5), and H(6) shifted downfield.

Confirming the formation of this cationic complex, a high resolution electrospray mass spectrum (HR-EMS) of the crude product exhibited a peak at m/z 615.17870 (calculated 615.17871) and with an appropriate isotope pattern (Figure 71). No iridium-containing species could be recognized in an HR-EMS operating in the negative mode, and thus the achiral complex is presumably not charged.

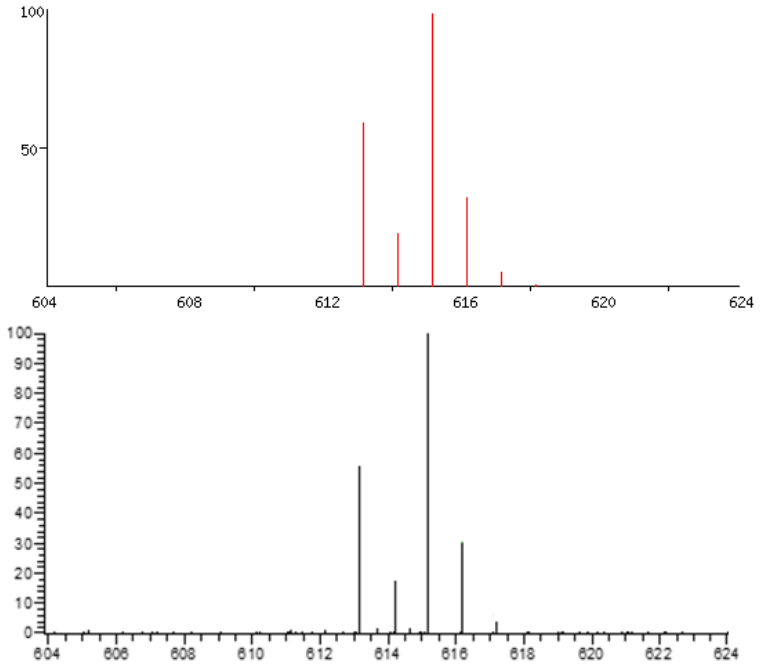

Figure 71. HR-EMS of $[Ir(COD)(I)]^+$ (bottom). The calculated isotope distribution is shown on top.

In view of the significant broadening of the COD vinyl resonance at δ 3.87 in Figure 68, the NMR spectrum of the product of the reaction between $[Ir(COD)Cl]_2$ and **I** was run at –65 °C, revealing that the broad peak at δ 3.87 decoalesced to two resonances at δ 3.64 and 3.79 while the other resonances in the spectrum changed relatively little (Figure 72). The intensities of the six 1H PHIN ring resonances, relative to the 3H P-Me

resonance, remained as above, and the ratios of intensities of the three COD vinyl resonances at δ 3.79, 3.64 and 3.31 were, respectively, ~2:4:2. These integrations confirm the presence in the reaction mixture of more than one type of COD group per PHIN ligand, as expected on the basis of the molar ratio of reactants added.

Indeed, the spectrum shown in Figure 72 suggests the presence of two different η^4-COD-iridium species, one in which the COD exists in an achiral environment, the other containing a planar chiral η^5-PHIN-Ir moiety such as the cation in [Ir(COD)(η^5-(**I**)]Cl.

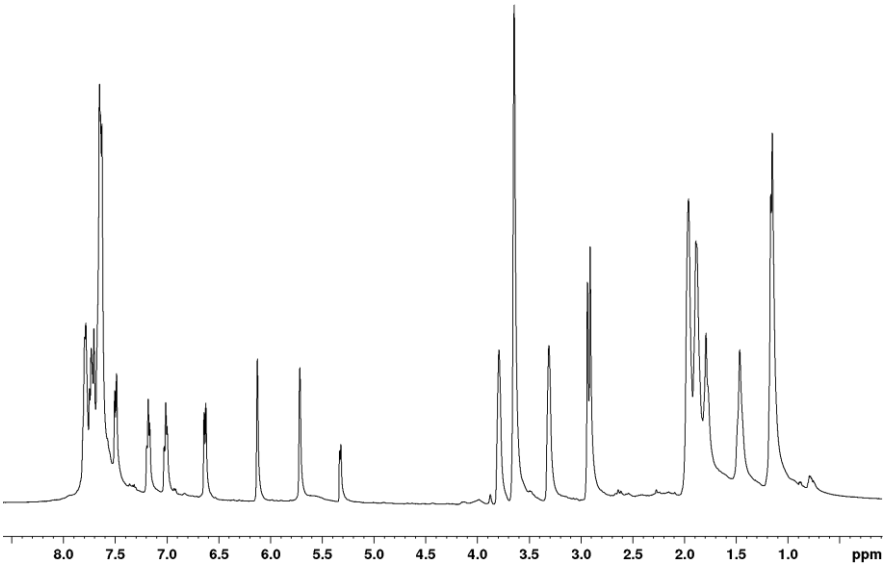

Figure 72. ^{1}H NMR spectrum of the product of reaction between $[Ir(COD)Cl]_2$ and (**I**) at –65 °C in CD_2Cl_2.

3.2.2 Synthesis of $[Ir(COD)(I\text{-}II)]BF_4$ (III-IV) and $[Rh(COD)(I\text{-}II)]BF_4$ (V-VI)

In a typical reaction, a mixture of $AgBF_4$ and either $[Ir(COD)Cl]_2$ or $[Rh(COD)Cl]_2$ in THF was stirred for 45 min and then filtered, and a solution containing

a PHIN in THF solution was added. The reaction mixture was then stirred for 4 h to afford [Ir(η^4-C_8H_{12})(**I-II**)]BF_4 (**III**, **IV**), or [Rh(η^4-C_8H_{12})(**I-II**)]BF_4 (**V**, **VI**) (Figure 73).

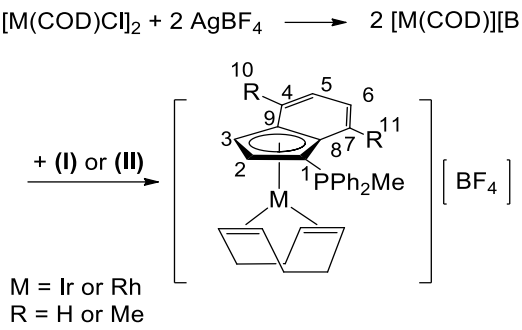

Figure 73. Synthesis of [M(η^4-C_8H_{12})(**I-II**)]BF_4 (**III**–**VI**), M = Ir or Rh.

3.2.3 Spectral Analysis of [Ir(η^4-C_8H_{12})(η^5-I)]BF_4 (III)

As described in **2.6.2**, **III** was synthesized, and ^{1}H and ^{13}C NMR assignments for **III** can be found in Table 6. In the ^{1}H NMR spectrum of **III** (Figure 74), the cyclooctadiene olefinic protons are readily identified as they appear as two multiplets at δ 3.39 and 3.89, while the CH_2 protons of the cyclooctadiene appear as multiplets from δ 1.58 to δ 2.0. The P-Me methyl resonance appears as a doublet at δ 2.85 with J_{H-P} = 13.3 Hz, which is consistent with previous reported coupling constant values.[54,55]

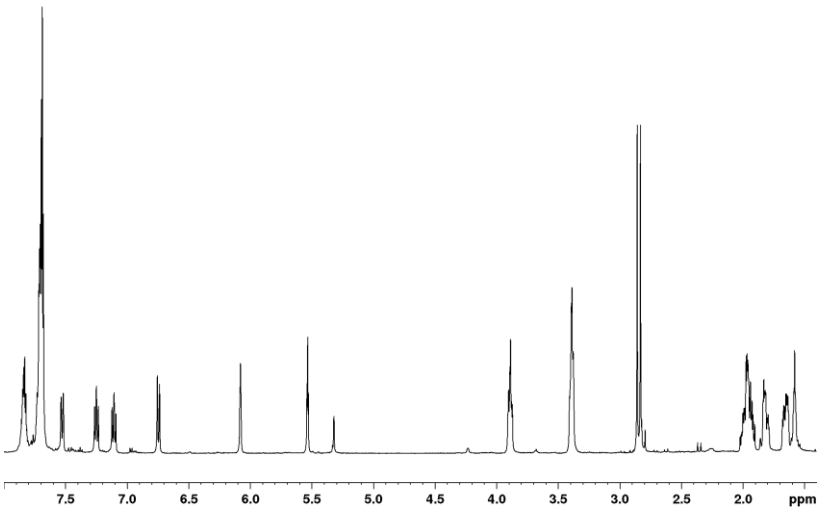

Figure 74. ^{1}H NMR spectrum of (**III**) in CD_2Cl_2.

In the NOESY spectrum of **III** (Figure 75), a correlation between the doublet at δ 2.85 and a triplet at δ 5.54 is used to assign the latter to H(2); in the COSY spectrum of **III** (Figure 76), a correlation between the triplet at δ 5.54 and the broad triplet at δ 6.08 is used to assign the latter to H(3).

Table 6. ^{1}H and ^{13}C NMR data of (**III**)

Position	δ (^{1}H)	δ (^{13}C)
1	-	60.76 (d, $^{1}J_{P-C}$ = 102.1)
2	5.54 (t, $J_{H-H} = J_{H-P}$ = 2.8)	89.30 (d, $^{2}J_{P-C}$ = 14.0)
3	6.08 (br t, $J_{H-H} = J_{H-P}$ = 4.8)	80.94 (d, $^{3}J_{P-C}$ = 9.6)
4	7.53 (d, J_{H-H} = 8.5)	123.74 (s)
5	7.24 (t, J_{H-H} = 7.4)	126.44 (s)
6	7.11 (t, J_{H-H} = 8.3)	128.24 (s)
7	6.75 (d, J_{H-H} = 8.7)	119.76 (s)
8[a]	-	107.65 (d, $^{2}J_{P-C}$ = 11.3)
9[a]	-	113.57 (d, $^{3}J_{P-C}$ = 9.4)
P-Me	2.85 (d, J_{H-P} = 13.3)	11.97 (d, $^{1}J_{P-C}$ = 62.5)
ipso-C	-	120.47 (d, $^{1}J_{P-C}$ = 90.6), 120.55 (d, $^{1}J_{P-C}$ = 88.8)
o-H, C[b]	7.68 – 7.73 (m)	133.15 (d, $^{2}J_{P-C}$ = 11.1), 133.31 (d, $^{2}J_{P-C}$ = 11.2)
m-H, C[b]	7.68 – 7.73 (m)	130.8 (d, $^{3}J_{P-C} \approx$ 13.4), 130.7 (d, $^{3}J_{P-C} \approx$ 12.9)
p-H, C	7.82 – 7.85 (m)	135.78 (d, $^{4}J_{P-C}$ = 3.0), 135.83 (d, $^{4}J_{P-C}$ = 2.8)
COD =CH	3.39 (m), 3.89 (m)	55.43 (s), 58.59 (s)
COD CH_2	1.58 – 2.0 (m)	33.56(s), 32.92 (s)

a. ^{13}C assignments of the C(8) and C(9) resonances may be reversed.

b. ^{13}C assignments of the *o*- and *m*-C resonances may be reversed.

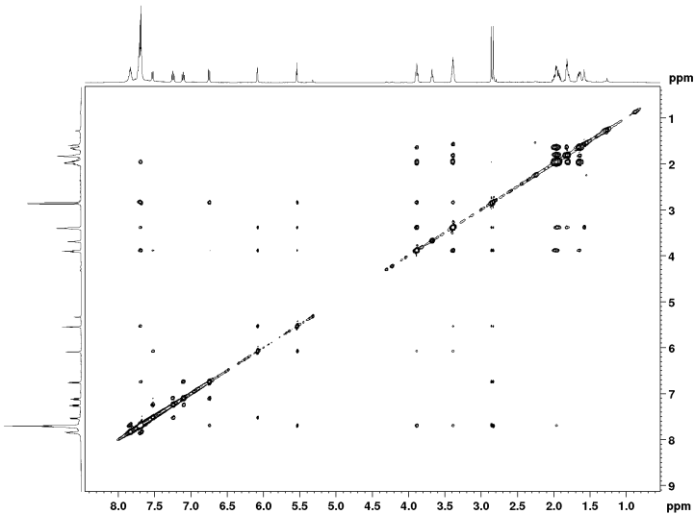

Figure 75. NOESY spectrum of (**III**) in CD_2Cl_2.

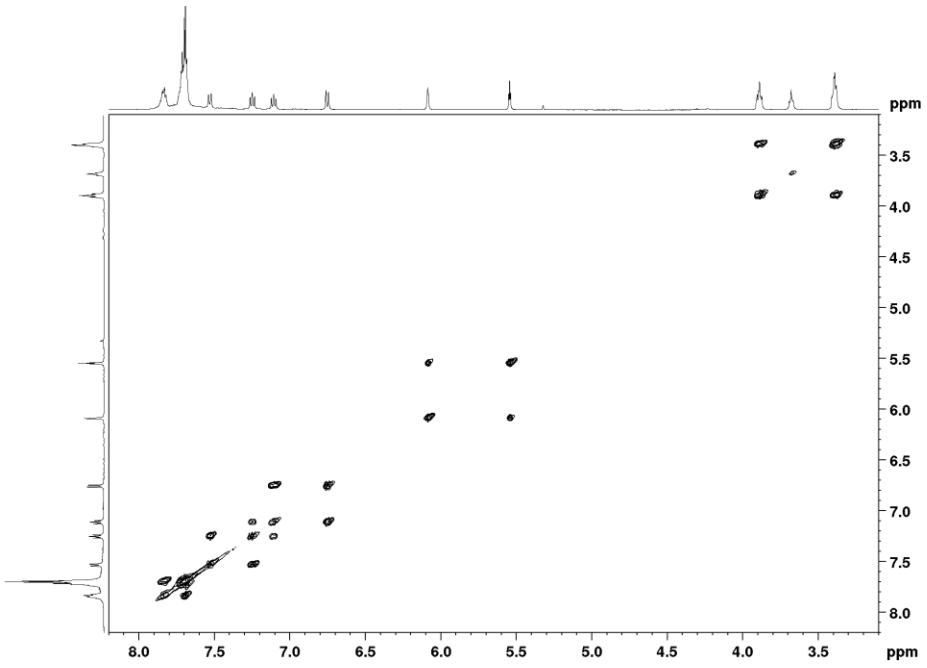

Figure 76. COSY spectrum of (**III**) in CD_2Cl_2.

Also in the NOESY spectrum of **III** (Figure 75), a correlation between the triplet at δ 6.08 (H(3)) and a doublet at δ 7.53 is used to assign this peak to H(4) and, in the

COSY spectrum (Figure 76), a correlation between the doublet at δ 7.53 (H(4)) and a triplet at δ 7.24 is used to assign this resonance to H(5). A COSY correlation between the triplet at δ 7.24 (H(5)) and a triplet at δ 7.11 is used to assign this triplet to H(6). The NOESY spectrum showed correlations between the two multiplets at δ 3.39 and δ 3.89 and H(2), H(3), H(4), H(7), and cyclooctadiene CH_2 resonance, confirming the proposed structure of [Ir(η^4-C_8H_{12})(η^5-**I**)]BF_4. ^{13}C NMR, HMBC, and HSQC spectra used for ^{13}C assignments (See Appendix, Figures A 11-A 13). The resonances of the cyclooctadiene olefinic protons are shifted upfield upon coordination, but it is difficult to compare the chemical shifts of the corresponding CH_2 protons with those of free cyclooctadiene because of the multiplicity of these peaks.

Upon coordination of **I** to Ir, protons H(2) and H(3) shifted upfield and all carbons of the C_5 ring also shifted upfield. All carbons of the C_6 ring are shifted downfield, but there is no shielding or deshielding trend in the chemical shifts of the protons of the C_6 ring as H(4), and H(7) shifted upfield, but H(5), and H(6) shifted downfield.

The ^{31}P NMR spectrum of **III** showed a 11 ppm downfield shift compared with free **I**, akin to previously reported chromium and ruthenium phosphonium indenylide complexes.[54,55] A ^{1}H-^{31}P HMBC spectrum (Figure 77) showed that the P-Me, H(2), H(3) and H(4) resonances were all coupled to the ^{31}P resonance at 16.98. The HR-EMS (Figure 78) of **III**, along with that calculated for [Ir(COD)(η^5-**I**)]$^+$, and elemental analyses of **III** are in excellent agreement with the structure proposed.

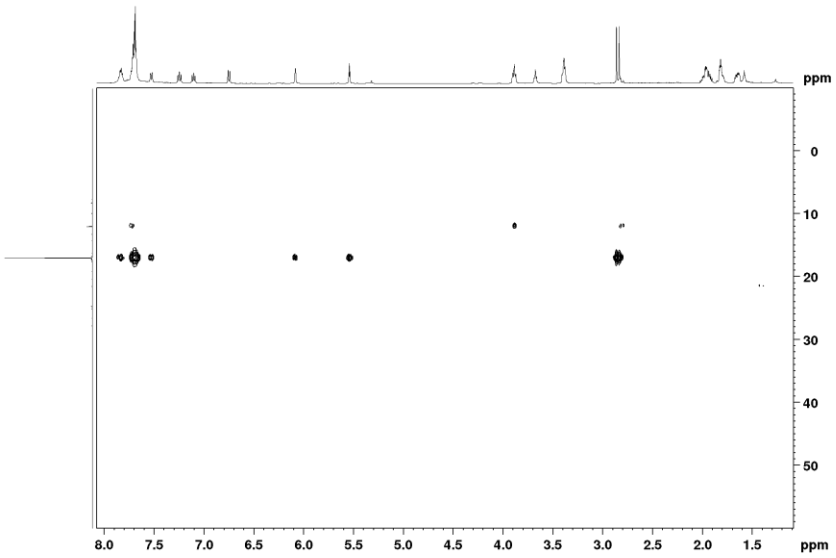

Figure 77. ^{1}H-^{31}P HMBC spectrum of (**III**) in CD_2Cl_2.

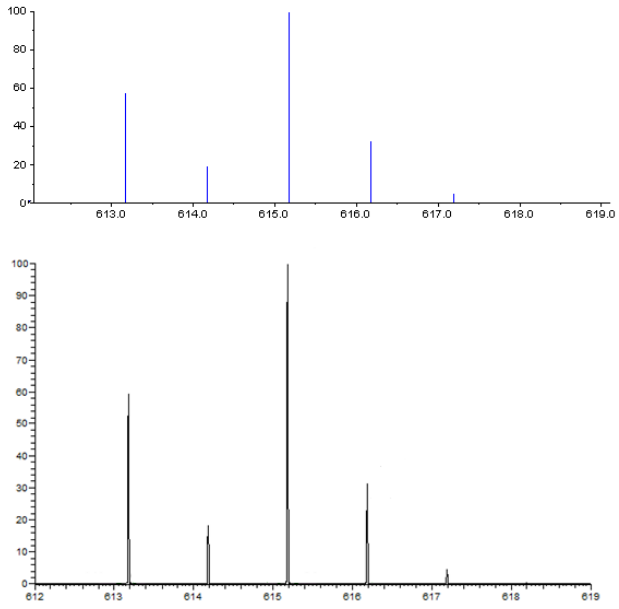

Figure 78. HR-EMS of [Ir(COD)(η^5-**I**)]$^+$ (bottom) and the calculated isotope distribution (top).

As the approach taken to synthesize **III** presumed the intermediacy of [Ir(COD)][BF_4], an attempt was made to prepare this complex in THF. Unfortunately, ^{1}H NMR and COSY spectra exhibited several broad peaks (See Appendix, Figure A 14, and A 15) and thus a mixture was present. It seems that this compound is not stable enough to be isolated and characterized.

3.2.4 Spectral Analysis of [Rh(η^4-C_8H_{12})(η^5-I)]BF_4 (V)

As described in **2.6.4**, **V** was synthesized, and ^{1}H and ^{13}C NMR assignments for **V** can be found in Table 7. In the ^{1}H NMR spectrum of **V** (Figure 79), the COD olefinic resonances are readily identified as they appear as two multiplets at δ 3.70 and 4.19. The COD CH_2 resonances appear as a sets of multiplets from δ 1.70 to δ 2.05. The P-Me resonance appears as a doublet at δ 2.80 (J_{H-P} = 13.5 Hz), consistent with previously reported coupling constants.[54,55]

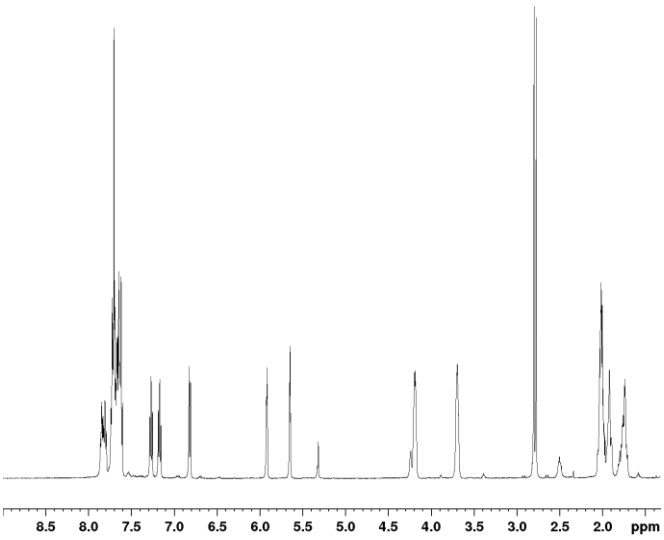

Figure 79. ^{1}H NMR spectrum of (**V**) in CD_2Cl_2.

Table 7. ^{1}H and ^{13}C NMR data of (**V**)

Position	δ (^{1}H)	δ (^{13}C)
1	-	65.94 (dd, $^{1}J_{P-C}$ = 100.0, J_{Rh-C} = 5.1)
2	5.94 (t, J_{H-H} = J_{H-P} = 2.5)	100.39 (dd, $^{2}J_{P-C}$ = 14.1, J_{Rh-C} = 4.6)
3	5.67 (t, J_{H-H} = J_{H-P} = 2.5)	83.28 (dd, $^{3}J_{P-C}$ = 10.7, J_{Rh-C} = 4.1)
4	7.64 (d, J_{H-H} = 7.1)	122.92 (s)
5	7.27 (t, J_{H-H} = 7.3)	124.99 (s)
6	7.17 (t, J_{H-H} = 7.5)	127.07 (s)
7	6.84 (d, J_{H-H} = 8.5)	118.20 (s)
8[a]	-	113.94 (br d, $^{2}J_{P-C}$ = 11.5, J_{Rh-C} < 1)
9[a]	-	117.85 (br d, $^{3}J_{P-C}$ = 9.4, J_{Rh-C} < 1)
P-Me	2.80 (d, J_{H-P} = 13.5)	11.47 (d, $^{1}J_{P-C}$ = 61.3)
ipso-C	-	121.00 (d, $^{1}J_{P-C}$ = 88.7), 121.21 (d, $^{1}J_{P-C}$ = 91.0)
o-H, C[b]	7.65 – 7.86 (m)	133.09 (d, $^{2}J_{P-C}$ = 5.2), 133.00 (d, $^{2}J_{P-C}$ = 4.8)
m-H, C[b]	7.65 – 7.86 (m)	130.75 (d, $^{3}J_{P-C}$ = 12.8), 130.88 (d, $^{3}J_{P-C}$ = 12.8)
p-H, C	7.65 – 7.86 (m)	~135.6 (m, Δδ < 0.01 ppm, $^{4}J_{P-C}$ < 1)
COD =CH	3.70 (m), 4.19 (m)	71.96 (d, $^{1}J_{Rh-C}$ = 13.7), 74.58 (d, $^{1}J_{Rh-C}$ = 13.5)
COD CH_2	1.70 – 2.05 (m)	32.38 (s), 30.85 (s)

a. ^{13}C assignments of the C(8) and C(9) resonances may be reversed.

b. ^{13}C assignments of the *o*- and *m*-C resonances may be reversed.

In the NOESY spectrum of **V** (Figure 80), a correlation between the -PMe doublet at δ 2.80 and a triplet at δ 5.94 is used to assign the latter to H(2), while a COSY correlation (Figure 81) between the resonance at δ 5.94 and a triplet at δ 5.67 is used to assign the latter to H(3). Similarly a NOSEY correlation between the resonance of H(3) and a doublet at δ 7.64 is used to assign the latter to H(4). Further COSY correlations between the doublet at δ 7.64 of H(4) and a triplet at δ 7.27, and between the latter and a triplet at δ 7.17 are used to assign the latter two resonances to H(5) and H(6),

respectively. A COSY correlation between the triplet at δ 7.17 of H(6) and a doublet at δ 6.84 is used to assign the latter resonance to H(7).

The NOESY spectrum also showed correlations between the COD olefinic and CH_2 resonances with the resonances of H(2), H(3), H(4) and H(7). ^{13}C NMR and HMBC, and HSQC spectra used to make ^{13}C assignments (See Appendix, Figures A 16-A 18).

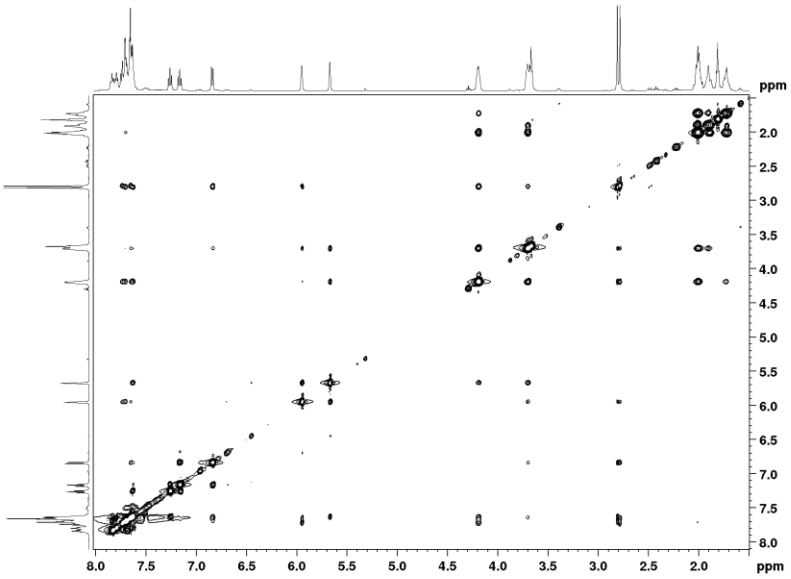

Figure 80. NOESY spectrum of (**V**) in CD_2Cl_2.

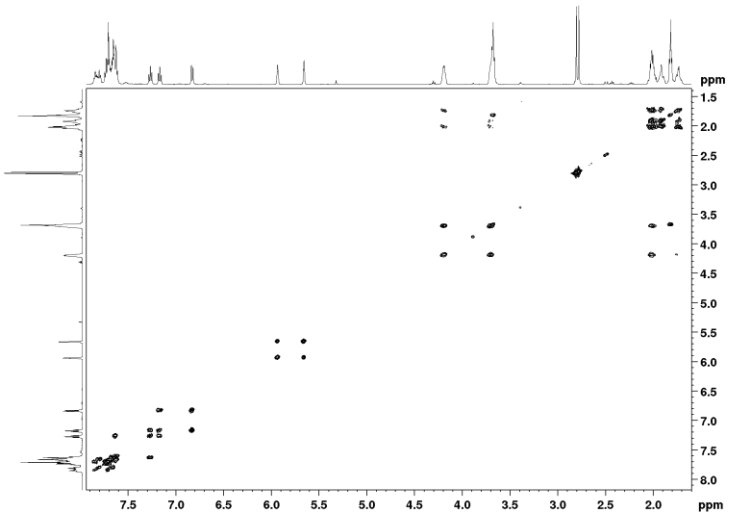

Figure 81. COSY spectrum of (**V**) in CD_2Cl_2.

Upon coordination of **I** to rhodium, the resonances of H(2) and H(3) and of all carbons of the C_5 ring shifted upfield. All carbons of the C_6 ring shifted downfield; H(4), and H(7) shifted upfield but H(5), H(6) shifted downfield.

The ^{31}P NMR spectrum of **I** showed a 11.5 ppm downfield shift compare with **I**, akin to formerly reported chromium phosphonium indenylide,[55] and ruthenium phosphonium indenylide complexes.[54] A ^{1}H-^{31}P HMBC (Figure 82) showed that the P-Me, H(2), H(3), H(4), and *p*-H resonances were coupled with the phosphonium resonance at δ 17.15. A HR-EMS (Figure 83) of **V**, along with that calculated for $[Rh(COD)(\eta^5\text{-}\mathbf{I})]^+$ and elemental analyses of **V** are in excellent agreement.

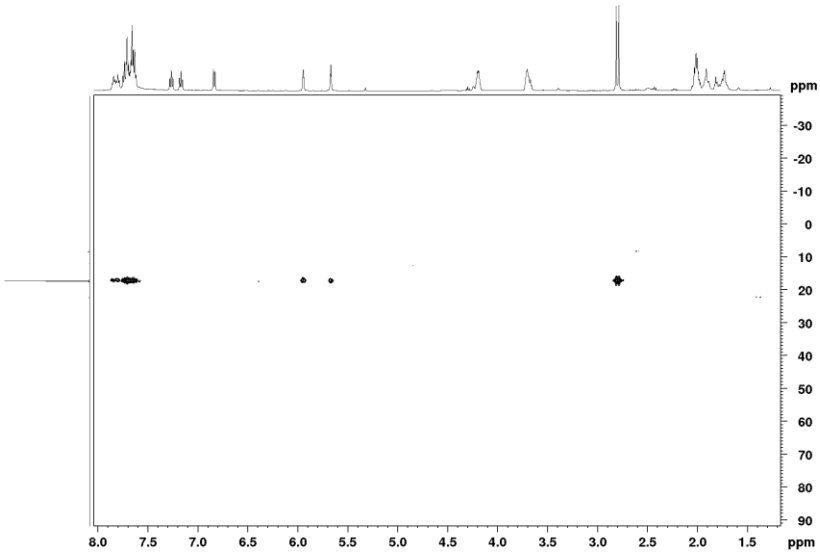

Figure 82. ^{1}H-^{31}P HMBC spectrum of (**V**) in CD_2Cl_2.

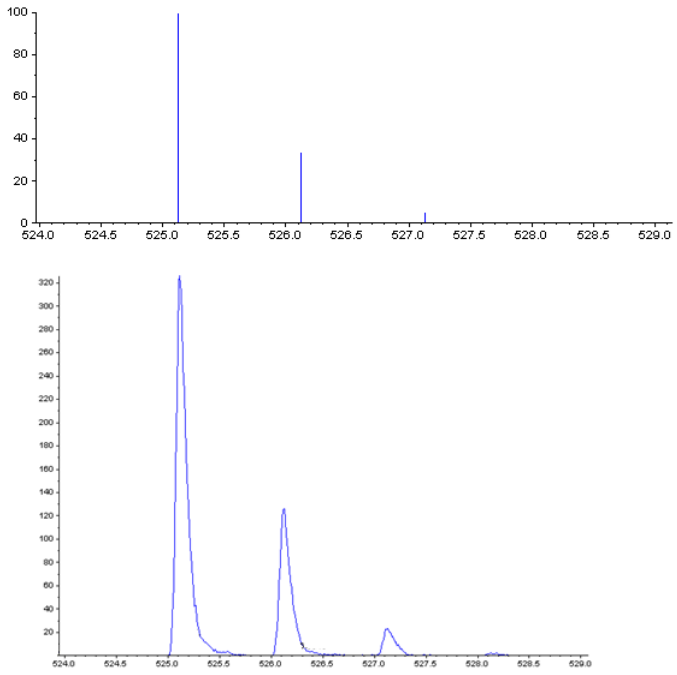

Figure 83. HR-EMS of $[Rh(COD)(\eta^5$-**I**$)]^+$ (bottom) and the calculated isotopic distribution (top).

As with the iridium analogue, isolation of [Rh(COD)][BF_4] in THF was attempted in order to establish its role as an intermediate in the formation of [Rh(COD)(η^5-**I**)][BF_4]. In contrast to [Ir(COD)][BF_4], [Rh(COD)][BF_4] was stable enough to be isolated and characterized and ^{1}H NMR and COSY spectra (See Appendix, Figure A 19, and A 20) of the compound were obtained. In a ^{1}H NMR spectrum, the COD CH_2 resonances appeared as two multiplets at δ 1.67 and 2.53, while the COD olefin resonance appeared as a broad peak at δ 4.19. A COSY spectrum showed a correlation between olefinic resonance and the CH_2 resonance at δ 2.53, consistent with the structure proposed.

3.2.5 Spectral Analysis of [Ir(η^4-C_8H_{12})(η^5-II)]BF_4 (IV)

Complex **IV** was synthesized as described in **2.6.3**, and a ^{1}H spectrum is shown in Figure 84, ^{1}H and ^{13}C NMR assignments for **IV** can be found in Table 8.

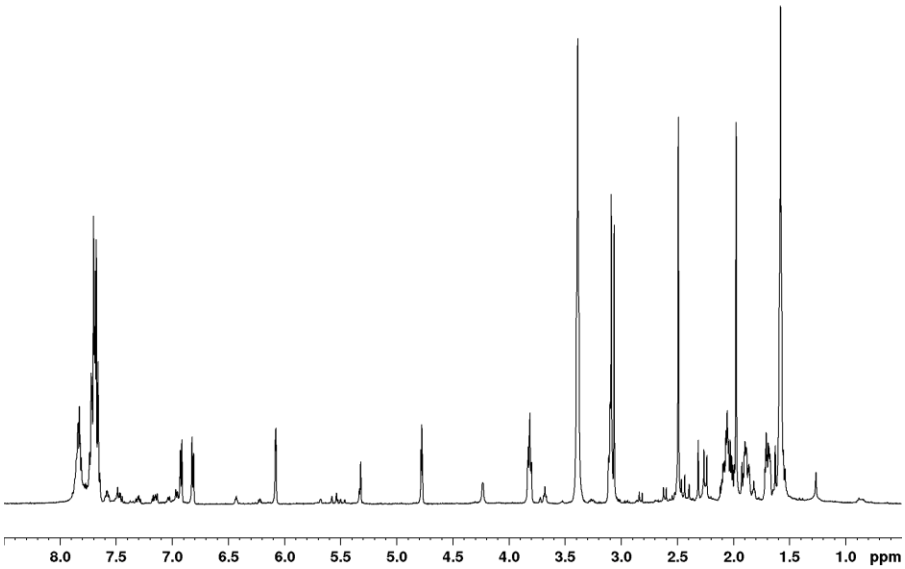

Figure 84. ^{1}H NMR spectrum of (**IV**) in CD_2Cl_2.

In the ^{1}H NMR spectrum of **IV**, the olefinic resonances of the COD ligand are readily identified as they appear as multiplets at δ 3.39 and 3.81. The CH_2 resonances of the COD ligand appear as multiplet in the region δ 1.54-2.0 while the -PMe resonance appears as a doublet at δ 3.07 with 13.1 Hz coupling constant, consistent with previous reported coupling constant values.[54,55]

Table 8. ^{1}H and ^{13}C NMR data of (**IV**)

Position	δ (^{1}H)	δ (^{13}C)
1	-	61.34 (d, $^{1}J_{P-C}$ = 100.1)
2	4.77 (t, J_{H-H} = J_{H-P} = 3.5)	91.36 (d, $^{2}J_{P-C}$ = 15.6)
3	6.08 (t, J_{H-H} = J_{H-P} = 2.3)	81.27 (d, $^{3}J_{P-C}$ = 10.5)
4	-	130.90 (s)
5	6.92 (d, $^{3}J_{H-H}$ = 6.8)	125.64 (s)
6	6.82 (d, $^{3}J_{H-H}$ = 6.8)	129.2 (s)
7	-	127.65 (s)
8[a]	-	104.37 (d, $^{2}J_{P-C}$ = 10.1)
9[a]	-	114.5 (d, $^{3}J_{P-C}$ = 9.3)
10	2.49 (s)	18.84 (s)
11	1.97 (s)	23.21 (s)
P-Me	3.07 (d, $^{2}J_{H-P}$ = 13.1)	16.9 (d, $^{1}J_{P-C}$ = 63.8)
ipso-C	-	122.00 (d, $^{1}J_{P-C}$ = 91.6), 122.21 (d, $^{1}J_{P-C}$ = 87.9)
o-H, C[b]	7.64-7.76 (m)	133.2 (d, $^{2}J_{P-C}$ = 10.1), 133.0 (d, $^{2}J_{P-C}$ = 10.7)
m-H, C[b]	7.64-7.76 (m)	130.74 (d, $^{3}J_{P-C}$ = 12.6), 131.08 (d, $^{3}J_{P-C}$ = 12.9)
p-H, C	7.76-7.89 (m)	135.61(d, $^{4}J_{P-C}$ = 2.9), 135.74 (d, $^{4}J_{P-C}$ = 3.1)
COD =CH	3.39 (m), 3.81 (m)	59.29 (s), 54.00 (s)
COD CH_2	1.54 - 2.0 (m)	33.27 (s), 32.99 (s)

a. ^{13}C assignments of the C(8) and C(9) resonances may be reversed.

b. ^{13}C assignments of the *o*- and *m*-C resonances may be reversed.

NOESY and COSY spectra of **IV** are shown in Figures 85 and 86, respectively, and an NOESY correlation in the former between the -PMe doublet at δ 3.07 and a triplet at δ 4.77 is used to assign the latter to H(2). A COSY correlation between the triplet at δ 4.77 and a triplet at δ 6.08 is used to assign the latter to H(3). In the NOESY spectrum, a correlation between the resonance of H(3) and a singlet at δ 2.49 is used to assign the latter to CH_3(10), while a NOESY correlation between the singlet at δ 2.49 and a doublet at δ 6.92 is used to assign the latter to H(5); a COSY correlation between the resonance of H(5) and a doublet at δ 6.82 is used then to assign the latter to H(6). We also note correlations in the NOESY spectrum of **IV** (Figure 85) between the two multiplets at δ 3.39 and δ 3.81 and H(2), H(3), CH_3(10), CH_3(11), CH_3(12) and CH_2 of the cyclooctadiene, confirming the proposed structure of **IV**. ^{13}C NMR and HMBC, and HSQC spectra used for ^{13}C assignments (See Appendix, Figures A 21-A 23). With the aid of HSQC and HMBC experiments, all the carbons of **IV** were assigned.

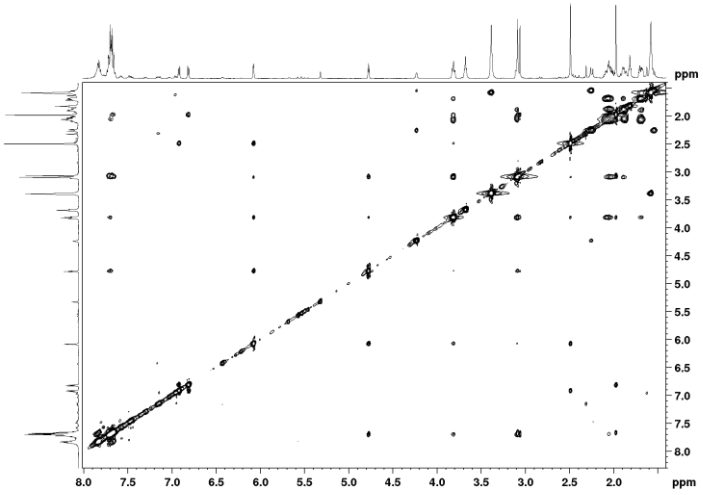

Figure 85. NOESY spectrum of (**IV**) in CD_2Cl_2.

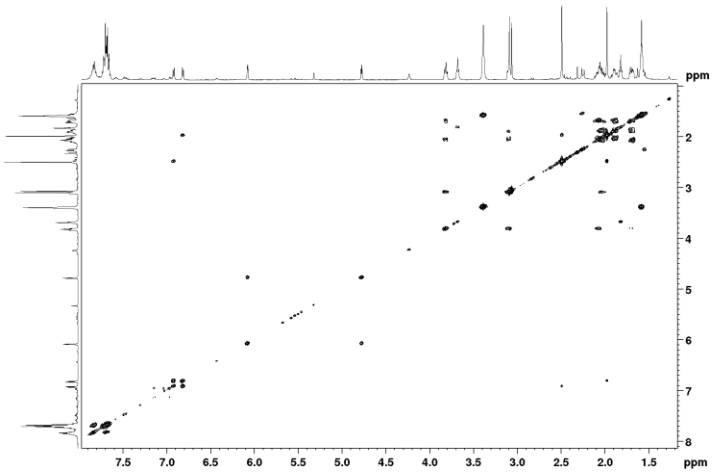

Figure 86. COSY spectrum of (**IV**) in CD_2Cl_2.

The COD olefinic resonances are shifted upfield upon coordination, but it is difficult to compare the chemical shifts of the CH_2 protons of coordinated cyclooctadiene and free cyclooctadiene because of the complexity of these peaks. Upon coordination of **II** to Ir, protons H(2) and H(3) and all carbons of the C_5 ring shifted upfield. The chemical shifts of two methyl groups at position 10 and 11 did not change significantly, but the P-Me resonance shifted 0.55 ppm downfield. All carbons of the C_6 ring are shifted downfield, as did H(5) and H(6).

The ^{31}P NMR spectrum of **IV** showed a 12 ppm downfield shift of the ^{31}P resonance compared with **II**, akin to formerly reported chromium[55] and ruthenium phosphonium indenylide,[54] complexes. A ^{1}H-^{31}P HMBC (Figure 87) showed that the P-Me, H(2), H(3), and *o*, *m*, *p*-H resonances correlated with the phosphonium ^{31}P resonance at 17.59. The HR-EMS (Figure 88) of **V**, along with that calculated for [Ir(COD)(η^5-**II**)]$^+$ and elemental analyses of **IV** are in excellent agreement.

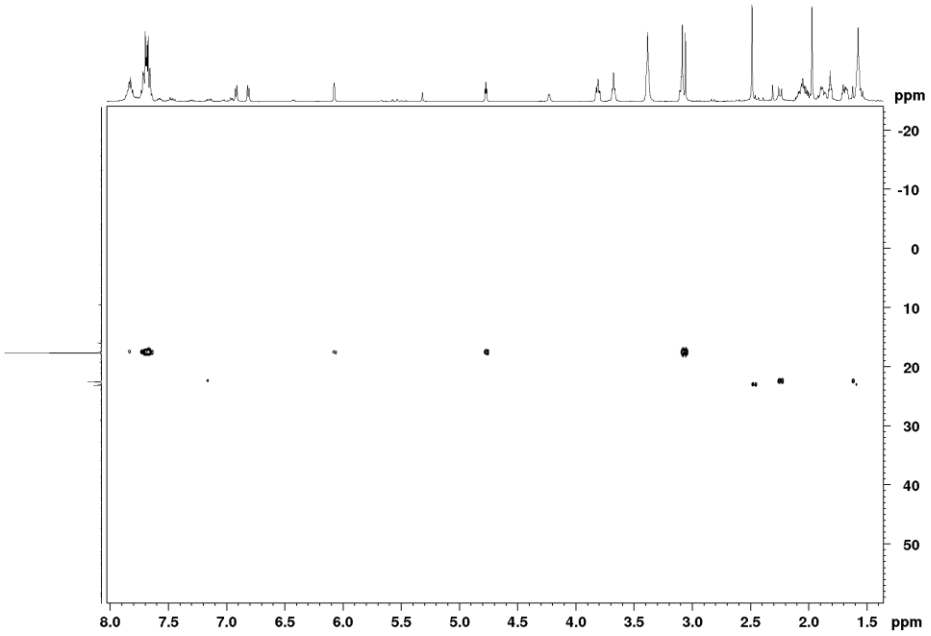

Figure 87. ^{1}H-^{31}P HMBC spectrum of (**IV**) in CD_2Cl_2.

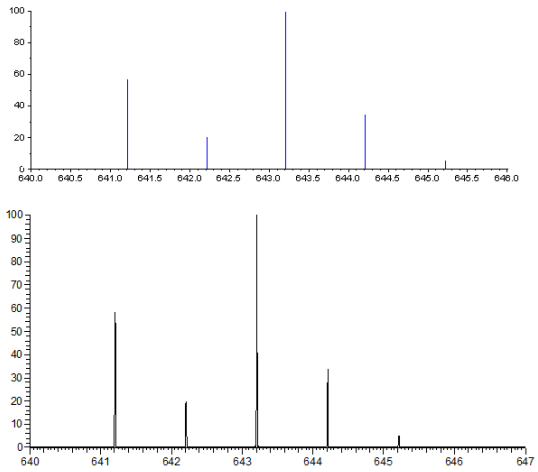

Figure 88. HR-EMS of [Ir(COD)(η^5-**II**)]$^+$ (bottom), and the calculated isotopic distribution (top).

3.2.6 Spectral Analysis of $[Rh(\eta^4\text{-}C_8H_{12})(\eta^5\text{-}II)]BF_4$ (VI)

As described in **2.6.5**, **VI** was synthesized, and ^1H and ^{13}C NMR assignments for **VI** can be found in Table 9. In the ^1H NMR spectrum of **VI** (Figure 89), the olefinic protons of cyclooctadiene are readily identified as they appear as two multiplets at δ 3.39 and 4.18. The CH_2 protons of cyclooctadiene appear as a sets of multiplet from δ 1.53 to δ 1.87 and from δ 2.06 to δ 2.17. The P-Me methyl resonance appears as a doublet at δ 3.02 with $J_{H\text{-}P}$ = 13.0 Hz, consistent with previous reported coupling constant values.[54,55]

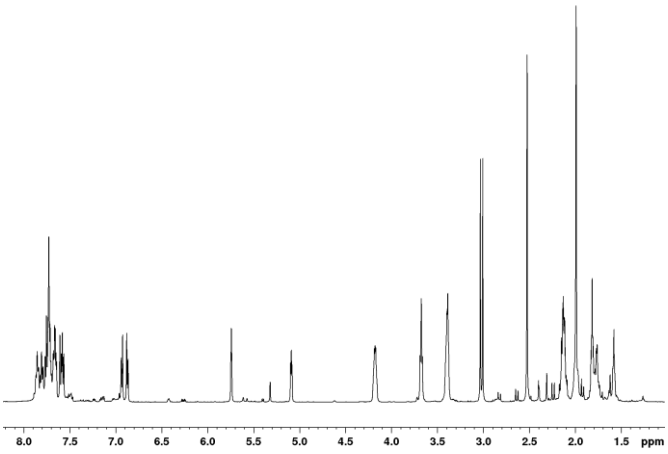

Figure 89. ^1H NMR spectrum of (**VI**) in CD_2Cl_2.

Table 9. ^{1}H and ^{13}C NMR data of (**VI**)

Position	δ (^{1}H)	δ (^{13}C)
1	-	66.91 (dd, $^{1}J_{P-C}$ = 99.3, J_{Rh-C} = 4.9)
2	5.09 (t, J_{H-H} = J_{H-P} = 4.5)	101.80 (dd, $^{2}J_{P-C}$ = 15.6, J_{Rh-C} = 4.0)
3	5.74 (t, J_{H-H} = J_{H-P} = 2.7)	83.51 (dd, $^{3}J_{P-C}$ = 11.5, J_{Rh-C} = 3.7)
4	-	130.78 (s)
5	6.93 (d, $^{3}J_{H-H}$ = 7.0)	124.5 (s)
6	6.87 (d, $^{3}J_{H-H}$ = 7.1)	128.7 (s)
7	-	126.08 (s)
8[a]	-	110.43 (br dd)
9[a]	-	118.12 (dd, $^{4}J_{P-C}$ = 9.6, J_{Rh-C} = 1.5)
10	2.52 (s)	19.11 (s)
11	1.99 (s)	23.17 (s)
P-Me	3.02 (d, $^{2}J_{H-P}$ = 13.0)	16.2 (d, $^{1}J_{P-C}$ = 63.1)
ipso-C	-	122.80 (d, $^{1}J_{P-C}$ = 92.2), 122.90 (d, $^{1}J_{P-C}$ = 88.1)
o-H, C[b]	7.56-7.68 (2 br d)	132.8 (d, $^{2}J_{P-C}$ = 10.6), 133.1 (d, $^{2}J_{P-C}$ = 10.3)
m-H, C[b]	7.56-7.68 (2 br t)	130.64 (d, $^{3}J_{P-C}$ = 12.9) 131.02, (d, $^{3}J_{P-C}$ = 12.8)
p-H, C	7.79-7.87 (2 br t)	135.42 (d, $^{4}J_{P-C}$ = 2.8), 135.56 (d, $^{4}J_{P-C}$ = 2.8)
COD =CH	3.39 (m), 4.18 (m)	70.17 (d, $^{1}J_{Rh-C}$ = 14.1), 75.68 (d, $^{1}J_{Rh-C}$ = 13.8)
COD CH_2	1.53-1.87 (m)	31.04 (s), 33.0 (s)

a. ^{13}C assignments of the C(8) and C(9) resonances may be reversed.

b. ^{13}C assignments of the *o*- and *m*-C resonances may be reversed.

In the NOESY spectrum of **VI** (Figure 90), a correlation between the doublet at δ 3.02 and a triplet at δ 5.09 is used to assign this peak to H(2), while in the COSY spectrum of **VI** (Figure 91), a COSY correlation between this triplet at δ 5.09 (H2) and the triplet at δ 5.74 is used to assign this peak to H(3). In the NOESY spectrum of **VI** (Figure 90), a correlation between the triplet at δ 5.74 (H(3)) and a singlet at δ 2.52 is used to assign this peak to CH_3(10). Similarly a NOESY correlation between the singlet at δ 2.52 and a doublet at δ 6.93 is used to assign this peak to H(5), while a COSY correlation (Figure 91) between this doublet at δ 6.93 and the doublet at δ 6.87 is used to

assign this peak to H(6). The NOESY spectrum also exhibited correlations between the multiplets of the olefinic hydrogen of COD at δ 3.39, and δ 4.18 with the resonances of H(2), H(3), CH_3(10), CH_3(11), CH_3(12) and CH_2 of the cyclooctadiene, confirming the proposed structure of **VI**. ^{13}C NMR and HMBC, and HSQC spectra were used for ^{13}C assignments (See Appendix, Figures A 24-A 26).

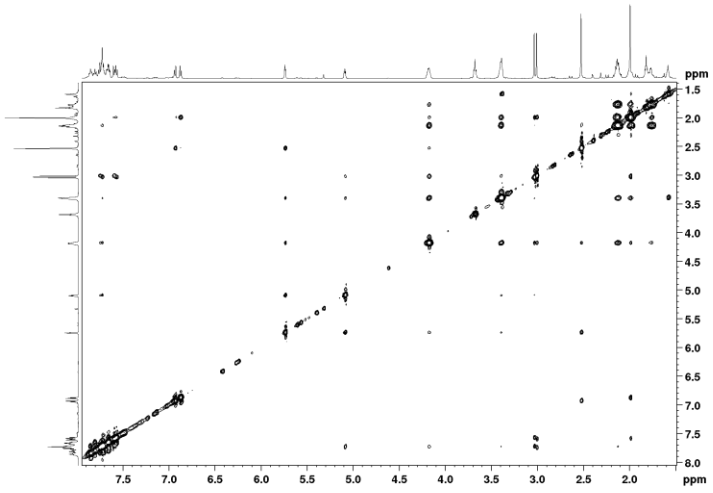

Figure 90. NOESY spectrum of (**VI**) in CD_2Cl_2.

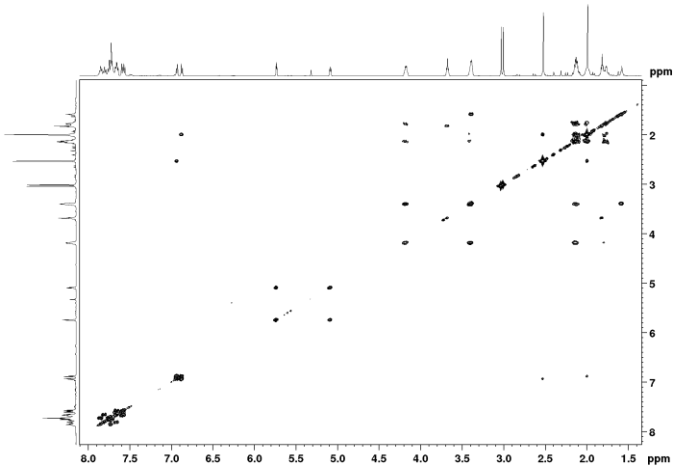

Figure 91. COSY spectrum of (**VI**) in CD_2Cl_2.

Upon coordination of **II** to Rh, the resonances of H(2) and H(3) and the resonances of all carbons of the C_5 ring shifted upfield. The chemical shift of the methyl group at position 11 did not change, but that of the methyl group at position 10 shifted 0.04 ppm downfield. The chemical shifts of the P-Me group shifted 0.50 ppm downfield on coordination. All carbons of **VI** at positions 4, 5, 6, and 7 shifted downfield, and the chemical shifts of the two protons at position 5 and 6 shifted downfield, as well.

The ^{31}P chemical shift of **VI** was 11.04 ppm downfield compared with free **II**, akin to previously reported chromium[55] and ruthenium phosphonium indenylide, complexes.[54] A ^{1}H-^{31}P HMBC (Figure 92) showed that the P-Me, H(2), H(3), and *o*, *m*, *p*-H protons correlated with the ^{31}P resonance at 17.68. The HR-EMS (Figure 93) of **VI**, along with that calculated for [Rh(COD)(η^5-**II**)]$^+$, and elemental analyses of **VI** are in excellent agreement with the proposed structure.

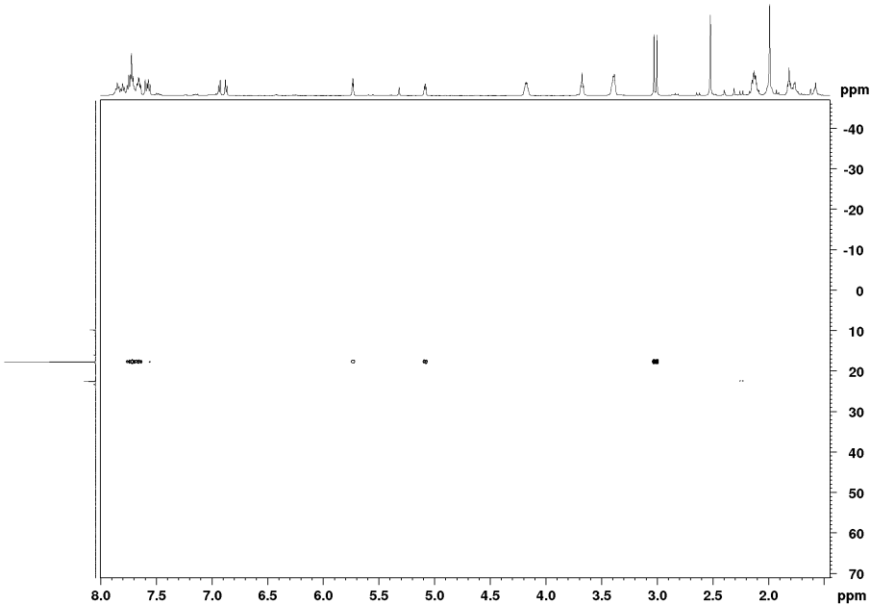

Figure 92. ^{1}H-^{31}P HMBC spectrum of (**VI**) in CD_2Cl_2.

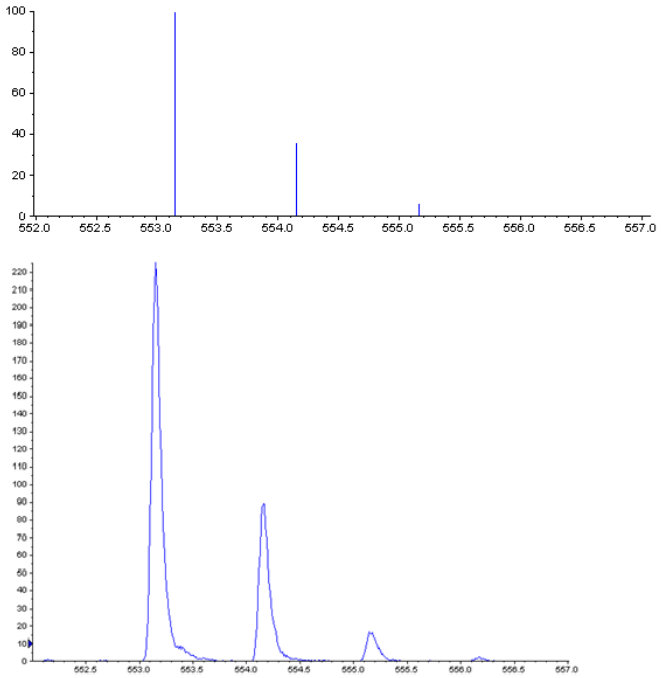

Figure 93. HR-EMS of [Rh(COD)(η^5-**II**)] (bottom), and the calculated isotopic distribution (top).

3.3 Attempted Oxidation Addition of MeI and $PhCH_2Cl$ to [M(η^4-C_8H_{12})(η^5-(I-II))]BF_4, M = Ir and Rh (III-VI)

It was expected that iridium(I) and rhodium(I) complexes **III-VI** would undergo oxidative addition reactions with MeI and $PhCH_2Cl$ (Figure 94).

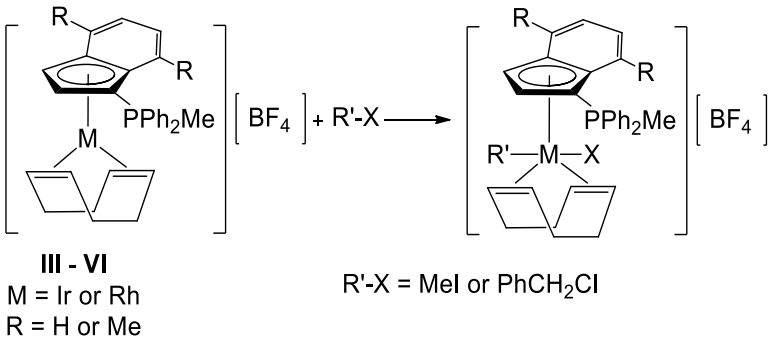

Figure 94. Oxidative addition of R'-X to (**III-VI**).

As described in **2.7.1**, a mixture of **III**, MeI and CD_2Cl_2 in an NMR tube was shaken for 5 min and NMR spectra were run, but both ^{1}H and ^{13}P NMR spectra indicated that no reaction had occurred after ~15 min (See Appendix, Figure A 27 and A 28). After 8 days, however, the ^{1}H and ^{31}P NMR spectra showed that the starting material had been consumed (See Appendix, Figure A 29 and A 30) and crystals had formed in the NMR tube. The crystals were isolated and a crystal structure was obtained, as shown in Figure 95. The crystal structure revealed that the products was $[IrMeI(\eta^4\text{-}C_8H_{12})(\mu\text{-}I)]_2$, suggesting that oxidation addition had occurred but not to form a complex of **I**. Selected bond lengths and angles can be found in Table 10.

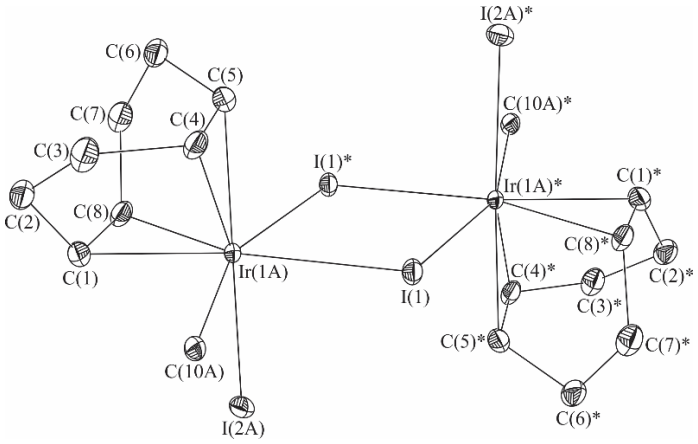

Figure 95. Molecular structure of $[IrMeI(\eta^4\text{-}C_8H_{12})(\mu\text{-}I)]_2$.

Similar experiments with **V** and **VI** also proved unsuccessful. As described in **2.7.2** and **2.7.3**, mixtures of MeI and either **V** or **VI** in CD_2Cl_2 in NMR tubes were shaken for 5 min and both ^{1}H and ^{31}P NMR spectra were obtained after 15 min, but no reaction had occurred in either cases after ~15 min (See Appendix, Figures A 31-A 34).

As described in **2.7.4**, **2.7.5**, and **2.7.6**, similar NMR experiments involving $PhCH_2Cl$ and **III**, **V**, and **VI** also failed to yield any products of oxidative addition; see Appendix, Figures A 35-A 40 which exhibit only the resonance of the starting compounds.

Table 10. X-ray data for $[IrMeI(\eta^4\text{-}C_8H_{12})(\mu\text{-}I)]_2$

Bond	Bond Length (Å)	Bond Angle	Bond Angle (°)
Ir(1A)-C(10A)	2.149(8)	I(1)-Ir(1A)-I(1)*	80.870(18)
Ir(1A)-C(8)	2.190(8)	C(10A)-Ir(1A)-I(2A)	84.0(2)
Ir(1A)-C(1)	2.197(8)	C(4)-Ir(1A)-I(2A)	160.4(2)
Ir(1A)-C(4)	2.211(8)	C(10A)-Ir(1A)-C(8)	115.9(3)
Ir(1A)-C(5)	2.219(8)	C(10A)-Ir(1A)-C(1)	78.9(3)
Ir(1A)-I(1)	2.6996(6)	C(4)-Ir(1A)-C(5)	36.3(3)
Ir(1A)-I(2A)	2.7177(6)	Ir(1A)-I(1)-Ir(1A)*	99.130(18)
Ir(1A)-I(1)*	2.8502(6)	C(4)-Ir(1A)-I(1)*	115.0(2)
I(1)-Ir(1A)*	2.8502(6)	C(5)-Ir(1A)-I(1)*	80.0(2)
C(1)-C(8)	1.415(12)	C(8)-Ir(1A)-C(1)	37.6(3)
C(1)-C(2)	1.518(11)	C(8)-Ir(1A)-C(4)	94.6(3)
C(2)-C(3)	1.525(13)	C(8)-Ir(1A)-C(5)	79.8(3)
C(3)-C(4)	1.520(12)	C(1)-Ir(1A)-C(4)	79.8(3)
C(4)-C(5)	1.381(12)	C(1)-Ir(1A)-C(5)	88.0(3)
C(5)-C(6)	1.525(12)	C(8)-C(1)-C(2)	121.9(7)
C(6)-C(7)	1.538(12)	C(8)-C(1)-Ir(1A)	70.9(5)
C(7)-C(8)	1.496(12)	C(7)-C(8)-Ir(1A)	112.5(6)

3.4 Attempted Reaction of H_2 and III or V

It was anticipated that complexes **III**–**VI** would react with H_2 to form $[M(H)_2(\eta^5$-(**I**-**II**))]BF_4, M = Ir and Rh, and cyclooctane or cyclooctene (Figure 96).

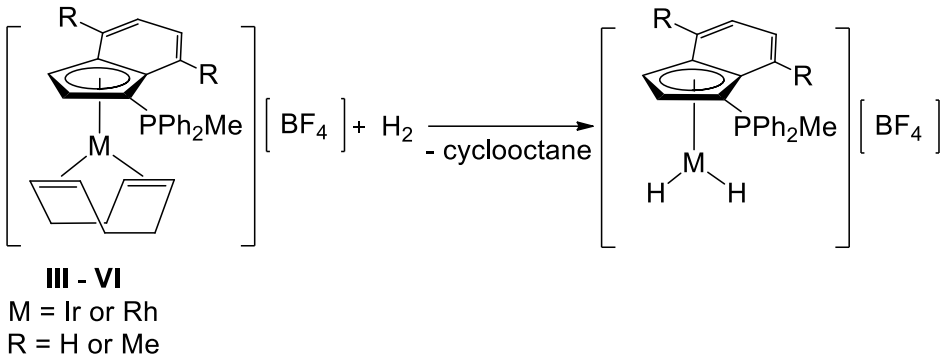

Figure 96. Reaction of H_2 and (**III**-**VI**).

As described in **2.8.1**-**2.8.3**, a reaction of **V** with H_2 gas at one bar for 24 h at room temperature resulted in no color change. Removal of solvent under reduced pressure gave a green solid, but both ^1H and ^{13}P NMR spectra (See Appendix, Figure A 41 and A 42) indicated that no reaction had occurred. Similar reactions of **V** at 10 bar H_2 in EtOH for 5.5 or 24 h at room temperature followed by removal of solvent under reduced pressure gave dark brown solids and in these cases ^1H and ^{31}P NMR spectra indicated that a reaction had occurred (See Appendix, Figures A 43-A 46). Thus the ^{31}P NMR spectrum of the latter reaction exhibited two resonances at δ 13.08 and 25.77 while the reaction run for 5.5 h exhibited only a single resonance at δ 25.62. None of the ^{31}P resonances is attributable to starting material, and assignments, but no hydride resonances were observed in the high field region of ^1H NMR spectra and the reactions were not investigated further.

As described in **2.8.3**, a similar high pressure reaction was attempted with **III** in EtOH. In this case a ^{1}H NMR spectrum (See Appendix, Figure A 47) showed broad peaks while a ^{13}P NMR spectrum (See Appendix, Figure A 48) showed a single resonance at δ 25.62. All starting material was consumed because no ^{31}P resonance was observed at 16.98, but again no hydride resonance was observed and the reaction was abandoned.

3.5 Attempted Synthesis of [(η^6-toluene)Rh(PPh_3)$_2$][X] and its Reaction with I

The synthesis of [(η^6-toluene)Rh(PPh_3)$_2$]$^+$ was reported previously,[74] and it was anticipated that the reaction between [(η^6-toluene)Rh(PPh_3)$_2$][X] and **I** might result in the formation of [(η^5-**I**)Rh(PPh_3)$_2$][X], because **I** is a better electron donor ligand than toluene. Synthesis of complexes of the type [(arene)Rh(PPh_3)$_2$][BAr^f] (arene = benzene, or toluene ; Ar^f = $C_6H_3(CF_3)_2$-3,5) have been reported using $NaBAr^f$ for chloride abstraction in the presence of excess arene (Figure 97).[74]

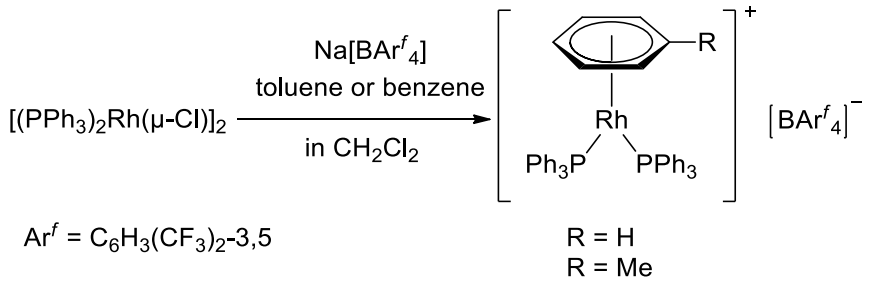

Figure 97. Synthesis of [(arene)Rh(PPh_3)$_2$][BAr^f].

We used $AgNO_3$ as the chloride abstractor instead of Na(BAr^f) in the presence of excess toluene (Figure 98). As described in **2.9.1**, a mixture of [(PPh_3)$_2$Rh(μ-Cl)]$_2$, $AgNO_3$ and toluene in CH_2Cl_2 were stirred for 24 h in a Schlenk flask. A dark brown

slurry was obtained, and this was filtered to give a brown solution from which the volatiles were removed under reduced pressure to yield an oily dark brown product.

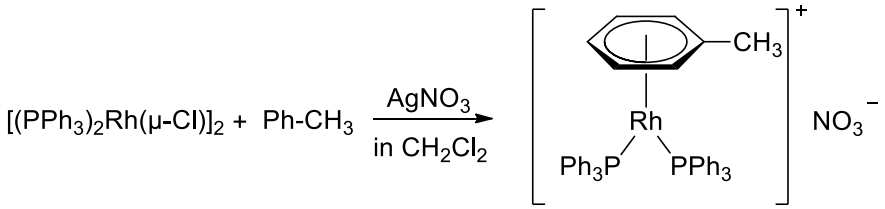

Figure 98. Synthesis of $[(\eta^6\text{-toluene})Rh(PPh_3)_2][NO_3]$.

In the ^1H NMR spectrum (See Appendix, Figure A 49), the methyl resonance of residual free toluene was readily identified as a singlet at δ 2.34, but no resonance for coordinated toluene was evident. The ^{31}P NMR spectrum (See Appendix, Figure A 50) exhibited a singlet at δ 28.45 as a major peak and doublets at δ 30.7 ($J_{Rh\text{-}H}$ = 126.6 Hz) and δ 44.69 ($J_{Rh\text{-}H}$ = 158.0 Hz) as minor products. The ^{31}P NMR spectrum of $[(\eta^6\text{-toluene})Rh(PPh_3)_2][BAr^f]$ is reported to exhibit a doublet resonance at δ 44.4 ($J_{Rh\text{-}P}$ = 205.4 Hz),[74] and thus it seems that the desired product, $[(\eta^6\text{-toluene})Rh(PPh_3)_2][NO_3]$, was not formed.

As described in **2.9.2**, we also carried out a similar reaction in acetonitrile, in which $AgNO_3$ is soluble. After work-up as above, the ^1H NMR spectrum (See Appendix, Figure A 51) again exhibited only the methyl resonance of free toluene while the ^{31}P NMR spectrum (See Appendix, Figure A 52) exhibited only a singlet at δ 28.48 as a major peak and a weak doublet at δ 30.7 ($J_{Rh\text{-}P}$ = 126.0 Hz). Thus again $[(\eta^6\text{-toluene})Rh(PPh_3)_2][NO_3]$ was clearly not formed.

As described in **2.9.3**, triphenylcarbonium tetrakis(pentafluorophenyl)borate was used as a chloride abstractor with $[(PPh_3)_2Rh(\mu\text{-}Cl)]_2$ and toluene in CH_2Cl_2 in an attempt to synthesize $[(\eta^6\text{-toluene})Rh(PPh_3)_2][B(C_6F_5)_4]$ (Figure 99).

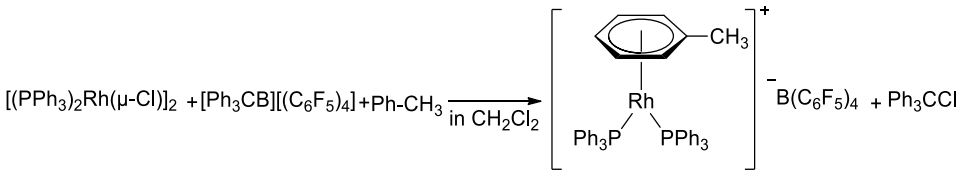

Figure 99. Synthesis of $[(\eta^6\text{-toluene})Rh(PPh_3)_2][B(C_6F_5)_4]$.

A solution of $[(PPh_3)_2Rh(\mu\text{-}Cl)]_2$, $[Ph_3C][B(C_6F_5)_4]$ and toluene in CH_2Cl_2 was stirred for 5 h, after which the solvent volume was reduced and the solution was stored at –30 °C overnight. No precipitate formed, and volatiles were therefore removed under reduced pressure to give an oily dark brown mixture. A ^1H NMR spectrum of the oily dark brown mixture (Figure 100) revealed that $[(\eta^6\text{-toluene})Rh(PPh_3)_2][B(C_6F_5)_4]$ had formed as a ^1H NMR spectrum exhibited the resonances reported previously for $[(\eta^6\text{-toluene})Rh(PPh_3)_2][BAr^f]$.[74]

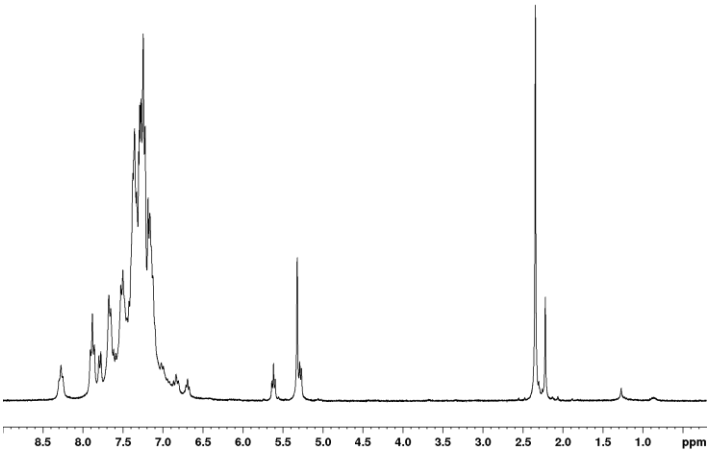

Figure 100. ^{1}H NMR spectrum of [η^6-toluene)Rh(PPh_3)$_2$][$B(C_6F_5)_4$] in CD_2Cl_2.

Thus the methyl resonance of coordinated toluene was assigned to a singlet at δ 2.22, compared with the methyl resonance of free toluene observed at δ 2.34. The ortho protons of the coordinated toluene were assigned to a doublet at δ 5.28 ($^3J_{H-H}$ = 6.4 Hz), the meta protons to a triplet at δ 5.61 ($^3J_{H-H}$ = 6.4 Hz) and the para proton to a triplet at δ 6.69 ($^3J_{H-H}$ = 6.1 Hz), all very similar to data reported previously for [(η^6-toluene)Rh(PPh_3)$_2$][BAr^f].[74] The ^{31}P NMR spectrum (Figure 101) confirmed the formation of desired product as it exhibited a doublet at δ 44.91 (J_{Rh-P} = 206.4 Hz) which is very similar to the reported δ 44.4 (J_{Rh-P} = 205.4 Hz).[74]

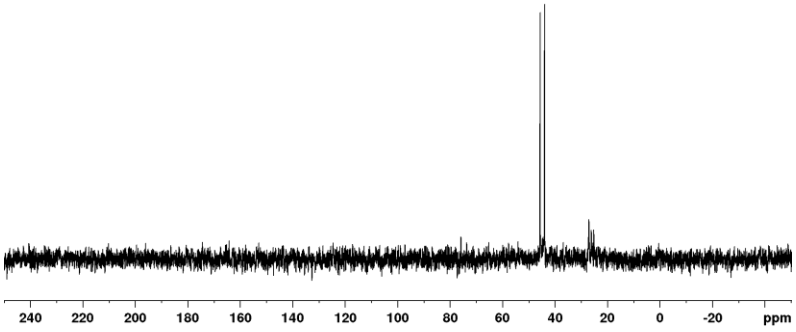

Figure 101. ^{31}P NMR spectrum of $[(\eta^6\text{-toluene})Rh(PPh_3)_2][B(C_6F_5)_4]$ in CD_2Cl_2.

The crude product was washed with hexanes in an unsuccessful attempt to purify it. As PHIN is a better electron donator compare to toluene,[55] it was thought that refluxing a solution of $[(\eta^6\text{-toluene})Rh(PPh_3)_2][B(C_6F_5)_4]$ and **I** in CH_2Cl_2 would result in the toluene ligand being replaced by **I** (Figure 102).

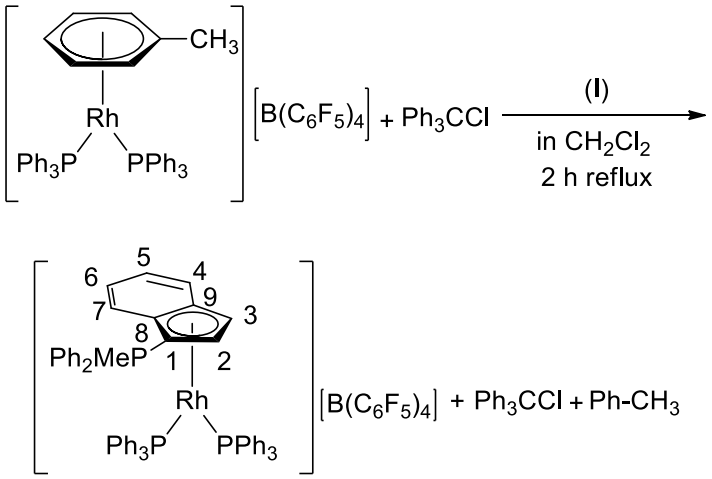

Figure 102. Reaction between $[(\eta^6\text{-toluene})Rh(PPh_3)_2][B(C_6F_5)_4]$ and (**I**).

As described in **2.9.4**, a reaction between [(η^6-toluene)Rh(PPh_3)$_2$][$B(C_6F_5)_4$] and **I** was attempted, and ^{31}P and ^{1}H NMR spectra of the product of the reaction are shown in Figures 103 and 104, respectively. The ^{31}P NMR spectrum exhibited resonances of four different species, and also showed that all of the PHIN had been consumed as there was no resonance at δ 5.69. It was not known initially if the doublet ^{31}P resonance at δ 51.37 should be assigned to the PPh_3 group of [(PPh_3)$_2$Rh(μ-Cl)]$_2$ or to a new product.

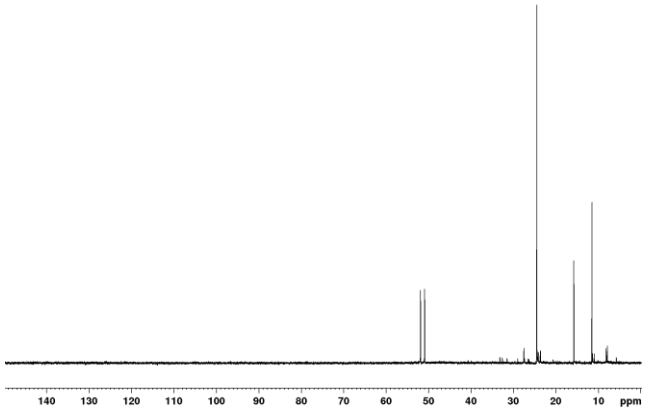

Figure 103. ^{31}P NMR spectrum of the product of reaction between [(η^6-toluene)Rh(PPh_3)$_2$][$B(C_6F_5)_4$] and (**I**) in CD_2Cl_2.

A ^{1}H NMR spectrum (Figure 104) exhibited several P-Me doublets at δ 1.58 ($^2J_{H-P}$ = 13.5 Hz), 2.24 ($^2J_{H-P}$ = 12.8 Hz), and 2.67 ($^2J_{H-P}$ = 13.3 Hz), indicating the formation of several products. All these doublets showed J_{H-P} ~13 Hz which is characteristic for methyl group of PHIN ligands. As the aromatic region is extremely complex, no assignment were possible.

The discussion on the following pages presents a possible rationalization of the ^{1}H and ^{31}P NMR data, but one which ultimately turned out to not be conclusive. It is

included here because of its relevance to complementary experimentation which did ultimately prove useful.

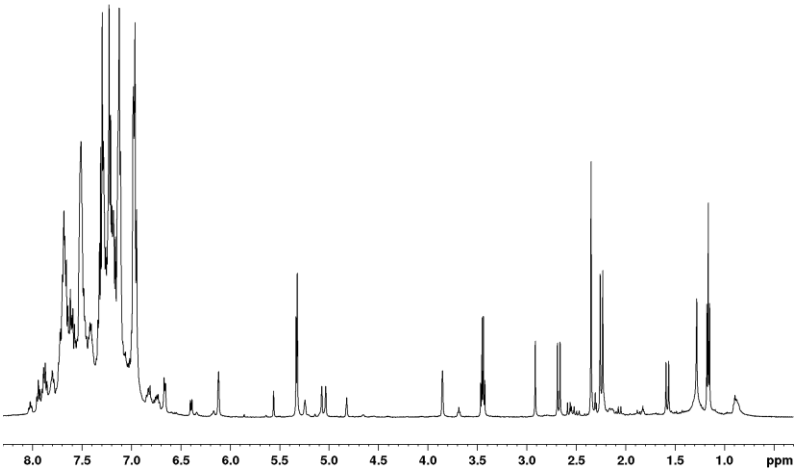

Figure 104. ^{1}H NMR spectrum of the product of reaction between [(η^{6}-toluene)$Rh(PPh_3)_2$][$B(C_6F_5)_4$] and (**I**) in CD_2Cl_2.

By analyzing the ^{1}H-^{31}P HMBC spectrum of the product (Figure 105), it was found that phosphorus resonances at δ 11.48, 15.76 and 24.45 exhibited ^{31}P HMBC correlations with the P-Me doublets at δ 2.67, 1.57 and 2.24 (P-*Me*), respectively.

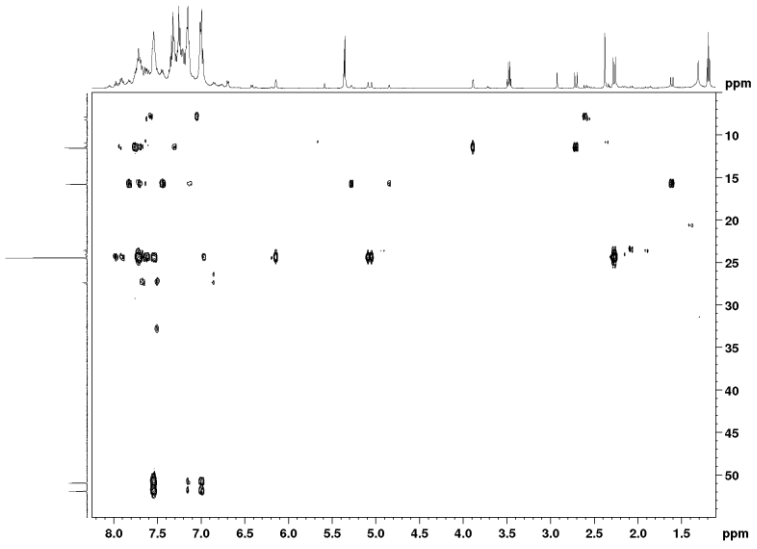

Figure 105. ^{1}H-^{31}P HMBC spectrum of the product of reaction between impure [(η^6-toluene)$Rh(PPh_3)_2$][$B(C_6F_5)_4$] and (**I**) in CD_2Cl_2.

As mentioned above, the phosphorus resonance at δ 15.76 correlates in the ^{1}H-^{31}P HMBC spectrum with the methyl resonance of P-Me at 1.57; it also correlates with two broad triplets at δ 4.8 and 5.25 which are the two protons of five membered ring, (H2) and (H3). This assignment was also confirmed by COSY spectrum (Figure 106), as the two broad triplets at δ 4.8 and 5.25 exhibited mutual correlations. In a NOESY spectrum (Figure 107), the P-Me doublet at δ 1.57 correlates with a doublet at δ 6.39, which is therefore assigned to the proton at position 7. The COSY spectrum showed a correlation between protons at position 7 (δ 6.39) with the proton at position 6 at δ 7.16. As the aromatic region is crowded by broad peaks, it is difficult to distinguish all the protons, but it seems that there is a correlation in the COSY spectrum between the proton at position 6 (δ 7.12) with the proton at position 5 (δ 7.27), which is correlated with proton at position 4 at δ 7.68. ^{13}C NMR, HMBC, and HSQC spectra can be found in Appendix,

Figures A 53-A 55). The full characterization of the desired product was abandonded due to the formation of several products and complex ^{1}H and ^{13}C NMR spectra.

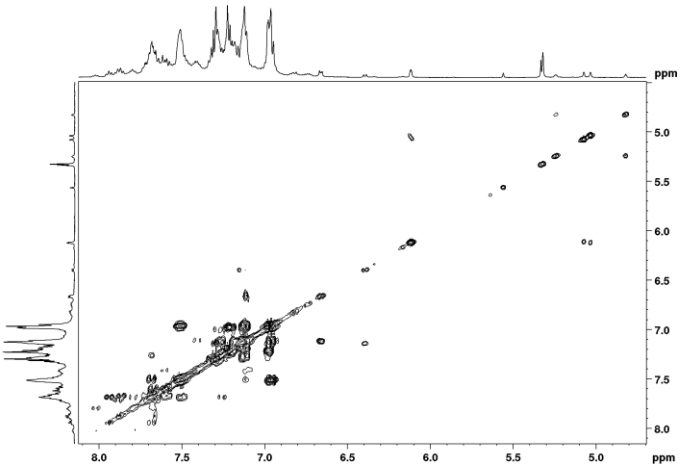

Figure 106. COSY spectrum of the product of reaction between impure [(η^6-toluene)$Rh(PPh_3)_2$][$B(C_6F_5)_4$] and (**I**) (aromatic region) in CD_2Cl_2.

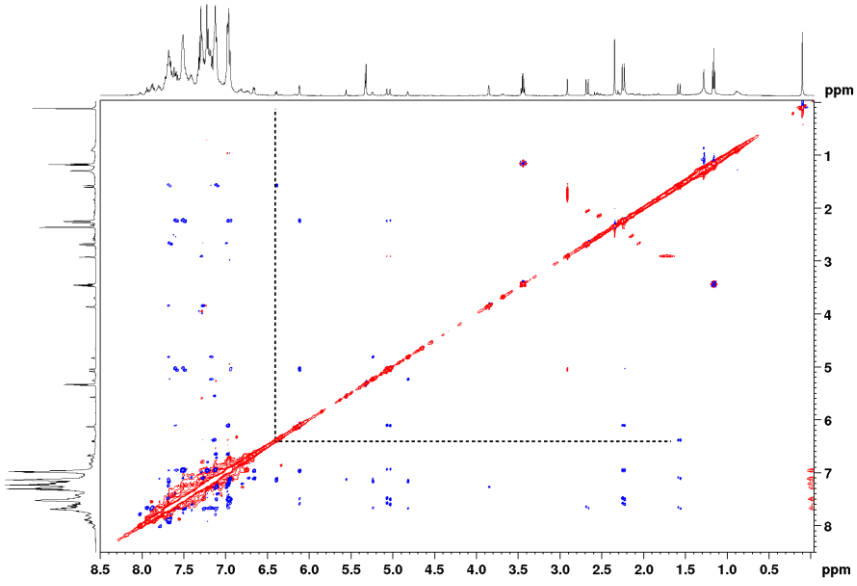

Figure 107. NOESY spectrum of the product of reaction between impure [(η^6-toluene)$Rh(PPh_3)_2$][$B(C_6F_5)_4$] and (**I**) in CD_2Cl_2.

In view of the uncertainties on assignments of the resonances in the ^{31}P NMR spectrum (Figure 103), we decided to ensure accurate integrations by use of the well-known relaxation reagent chromium(III) acetylacetonate, $Cr(acac)_3$, which is frequently used as a relaxation agent in NMR experiments involving nuclei such as ^{13}C and ^{31}P because its paramagnetisim both shortens relaxation times and minimizes Overhauser effects, thus permitting acquisition of more accurate integration data.[104,105] In this way we hoped, by taking the resonance at δ 24.61 as one, that we would be able to ascertain if the doublet at 51.38 has the appropriate integrated intensity to be assignable to the two PPh_3 phosphorus atoms of the putative product.

As described in **2.9.5.1**, each of three NMR solutions of the product of a reaction of $[(\eta^6\text{-toluene})Rh(PPh_3)_2][B(C_6F_5)_4]$ with **I**, each containing ~0.03 mmol of product, were combined with 0.15, 0.30, and 0.45 mmol of $Cr(acac)_3$ and ^{31}P NMR spectra were obtained (See Appendix, Figures A 56-A 58). The ^{31}P NMR spectra were integrated, and the ratios of the doublet at δ 51.38 to the singlet at δ 24.61 were found to be 1.72, 1.64, and 1.41, respectively, not edging toward 2:1. Thus the ratio of intensities is not consistent with the resonances being assigned to a complex such as $[(\eta^5\text{-}\mathbf{I})Rh(PPh_3)_2]B(C_6F_5)_4$. The resonance at δ 24.61, and quite likely those at δ 11.48, 15.76 and 24.45 are attributable to PHIN species of some kind but the doublet at δ 51.38 is assigned to unreacted $[(PPh_3)_2Rh(\mu\text{-Cl})]_2$ and the apparent absence of PPh_3 resonance(s) of the product(s) is puzzling (but see below).

An alternative route, via chloride abstraction from $[(PPh_3)_2Rh(\mu\text{-Cl})]_2$ using $[Ph_3C][B(C_6F_5)_4]$ followed by the addition of **I**, was considered as described in **2.9.6**, (Figure 108).

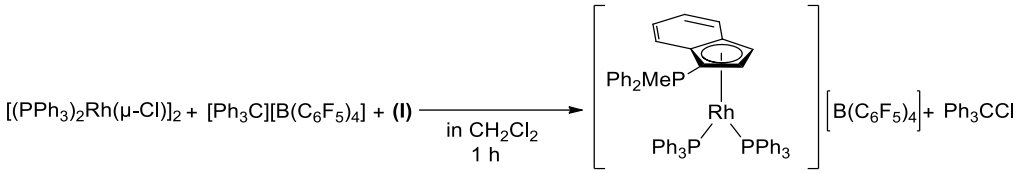

Figure 108. Attempted synthesis of [(η^5-**I**)Rh(PPh_3)$_2$][$B(C_6F_5)_4$].

A ^{1}H NMR spectrum (See Appendix, Figure A 59) showed a doublet at δ 2.23 and 2.68 with J_{H-P} ~13.0 Hz which is characteristic for -PMe groups of indenylide ligands and very similar to the ^{1}H NMR spectrum of the product of the reaction between [(η^6-toluene)Rh(PPh_3)$_2$]$B(C_6F_5)_4$ and **I** (See Figure 104). The ^{1}H NMR spectrum also exhibited broad peaks at δ 3.86, 5.63 and 6.11, again very similar to the ^{1}H NMR spectrum of the product of reaction between [(η^6-toluene)Rh(PPh_3)$_2$]$B(C_6F_5)_4$ and **I** (See Figure 104) but the spectrum was complex and clearly a number of species was present. The ^{31}P NMR spectrum (See Appendix, Figure A 60) exhibited singlets at δ 12.00 and 25.52 and a doublet at δ 52.58 with J_{Rh-P} = 196.7 Hz, again similar to the ^{31}P NMR spectrum of the products of the reaction between [(η^6-toluene)Rh(PPh_3)$_2$]$B(C_6F_5)_4$ and **I** (Figure 103).

For purpose of comparison, an NMR scale reaction between **I** and [Ph_3C][$B(C_6F_5)_4$] was carried out (See Appendix, Figure A 61 and A 62). Interestingly, the ^{1}H NMR spectrum of the mixture exhibited a P-Me doublet at δ ~2.23 with J_{H-P} ~12.7 Hz while the ^{31}P NMR spectrum exhibited a singlet peak at δ 25.52, both apparently corresponding to resonances in the spectra of the reaction of [(PPh_3)$_2$Rh(μ-Cl)]$_2$, [Ph_3C][$B(C_6F_5)_4$] and **I**. On the other hand, an NMR scale reaction of [(PPh_3)$_2$Rh(μ-Cl)]$_2$ and [Ph_3C][$B(C_6F_5)_4$] produced a product mixture which exhibited in a ^{31}P NMR

spectrum a singlet at δ 25.39, a doublet at δ 39.07 (J_{Rh-P} = 170.5 Hz) and a doublet at δ 44.94 (J_{Rh-P} = 206.7 Hz) (See Appendix, Figure A 63 and A 64), quite unlike the spectra of the reaction of $[(PPh_3)_2Rh(\mu\text{-}Cl)]_2$, $[Ph_3C][B(C_6F_5)_4]$ and **I**.

As described in **2.9.7**, $AgBF_4$ was used as a chloride abstractor with $[(PPh_3)_2Rh(\mu\text{-}Cl)]_2$ and **I** in CH_2Cl_2 to synthesize $[(\eta^5\text{-}\mathbf{I})Rh(PPh_3)_2][BF_4]$ (Figure 109).

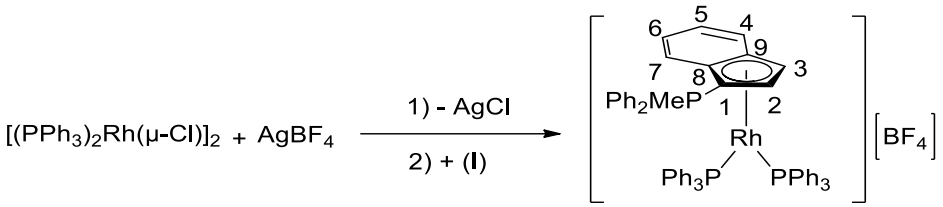

Figure 109. Synthesis of $[(\eta^5\text{-}\mathbf{I})Rh(PPh_3)_2][BF_4]$.

Both ^1H and ^{31}P NMR spectra of $[(\eta^5\text{-}\mathbf{I})Rh(PPh_3)_2][BF_4]$ (Figures 110 and 111) showed that the crude material contained other than just the desired product. ^1H NMR spectrum exhibited two P-Me doublets at δ 1.69 and 2.87 with $^2J_{H-P}$ ~13.0 Hz. ^{31}P NMR spectrum exhibited several resonances in the region δ 7.00-30.00, a doublet at δ 51.46 with J_{Rh-P} = 196.5 Hz which is possibly attributable to starting material $[(PPh_3)_2Rh(\mu\text{-}Cl)]_2$, and a broad peak centered at δ 40-50.

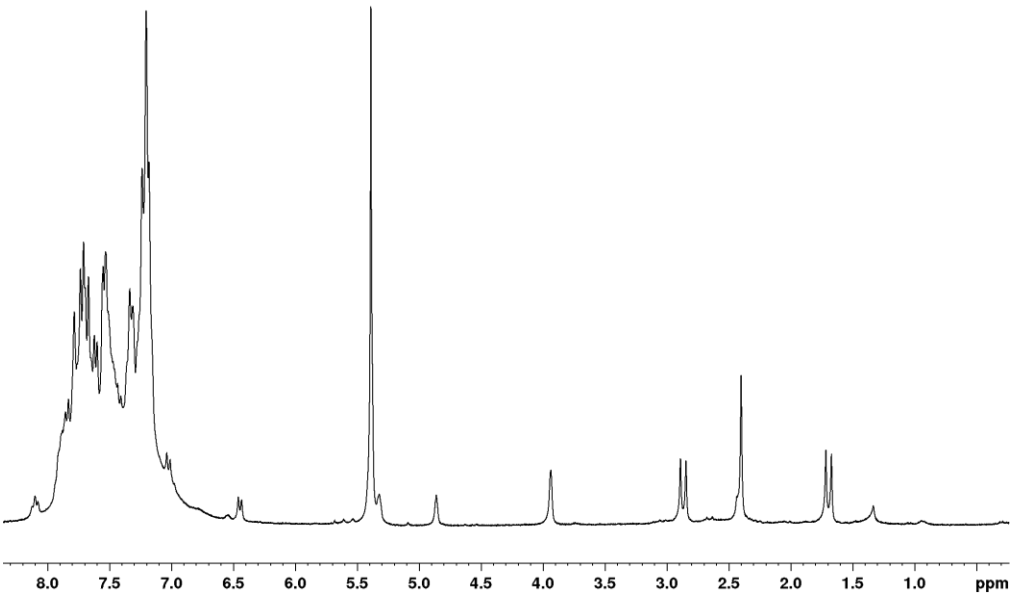

Figure 110. ^{1}H spectrum of crude [(η^5-**I**)Rh(PPh_3)$_2$][BF_4] at room temperature in CD_2Cl_2.

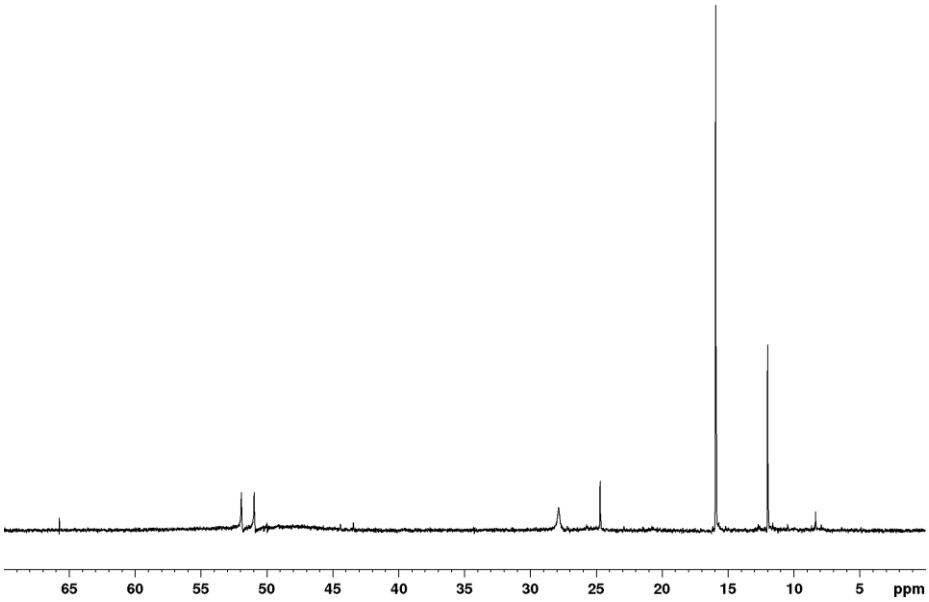

Figure 111. ^{31}P NMR spectrum of crude [(η^5-**I**)Rh(PPh_3)$_2$][BF_4] at room temperature in CD_2Cl_2.

To investigate the apparent exchange process indicated by the broad band in the ^{31}P NMR spectrum, ^{31}P NMR spectra were obtained at –50 °C, –60 °C and –75 °C (Figures 112-114).

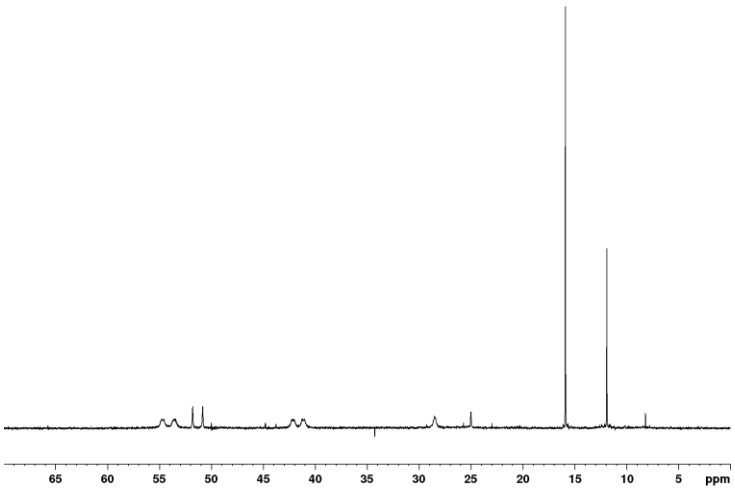

Figure 112. ^{31}P NMR spectrum of crude $[(\eta^5\text{-}\mathbf{I})Rh(PPh_3)_2][BF_4]$ at –50 °C in CD_2Cl_2.

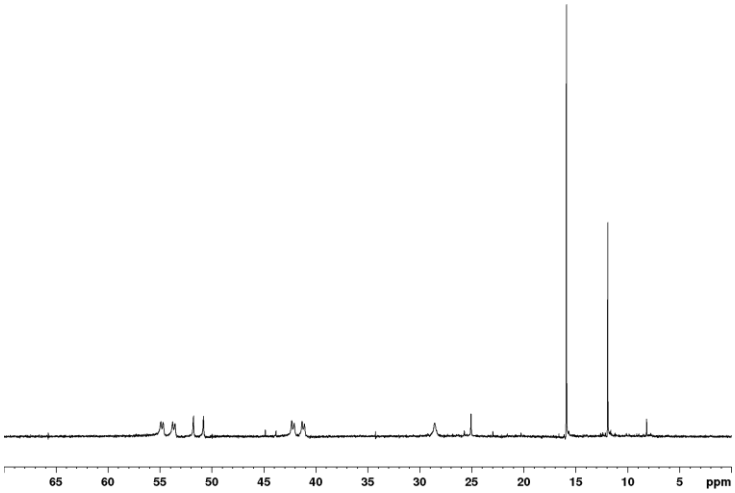

Figure 113. ^{31}P NMR spectrum of crude $[(\eta^5\text{-}\mathbf{I})Rh(PPh_3)_2][BF_4]$ at –60 °C in CD_2Cl_2.

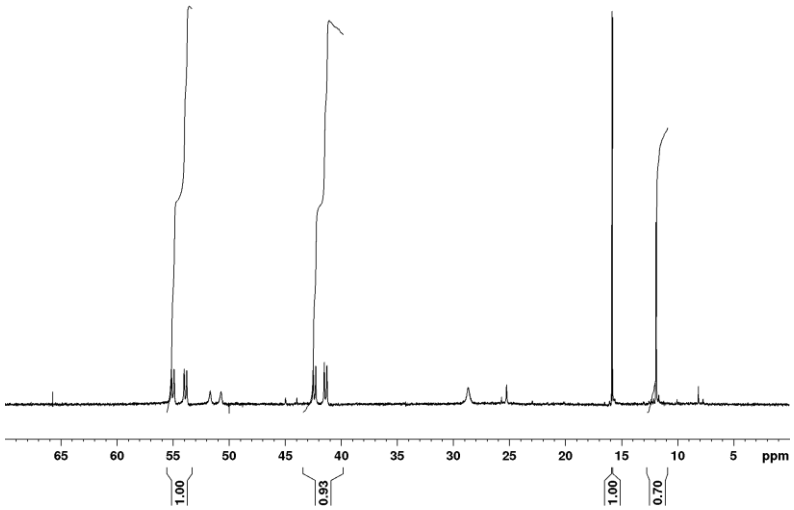

Figure 114. ^{31}P NMR spectrum of crude [(η^5-**I**)Rh(PPh_3)$_2$][BF_4] at −75 °C in CD_2Cl_2.

As can be seen, although there is little change in most of the spectrum, the broad band at δ 40-50 has decoalesced at −75 ºC to two doublets of doublets centered at δ 41.87 ($^2J_{P\text{-}P}$ = 47.0 Hz, $J_{Rh\text{-}P}$ = 201.11 Hz) and δ 54.45 ($^2J_{P\text{-}P}$ = 47.0 Hz, $J_{Rh\text{-}P}$ = 228.38 Hz). The relative integrations of the doublets at δ 41.87 and 54.45 and the singlet at δ 15.83 in the spectrum at −75 °C were ~1:1:1, with all other resonances being significantly weaker, and thus we attribute the resonances at δ 41.87 and 54.45 to two non-equivalent PPh_3 ligands and that at δ 15.83 to the phosphorus of the coordinated **I** in [(η^5-**I**)Rh(PPh_3)$_2$][BF_4]. The PPh_3 ligands are diastereotopic because of the coordinated planar chiral PHIN ligand.

The nature of the exchange process is not known. Simple rotation of the PHIN ligand would not result in exchange of the magnetically non-equivalent phosphorus atoms, it seems likely that the mechanism of exchange is either dissociative in nature or that it involves intermolecular exchange with a trace amount of free PPh_3.

Full assignments of the ^{1}H NMR spectrum were not possible because of overlap by the very broad phenyl resonances; however, by assigning the phosphorus resonance of the coordinated **I** to δ 15.83 and using a ^{1}H-^{31}P HMBC spectrum (Figure 115), it was found that the phosphorus resonance at δ 15.83 correlated with a P-Me resonance at δ 1.62 (d, $J_{P\text{-}Me}$ = 13.5 Hz) in addition to two broad triplets at δ 4.8 and 5.25 which are the two protons of five membered ring, H(2) and H(3).

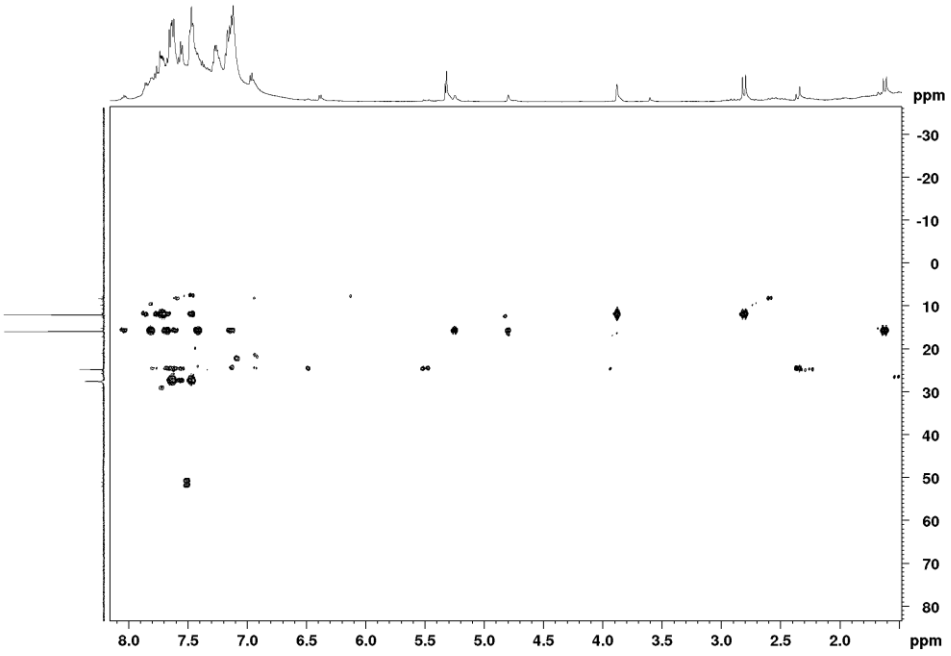

Figure 115. ^{1}H-^{31}P HMBC of [(η^{5}-**I**)Rh(PPh_3)$_2$][BF_4] in CD_2Cl_2.

The assignment was confirmed by correlation between the two broad triplets at δ 4.8 and 5.25 in a COSY experiment (Figure 116). A NOESY spectrum (Figure 117) showed a correlation between the P-Me doublet at δ 1.62 and a doublet at δ 6.39, and the latter is assigned to H(7). A COSY correlation of the resonance at δ 6.39 with another at δ 7.12 let to assignment of the latter to H(6), and similar correlations resulted in tentative assignments of resonances at δ 7.12 and δ 7.67 to H(5) and H(4), respectively, although

these resonances were obscured by overlap by the strong phenyl resonances. Figure A 65–A 67 in the Appendix provide ^{13}C NMR, ^{1}H-^{13}C HMBC, and ^{1}H-^{13}C HSQC spectra which were used in the attempts to further characterize the product.

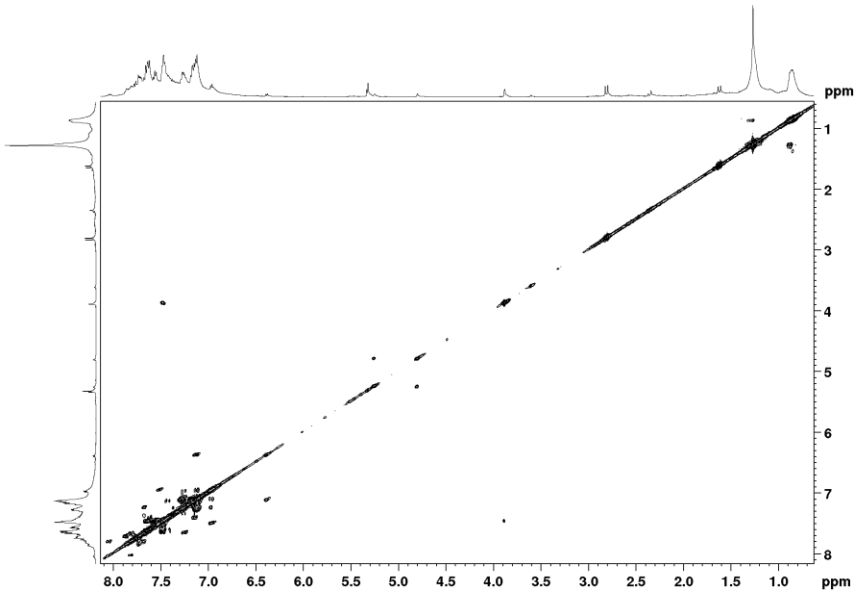

Figure 116. COSY spectrum of $[(\eta^5\text{-}\mathbf{I})Rh(PPh_3)_2][BF_4]$ in CD_2Cl_2.

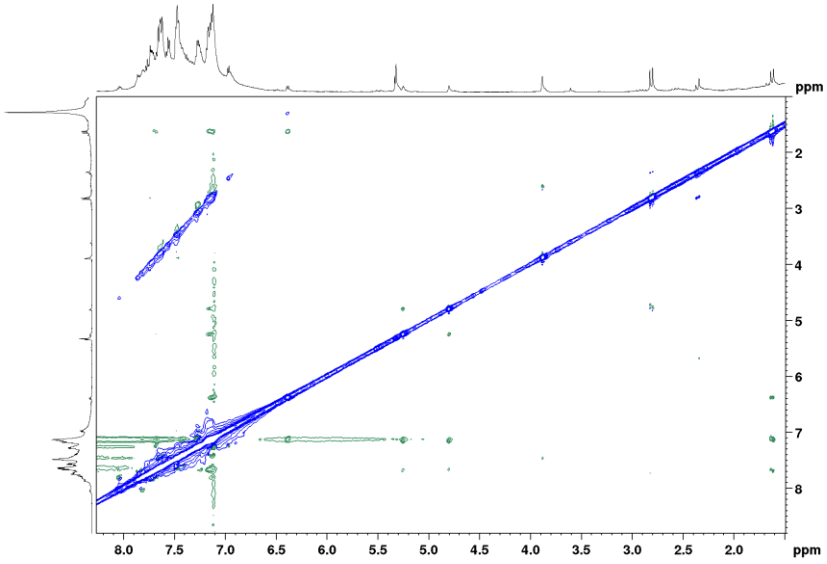

Figure 117. NOESY spectrum of $[(\eta^5\text{-}\mathbf{I})Rh(PPh_3)_2][BF_4]$ in CD_2Cl_2.

Consistent with the structure shown in Figure 109, the observed HR-EMS spectrum of the crude reaction mixture exhibited an ion with m/z value (941.2067) in an excellent agreement with the calculated value (941.2097) and exhibiting the expected isotope distribution (Figure 118).

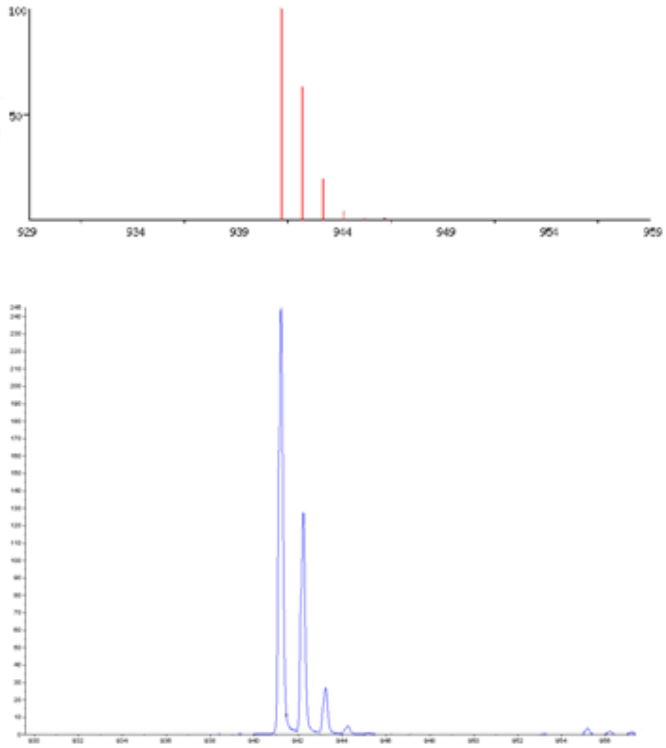

Figure 118. HR-EMS of $[(\eta^5\text{-}\mathbf{I})Rh(PPh_3)_2]^+$ (bottom), and the calculated isotopic distribution (top).

3.6 Attempted Oxidative Addition Reaction to $[(\eta^5\text{-I})Rh(PPh_3)_2][BF_4]$ on an NMR Scale

As described in **2.10.1**, oxidative addition of MeI to the rhodium(I) complex, $[(\eta^5\text{-}\mathbf{I})Rh(PPh_3)_2]BF_4$, was attempted on an NMR scale with a view to producing a rhodium(III) complex such as $[(\eta^5\text{-}\mathbf{I})Rh(Me)(I)]BF_4$ (Figure 119).

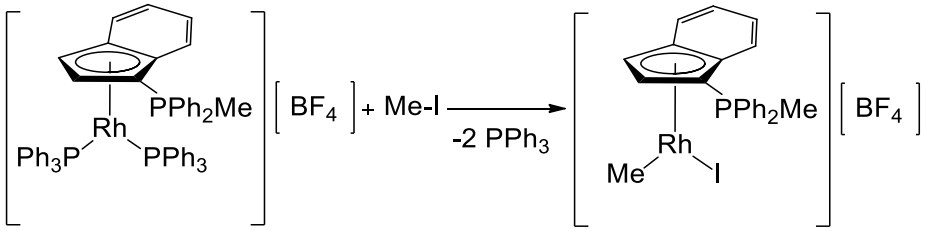

Figure 119. Oxidative addition of MeI to $[(\eta^5\text{-}\mathbf{I})Rh(PPh_3)_2]BF_4$.

The ^1H and ^{31}P NMR spectra of the product (Appendix, Figure A 68 and A 69) were both very complex and hence uninformative, and the reaction was not pursued further.

As described in **2.11**, the reaction of H_2 to $[(\eta^5\text{-}\mathbf{I})Rh(PPh_3)_2]BF_4$ was attempted with a view to producing the oxidative addition product $[(\eta^5\text{-}\mathbf{I})Rh(H)_2(PPh_3)]BF_4$ (Figure 120). ^1H and ^{31}P NMR spectra can be found in Appendix, Figure A 70 and A 71, and are decidedly uninformative. If $[(\eta^5\text{-}\mathbf{I})Rh(H)_2(PPh_3)]BF_4$ were produced, hydride resonances should be observed in the negative region of the ^1H NMR spectrum, and their absence shows clearly that no hydride was formed.

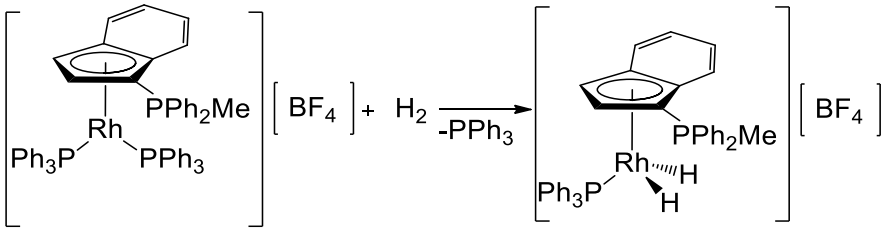

Figure 120. Attempted Reaction of H_2 and $[(\eta^5\text{-}\mathbf{I})Rh(PPh_3)_2][BF_4]$.

3.7 Coordination of I to Group IV Metals

Several attempts have been made in the Baird lab in recent years to coordinate **I** to the group IV metals titanium and zirconium. Littlefield, in her Queen's University

MSc thesis,[79] describes experiments in which direct addition of **I** to $TiCl_4$ or $TiCl_4(THF)_2$ was carried out with a view to synthesizing cationic species such as $[TiCl_3(\eta^5\text{-}\mathbf{I})]^+$ or $[TiCl_2(\eta^5\text{-}\mathbf{I})_2]^{2+}$. A similar approach had earlier been reported by Holy *et al.*[26] to prepare the complex $[CpPPh_3)_2TiCl_2]Cl_2$, but all attempts involving **I**, even in excess, were unsuccessful because brown solution containing complex mixtures of inseparable products were formed.

A latter attempt was based on a report that coordination of the electron-rich arene C_6Me_6 to titanium to form $[(\eta^6\text{-}C_6Me_6)TiCl_3][Ti_2Cl_9]$, as in Figure 121, could be achieved by adding an excess of $TiCl_4$ rather than of arene.[69,70] The excess Lewis acid apparently served to abstract a chloride ion and generate a reactive species such as $[TiCl_3]^+$.

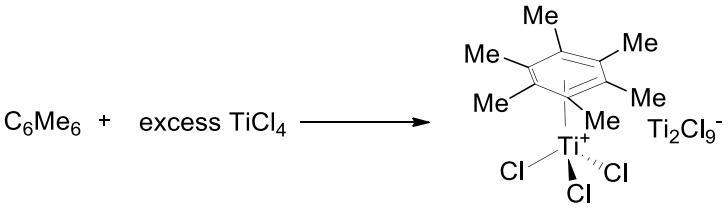

Figure 121. Coordination of C_6Me_6 to titanium.

As **I** is better electron donor ligand compared with arenes,[22,39] it was anticipated that much the same approach could be used to synthesize titanium complex of **I**[80] and, as described in **2.12.1**, coordination of **I** to titanium was attempted in CD_2Cl_2, using four-fold molar excess of $TiCl_4$ (Figure 122).[80] As with C_6Me_6 a deep red solution was obtained, indicating that PHIN coordination had indeed occurred.

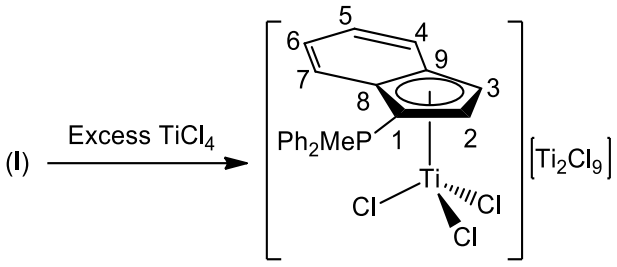

Figure 122. Presumed structure of the product of coordination of (**I**) to titanium, using a four-fold excess of $TiCl_4$.

Although pure product(s) could not be obtained, ^{1}H and ^{31}P NMR spectra could be obtained and are shown in Figures 123 and 124 while ^{1}H and ^{13}C assignments may be found in Table 11. With the aid of COSY, HSQC and HMBC experiments (See Appendix, Figures A 72-A 74) all the protons and carbons of the presumed product of coordination of **I** to titanium ($[(\eta^5\text{-}\mathbf{I})TiCl_3]^+$) were assigned.[80]

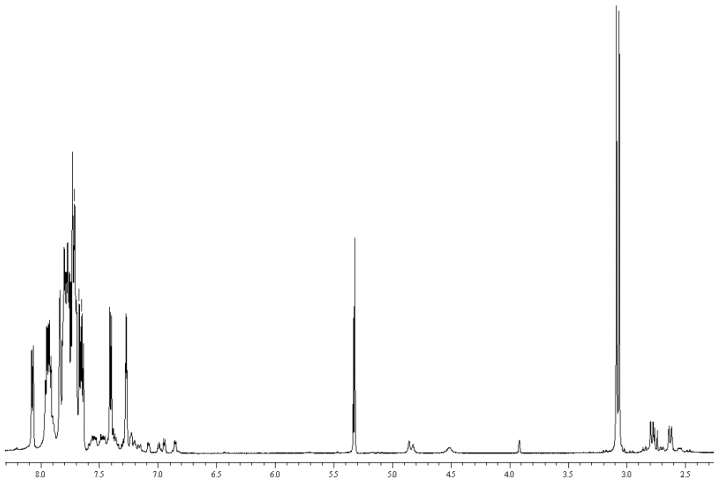

Figure 123. ^{1}H NMR spectrum of the product obtained using a four-fold excess of $TiCl_4$ in CD_2Cl_2.

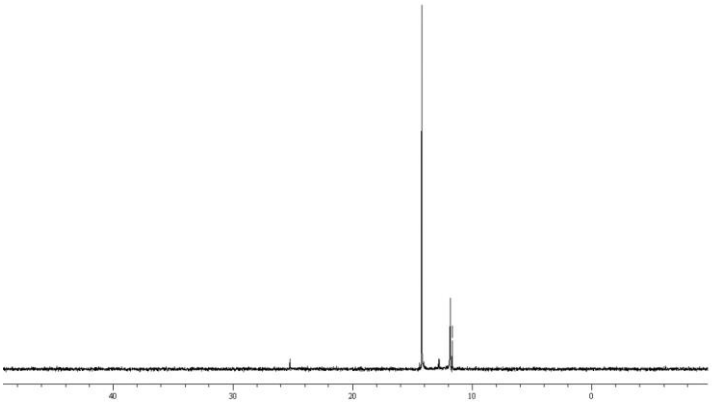

Figure 124. ^{31}P NMR spectrum of the product obtained using a four-fold excess of $TiCl_4$ in CD_2Cl_2.

Table 11. ^{1}H and ^{13}C NMR data for the species obtained on reaction **I** with $TiCl_4$

Position	δ (^{1}H)	δ (^{13}C)
1	-	102.2
2	7.29 (t, $J_{H-H} = J_{H-P} = 4.0$)	128.6
3	7.84 (t, $J_{H-H} = J_{H-P} = ?$)	121.0
4	8.07 (d, $J_{H-H} = 8.1$)	128.7
5	7.71 (m)	131.4
6	7.74 (m)	133.0
7	7.41 (d, $J_{H-H} = 8.5$)	124.8
8	-	132.1
9	-	132.8
P-Me	3.08 (d, $^{2}J_{H-P} = 13.2$)	11.0
ipso-C	-	116.7
o-H, C	7.66, 7.71 (2 m)	131.4, 131.5
m-H, C	7.77, 7.80 (2 m)	133.1, 133.2
p-H, C	7.92, 7.95 (2 m)	136.9

The apparent compound [(η^5-**I**)$TiCl_3$][Ti_2Cl_9] was thought to assume a piano-stool type structure about the titanium atom (Figure 122).

In spite of this apparent success,[79,80] no pure crystalline titanium complex was obtained and it was anticipated that using a more concentrated solution of $TiCl_4$ (more than four-fold excess of $TiCl_4$) might force the reaction farther to the right and make possible isolation of a single product containing the cationic species $[(\eta^5\text{-}\mathbf{I})TiCl_3]^+$. As described in **2.12.2**-**2.12.5**, reactions of **I** with excess $TiCl_4$ (~1:11 ratio) were attempted at various temperatures in CH_2Cl_2 and also in a solvent free reaction. At room temperature, the reaction of **I** and $TiCl_4$ (~1:11 ratio) in CH_2Cl_2 resulted in the rapid formation of a deep red solution which afforded a brown solid on removal of the solvent. A ^1H NMR spectrum of the product (See Appendix, Figure A 75) exhibited several P-Me doublets at δ 2.55-3.15 ($J_{P\text{-}Me}$ ~13.0 Hz), including one at δ 3.07 which may correspond to the P-Me doublet at δ 3.08 observed previously (Table 11). A ^{31}P NMR spectrum (See Appendix, Figure A 76) exhibited strong resonances at δ 12.82 and 15.18, and weak resonances at δ 13.13, and 24.01, and we note that the ^{31}P NMR spectrum of the product of the reaction using a four-fold excess of $TiCl_4$ exhibited two singlets at δ 11.8 and 14.2. Thus the reaction carried out here and involving a high ratio of $TiCl_4$ to **I** gave a product mixture similar to that found previously with a lower $TiCl_4$ to **I** ratio.

However, a crystalline sample of the new compound was not obtained, and we therefore carried out the reaction at low temperature hoping that the desired product would form and crystallize. As described in **2.12.3**, a reaction of **I** and excess $TiCl_4$ (~1:11 ratio) in CH_2Cl_2 was attempted at −78 °C and afforded a brown solid after removal of the solvent. Unfortunately, a ^1H NMR spectrum of the product (See Appendix, Figure A 77) exhibited several P-Me doublets at δ 2.18-2.82 but not a P-Me doublet at δ 3.07. The ^{31}P NMR spectrum (See Appendix, Figure A 78) exhibited four

major resonances at δ 11.81, 12.07, 12.16, and 24.08, quite different from the spectrum of the room temperature product. Thus the low temperature experiment was not successful in that it produced neither the major product formed at room temperature nor a crystalline product of any kind.

As described in **2.12.5**, a reaction of **I** and excess $TiCl_4$ (1:11 ratio) was therefore carried out in refluxing CH_2Cl_2, affording a dark red oily mixture after removal of the solvent. A ^1H NMR spectrum (See Appendix, Figure A 79) exhibited one major P-Me doublet at δ 3.08, very similar to the major product of the room temperature experiments discussed above, and two minor P-Me doublets at δ 2.64 and 2.78 ($J_{P\text{-}Me}$ ~13.0 Hz). The ^{31}P NMR spectrum (See Appendix, Figure A 80) exhibited a singlet at δ 15.17, again corresponding to the major product discussed above, and a multiplet at δ 12.80.

As described in **2.12.4**, a solvent free reaction of **I** and neat $TiCl_4$ was attempted and afforded a red solid after removing unreacted $TiCl_4$. A ^1H NMR spectrum (See Appendix, Figure A 81) exhibited several P-Me doublets at δ 2.60-3.15 ($J_{P\text{-}Me}$ ~13.0 Hz) while a ^{31}P NMR spectrum (See Appendix, Figure A 82) exhibited two strong resonances at δ 11.69 and 14.04 and four weak resonances at δ 11.53, 11.72, 12.00, and 22.87.

In summary, reactions of **I** with excess $TiCl_4$ under a variety of conditions failed to produce a single PHIN complex which could be isolated and properly characterized.

A variety of other known chloride abstractors, $AlCl_3$,[80] $[Ph_3C][B(C_6F_5)_4]$, and $GaCl_3$ were therefore used in attempts to obtain coordination complexes of **I** with $TiCl_4$ (Figure 125).

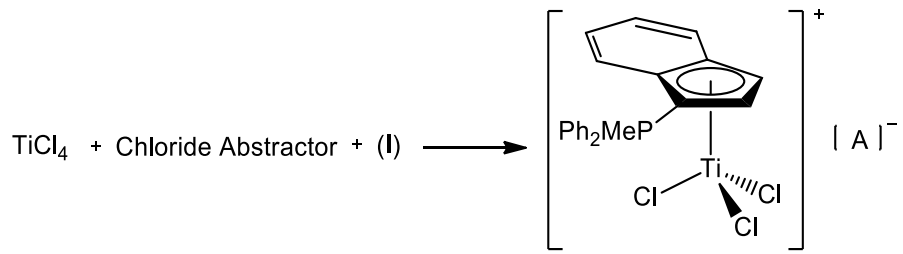

Chloride Abstractor = $Ph_3CB(C_6F_5)_4$, $GaCl_3$, or $AlCl_3$

A = $B(C_6F_5)_4$ or $GaCl_4$ or $AlCl_4$

Figure 125. Coordination of (**I**) to $TiCl_4$, using chloride abstractors.

As described in **2.12.6**, **2.12.7**, **2.12.8**, and **2.12.9**, experiments were performed, as with $TiCl_4$, to assess the possible use of $AlCl_3$, $[Ph_3C][B(C_6F_5)_4]$, and $GaCl_3$ as chloride abstractors, but only complex mixtures were obtained in all cases and the approach was discontinued. At this point we opted to assess the use of $TiCl_4(THF)_2$, which is an easily used solid, instead of $TiCl_4$ which is a fuming and corrosive liquid.[78] As described in **2.12.10**-**2.12.12**, $TiCl_4(THF)_2$ was synthesized and attempted to coordinate **I** in conjunction with chloride abstraction with $AgNO_3$. These all failed to produce products which could be characterized. See Appendix, Figures A 87-A 94 for spectral information.

The reaction of Cp^*MMe_3 (M = Ti, Zr and Hf) with the highly electrophilic borane $B(C_6F_5)_3$ in the presence of arene (arene = benzene, toluene, *m*- and *p*-xylene, anisole, styrene and mesitylene) to synthesize $[Cp^*MMe_2(\eta^6\text{-arene})][MeB(C_6F_5)_3]$ was previously reported.[106-108] It was thought that the reaction of Cp^*ZrMe_3 with $[Ph_3C][B(C_6F_5)_4]$ in the presence of **I** will result in methyl carbanion abstraction and coordination of **I** to afford $[Cp^*ZrMe_2(\eta^5\text{-}\mathbf{I})][B(C_6F_5)_4]$. As described in **2.13.1**, the reaction of Cp^*ZrMe_3, **I** and $[Ph_3C][B(C_6F_5)_4]$, in CH_2Cl_2, was attempted, and a dark brown solid was obtained (Figure 126).

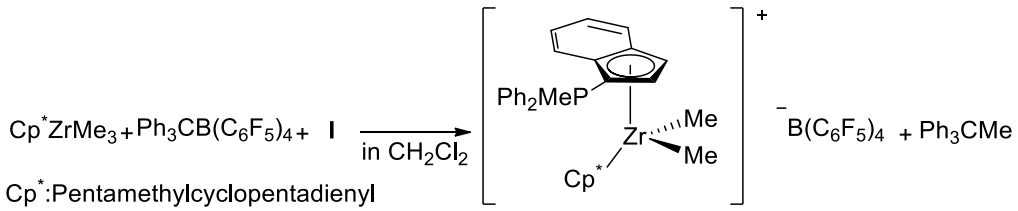

Figure 126. Attempted coordination of (**I**) to Cp^*ZrMe_3.

In the ^1H NMR spectrum (Figure 127), the two singlet peaks in the negative region were assigned to the two methyl groups on zirconium in the proposed structure in Figure 126. The ^{31}P NMR spectrum (Figure 128) depicted two singlet peaks, one major peak at δ 11.98 and one minor peak at δ 17.82. The final product was dissolved in CH_2Cl_2 and passed through a short silica gel column. The resulting filtrate showed no peak in the negative region of the ^1H NMR spectrum and the ^{31}P NMR showed a single peak at δ 11.98. This led us to assign the peak at δ 11.98 as undesired product which was the major product and the peak at δ 17.82 as the desired product which was the minor product. It was also found that no reaction occurred between **I**, and $[Ph_3C][B(C_6F_5)_4]$ due to the lack of a phosphorus peak at δ 25.73. No further study was attempted on this coordination.

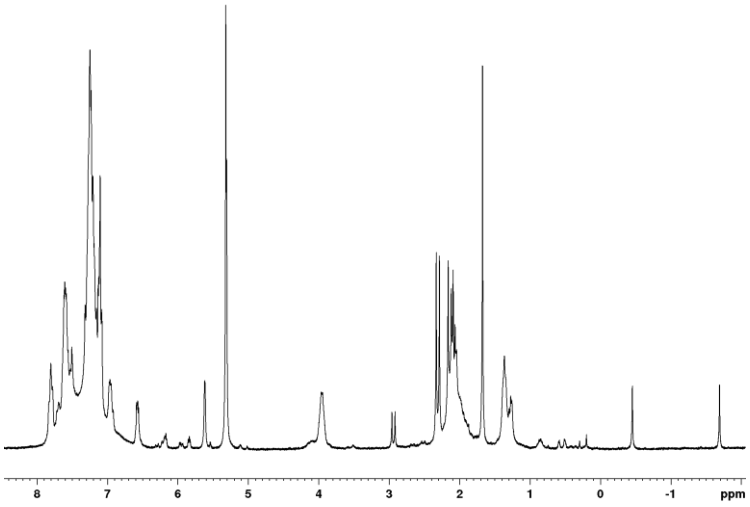

Figure 127. ^{1}H NMR spectrum of attempted coordination of **I** to Cp^*ZrMe_3 in CD_2Cl_2.

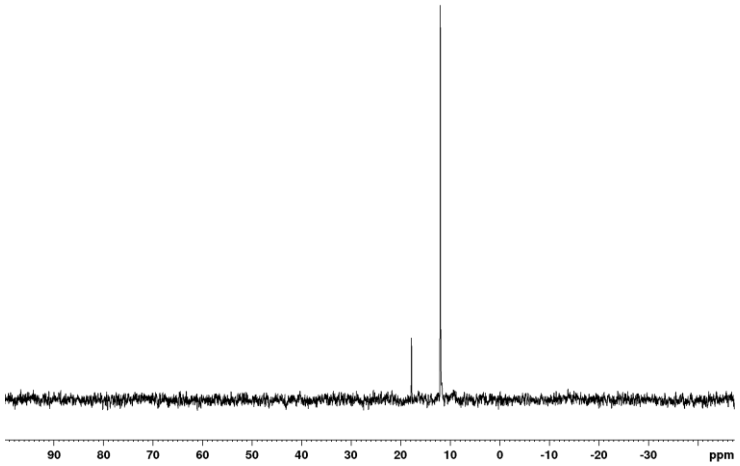

Figure 128. ^{31}P NMR spectrum of attempted coordination of **I** to Cp^*ZrMe_3 in CD_2Cl_2.

3.8 Attempted Coordination of I to $NiBr_2$(dimethyl ethylene glycol) or $NiBr_2$(DME)

The only study on the coordination of phosphonium cyclopentadienylides to nickel was reported in 1981 by Booth *et al*,[88] and they reported the synthesis of $[Ni(C_5H_4PPh_3)_2][PF_6]_2$ by the reaction of $C_5H_4PPh_3$ and nickelocene or $NiBr_2$, followed

by the addition of NH_4PF_6. To develop the nickel coordination to this class of ligand, it was thought that the coordination of nickel to PHIN should be attempted. After a series of solubility tests as described in **2.14.1**, it was found that $NiBr_2$(DME) is not soluble in THF, CH_2Cl_2, $CHCl_3$, Et_2O, toluene and chlorobenzene. Ethanol dissolved $NiBr_2$(DME) after a few minutes stirring, and acetonitrile dissolve $NiBr_2$(DME) partially.

The reaction of **I** and $NiBr_2$(DME) in CH_2Cl_2 was attempted as described in **2.14.2**, and after filtration, and removing solvent from filtrate, an oily dark brown mixture was obtained. ^1H and ^{31}P NMR spectra of the attempted coordination were obtained (Appendix, Figure A 95 and A 96). It was found that **I** was not consumed completely within 12 h due to the presence of a doublet peak at δ 2.49, in ^1H NMR spectrum, and also a singlet peak at δ 5.91 in ^{31}P NMR spectrum, which are characteristic for -PMe group of **I**. This reaction was repeated with longer time of stirring (48 h and 5 d) and ^{31}P NMR spectra of these reactions confirmed that all of **I** was consumed as the singlet peak at δ 5.91 had disappeared. ^1H and ^{31}P NMR spectra after 5 d are shown in Appendix, Figure A 97 and A 98. In ^1H NMR spectrum of the attempted coordination after 5 d (See Appendix, Figure A 97), the singlet peak at δ 3.35 was assigned for -OMe group in DME and the singlet peak at δ 3.51 was assigned for the CH_2 group of DME. ^{31}P NMR spectrum of the attempted coordination after 5 d (See Appendix, Figure A 98) depicted three singlet peaks at δ 11.25, 13.44 and 26.30 which revealed that three different products were formed in this reaction. It is possible that the two regioisomers of phosphonium salt of **I** were formed, as the two peaks at δ 13.44 and 26.30 are very similar to the phosphorus chemical shifts of phosphonium salts, δ 13.52 and 26.04. The singlet peak in ^{31}P NMR spectrum at δ 11.25 remained unidentified. The reaction of **I** and

$NiBr_2$(DME) was attempted in more vigorous condition, as described in **2.14.3**, by using toluene as solvent and refluxing the reaction for 2 h. Two fractions were obtained, a dark brown solid and a bright yellow solid. ^1H and ^{31}P NMR spectra were obtained from both fractions. It was found that the bright yellow solid was **I** as in ^{31}P NMR spectrum a singlet peak was seen at δ 5.91 which is characteristic for PMe group of **I** ligand. The ^1H NMR spectrum of dark brown solid (See Appendix, Figure A 99), showed a broad peak at δ 3.37 which was assigned for -OMe group in DME and the broad singlet peak at δ 3.54 assigned for CH_2 group of DME. The dark brown solid was also contained free toluene as there was a single peak at δ 2.34 in ^1H NMR spectrum. As described in **2.14.4**, the reaction of **I** and $NiBr_2$(DME) was refluxed in chlorobenzene, and two fractions were obtained, dark brown and green solids. ^1H and ^{31}P NMR spectra of the dark brown solid are shown in Appendix, Figure A 101, and A 102. The ^{31}P NMR spectrum revealed that three different products at least formed in this reaction as ^{31}P NMR spectrum depicted three different peaks at δ 5.92, 13.50, and 26.51. The singlet peak at δ 5.92 was assigned for the -PMe group in **I** and the peaks at 13.50, and 26.51 were assigned for the two regioisomers of phosphonium salts. As dissolving the dark green solid, obtained from filtration, was difficult in a variety of solvents, the NMR experiments were conducted by using DMSO-d_6. The green solid was determined to be **I**, as the ^{31}P NMR spectrum depicted one singlet peak at δ 7.20 which is identical with the ^{31}P NMR spectrum of **I** in DMSO-d_6. For comparison reason, NMR experiments of the dark brown solid which was obtained after filtration and removing solvent, was also conducted by using DMSO-d_6 as solvent, and the ^{31}P NMR spectrum depicted five different peaks at δ 7.3, 10.7, 14.48, 26.68 and 28.68. The singlet at δ 7.3 was assigned for -PMe group of **I**, the two singlet

peaks at δ 14.48, and 26.68 were assigned for the two regioisomers of phosphonium salts, the other two peaks at δ 10.7 and 28.68 were remained uncharacterized.

In summary, none of the attempted reactions afforded a single product, and none of the products was fully characterized due to the formation of minor products.

3.9 Attempted Coordination of I to HgX_2

The reaction of $C_5H_4PPh_3$ and HgX_2 (X = Cl, Br and I) in THF was previously reported by Holy *et al.* to synthesize $[(\eta^1\text{-}C_5H_4PPh_3)HgX_2]_2$.[86,87] Similarly, it was thought that the reaction of **I** and $HgCl_2$ would form $[(\eta^1\text{-}\mathbf{I})HgX_2]_2$, so the coordination of **I** to $HgCl_2$ was attempted, as described in **2.15.1**, and ^1H and ^{31}P NMR spectra were obtained (See Appendix, Figure A 103 and A 104). ^1H NMR spectrum was not too informative due to the presence of broad peaks. A broad peak at δ ~2.8 could be assigned for P-Me group which is characteristic for -PMe group of **I** ligand. ^{31}P NMR spectrum (See Appendix, Figure A 104) depicted two singlet peaks at δ 11.59 and 13.17. After precipitating a white solid by dissolving the reaction mixture in CH_2Cl_2 and isolate it by filtration, a dark green filtrate was obtained and the ^{31}P NMR spectrum depicted at least thirteen different peaks indicating the formation of several compounds. The white solid was insoluble in CH_2Cl_2, but it was soluble in DMSO. The ^1H NMR spectrum (See Appendix, Figure A 105) showed two doublet peaks at δ 2.76 and 3.00 with about 14.0 Hz coupling constants. The ^{31}P NMR spectrum (See Appendix, Figure A 106) showed two singlet peaks at δ 8.74 and 12.19. It was found that the white solid product was a mixture of two compounds and no further investigation was attempted to purify or characterize it. It was found that the white solid was not phosphonium salts as an NMR

experiment of phosphonium salts in DMSO-d_6 was attempted and compared with the NMR results of white solid. The ^{31}P NMR spectrum of phosphonium salts in DMSO-d_6 showed two singlet peaks at δ 14.49 and 26.71. Coordination of **I** to $HgBr_2$ was attempted as described in **2.15.2**, and ^{1}H and ^{31}P NMR spectra were obtained (See Appendix). The ^{1}H NMR spectrum (See Appendix, Figure A 107) showed a multiplet peak at δ ~2.8 which made it difficult to identify the doublet peaks of -PMe group of **I** ligand. The ^{31}P NMR spectrum (See Appendix, Figure A 108) depicted three singlet peaks at δ 10.83, 12.92 and 25.46. By comparing the phosphor chemical shifts of phosphonium salts which are δ 13.52 and 26.04 with the phosphor chemical shifts of this product, it was found that the two peaks at δ 12.92 and 25.46 could be attributed to the presence of two regioisomers of phosphonium salt in the final product. No further study was carried out on the coordination of **I** to HgX_2 (X = Cl and Br).

In summary, none of the attempted reactions afforded a single product, and none of the products was fully characterized due to the formation of minor products.

Chapter 4 : Conclusions and Future Work

4.1 Conclusions

In 2007, the synthesis of methyldiphenylphosphonium cyclopentadienylide ($C_5Ph_4PMePh_2$) and the group 6 complexes of methyldiphenylphosphonium cyclopentadienylide, $(\eta^5\text{-}C_5H_4PMePh_2)M(CO)_3$, (M = Cr, Mo, and W) were reported,[22] and later, in 2008, the synthesis of a new planar pro-chiral ligand, $C_9H_6PMePh_2$ (**I**), and its planar chiral chromium complex were studied.[55] In 2011, two new ligands of this class, dimethyldiphenylphosphonium indenylide ($1\text{-}C_9H_6PMe_2Ph$), and triphenylphosphonium indenylide ($1\text{-}C_9H_6PPh_3$), along with methyldiphenylphosphonium indenylide ($1\text{-}C_9H_6PMePh_2$, **I**) were synthesized and coordinated to form the ruthenium complexes of $[Ru(\eta^5\text{-}C_5H_5)(\eta^5\text{-}1\text{-}C_9H_6PMe_2Ph)]PF_6$, $[Ru(\eta^5\text{-}C_5H_5)(\eta^5\text{-}1\text{-}C_9H_6PPh_3)]PF_6$, and $[Ru(\eta^5\text{-}C_5H_5)(\eta^5\text{-}\mathbf{I})]PF_6$.[54]

To extend this field of research, the coordination of this class of ligand to different transition metals has been considered. In this work, the previously reported PHIN ligand, **I**, was synthesized, and has been coordinated to iridium(I) and rhodium(I) in the complexes $[Ir(\eta^4\text{-}C_8H_{12})(\eta^5\text{-}\mathbf{I})]BF_4$ (**III**), and $[Rh(\eta^4\text{-}C_8H_{12})(\eta^5\text{-}\mathbf{I})]BF_4$ (**V**). For further investigation, coordination of **I** to metals of groups 4, 10, and 12 was also studied. In terms of electron donating ability, ligand **I** donates six electrons like $CpPPh_3$ and C_6Me_6 and it was anticipated that ligand **I** could coordinate to titanium as do $CpPPh_3$[26] and C_6Me_6.[70] Titanium coordination to $CpPPh_3$ to form a sandwich complex, $[CpPPh_3)_2TiCl_2]Cl_2$, was reported in 1977 by using two-fold excess of $CpPPh_3$,[26] and coordination of C_6Me_6 to $TiCl_4$ was also reported in the synthesis of $[(\eta^6\text{-}C_6Me_6)TiCl_3][Ti_2Cl_9]$ by using four-fold excess of $TiCl_4$, in 1994.[70] Coordination of **I** to

titanium was previously attempted in the Baird lab by using either excess of **I** to synthesize a sandwich complex[79] or excess of $TiCl_4$ and $TiCl_4(THF)_2$ (four-fold excess) to synthesize a half sandwich complex,[78,80] but none of these attempts afforded a single product.

In this thesis, more concentrated solution of $TiCl_4$ (~eleven-fold excess) was used in hope of forcing the equilibrium to product more favorably. The reaction was also carried out in CH_2Cl_2 at different temperatures (room, −78 °C, and reflux temperature), and also in a solvent free reaction, but none of these attempts was successful. Several products were always formed and isolation of a single product was impossible. A variety of chloride abstractors was also tried to assist the formation of $[(\eta^5\text{-}\mathbf{I})TiCl_3]^+$, $AlCl_3$,[80] $[Ph_3C][B(C_6F_5)_4]$, and $GaCl_3$, but again mixtures of products were obtained.

Coordination of **I** to zirconium was also attempted by the reaction of **I**, Cp^*ZrMe_3 and $[Ph_3C][B(C_6F_5)_4]$. It was anticipated that $[Ph_3C][B(C_6F_5)_4]$ would abstract one methyl group from Cp^*ZrMe_3 to make a vacant site to coordinate to which **I** could coordinate to form $[Cp^*ZrMe_2(\eta^5\text{-}\mathbf{I})][B(C_6F_5)_4]$ While the ^1H NMR spectrum exhibited two singlet peaks in the negative region which could be attributed to the two methyl groups on zirconium, the reaction unfortunately formed more than one product and isolation of the desired product was unsuccessful.

Coordination of **I** to nickel was considered and it was found that the only nickel complex of this class of ligand, $[Ni(CpPPh_3)_2][PF_6]_2$, was reported in 1981.[88] Coordination of **I** to $NiBr_2(DME)$ was anticipated to occur because DME is a labile ligand and can possibly be replaced by **I**, but again attempted reactions in various solvents and at various temperatures always resulted in mixtures of products. Reaction of

I with mercuric halides were also considered since coordination of $CpPPh_3$ to HgX_2 (X = Cl, Br and I) was previously reported to result in formation of $[(\eta^1\text{-}C_5H_4PPh_3)HgX_2]_2$,[86,87] Unfortunately, none of the attempted reactions afforded a single product, and none of the products was fully characterized due to the formation of complex mixtures.

(Diphenylphosphino)-4,7-dimethyl-indene (4,7-dimethyl-1-$C_9H_5PPh_2$) was prepared before and characterized by ^1H, ^{13}C, and ^{31}P NMR, EI MS, and HR-MS, but its crystal structure has not been reported.[93] In this thesis, X-ray quality crystals of this compound were obtained and its structure has been determined. A novel PHIN ligand, **II**, was synthesized and characterized by ^1H, ^{13}C, and ^{31}P NMR, elemental analysis, and X-ray crystallography. **II** has been coordinated to iridium(I) and rhodium(I) to synthesize $[Ir(\eta^4\text{-}C_8H_{12})(\eta^5\text{-}\mathbf{II})]BF_4$ (**IV**), and $[Rh(\eta^4\text{-}C_8H_{12})(\eta^5\text{-}\mathbf{II})]BF_4$ (**VI**). All these complexes **III-VI** were characterized by NMR spectroscopy, HR-EMS, elemental analyses. Oxidative addition reactions of methyl iodide (MeI) and benzyl chloride ($PhCH_2Cl$) to **III-VI** were attempted, but no positive results were obtained, unfortunately. The reaction of H_2 to **III-VI** was attempted and no hydrogenated product was formed. Coordination of **I** to a variety of metals, group 4, 9, 10, and 12, was attempted unsuccessfully, and it was anticipated that all these unsuccessful attempted coordination resulted from the high reactivity of **I**, because in all these reactions the ligand (**I**) was completely consumed and there was no unreacted ligand (**I**) left at the end of each reaction.

4.2 Future work

The investigation of iridium and rhodium(I)-PHIN complexes is just started, and there is a lot left to work on. Further attempts need to be made to grow crystals of all the

coordinated complexes, **III-VI**, for the X-ray crystallography. This crystallization could be done by either using different solvents or using a combination of different solvents. It may also be possible to crystallize the complexes by changing the counter ion from BF_4^- to a different counter ion, for example PF_6^-, and this could be achieved by using a different chloride abstractor such as $AgPF_6$. In addition to characterizing these planar chiral complexes crystallographically, they will be resolved, by using a chiral, resolved anions, in order to prepare pure enantiomeric to be used as chiral catalysts in, for example, hydrogenation of different unsaturated compounds.

Since **I** and **II** are both planar pro-chiral, coordination of both to a transition metal discriminates the two enantiotopic faces[109] and results in the formation of a metal complex without a symmetry element.[110] One of the most important field of research in organometallic chemistry is the synthesis of chiral metal complexes due to the vast potential applications of these complexes in the field of natural product, pharmaceutical, and agricultural chemical synthesis.[111,112] The field of organometallic medicinal chemistry is another interesting aspect of the application of chiral metal complexes. Using chiral ligands to establish chirality in metal complexes has been introduced to organometallic chemistry long time ago, but these type of complexes are not applicable to all the organic transformations to synthesize the targeted product in high enantioselectivity.[113] Therefore, the study and exploration on the synthesis of chiral organometallic complexes where the chiral information is located at the metal center rather than at the ligand has become more appealing and caught attentions.

However, the synthesis and exploration of chiral organometallic complexes where chirality is established at the metal rather than the ligand remained virtually unexplored.

Consequently, coordination of ligands **I**, or **II** to a wide variety of transition metals can be studied and their asymmetric catalytic applications in the synthesis of different targeted products in high enantioselectivity can be investigated.

As a further experiment, it will be interesting to derivatize the phosphorus atoms of our PHIN ligands to study their structure, properties and ability to coordinate to iridium(I) or rhodium(I) because different phosphines should give rise to indenylides with different electronic properties and, therefore, different coordination chemistry. The ability to alter the electronic properties of a metal complex through slight modifications of a ligand can have great effects on applications in catalysis. Exploring oxidative additions to **III-VI** by using different alkyl halide or iodine could be considered. Additionally, the oxidative addition of H_2 to **III-VI** can be carried out under other conditions such as at higher pressure than 10 bar at room temperature or lower pressure at higher temperature.

In the field of coordination of PHINs to titanium, changing chloride abstractor might be beneficial to synthesize and crystallize the desired complex. Catalytic activities could be examined for polymerization of a variety of alkenes such as ethylene or propene.

Appendix A : NMR Spectra

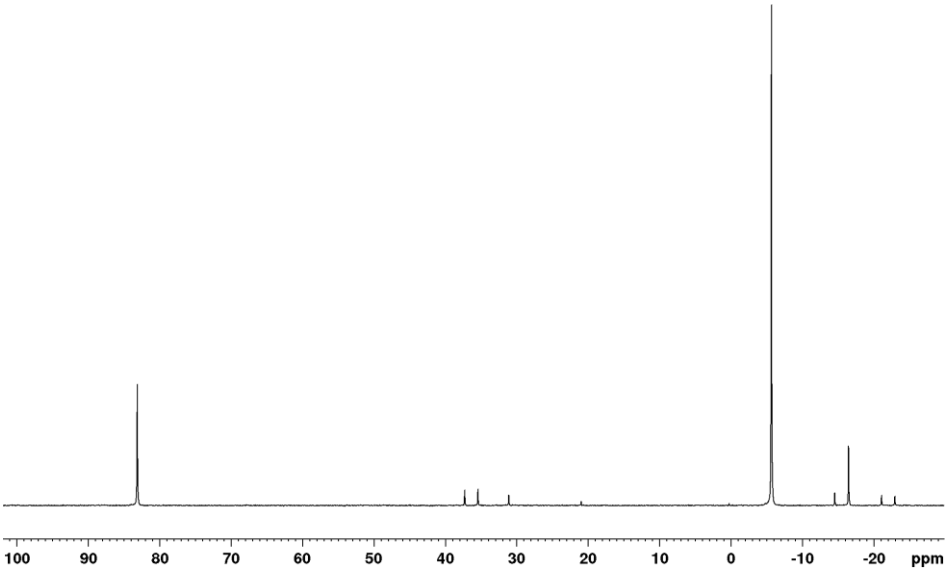

Figure A 1. ^{31}P NMR of 4,7-dimethyl-1-$C_9H_5PPh_2$ in CD_2Cl_2.

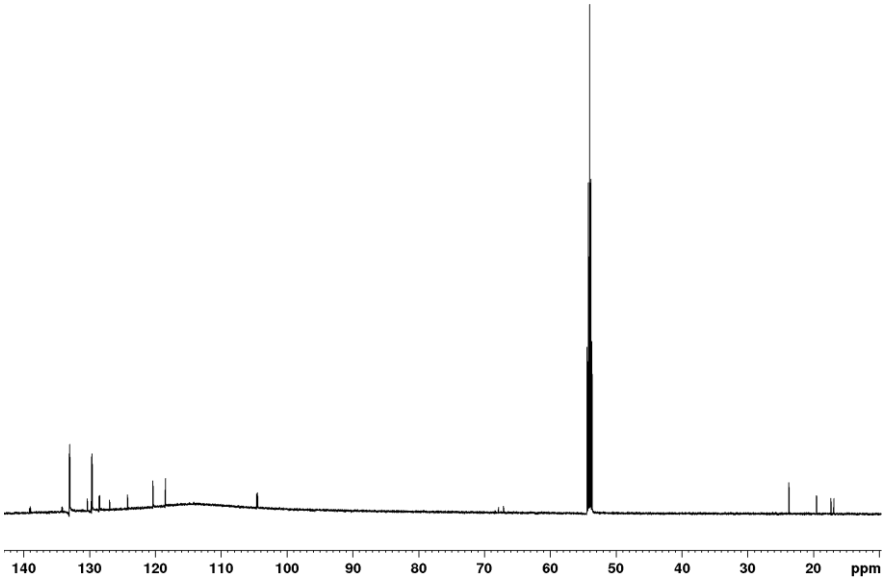

Figure A 2. ^{13}C NMR spectrum of 4,7-dimethyl-1-$C_9H_4PMePhe$ (II) in CD_2Cl_2.

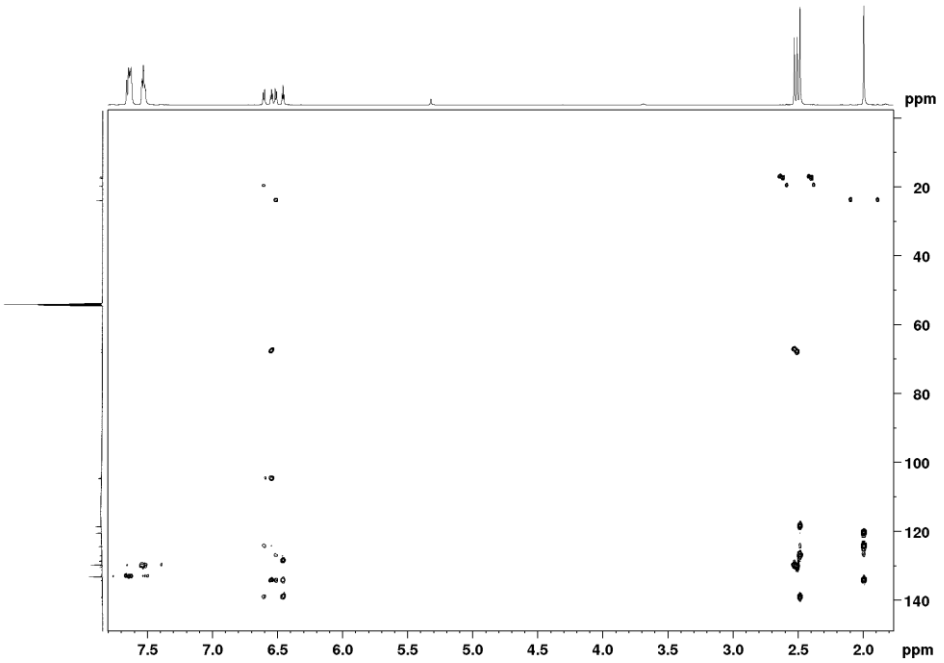

Figure A 3. ^{1}H-^{13}C HMBC spectrum of 4,7-dimethyl-1-$C_9H_4PMePh_2$ (II) in CD_2Cl_2.

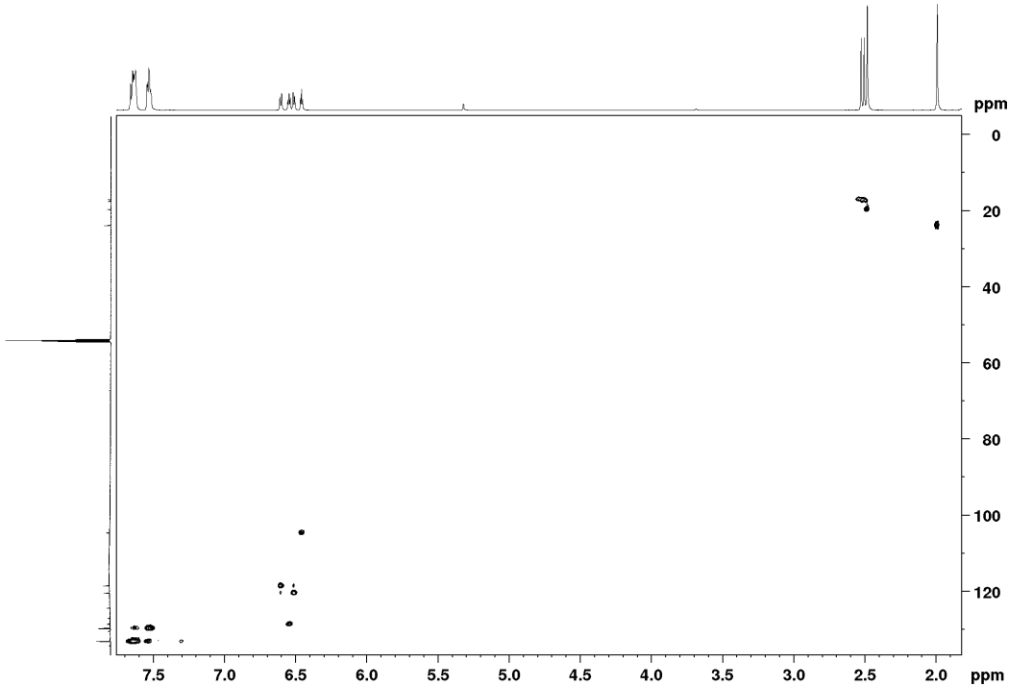

Figure A 4. ^{1}H-^{13}C HSQC spectrum of 4,7-dimethyl-1-$C_9H_4PMePh_2$ (II) in CD_2Cl_2.

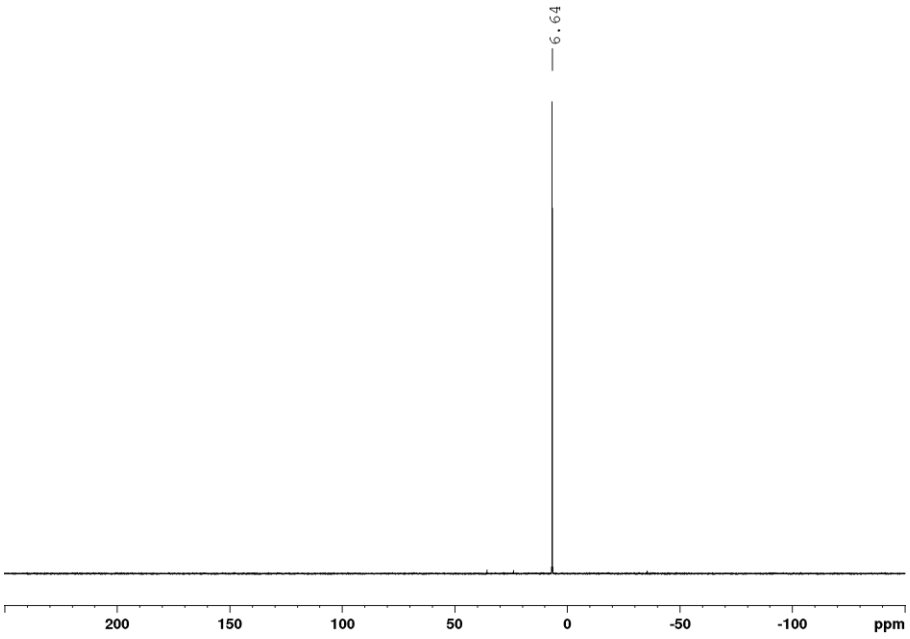

Figure A 5. ^{31}P NMR spectrum of 4,7-dimethyl-1-$C_9H_4PMePh_2$ (II) in CD_2Cl_2.

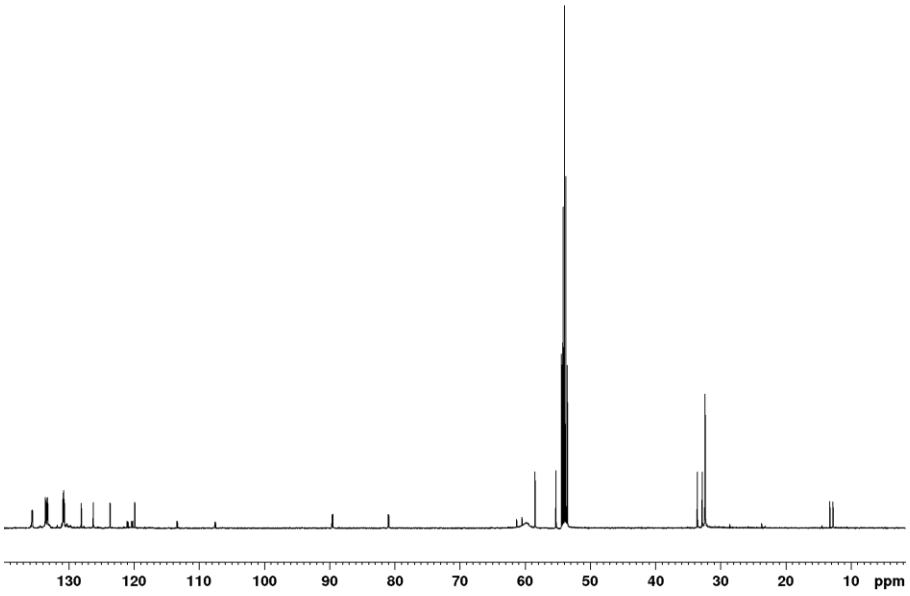

Figure A 6. ^{13}C NMR spectrum of the product of reaction between $[Ir(COD)Cl]_2$ and (I) in CD_2Cl_2.

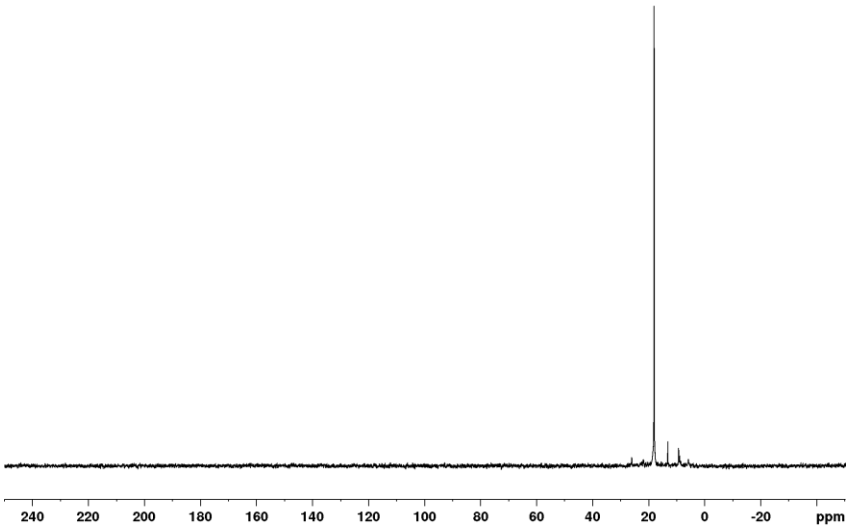

Figure A 7. ^{31}P NMR spectrum of the product of reaction between $[Ir(COD)Cl]_2$ and (I) in CD_2Cl_2.

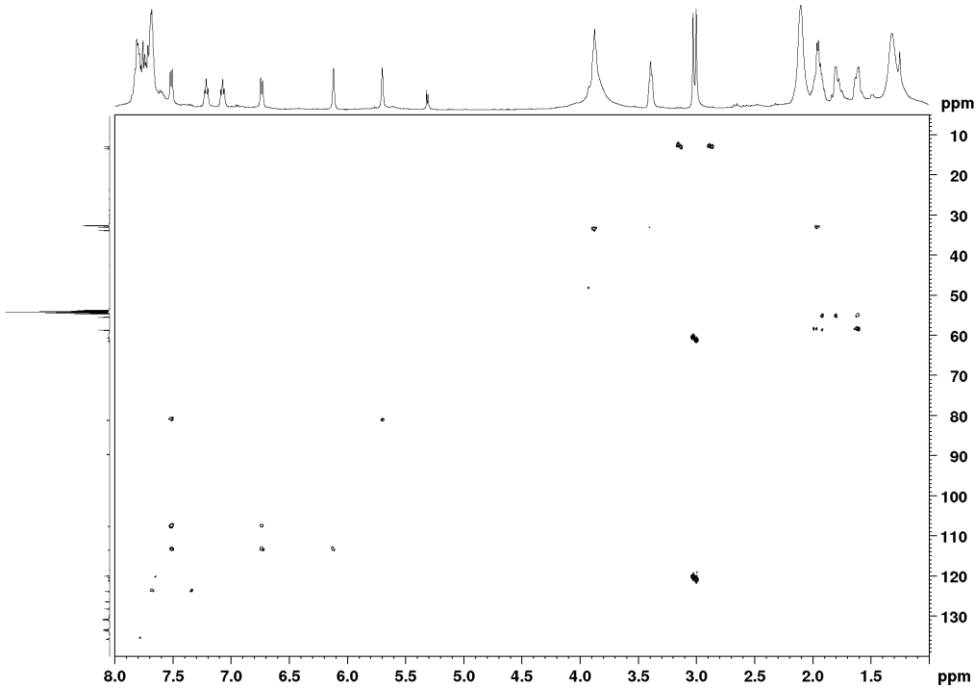

Figure A 8. ^{1}H-^{13}C HMBC spectrum of the product of reaction between $[Ir(COD)Cl]_2$ and (I) in CD_2Cl_2.

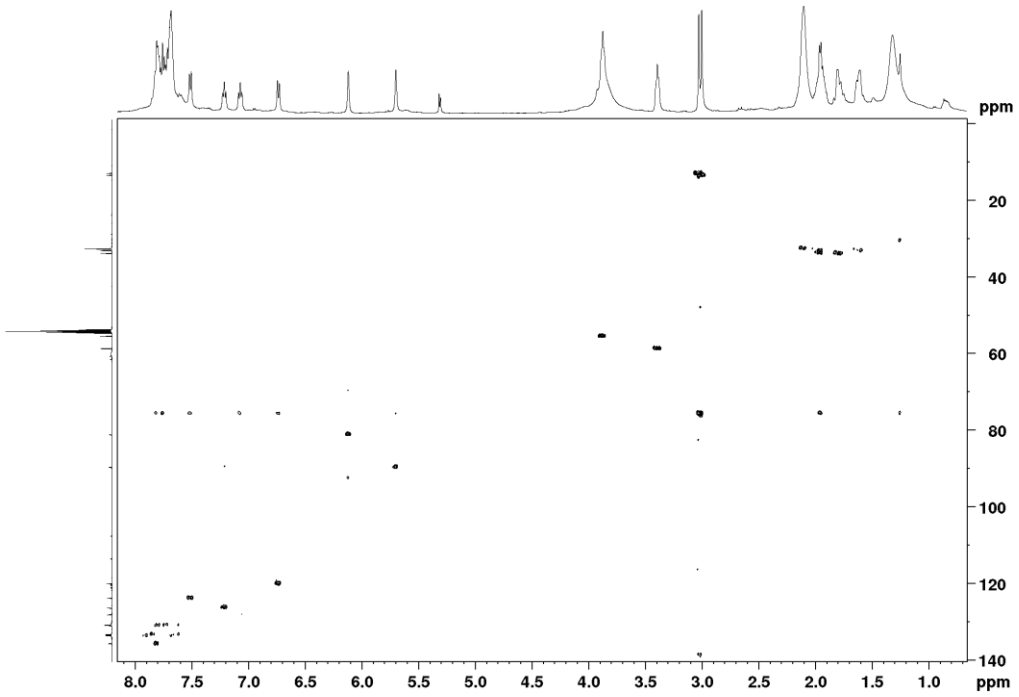

Figure A 9. ^{1}H-^{13}C HSQC spectrum of the product of reaction between $[Ir(COD)Cl]_2$ and (I) in CD_2Cl_2.

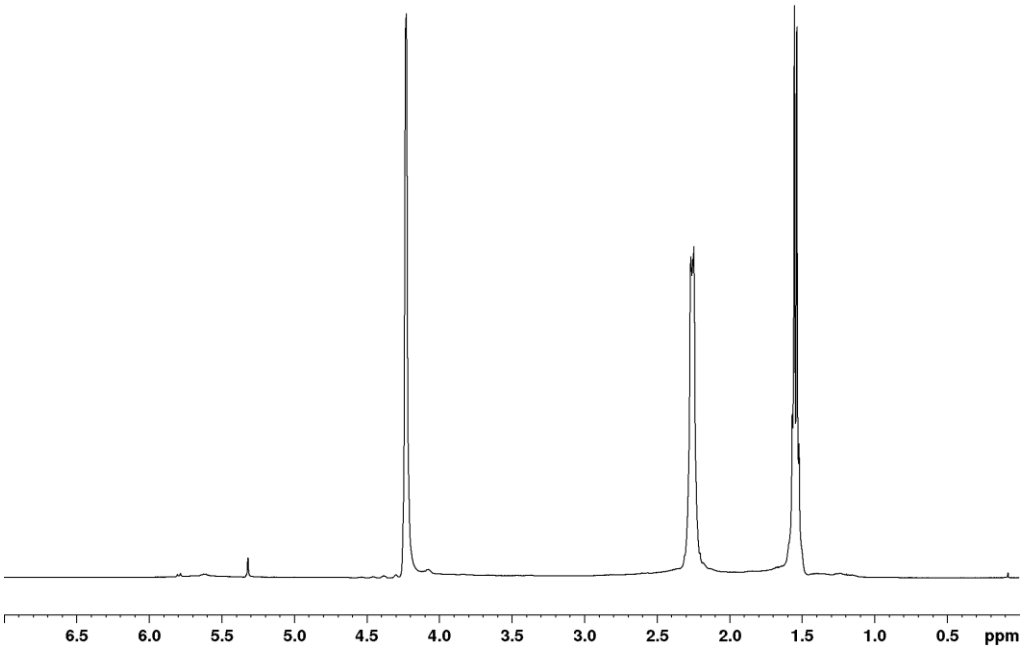

Figure A 10. ^{1}H NMR spectrum of $[Ir(COD)Cl]_2$ in CD_2Cl_2.

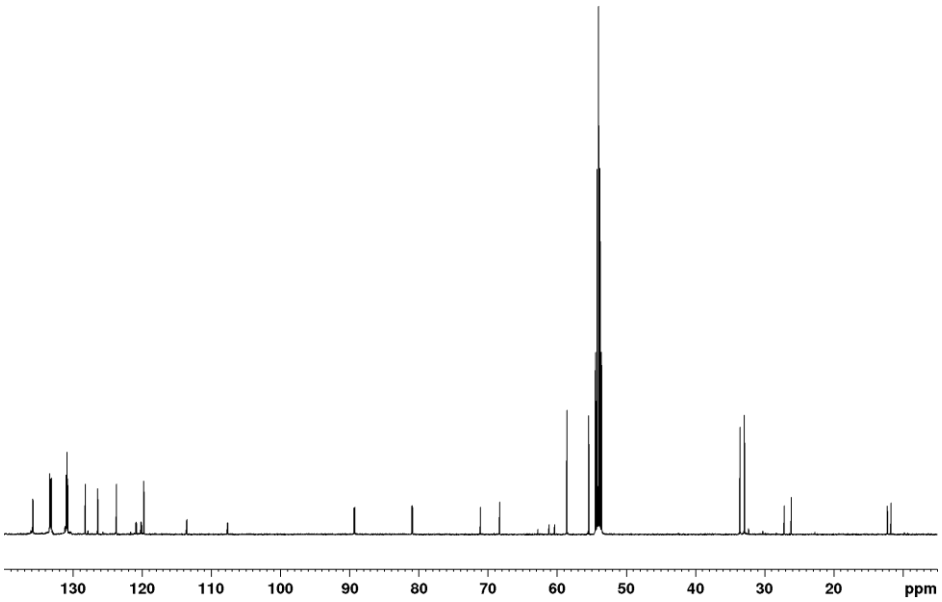

Figure A 11. ^{13}C NMR spectrum of (III) in CD_2Cl_2.

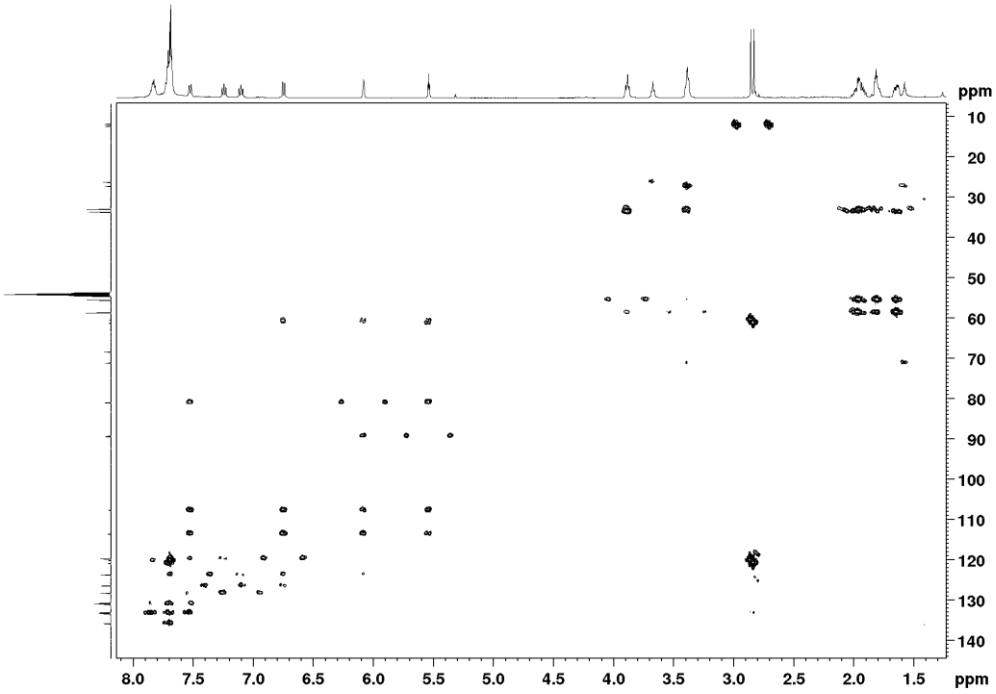

Figure A 12. ^{1}H-^{13}C HMBC spectrum of (III) in CD_2Cl_2.

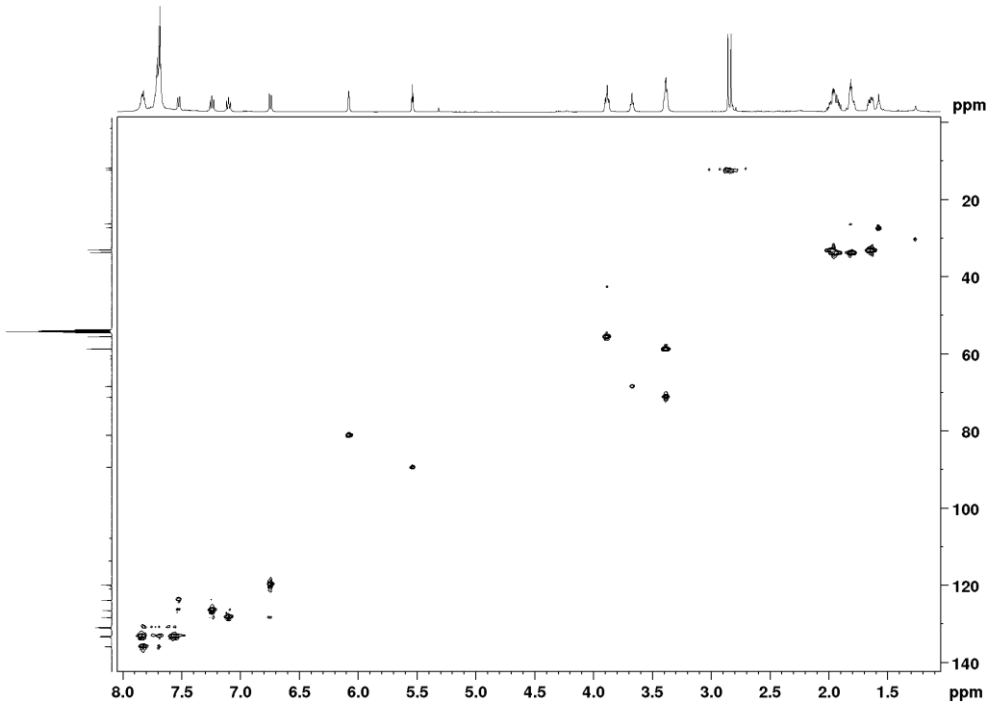

Figure A 13. ^{1}H-^{13}C HSQC spectrum of (III) in CD_2Cl_2.

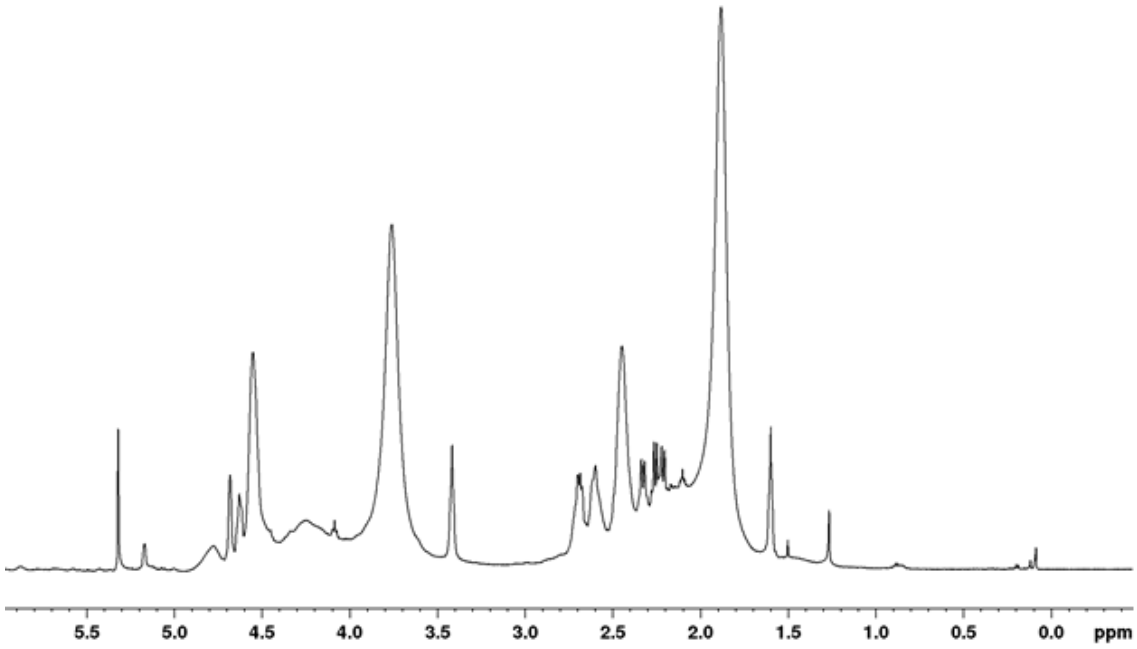

Figure A 14. ^{1}H NMR spectrum of [Ir(COD)][BF_4] in CD_2Cl_2.

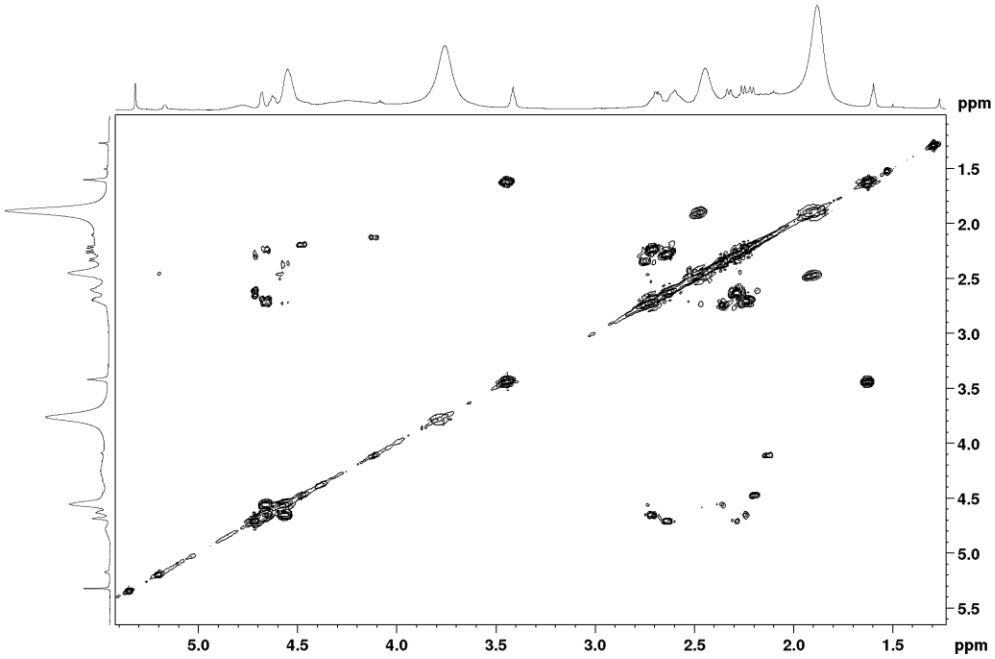

Figure A 15. COSY spectrum of [Ir(COD)][BF_4] in CD_2Cl_2.

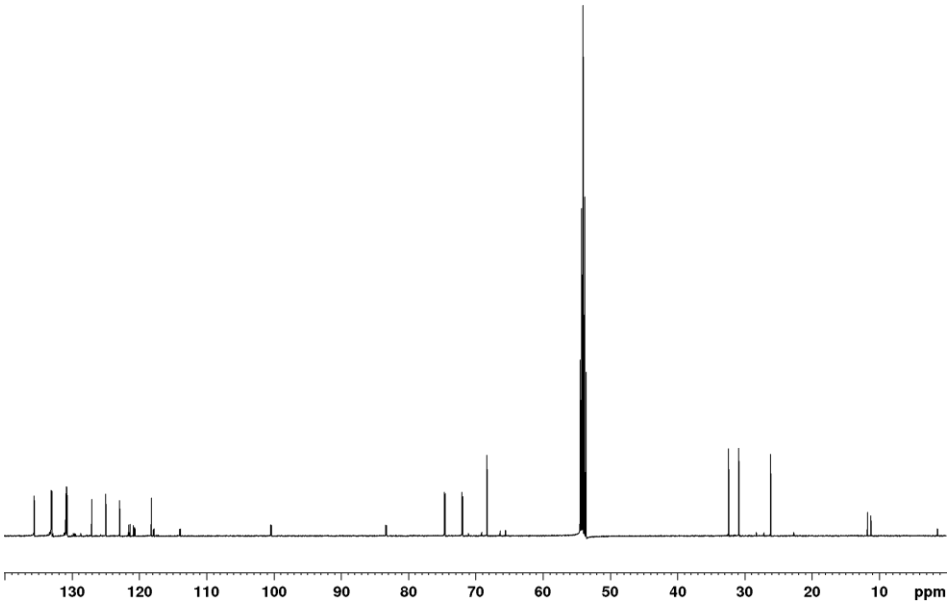

Figure A 16. ^{13}C NMR spectrum of (V) in CD_2Cl_2.

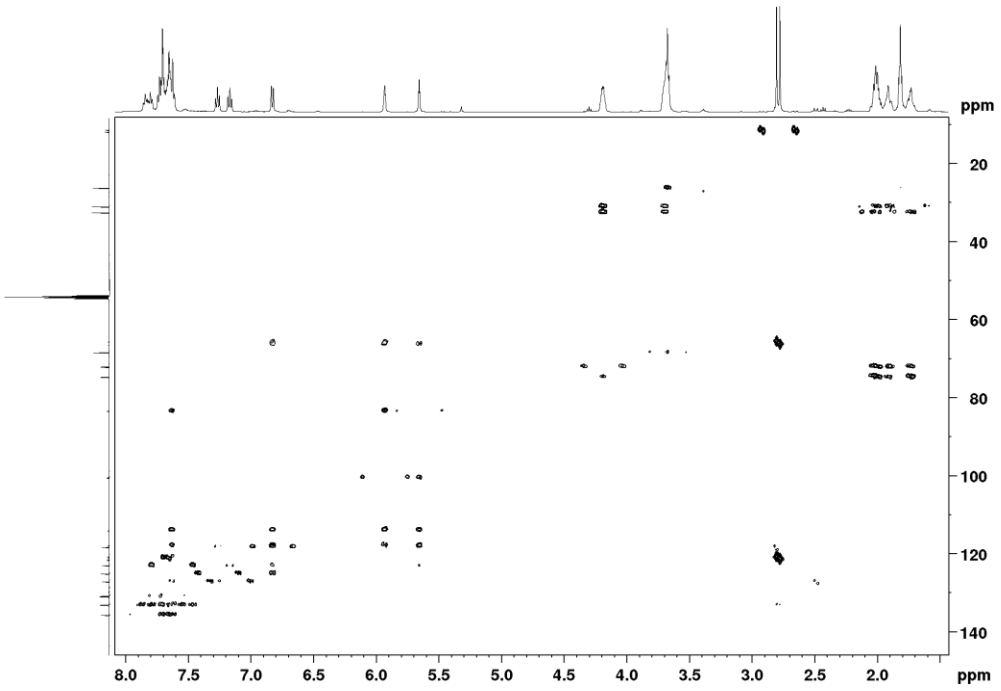

Figure A 17. ^{1}H-^{13}C HMBC spectrum of (V) in CD_2Cl_2.

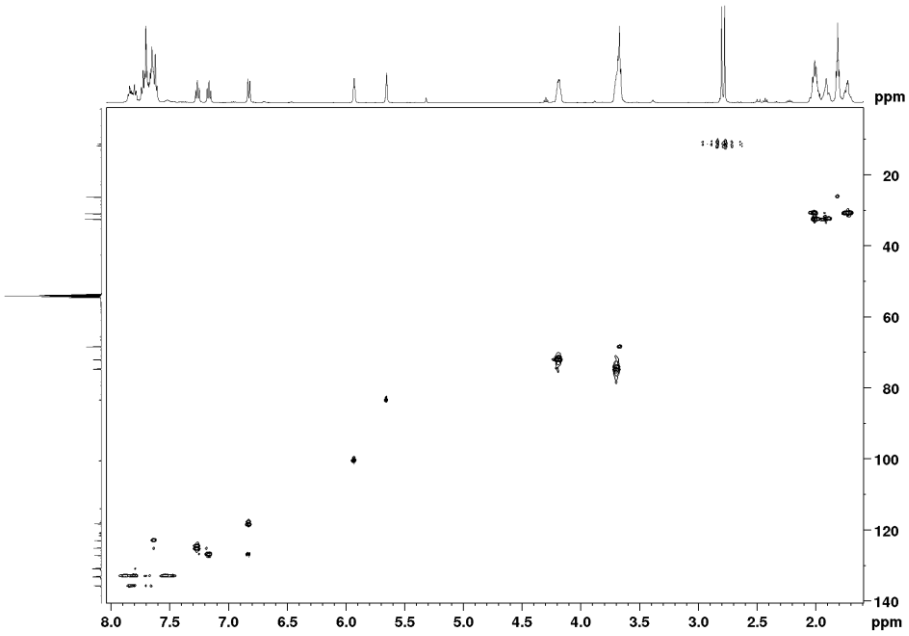

Figure A 18. ^{1}H-^{13}C HSQC spectrum of (V) in CD_2Cl_2.

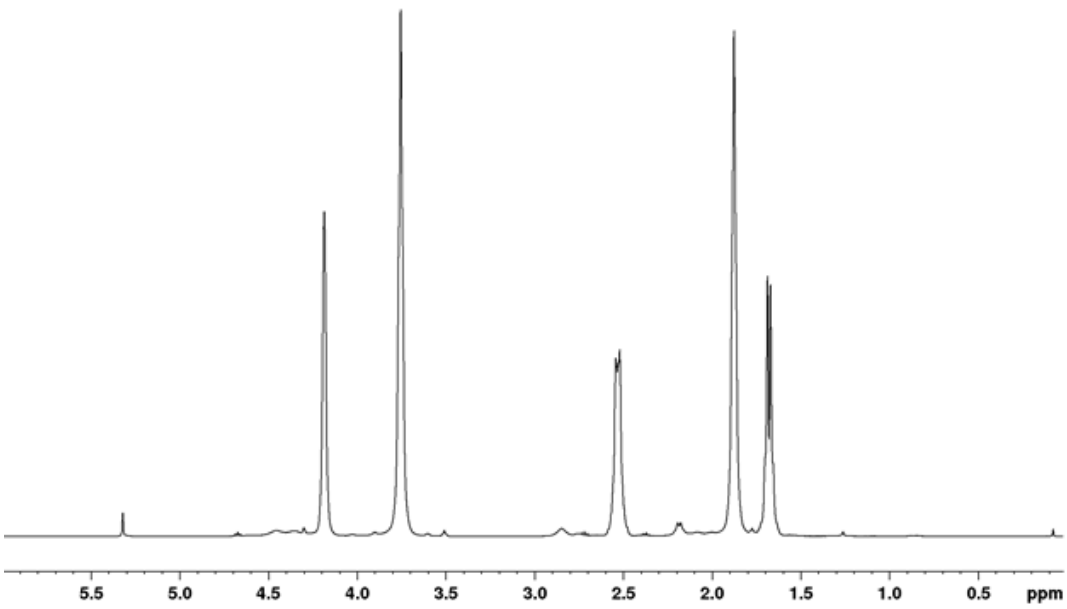

Figure A 19. ^{1}H NMR spectrum of [Rh(COD)][BF_4] in CD_2Cl_2.

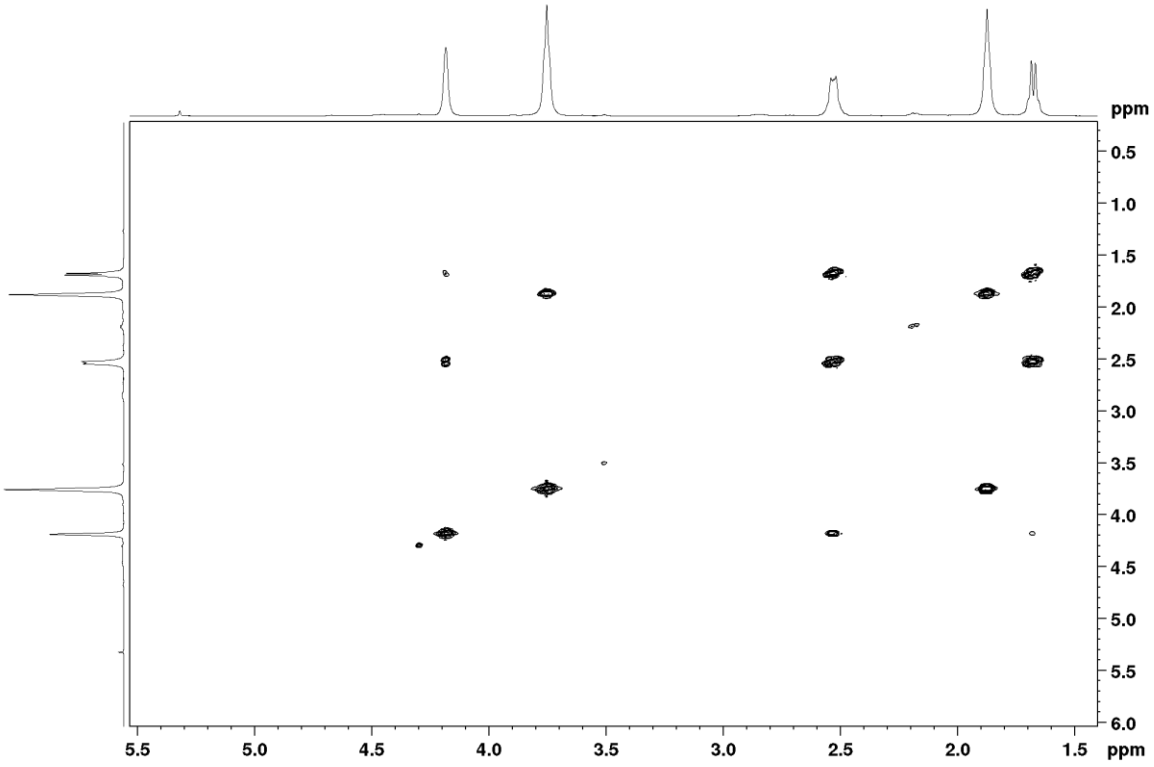

Figure A 20. COSY spectrum of [Rh(COD)][BF_4] in CD_2Cl_2.

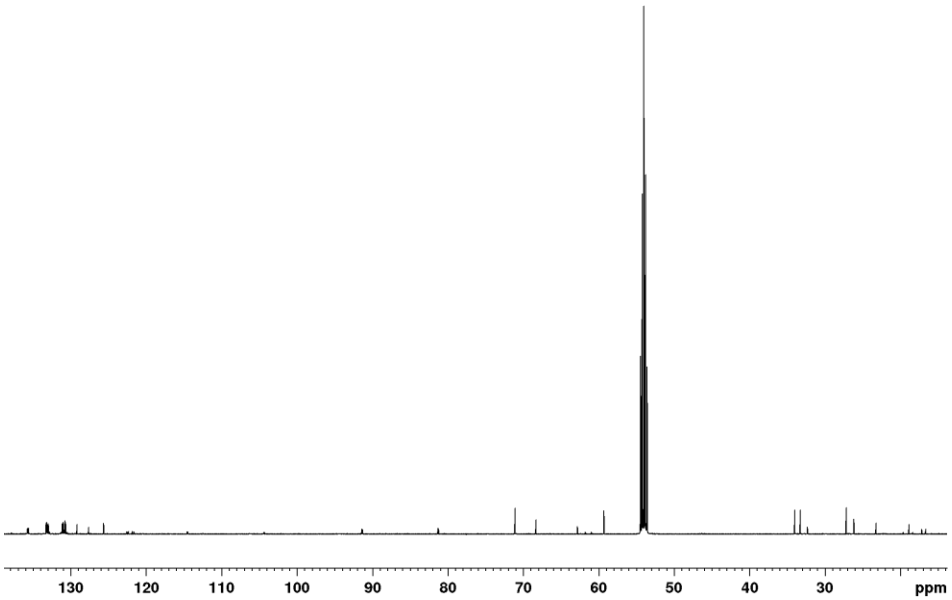

Figure A 21. ^{13}C NMR spectrum of (IV) in CD_2Cl_2.

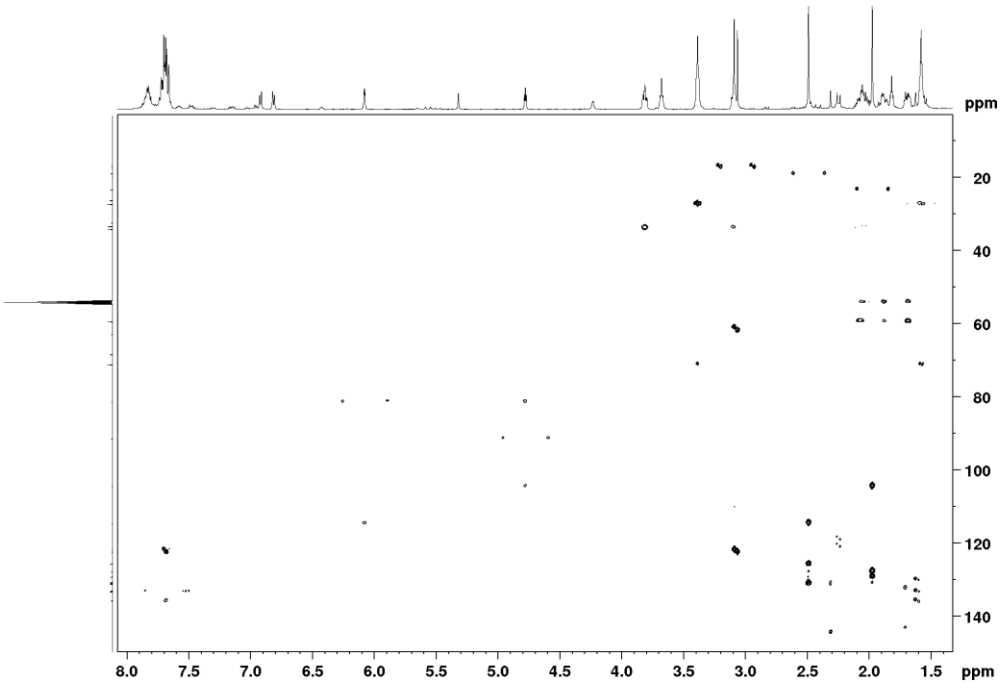

Figure A 22. ^{1}H-^{13}C HMBC spectrum of (IV) in CD_2Cl_2.

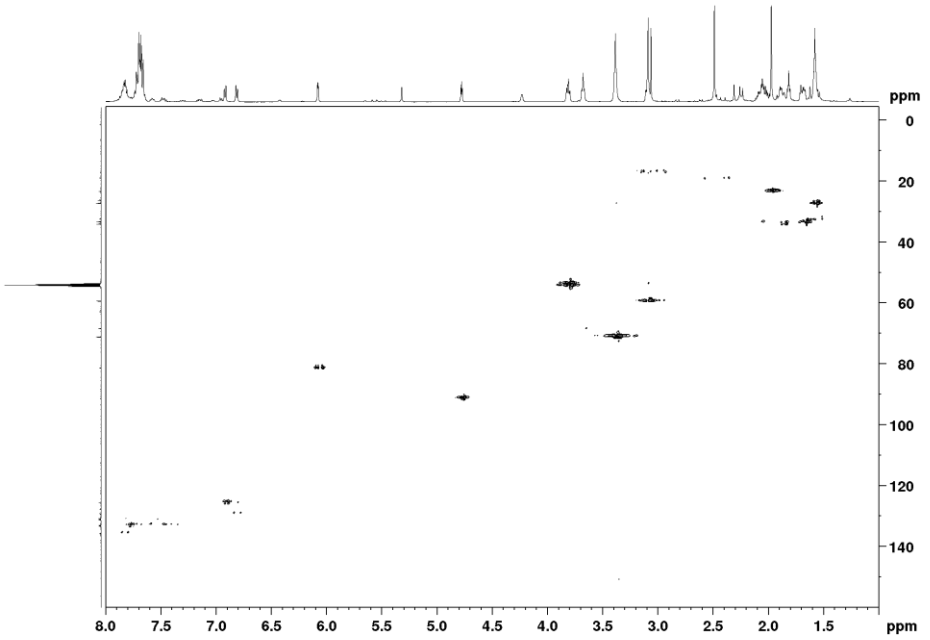

Figure A 23. ^{1}H-^{13}C HSQC spectrum of (IV) in CD_2Cl_2.

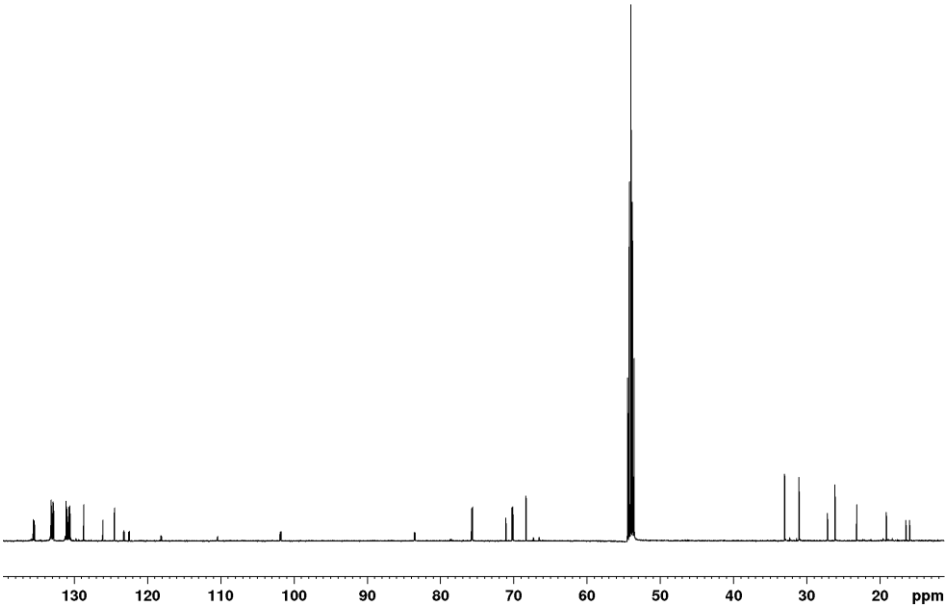

Figure A 24. ^{13}C NMR spectrum of (VI) in CD_2Cl_2.

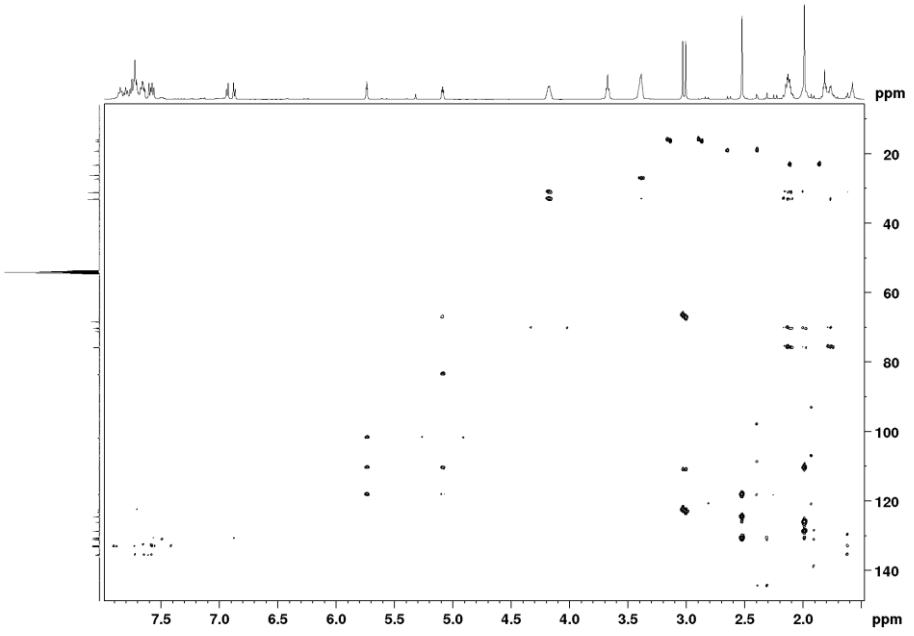

Figure A 25. ^{1}H-^{13}C HMBC spectrum of (VI) in CD_2Cl_2.

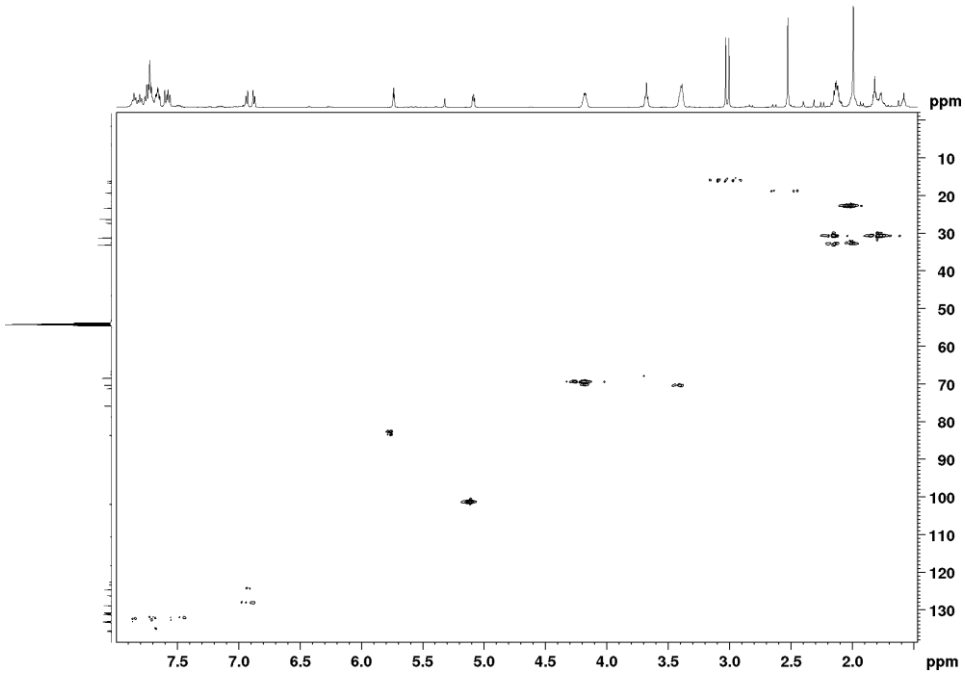

Figure A 26. ^{1}H-^{13}C HSQC spectrum of (VI) in CD_2Cl_2.

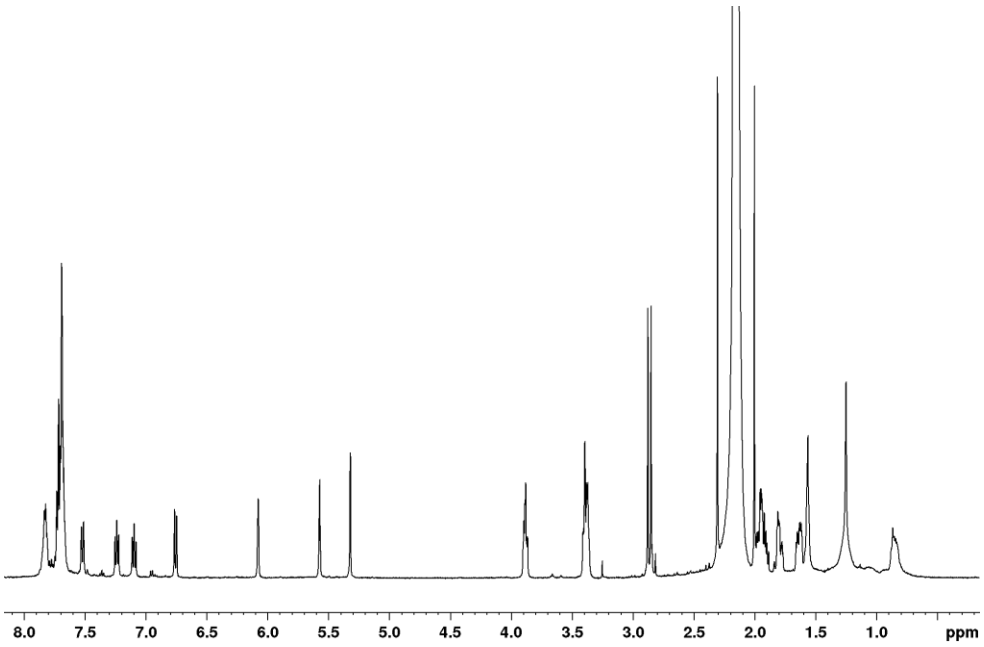

Figure A 27. ^{1}H NMR spectrum of the attempted oxidative addition of MeI to (III) in NMR scale after 5 min in CD_2Cl_2.

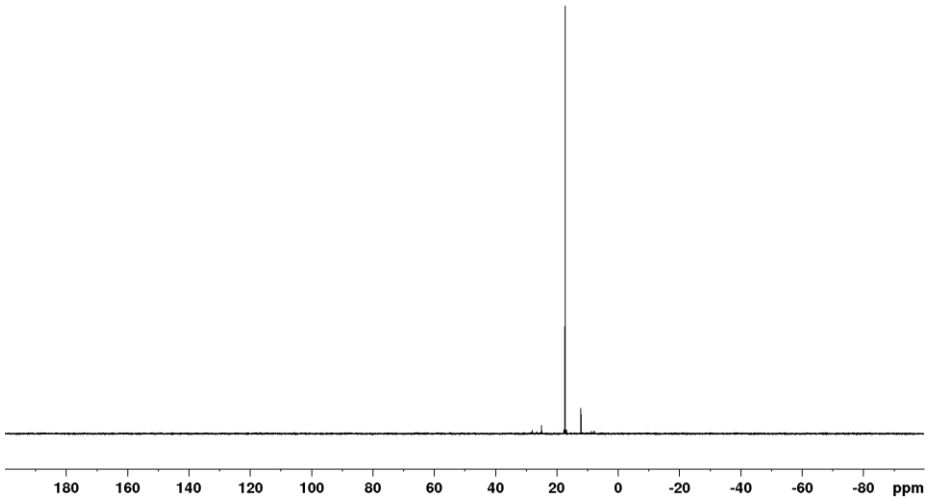

Figure A 28. ^{31}P NMR spectrum of the attempted oxidative addition of MeI to (III) in NMR scale after 5 min in CD_2Cl_2.

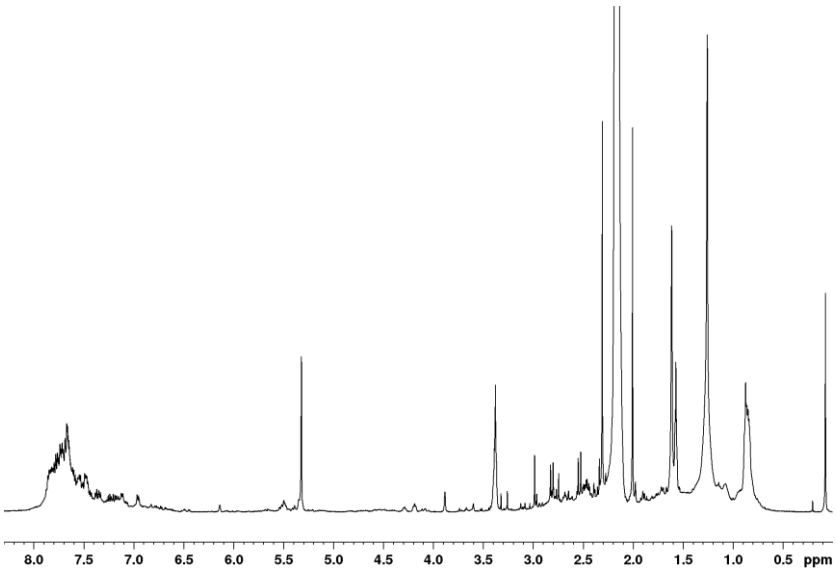

Figure A 29. ^{1}H NMR spectrum of the attempted oxidative addition of MeI to (III) in NMR scale after 8 d in CD_2Cl_2.

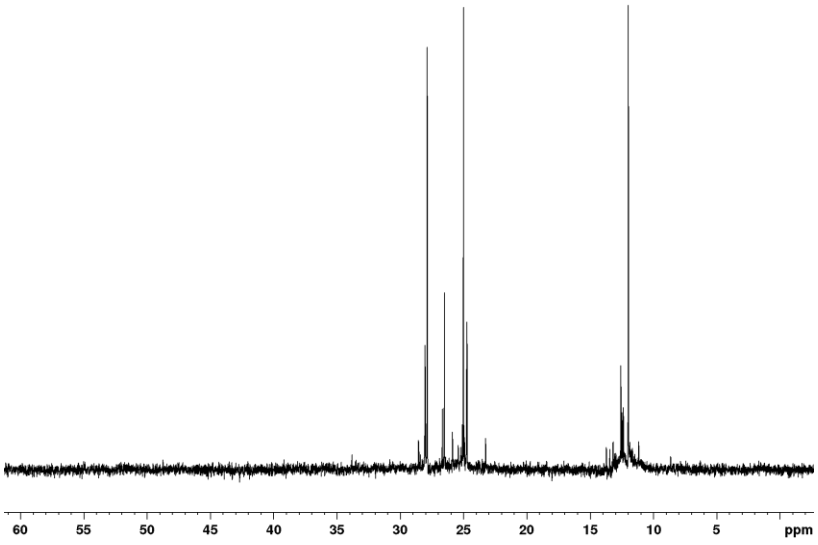

Figure A 30. ^{31}P NMR spectrum of the attempted oxidative addition of MeI to (III) in NMR scale after 8 d in CD_2Cl_2.

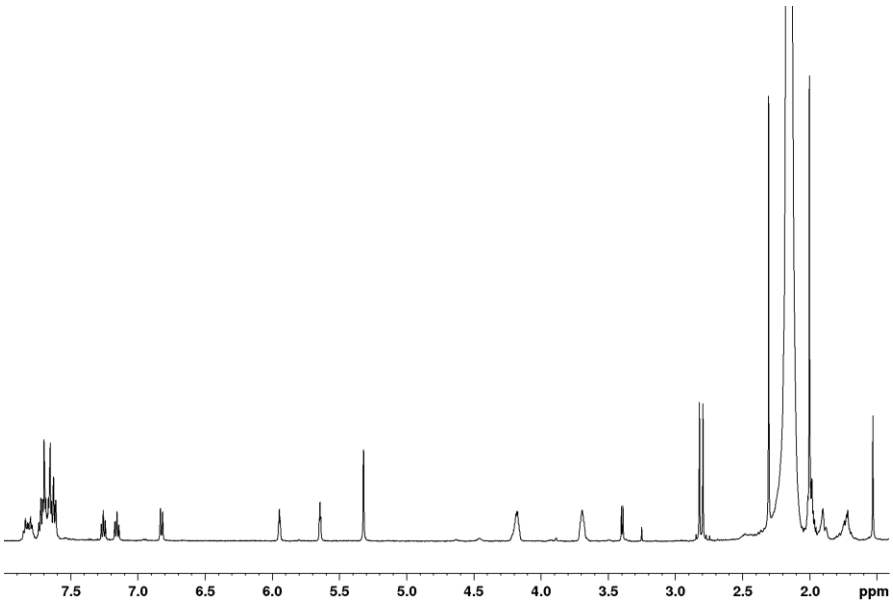

Figure A 31. ^{1}H NMR spectrum of the attempted oxidative addition of MeI to (V) in NMR scale after 5 min in CD_2Cl_2.

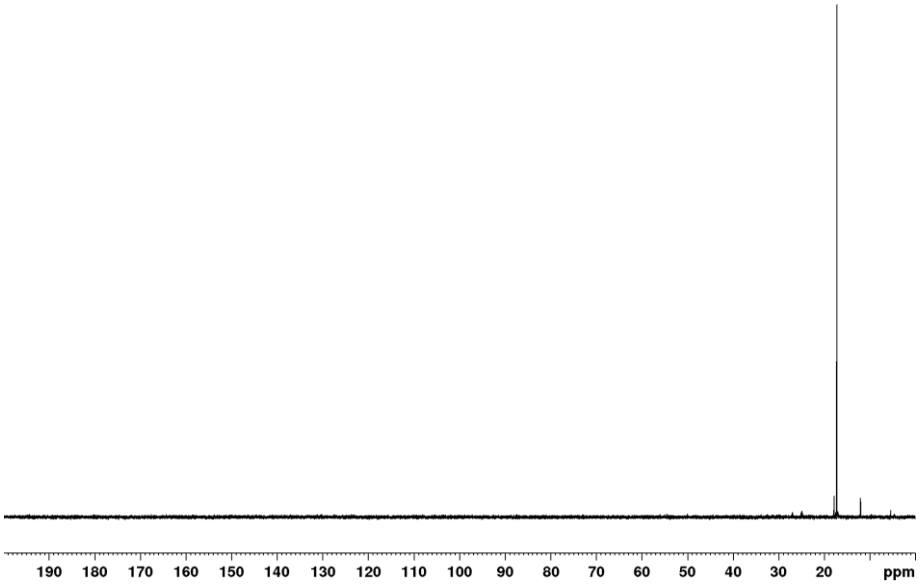

Figure A 32. ^{31}P NMR spectrum of the attempted oxidative addition of MeI to (V) in NMR scale after 5 min in CD_2Cl_2.

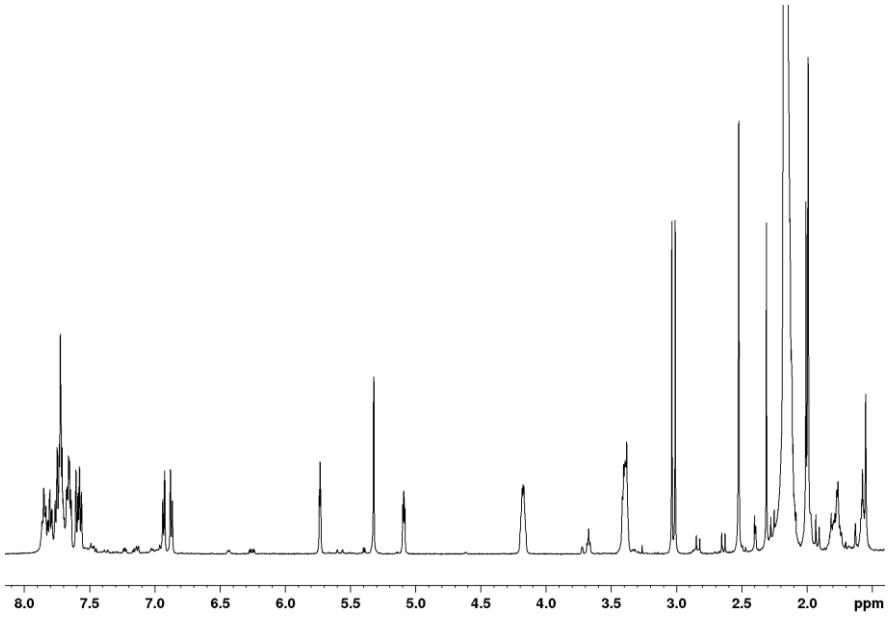

Figure A 33. ^{1}H NMR spectrum of the attempted oxidative addition of MeI to (VI) in NMR scale after 5 min in CD_2Cl_2.

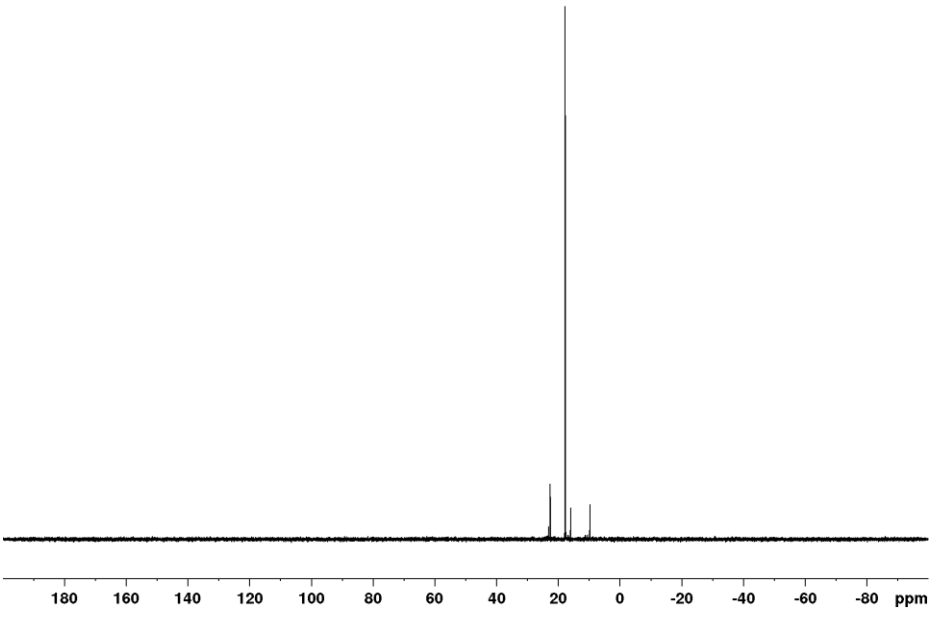

Figure A 34. ^{31}P NMR spectrum of the attempted oxidative addition of MeI to (VI) in NMR scale after 5 min in CD_2Cl_2.

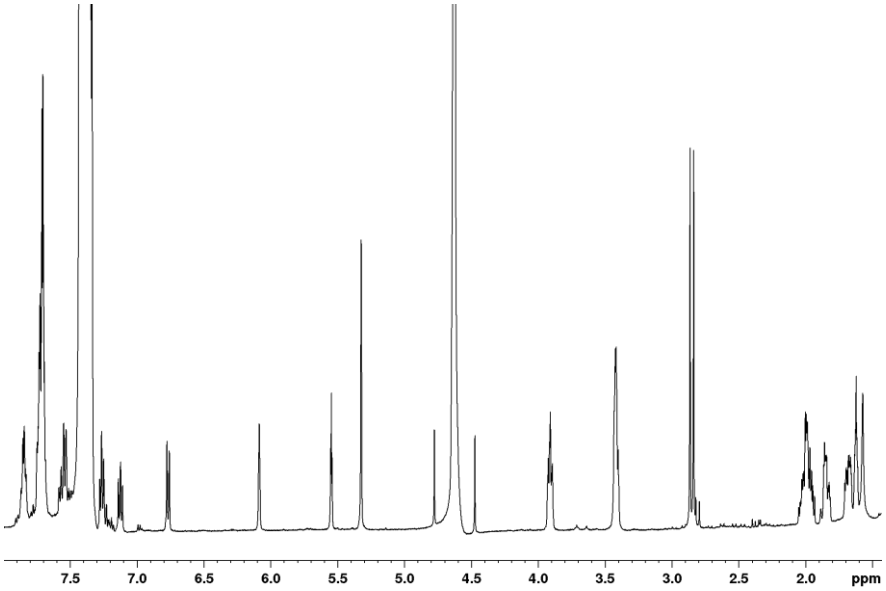

Figure A 35. ^{1}H NMR spectrum of the attempted oxidation addition of $PhCH_2Cl$ to (III) in NMR scale in CD_2Cl_2.

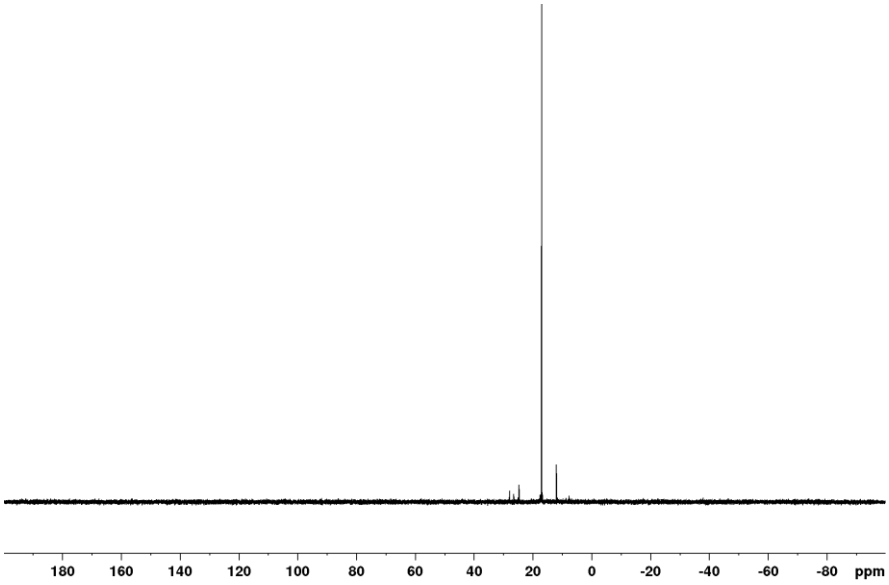

Figure A 36. ^{31}P NMR spectrum of the attempted oxidation addition of $PhCH_2Cl$ to (III) in NMR scale in CD_2Cl_2.

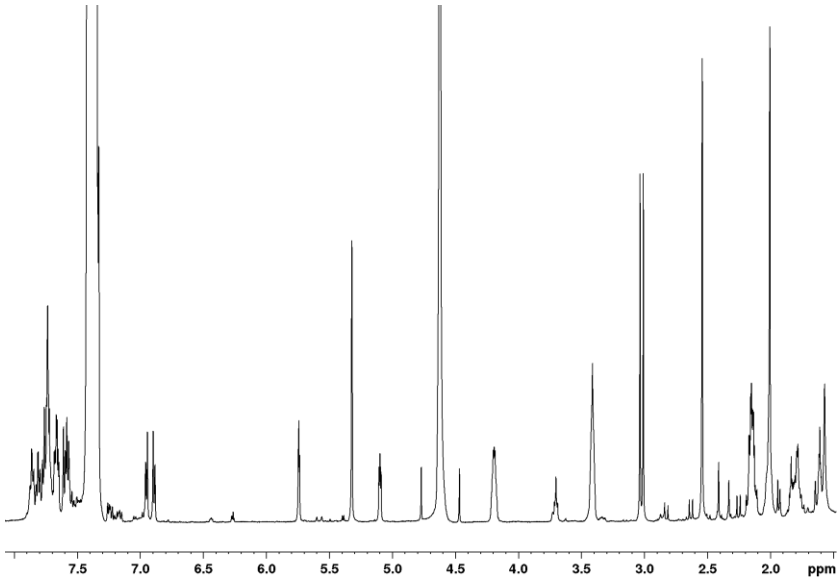

Figure A 37. ^{1}H NMR spectrum of the attempted oxidation addition of $PhCH_2Cl$ to (VI) in NMR scale in CD_2Cl_2.

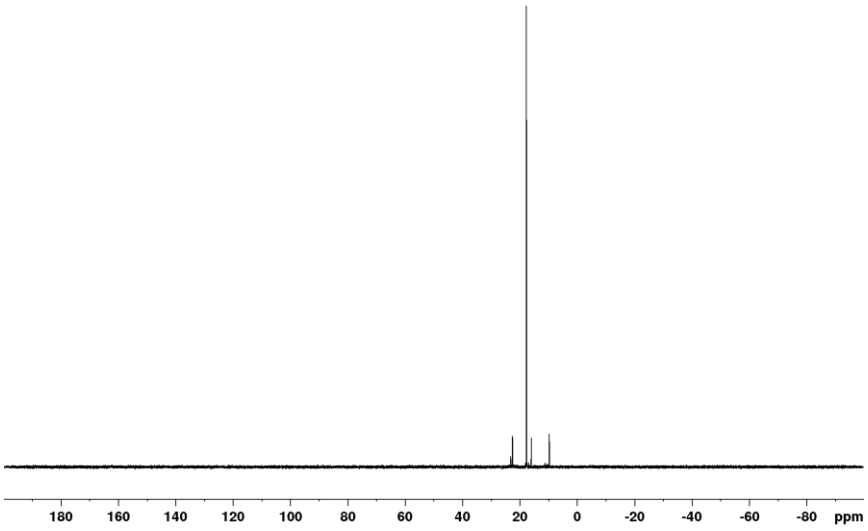

Figure A 38. ^{31}P NMR spectrum of the attempted oxidation addition of $PhCH_2Cl$ to (VI) in NMR scale in CD_2Cl_2.

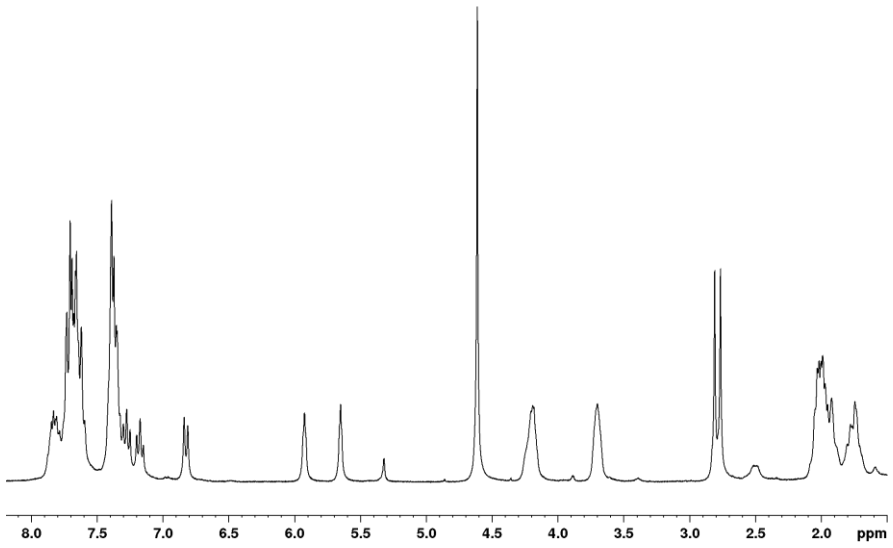

Figure A 39. ^{1}H NMR spectrum of the attempted oxidation addition of $PhCH_2Cl$ to (V) in benzene in CD_2Cl_2.

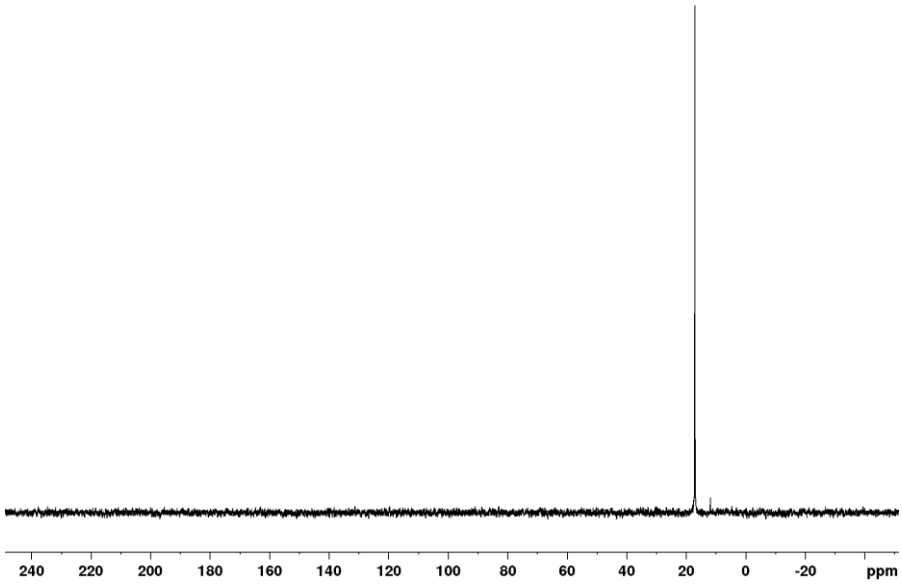

Figure A 40. ^{31}P NMR spectrum of the attempted oxidation addition of $PhCH_2Cl$ to (V) in benzene in CD_2Cl_2.

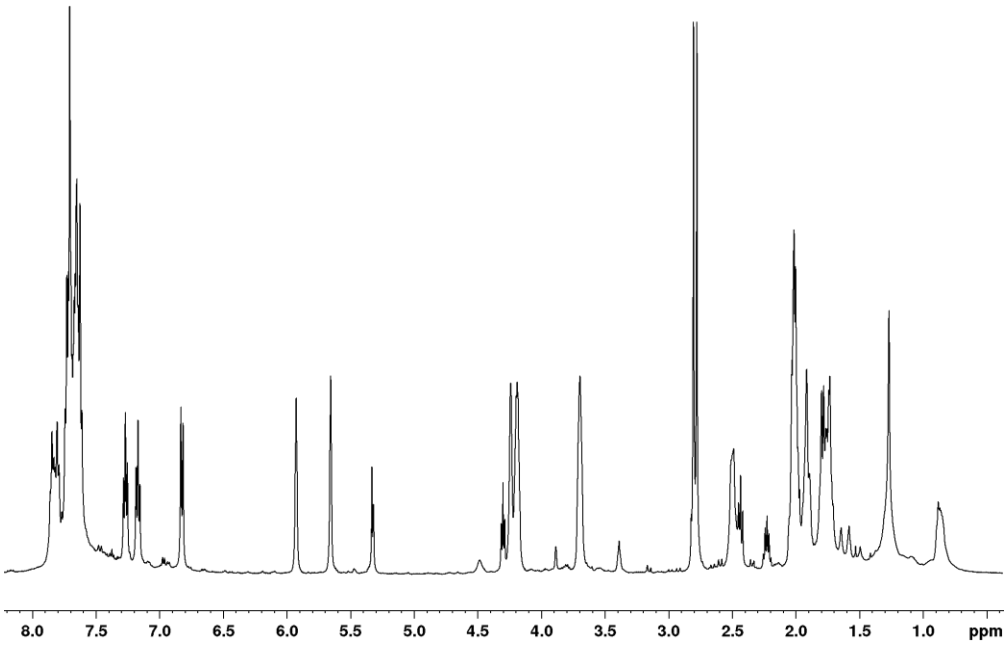

Figure A 41. ^{1}H NMR spectrum of the attempted reaction of H_2 and (V) after 24 h in CD_2Cl_2.

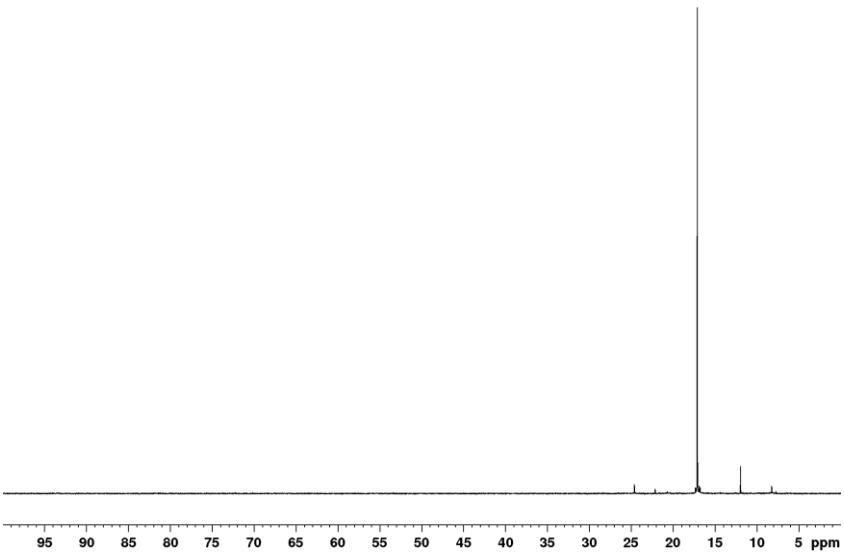

Figure A 42. ^{31}P NMR spectrum of the attempted reaction of H_2 and (V) after 24 h in CD_2Cl_2.

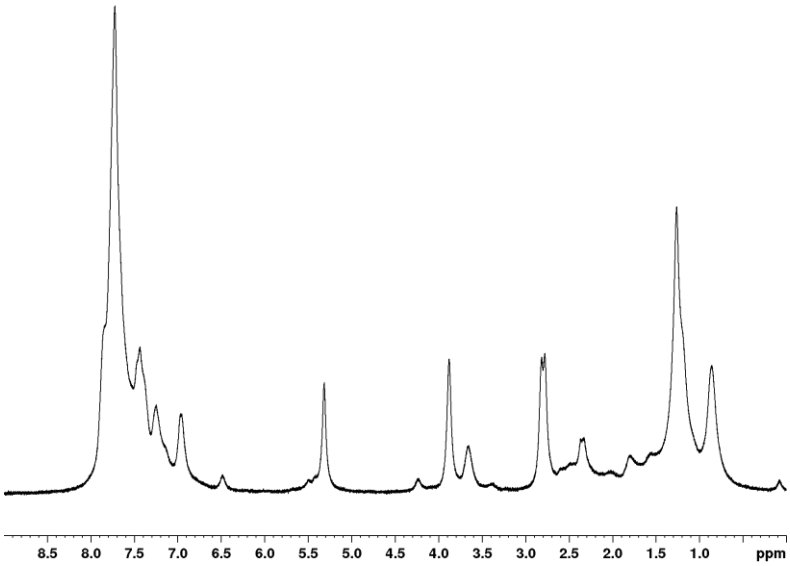

Figure A 43. ^{1}H NMR spectrum of the attempted reaction of H_2 and (V) after 24 h at 10 bar pressure in CD_2Cl_2.

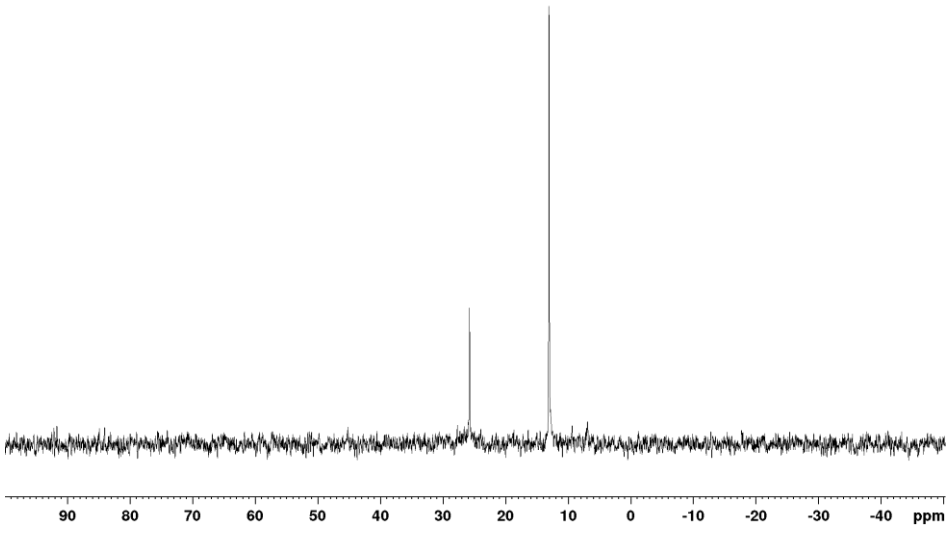

Figure A 44. ^{31}P NMR spectrum of the attempted reaction of H_2 and (V) after 24 h at 10 bar pressure in CD_2Cl_2.

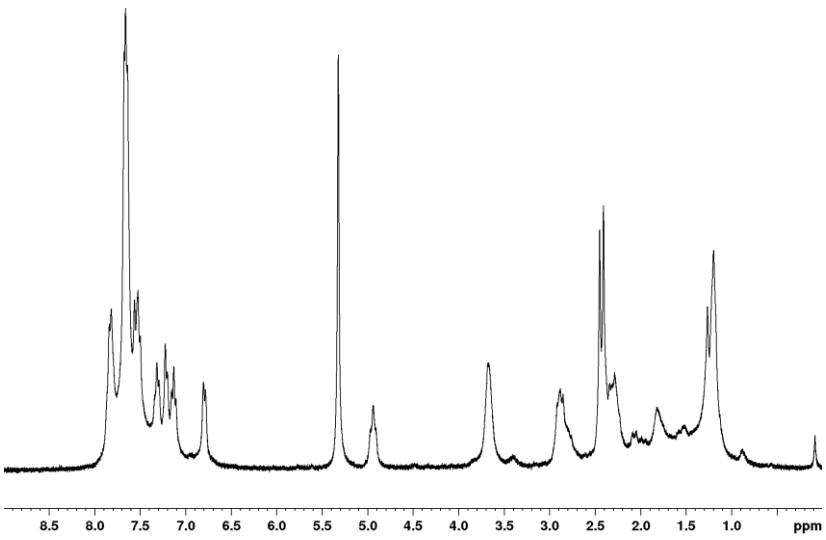

Figure A 45. ^{1}H NMR spectrum of the attempted reaction of H_2 and (V) after 5.5 h at 10 bar pressure in CD_2Cl_2.

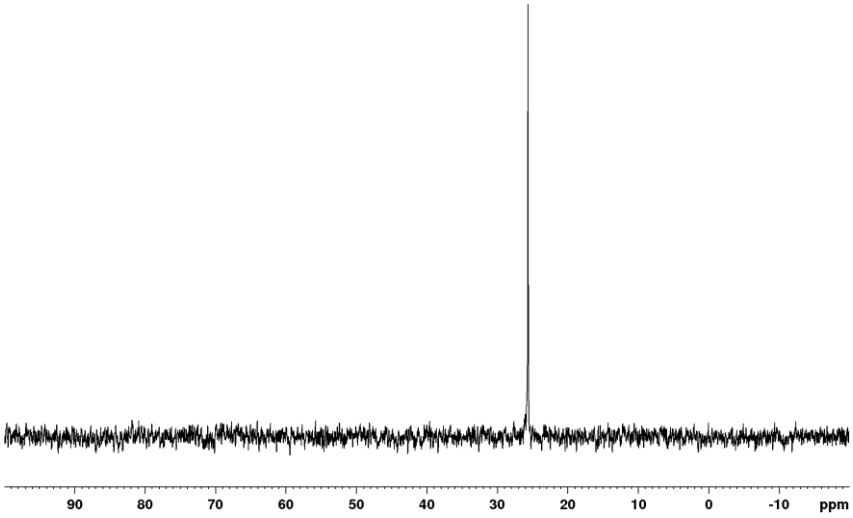

Figure A 46. ^{31}P NMR spectrum of the attempted reaction of H_2 and (V) after 5.5 h at 10 bar pressure in CD_2Cl_2.

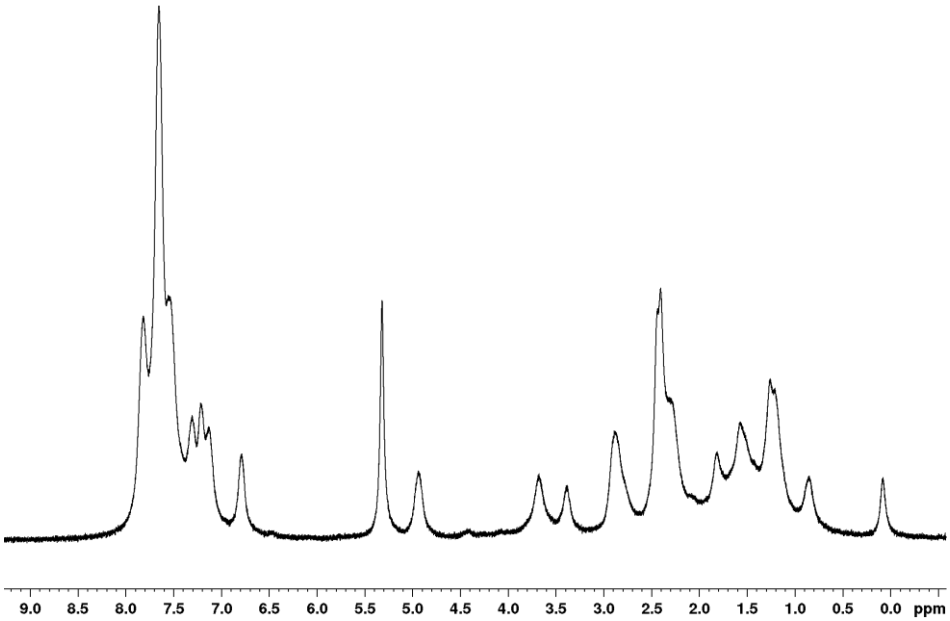

Figure A 47. ^{1}H NMR spectrum of the attempted reaction of H_2 and (III) after 24 h at 10 bar pressure in CD_2Cl_2.

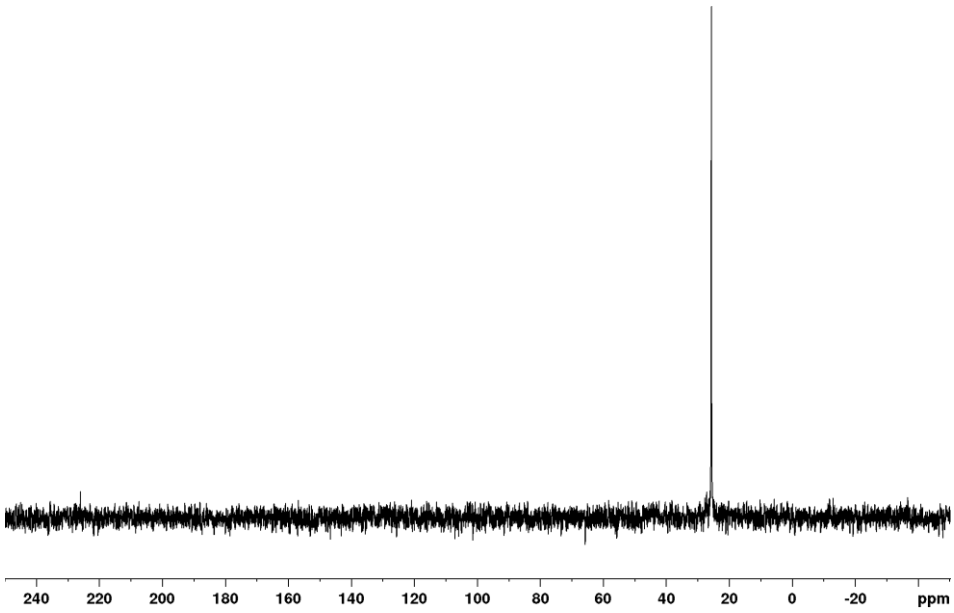

Figure A 48. ^{31}P NMR spectrum of the attempted reaction of H_2 and (III) after 24 h in CD_2Cl_2.

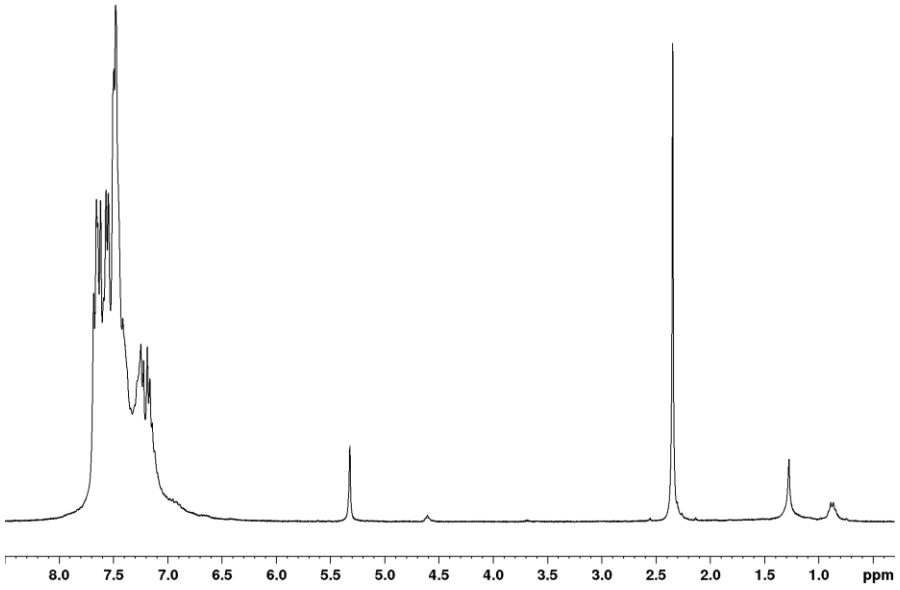

Figure A 49. ^{1}H NMR spectrum of the attempted synthesis of [(η^{6}-toluene)Rh(PPh_3)$_2$][NO_3] using $AgNO_3$ in CD_2Cl_2.

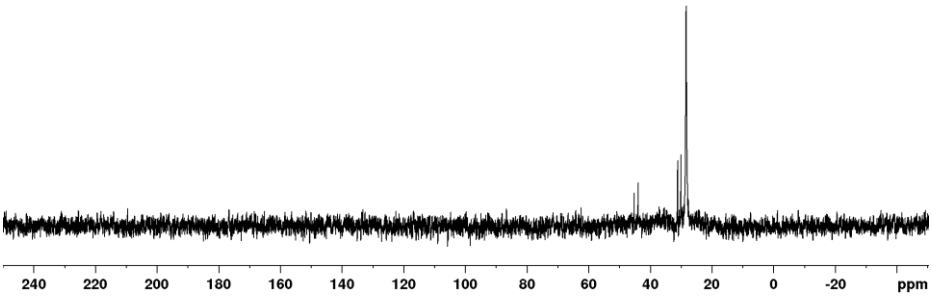

Figure A 50. ^{31}P NMR spectrum of the attempted synthesis of [(η^{6}-toluene)Rh(PPh_3)$_2$][NO_3] using $AgNO_3$ in CD_2Cl_2.

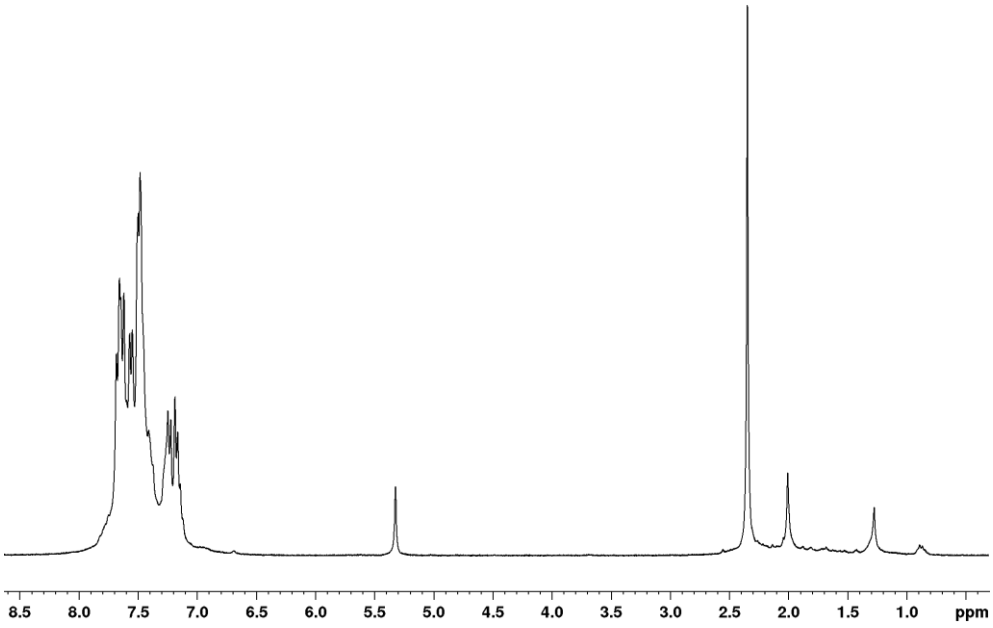

Figure A 51. ^{1}H NMR spectrum of the attempted synthesis of [η^{6}-toluene)Rh(PPh$_3$)$_2$][NO$_3$] using acetonitrile solution of AgNO$_3$ in CD$_2$Cl$_2$.

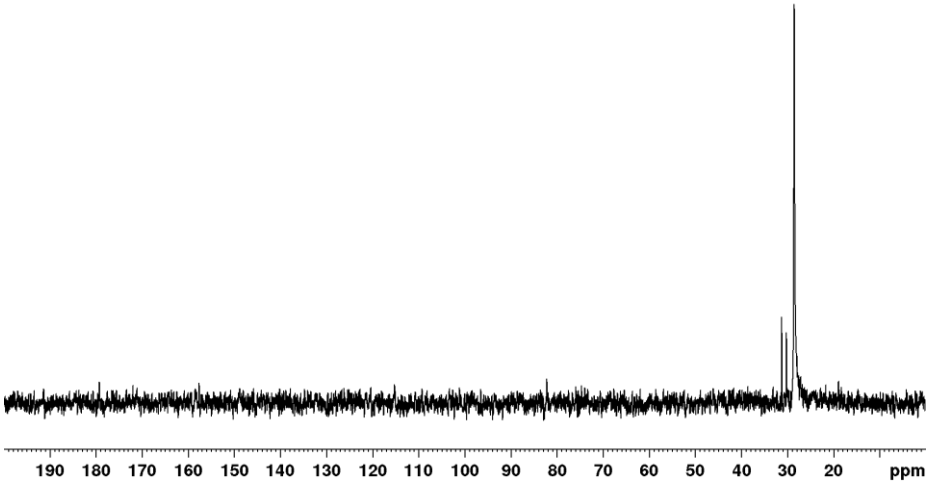

Figure A 52. ^{31}P NMR spectrum of the attempted synthesis of [η^{6}-toluene)Rh(PPh$_3$)$_2$][NO$_3$] using acetonitrile solution of AgNO$_3$ in CD$_2$Cl$_2$.

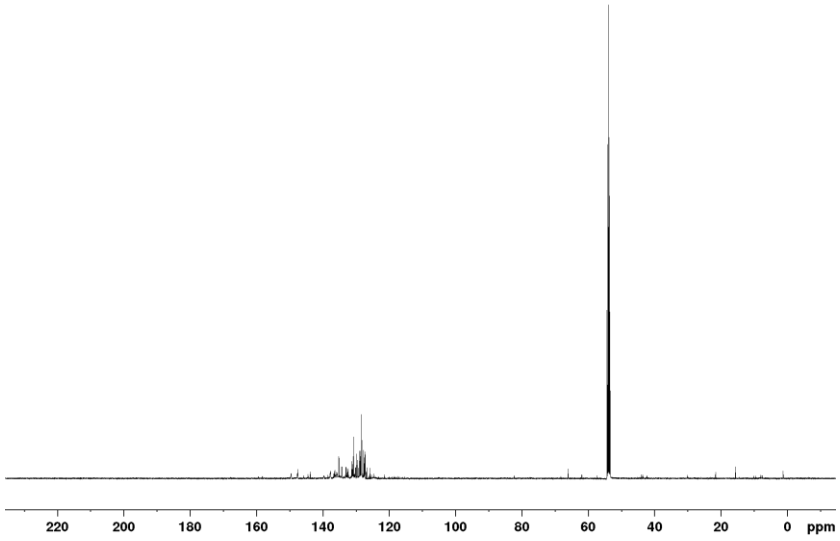

Figure A 53. ^{13}C NMR spectrum of the product of reaction between impure [(η^6-toluene)Rh(PPh_3)$_2$][$B(C_6F_5)_4$] and (I) in CD_2Cl_2.

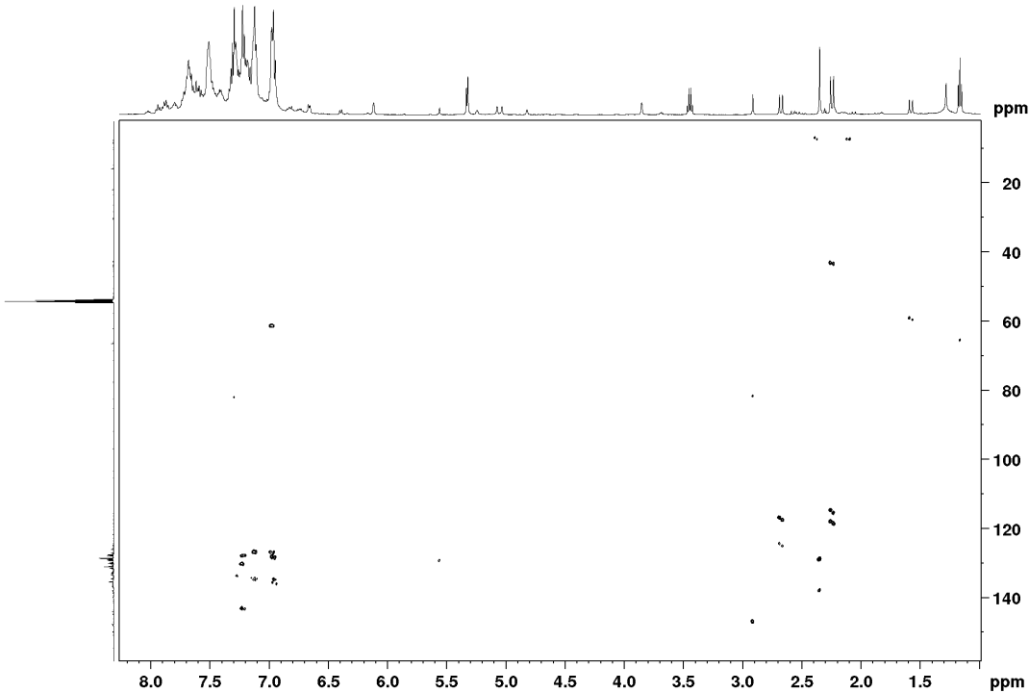

Figure A 54. ^{1}H-^{13}C HMBC spectrum of the product of reaction between impure [(η^6-toluene)Rh(PPh_3)$_2$][$B(C_6F_5)_4$] and (I) in CD_2Cl_2.

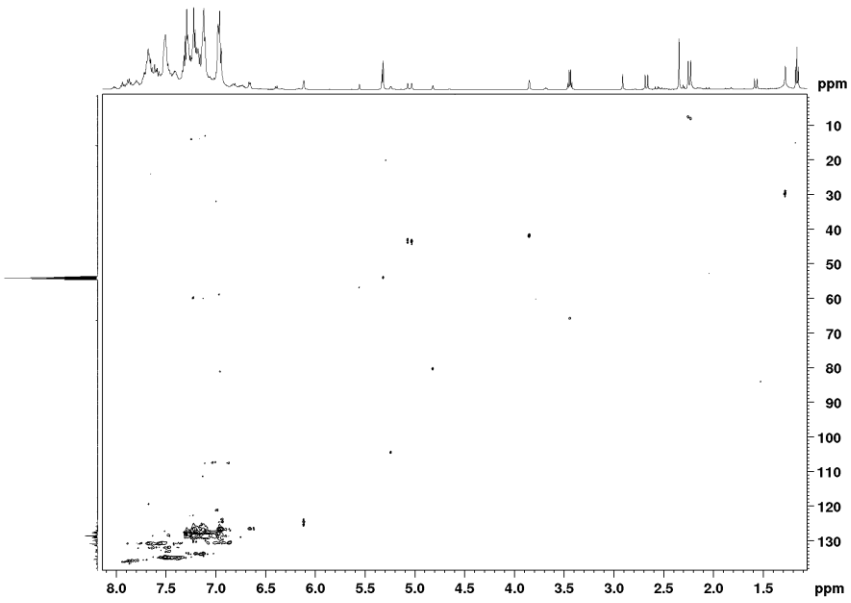

Figure A 55. ^{1}H-^{13}C HSQC spectrum of the product of reaction between impure $[(\eta^{6}\text{-toluene})Rh(PPh_3)_2][B(C_6F_5)_4]$ and (I) in CD_2Cl_2.

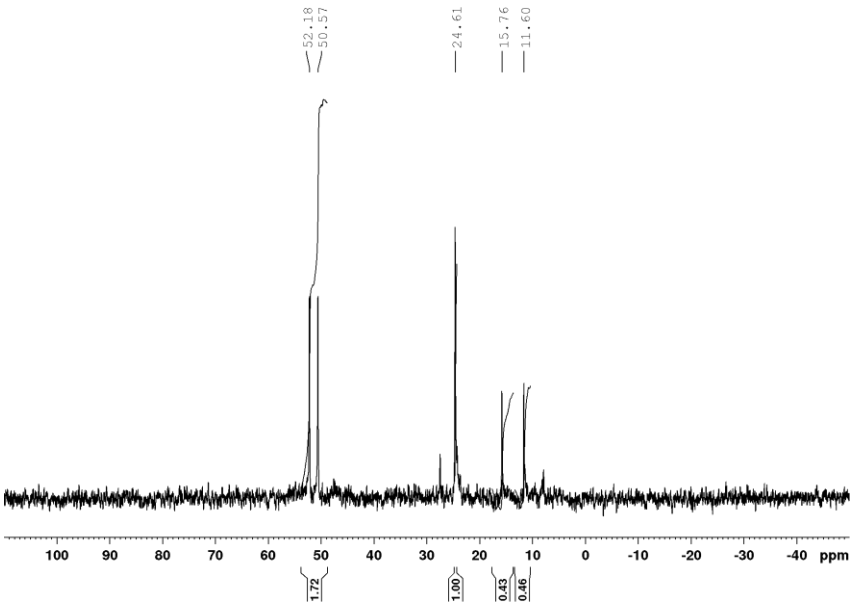

Figure A 56. ^{31}P NMR spectrum of the product of reaction between impure $[(toluene)Rh(PPh_3)_2][B(C_6F_5)_4]$ complex and (I) mixed with 0.15 mol of $Cr(acac)_3$ in CD_2Cl_2.

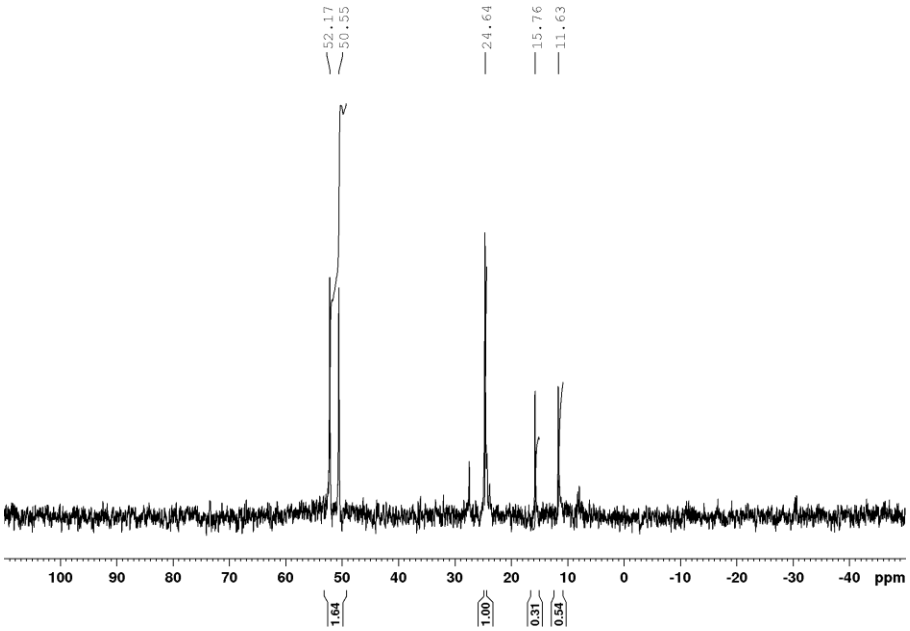

Figure A 57. ^{31}P NMR spectrum of the product of reaction between impure [(toluene)Rh(PPh$_3$)$_2$][B(C$_6$F$_5$)$_4$] complex and (I) mixed with 0.30 mol of Cr(acac)$_3$ in CD$_2$Cl$_2$.

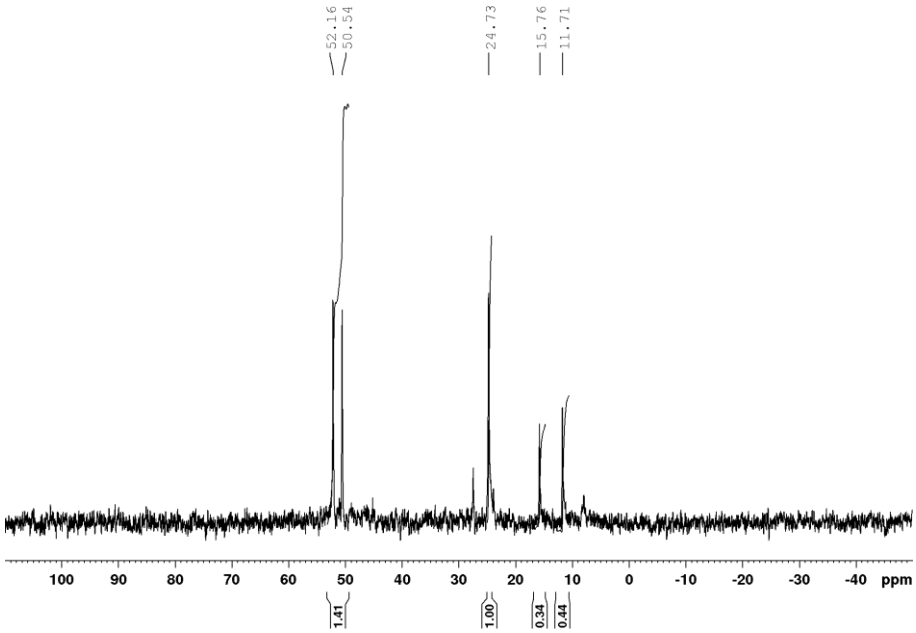

Figure A 58. ^{31}P NMR spectrum of the product of reaction between impure [(toluene)Rh(PPh$_3$)$_2$][B(C$_6$F$_5$)$_4$] complex and (I) mixed with 0.45 mol of Cr(acac)$_3$ in CD$_2$Cl$_2$.

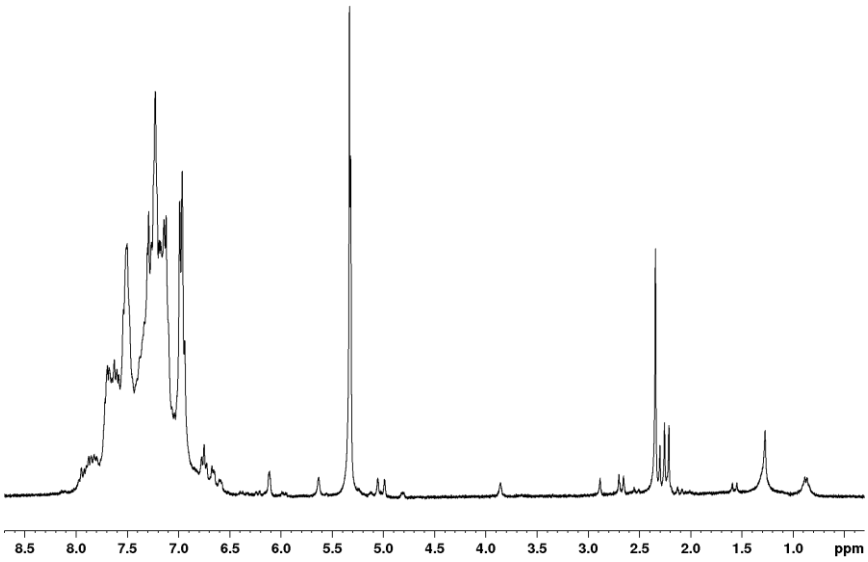

Figure A 59. ^{1}H NMR spectrum of attempted synthesis of [(η^5-I)Rh(PPh$_3$)$_2$][B(C$_6$F$_5$)$_4$] in CD$_2$Cl$_2$.

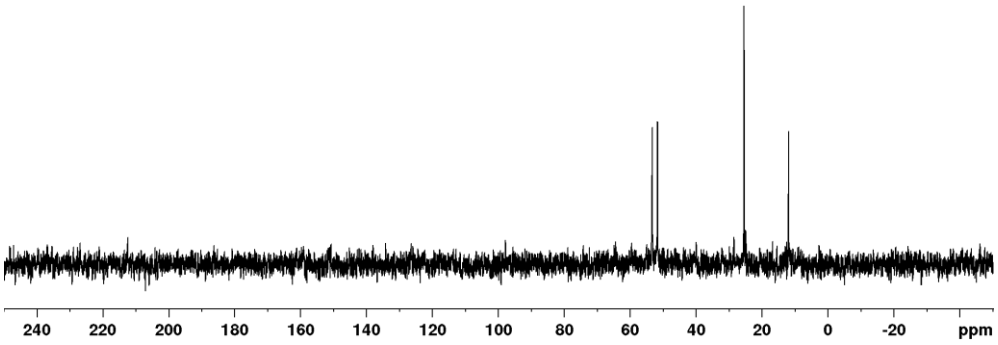

Figure A 60. ^{31}P NMR spectrum of attempted synthesis of [(η^5-I)Rh(PPh_3)$_2$][$B(C_6F_5)_4$] in CD_2Cl_2.

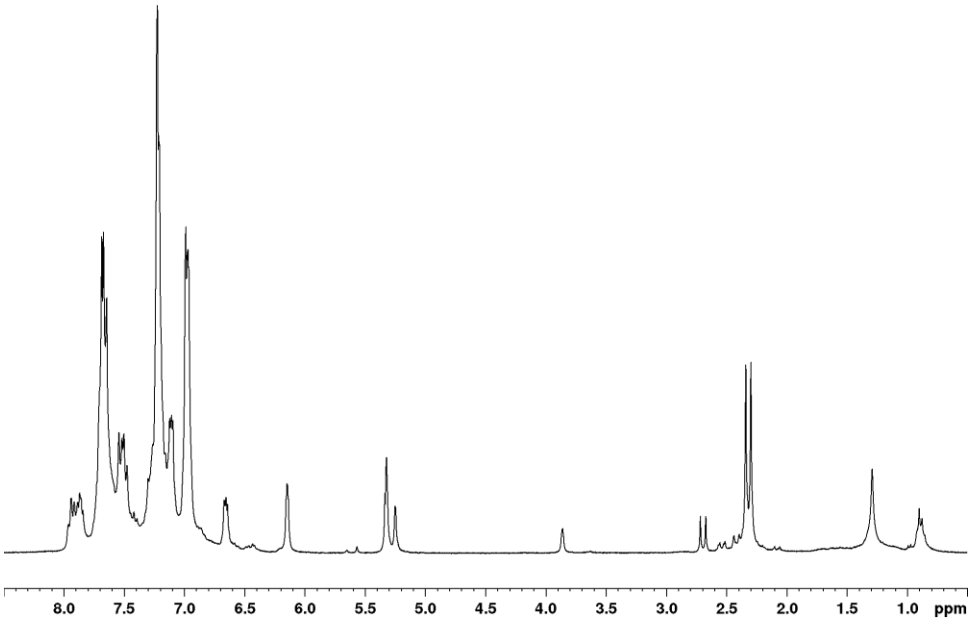

Figure A 61. ^{1}H NMR spectrum of the reaction between (I) and [Ph_3C][$B(C_6F_5)_4$] in NMR tube in CD_2Cl_2.

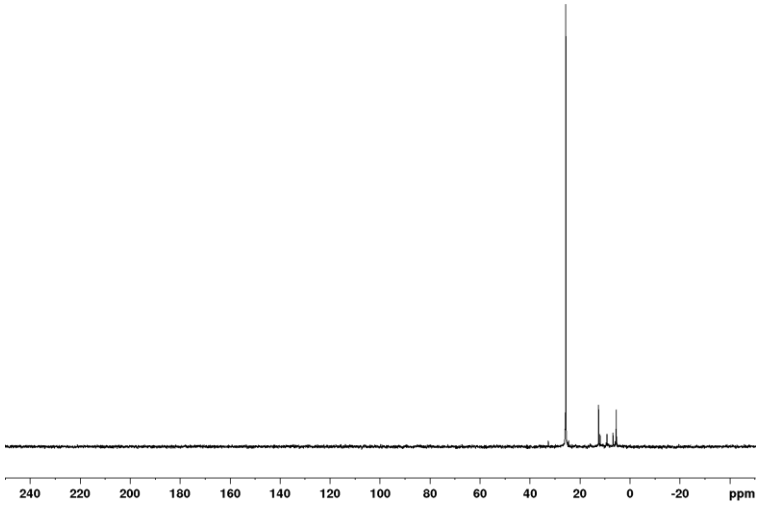

Figure A 62. ^{31}P NMR spectrum of the reaction between (I) and $[Ph_3C][B(C_6F_5)_4]$ in NMR tube in CD_2Cl_2.

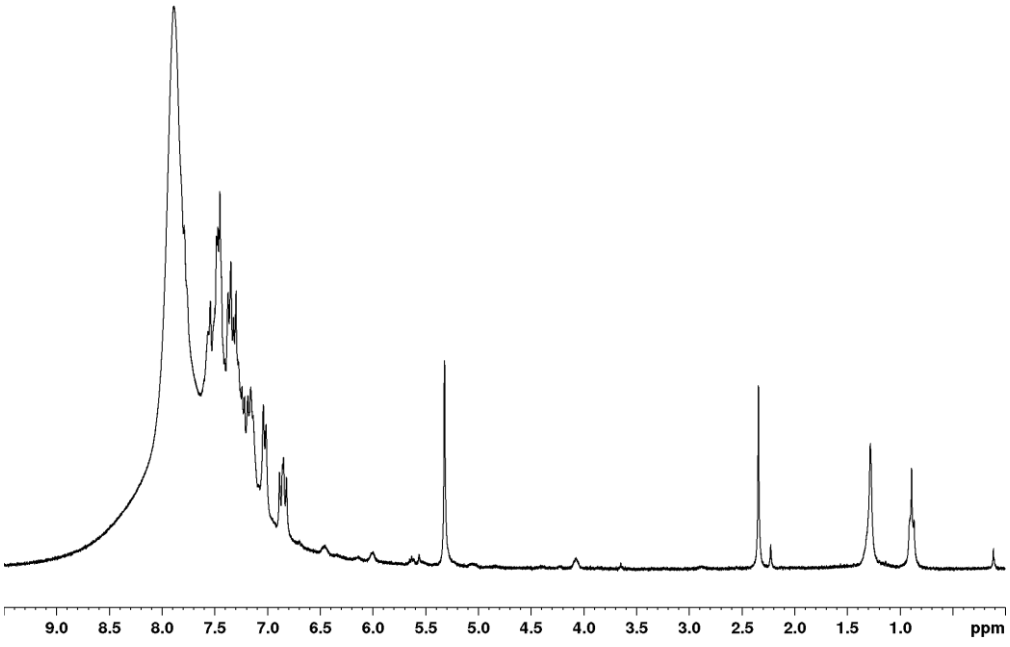

Figure A 63. ^{1}H NMR spectrum of the reaction between $[(PPh_3)_2Rh(\mu\text{-}Cl)]_2$ and $[Ph_3C][B(C_6F_5)_4]$ in NMR tube in CD_2Cl_2.

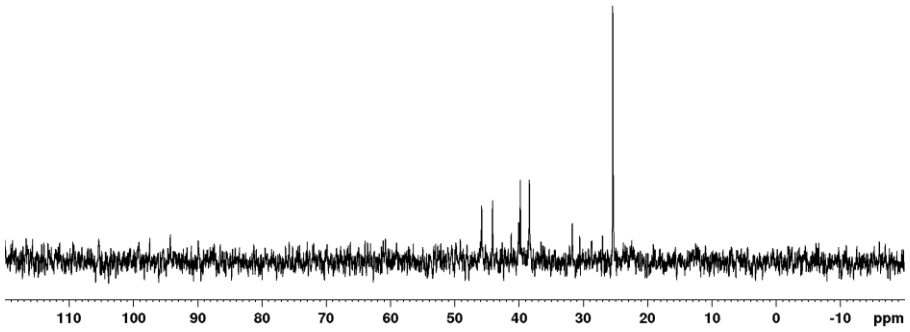

Figure A 64. ^{31}P NMR spectrum of the reaction between $[(PPh_3)_2Rh(\mu\text{-}Cl)]_2$ and $[Ph_3C][B(C_6F_5)_4]$ in NMR tube in CD_2Cl_2.

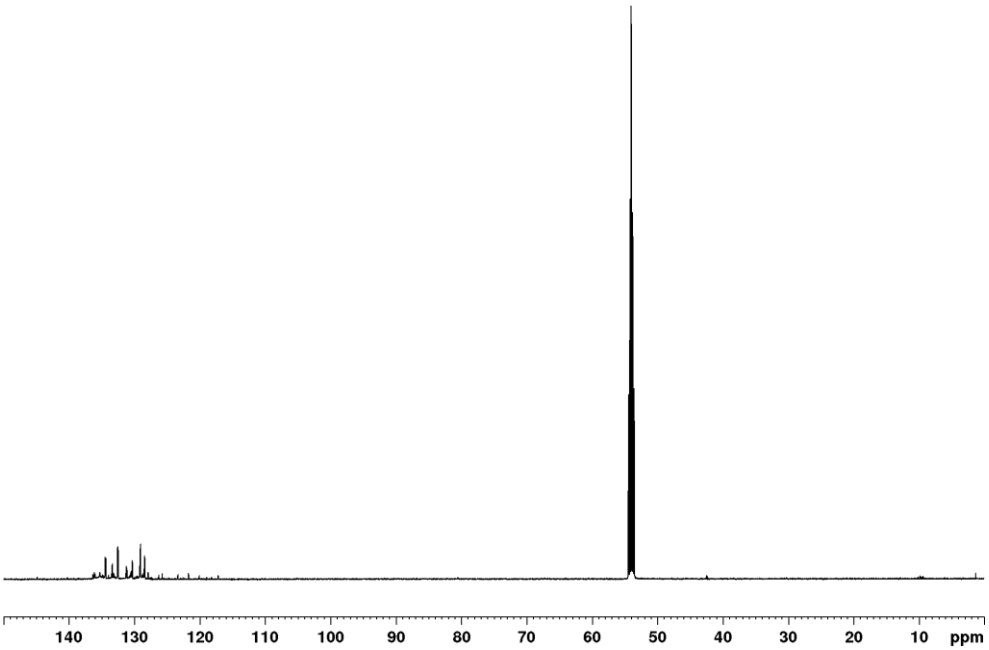

Figure A 65. ^{13}C NMR spectrum of $[(\eta^5\text{-}I)Rh(PPh_3)_2][BF_4]$ in CD_2Cl_2.

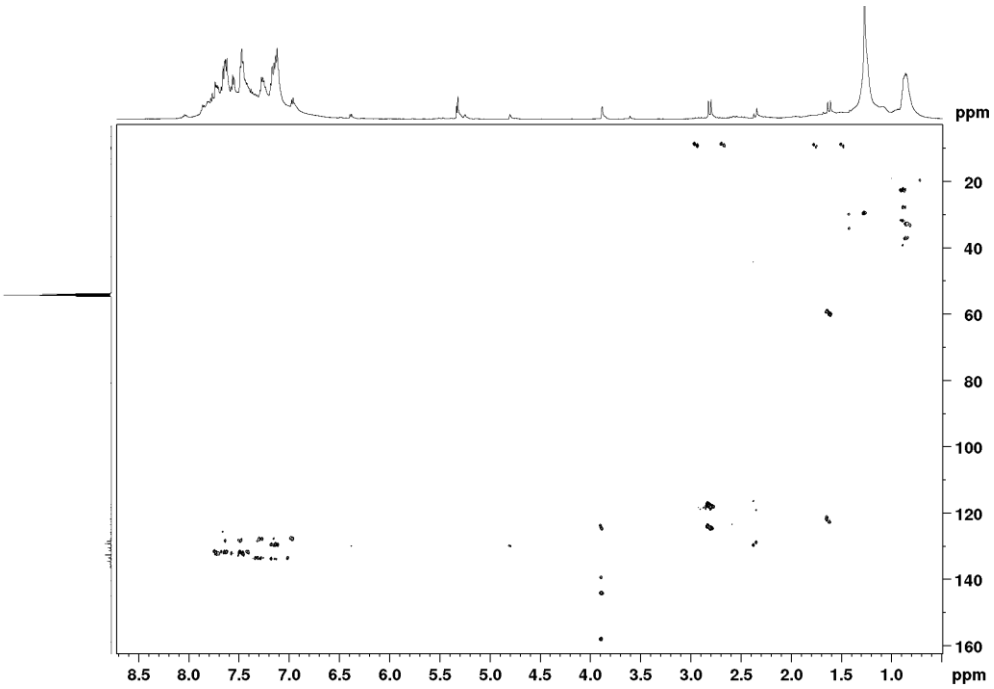

Figure A 66. ^{1}H-^{13}C HMBC spectrum of $[(\eta^5\text{-I})Rh(PPh_3)_2][BF_4]$ in CD_2Cl_2.

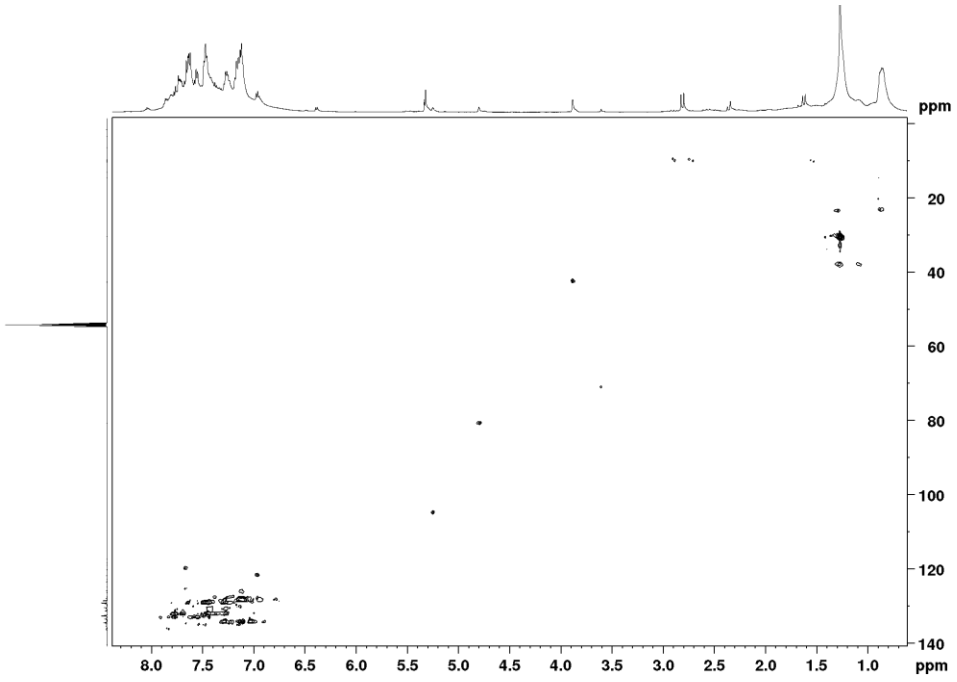

Figure A 67. ^{1}H-^{13}C HSQC spectrum of $[(\eta^5\text{-I})Rh(PPh_3)_2][BF_4]$ in CD_2Cl_2.

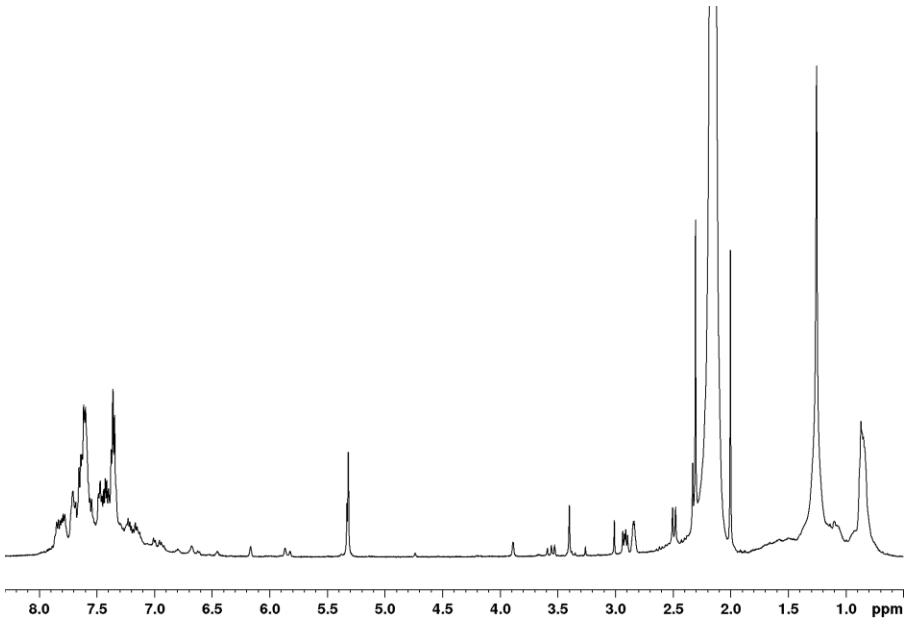

Figure A 68. ^{1}H NMR spectrum of attempted oxidative addition of MeI to [(η^5-I)Rh(PPh_3)$_2$][BF_4] in NMR scale in CD_2Cl_2.

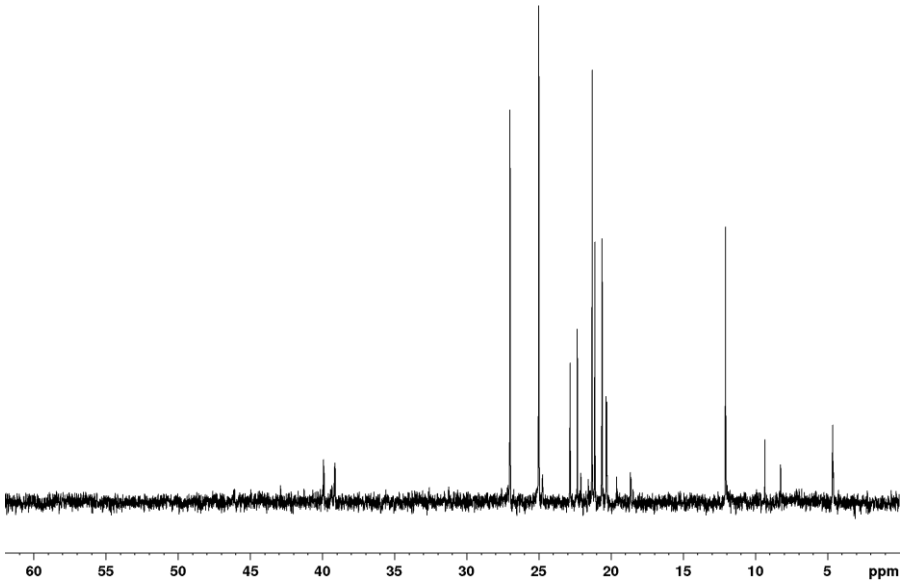

Figure A 69. ^{31}P NMR spectrum of attempted oxidative addition of MeI to [(η^5-I)Rh(PPh_3)$_2$][BF_4] in NMR scale in CD_2Cl_2.

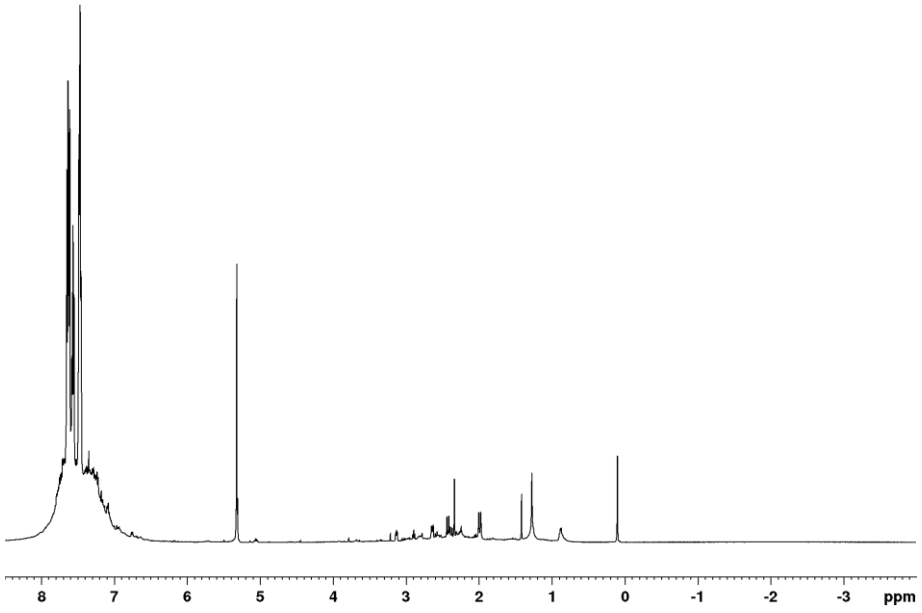

Figure A 70. ^{1}H NMR spectrum of attempted reaction of H_2 and [(η^5-I)Rh(PPh_3)$_2$]BF_4 in CD_2Cl_2.

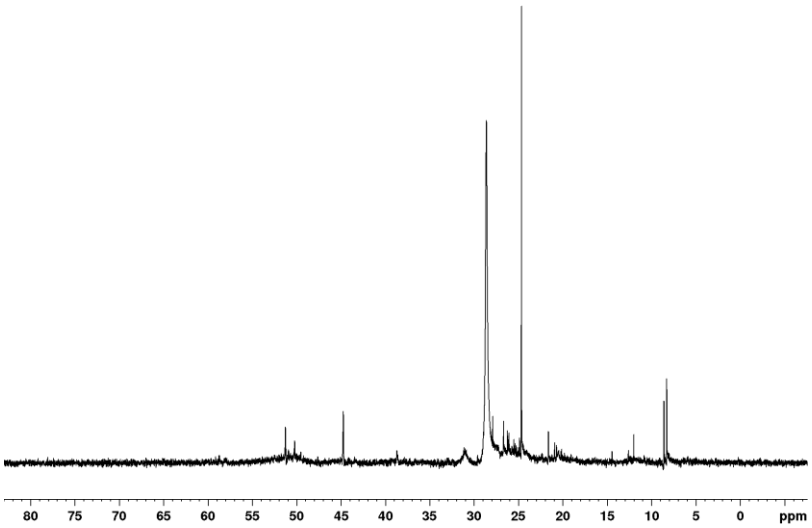

Figure A 71. ^{31}P NMR spectrum of attempted reaction of H_2 and [(η^5-I)Rh(PPh_3)$_2$]BF_4 in CD_2Cl_2.

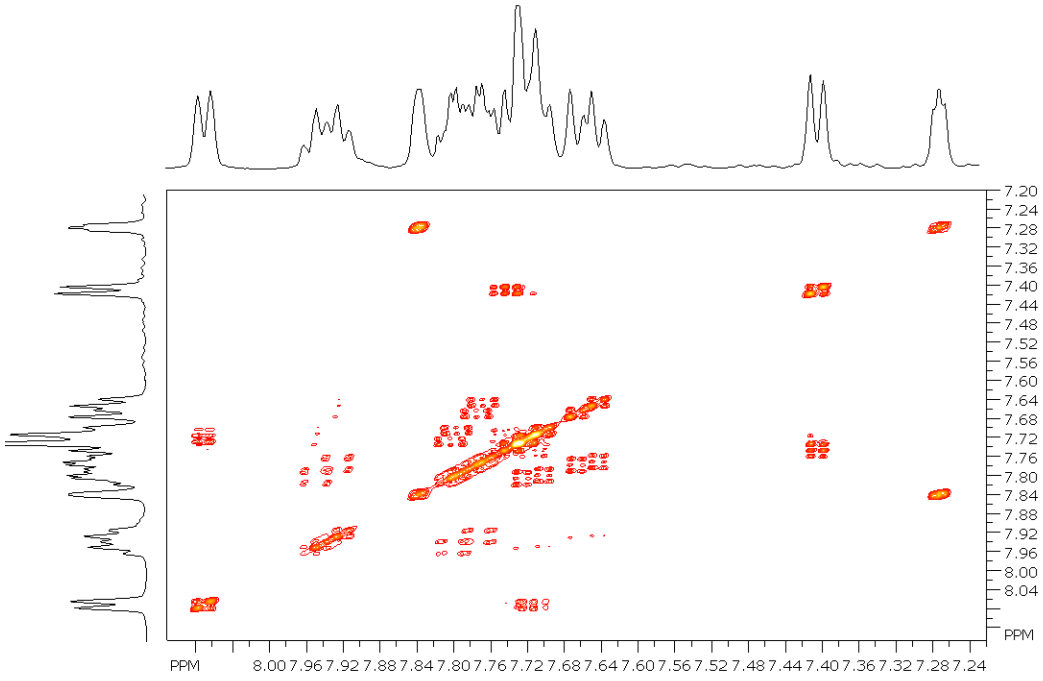

Figure A 72. COSY spectrum of coordination of (I) to titanium, using four-fold excess of $TiCl_4$ (aromatic region) in CD_2Cl_2.

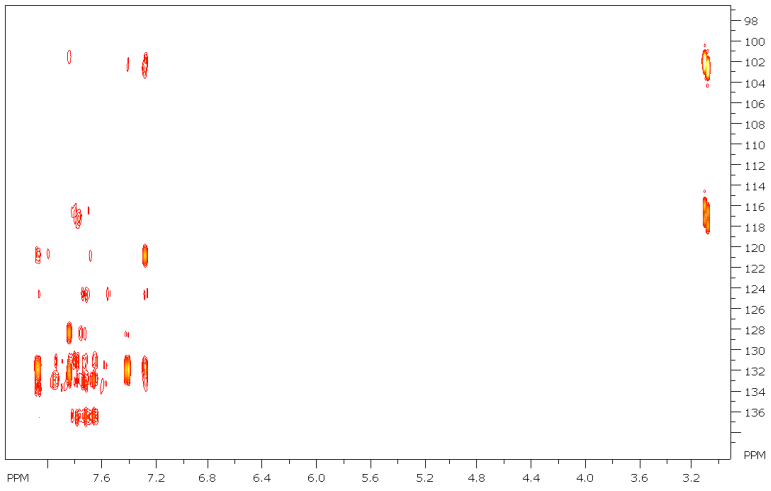

Figure A 73. ^{1}H-^{13}C HSQC spectrum of coordination of (I) to titanium, using four-fold excess of $TiCl_4$ in CD_2Cl_2.

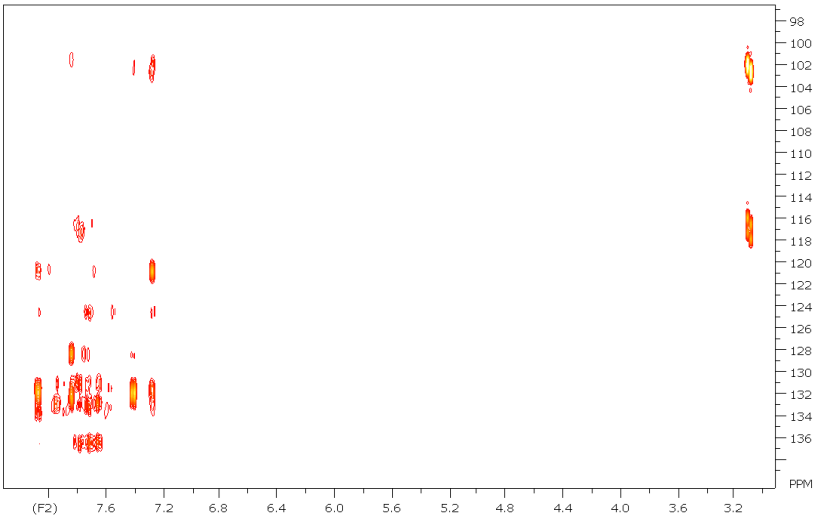

Figure A 74. ^{1}H-^{13}C HMBC spectrum of coordination of (I) to titanium, using four-fold excess of $TiCl_4$ in CD_2Cl_2.

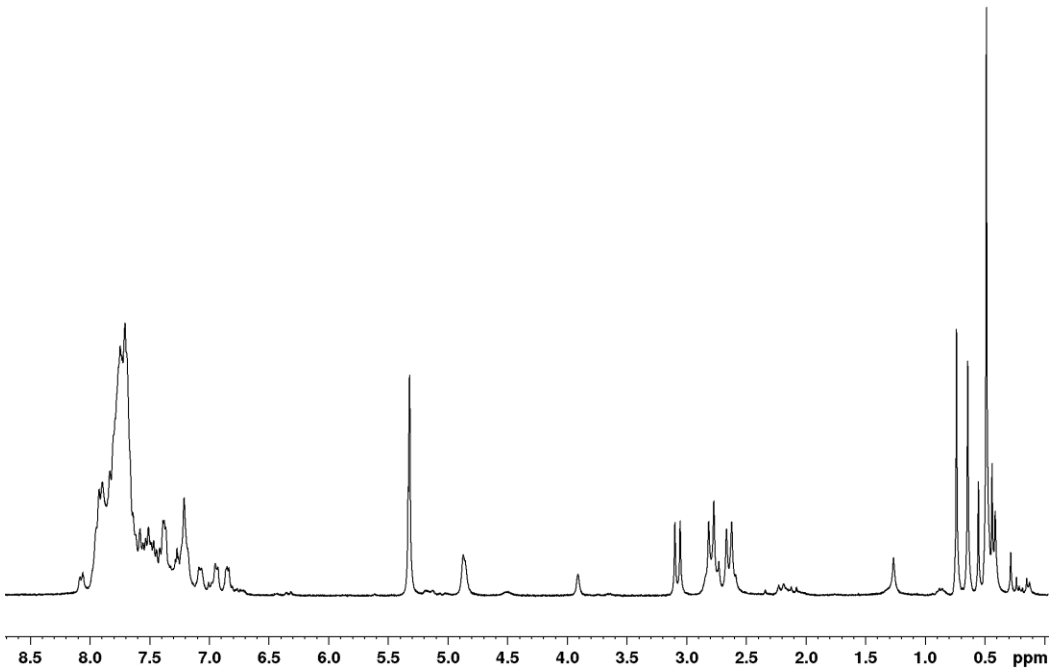

Figure A 75. ^{1}H NMR spectrum of the reaction of (I) and excess $TiCl_4$ (1:11 ratio) at room temperature in CD_2Cl_2.

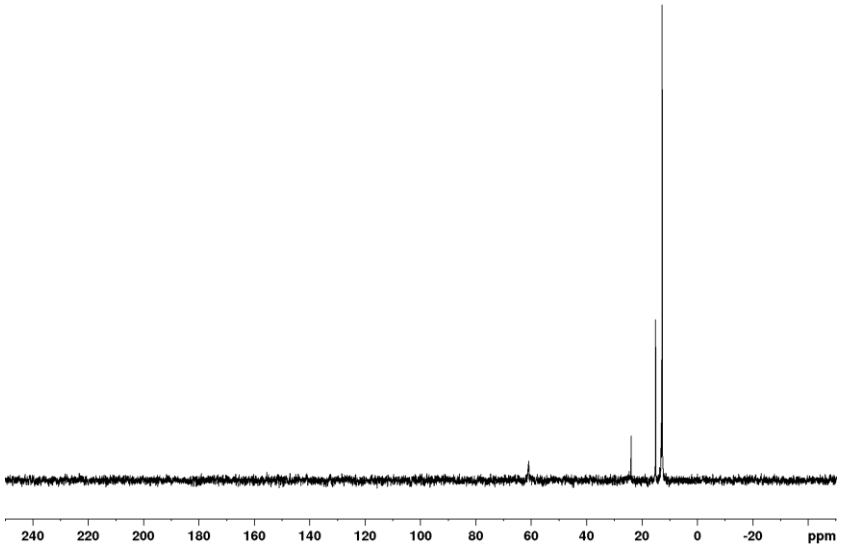

Figure A 76. ^{31}P NMR spectrum of the reaction of (I) and excess $TiCl_4$ (1:11 ratio) at room temperature in CD_2Cl_2.

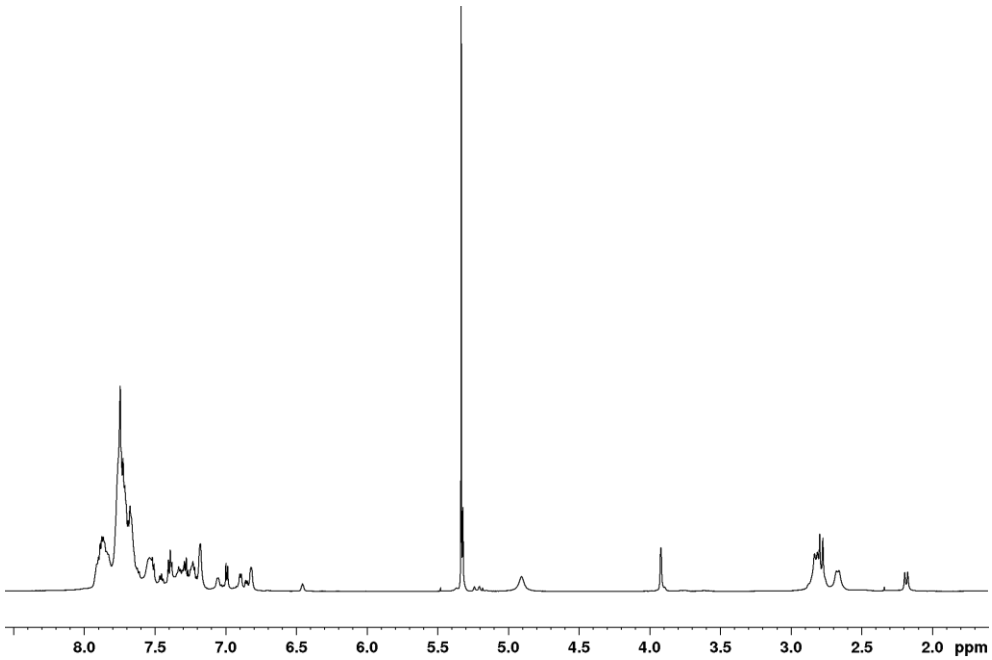

Figure A 77. ^{1}H NMR spectrum of the reaction of (I) and excess $TiCl_4$ (1:11 ratio) at low temperature in CD_2Cl_2.

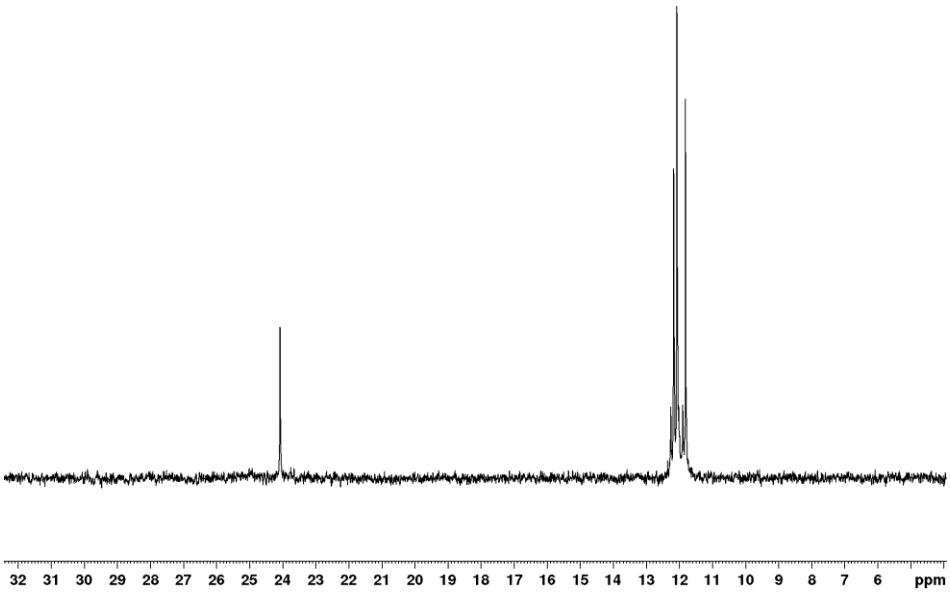

Figure A 78. ^{31}P NMR spectrum of the reaction of (I) and excess $TiCl_4$ (1:11 ratio) at low temperature in CD_2Cl_2.

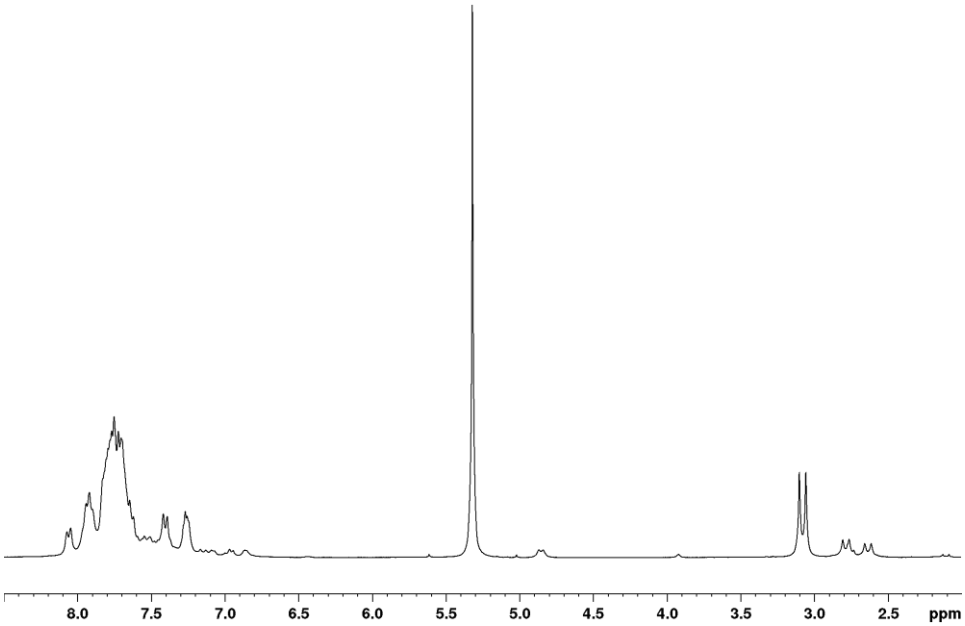

Figure A 79. ^{1}H NMR spectrum of the reaction of (I) and excess $TiCl_4$ (1:11 ratio) at high temperature (refluxing) in CD_2Cl_2.

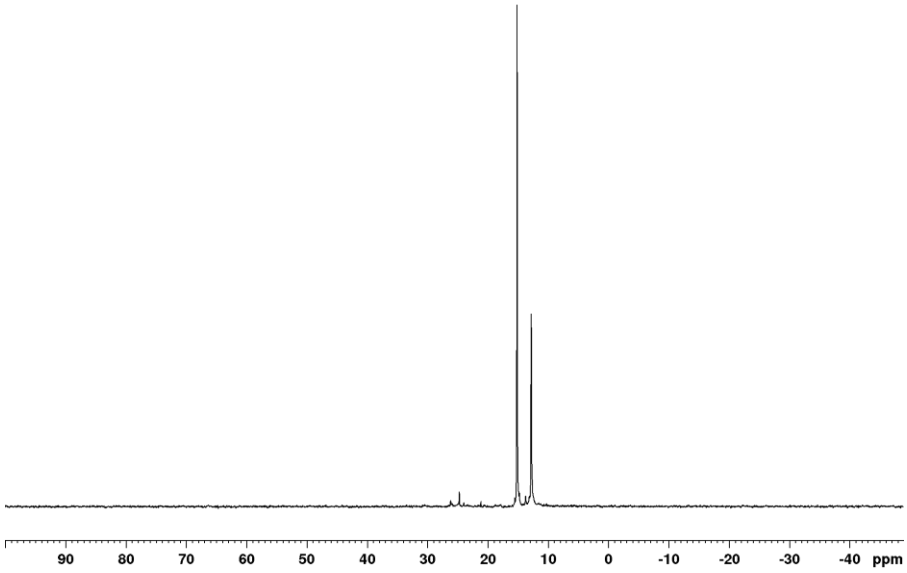

Figure A 80. ^{31}P NMR spectrum of the reaction of (I) and excess $TiCl_4$ (1:11 ratio) at high temperature (refluxing) in CD_2Cl_2.

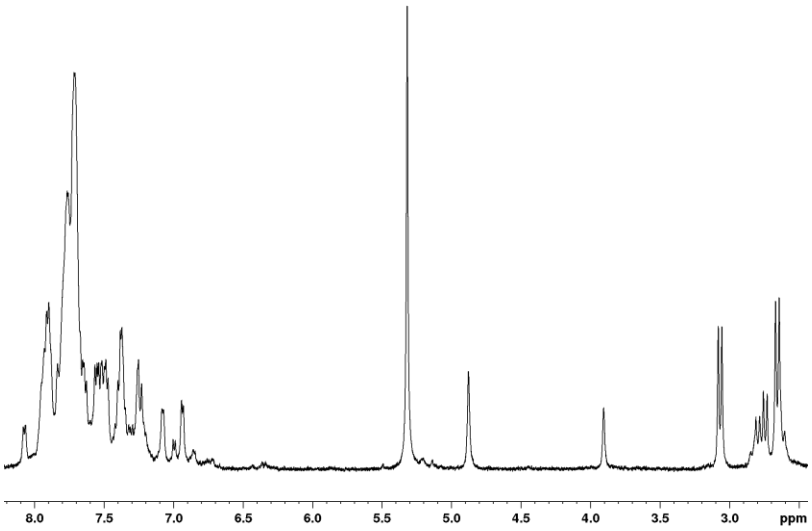

Figure A 81. ^{1}H NMR spectrum of the solvent free reaction of (I) and excess $TiCl_4$ (1:11 ratio) at room temperature in CD_2Cl_2.

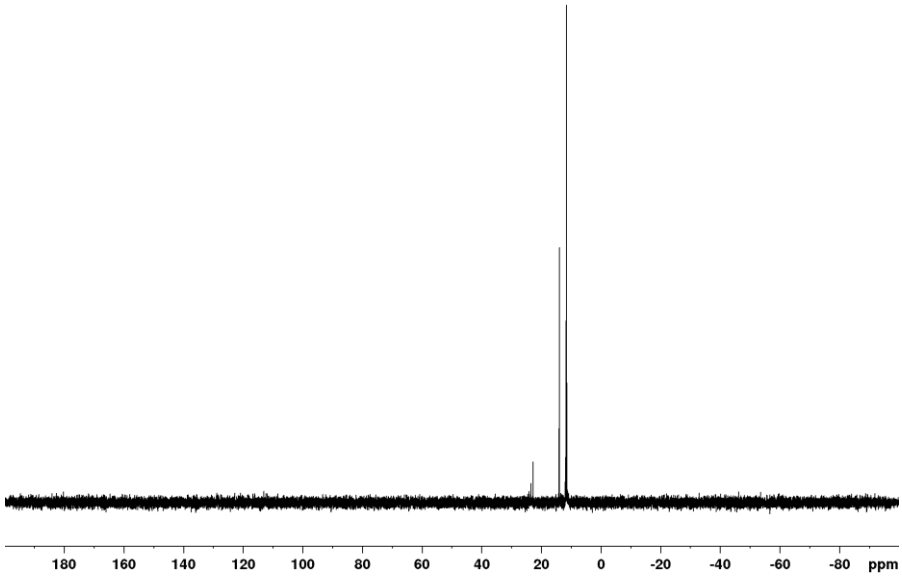

Figure A 82. ^{31}P NMR spectrum of the solvent free reaction of (I) and excess $TiCl_4$ (1:11 ratio) at room temperature in CD_2Cl_2.

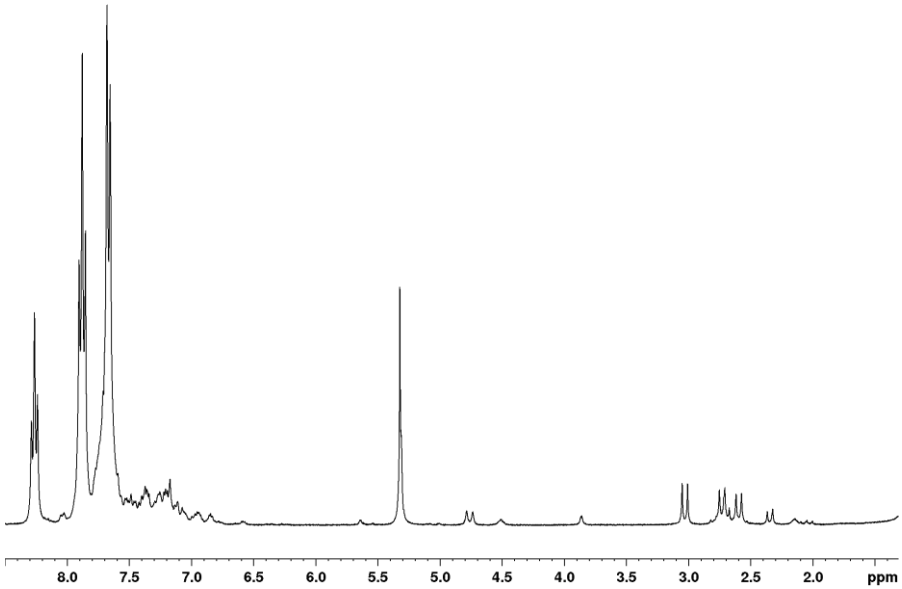

Figure A 83. ^{1}H NMR spectrum of the reaction of $TiCl_4$, (I), and $[Ph_3C][B(C_6F_5)_4]$ in CD_2Cl_2.

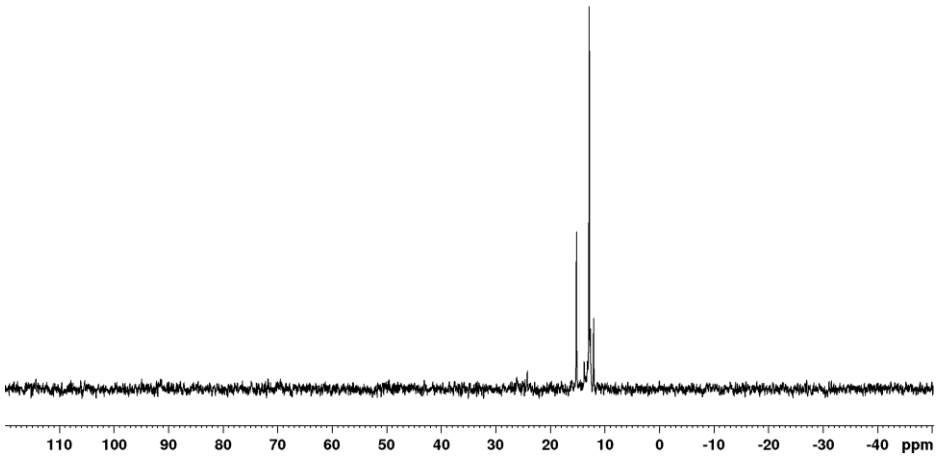

Figure A 84. ^{31}P NMR spectrum of the reaction of $TiCl_4$, (I), and $[Ph_3C][B(C_6F_5)_4]$ in CD_2Cl_2.

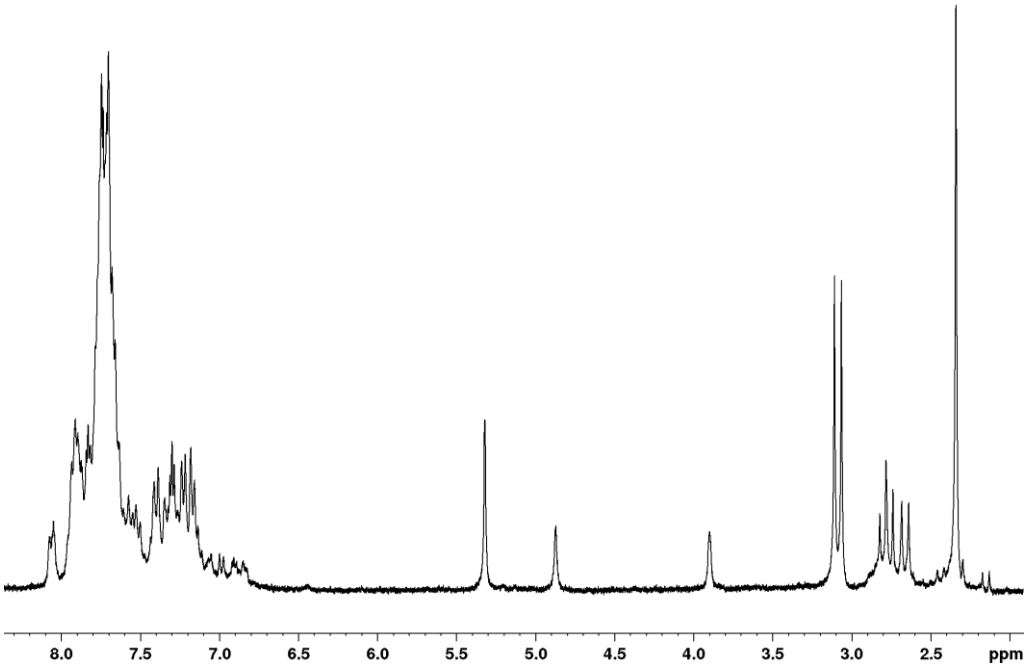

Figure A 85. ^{1}H NMR spectrum of the reaction of $TiCl_4$, (I), and $GaCl_3$ in toluene in CD_2Cl_2.

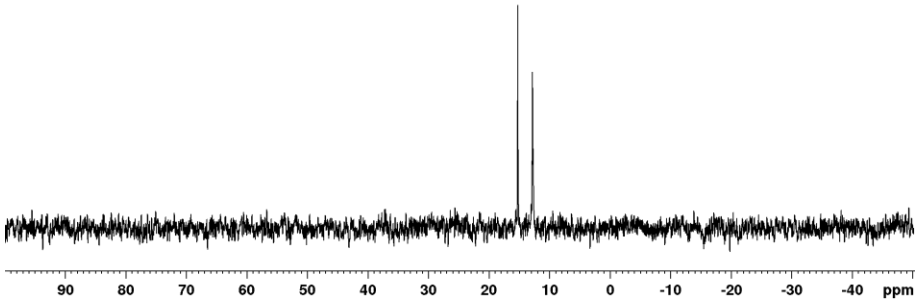

Figure A 86. ^{31}P NMR spectrum of the reaction of $TiCl_4$, (I), and $GaCl_3$ in toluene in CD_2Cl_2.

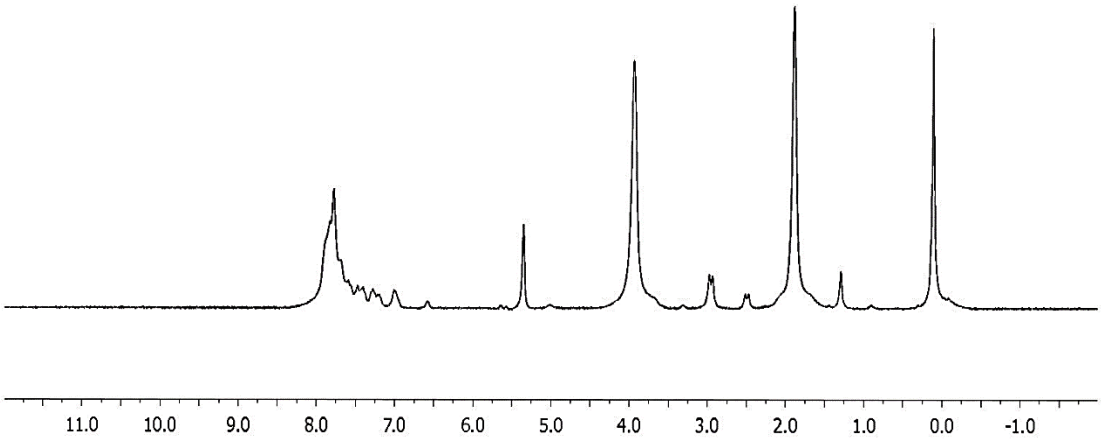

Figure A 87. ^{1}H NMR spectrum of the first attempted coordination of (I) to $TiCl_4.(THF)_2$ using $AgNO_3$ in CD_2Cl_2.

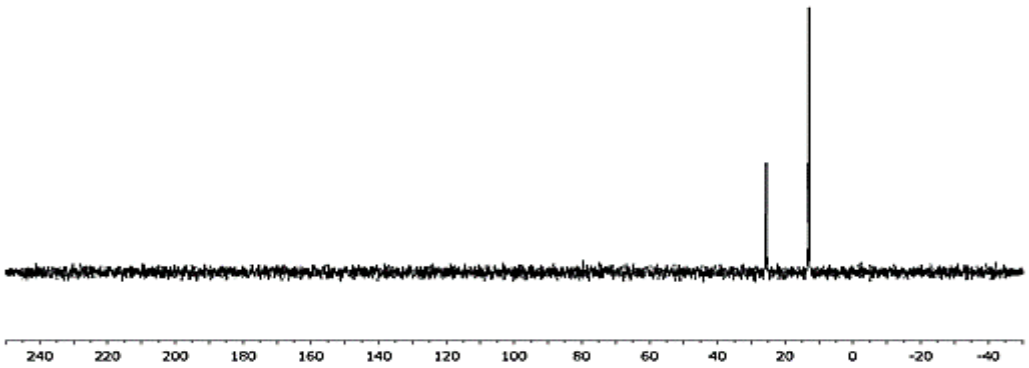

Figure A 88. ^{31}P NMR spectrum of the first attempted coordination of (I) to $TiCl_4.(THF)_2$ using $AgNO_3$ in CD_2Cl_2.

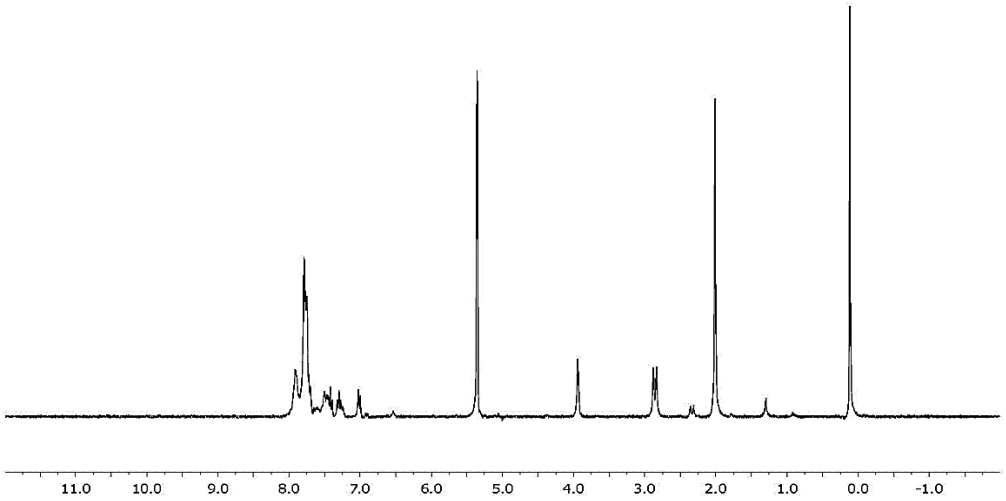

Figure A 89. ^{1}H NMR spectrum of the second attempted coordination of (I) to $TiCl_4.(THF)_2$ using $AgNO_3$ in CD_2Cl_2.

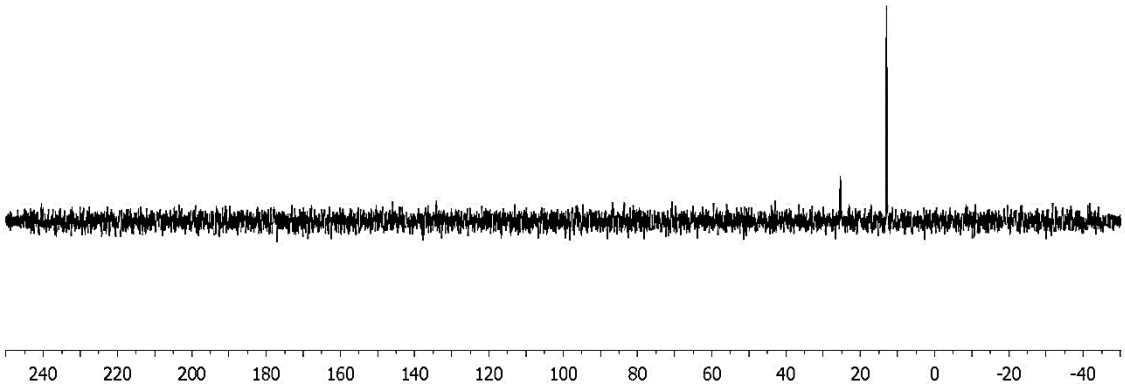

Figure A 90. ^{31}P NMR spectrum of the second attempted coordination of (I) to $TiCl_4.(THF)_2$ using $AgNO_3$ in CD_2Cl_2.

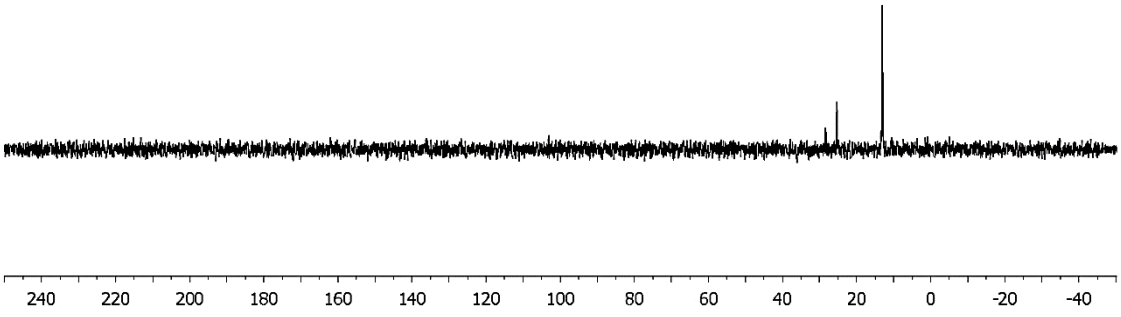

Figure A 91. ^{31}P NMR spectrum of the supernatant from the attempted coordination of (I), and four-fold excess of $TiCl_4(THF)_2$, in CH_2Cl_2 (in CD_2Cl_2).

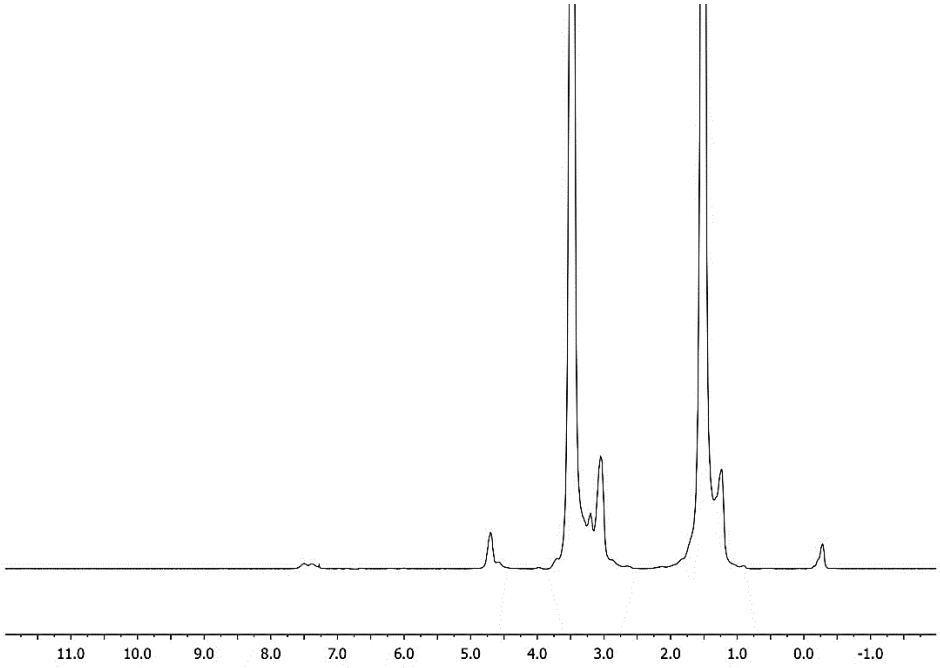

Figure A 92. ^{1}H NMR spectrum of the supernatant from the attempted coordination of (I), and four-fold excess of $TiCl_4(THF)_2$, in THF (in CD_2Cl_2).

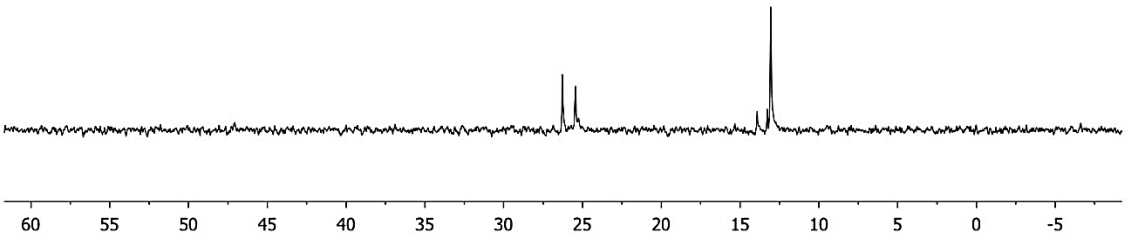

Figure A 93. ^{31}P NMR spectrum of the supernatant from the attempted coordination of (I), and four-fold excess of $TiCl_4(THF)_2$, in THF (in CD_2Cl_2).

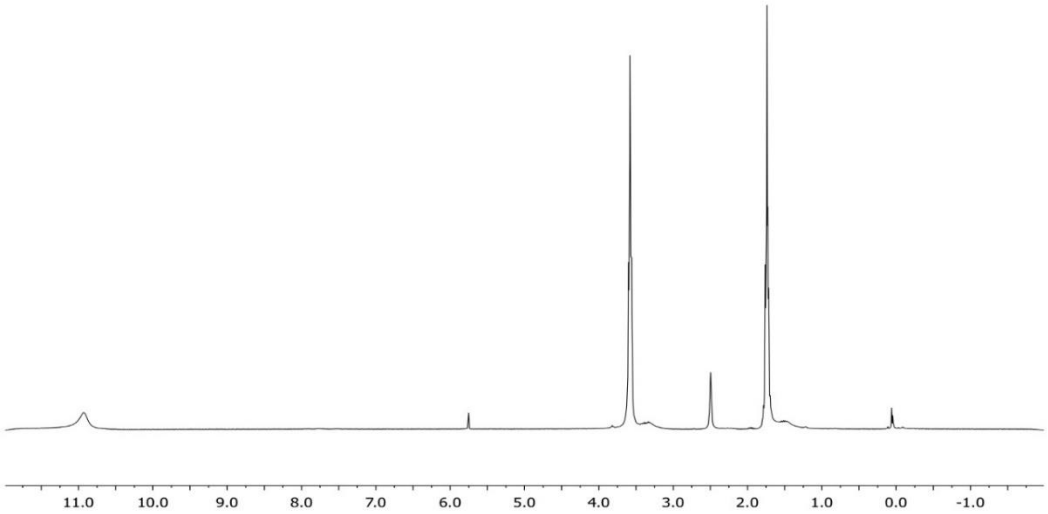

Figure A 94. ^{1}H NMR spectrum of the yellow precipitate from the attempted coordination of (I), and four-fold excess of $TiCl_4(THF)_2$, in CH_2Cl_2 (in CD_2Cl_2).

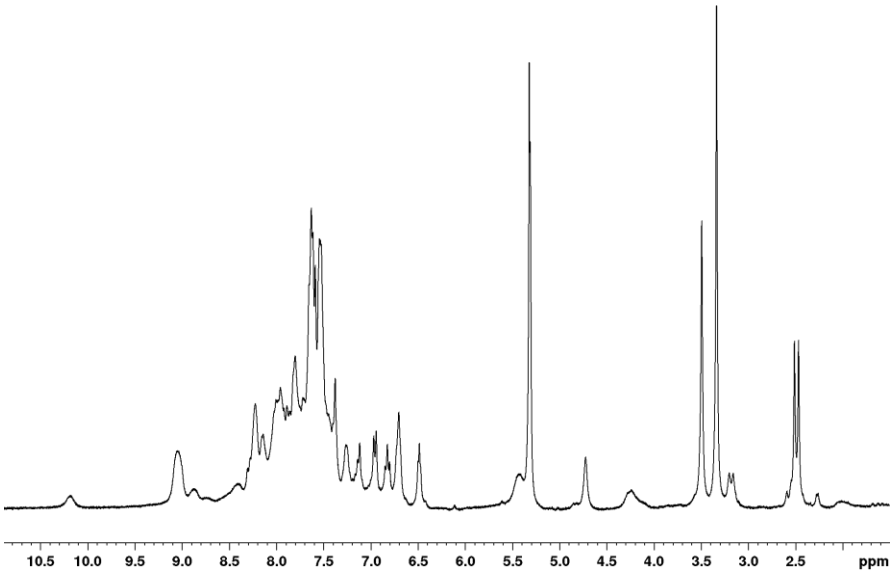

Figure A 95. ^{1}H NMR spectrum of attempted coordination of (I) to $NiBr_2$(DME) in CH_2Cl_2, after 12 h (in CD_2Cl_2).

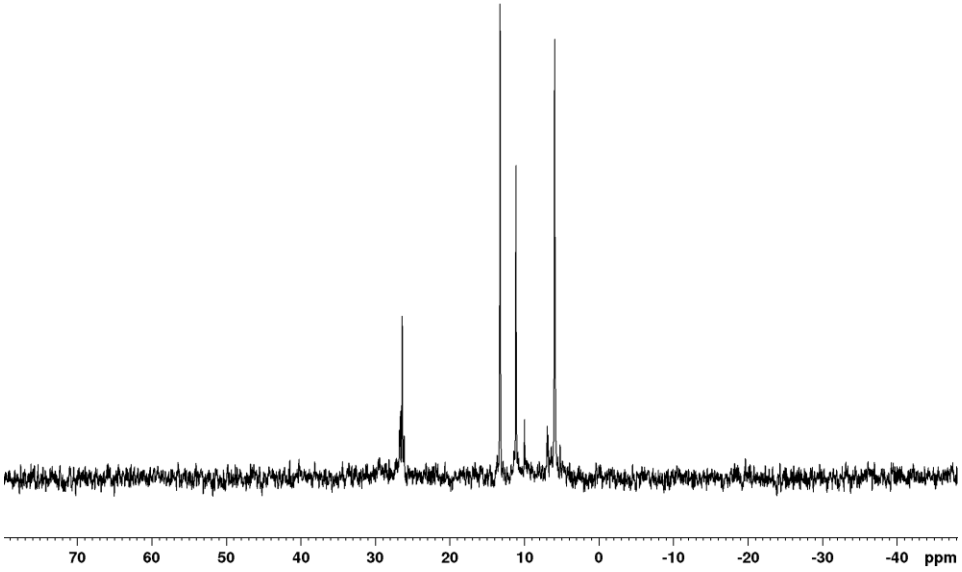

Figure A 96. ^{31}P NMR spectrum of attempted coordination of (I) to $NiBr_2$(DME) in CH_2Cl_2, after 12 h (in CD_2Cl_2).

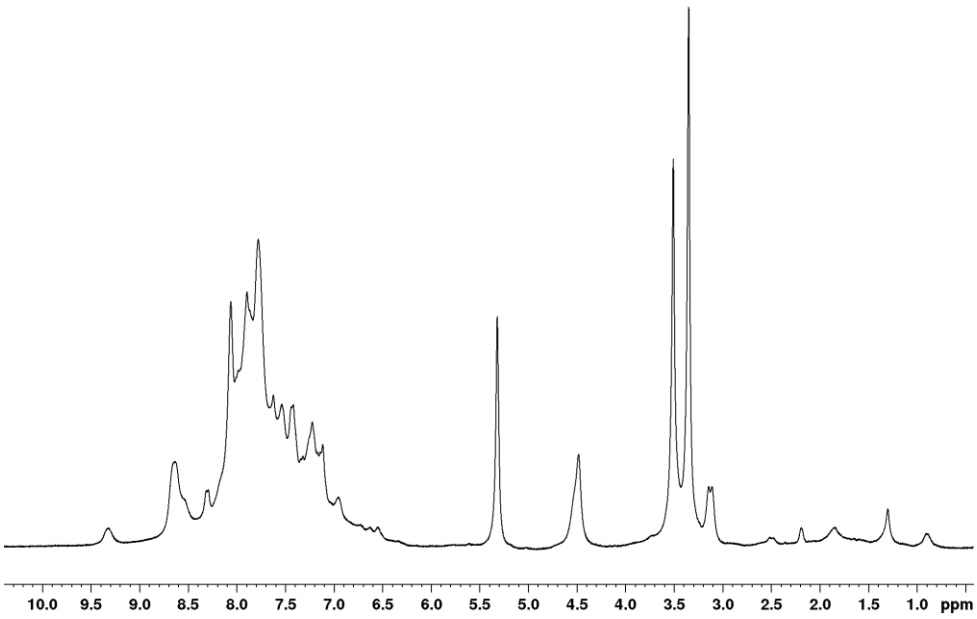

Figure A 97. ^{1}H NMR spectrum of attempted coordination of (I) to $NiBr_2$(DME) in CH_2Cl_2 after 5 d (in CD_2Cl_2).

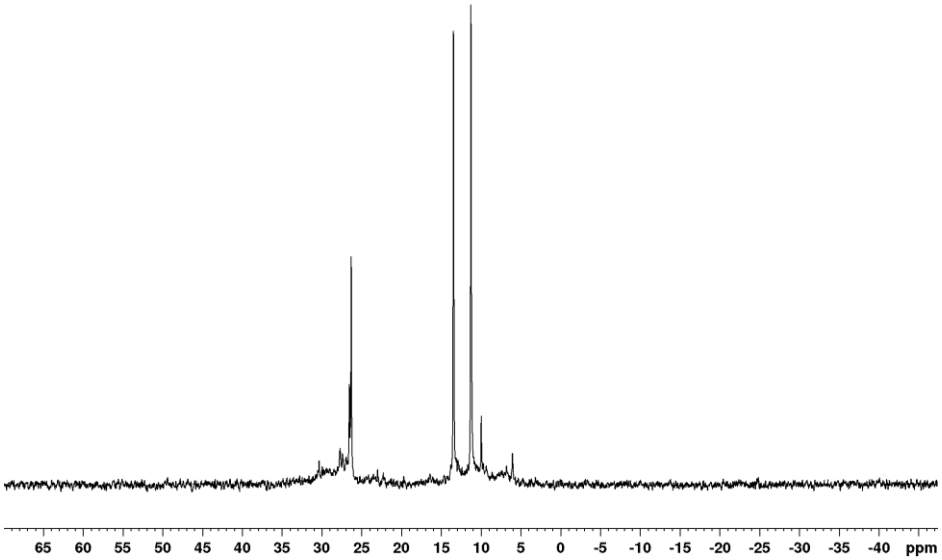

Figure A 98. ^{31}P NMR spectrum of attempted coordination of (I) to $NiBr_2$(DME) in CH_2Cl_2 after 5 d (in CD_2Cl_2).

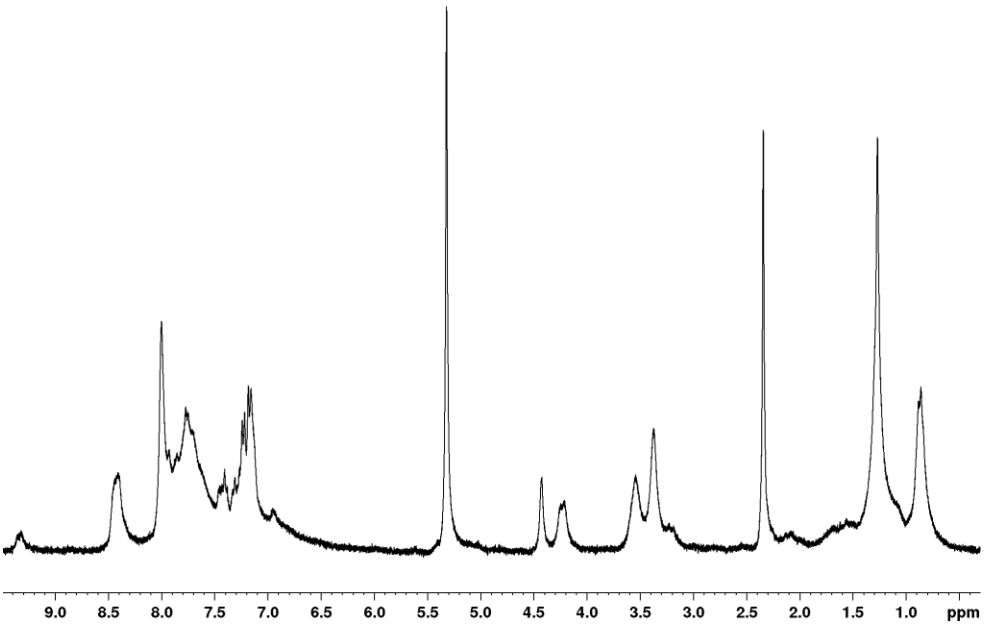

Figure A 99. ^{1}H NMR spectrum of dark brown solid of attempted coordination of (I) to $NiBr_2$(DME) in toluene (in CD_2Cl_2).

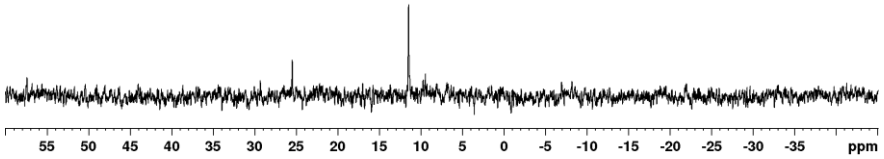

Figure A 100. ^{31}P NMR spectrum of dark brown solid of attempted coordination of (I) to $NiBr_2$(DME) in toluene (in CD_2Cl_2).

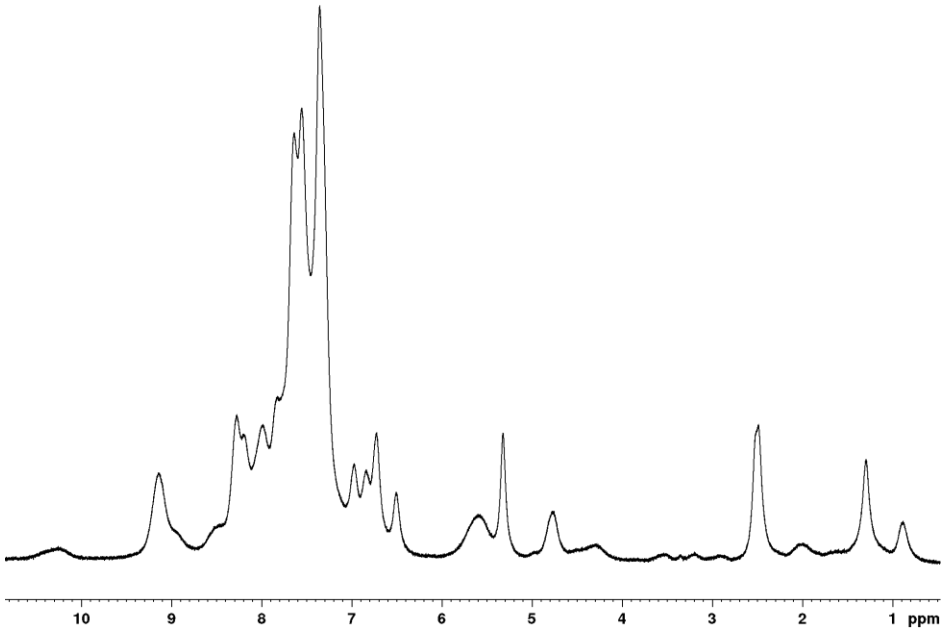

Figure A 101. ^{1}H NMR spectrum of dark brown solid from attempted coordination of (I) to $NiBr_2$(DME) in chlorobenzene (in CD_2Cl_2).

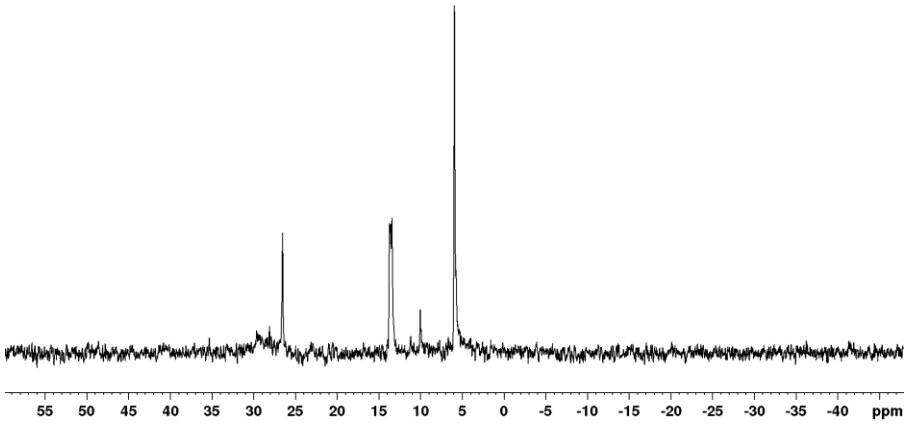

Figure A 102. ^{31}P NMR spectrum of dark brown solid from attempted coordination of (I) to $NiBr_2$(DME) in chlorobenzene (in CD_2Cl_2).

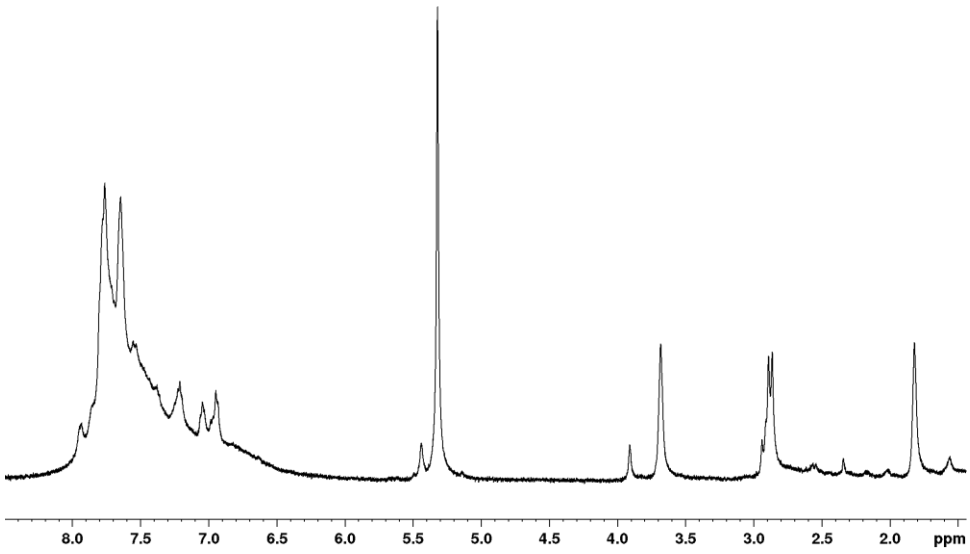

Figure A 103. ^{1}H NMR spectrum of attempted coordination of (I) to $HgCl_2$ in CD_2Cl_2.

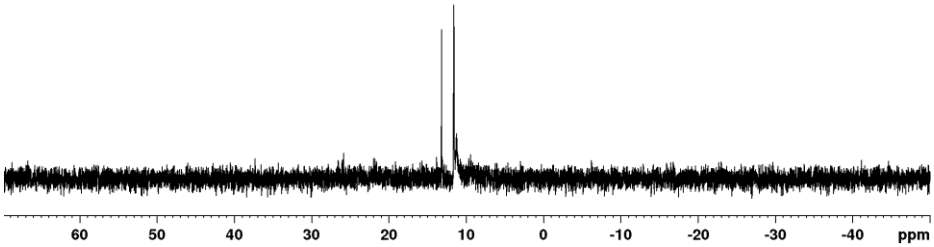

Figure A 104. ^{31}P NMR spectrum of attempted coordination of (I) to $HgCl_2$ in CD_2Cl_2.

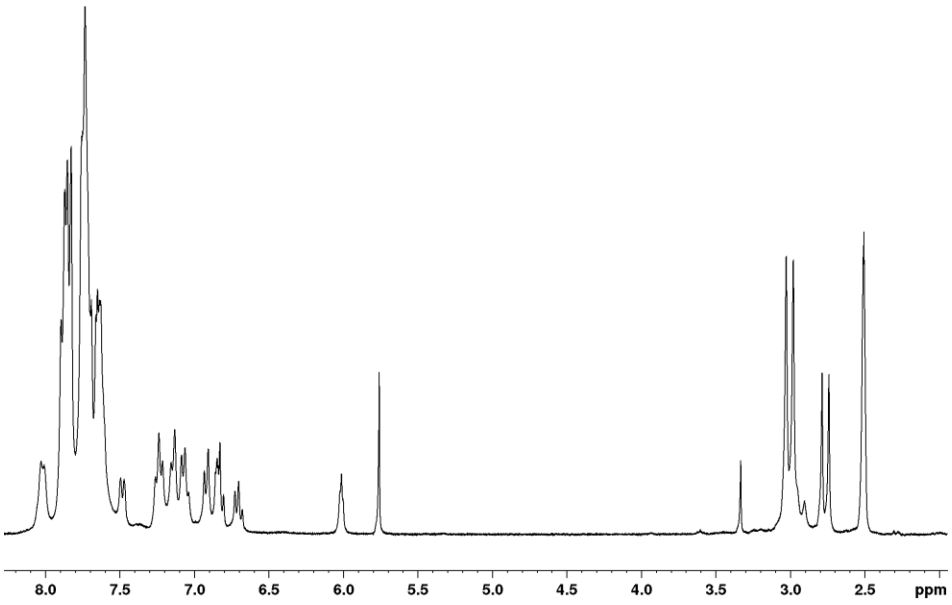

Figure A 105. ^{1}H NMR spectrum of white solid from attempted coordination of (I) to $HgCl_2$ in DMSO-d_6.

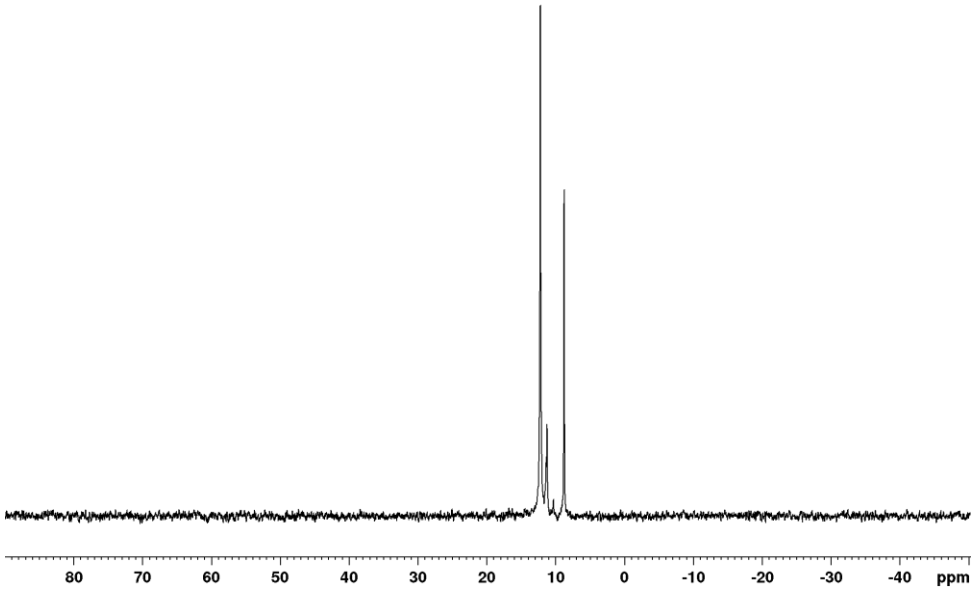

Figure A 106. ^{31}P NMR spectrum of white solid from attempted coordination of (I) to $HgCl_2$ in DMSO-d_6.

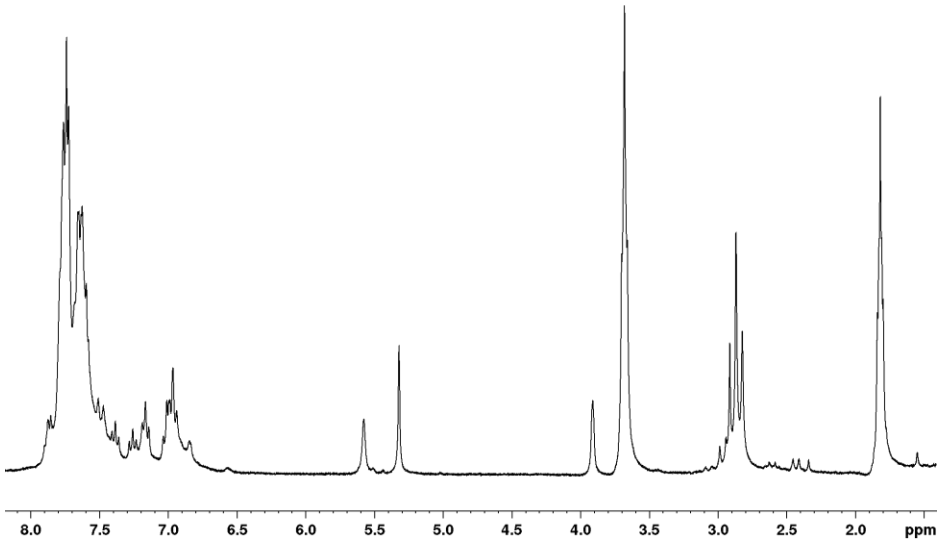

Figure A 107. ^{1}H NMR spectrum of attempted coordination of (I) to $HgBr_2$ in CD_2Cl_2.

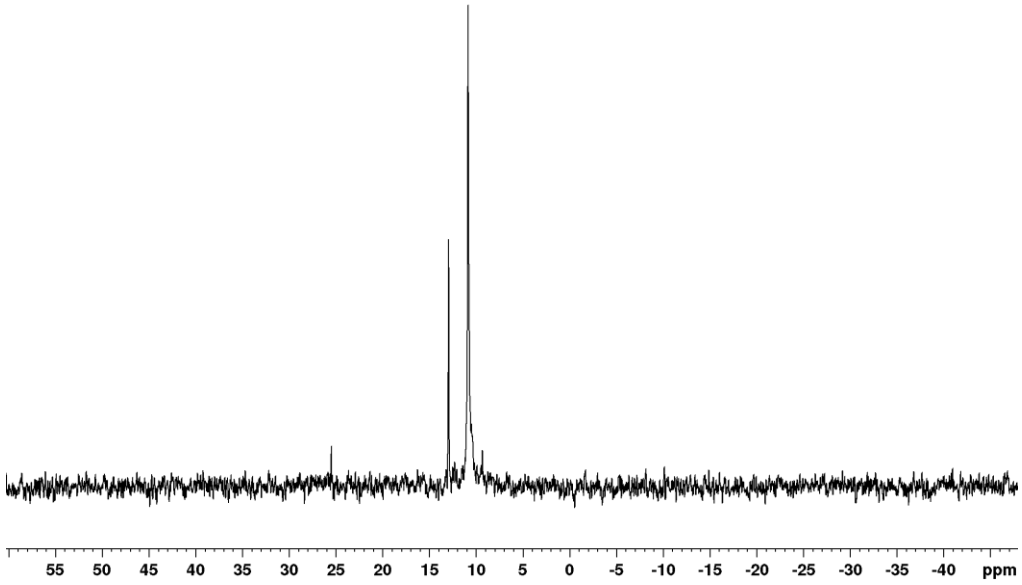

Figure A 108. ^{31}P NMR spectrum of attempted coordination of (I) to $HgBr_2$ in CD_2Cl_2.

Appendix B : X-ray Crystallographic Data

Crystal Data of 4,7-dimethyl-1-$C_9H_5PPh_2$

Empirical formula	$C_{23}H_{21}P_1$
Formula weight	328.37
Temperature	-93(2) °C [180(2) K]
Wavelength (Mo K_α)	0.71073 Å
Crystal system	monoclinic
Space group	$P2_1/c$ [No. 14]
Unit cell parameters	a = 8.3278(4) (Å) α = 90°
	b = 17.6372(8) (Å) β = 93.553(3)°
	c = 12.0862(5) (Å) γ = 90°
Volume	1771.90(14) $Å^3$
Z	4
Density (calculated)	1.231 Mg/m^3
Absorption coefficient	0.155 mm^{-1}
F(000)	696
Crystal dimensions	0.209 × 0.168 × 0.158 mm^3
Theta range for data collection	2.045 to 27.208°.
Index ranges	$-10 \le h \le 10$, $-22 \le k \le 18$, $-15 \le l \le 15$
Reflections collected	15480
Independent reflections	3945 [R(int) = 0.0299]
Completeness to theta = 25.242°	99.8%
Absorption correction method	multi-scan
Max. and min transmission	0.7455 and 0.7023
Refinement method	Full-matrix least-squares on F^2
Data / restraints / parameters	3945/ 0 / 219
Goodness-of-fit on F^2	1.041
Final R indices	
$R1 = [\Sigma\|\|F_o\|-\|F_c\|\|]/[\Sigma\|F_o\|]$ for $[F_o^2 > 2\sigma(F_o^2)]$	0.0429
$wR2 = ([\Sigma w(F_o^2-F_c^2)^2]/[\Sigma w(F_o^2)^2])^{1/2}$ [all data]	0.1077
Largest difference peak and hole	0.310 and -0.296 e.$Å^{-3}$

Crystal Data of 4,7-dimethyl-1-$C_9H_4PMePh_2$ (II)

Empirical formula	$C_{24}H_{23}P$	
Formula weight	342.39	
Temperature	180(2) K	
Wavelength	0.71073 Å	
Crystal system	Monoclinic	
Space group	C2/c	
Unit cell dimensions	a = 16.6549(2) Å	α= 90°.
	b = 11.23230(10) Å	β= 96.4639(4)°.
	c = 20.2304(2) Å	γ = 90°.
Volume	3760.50(7) $Å^3$	
Z	8	
Density (calculated)	1.210 Mg/m^3	
Absorption coefficient	0.149 mm^{-1}	
F(000)	1456	
Crystal size	0.30 x 0.25 x 0.20 mm^3	
Theta range for data collection	2.19 to 25.99°.	
Index ranges	-21<=h<=21, -14<=k<=14, -26<=l<=26	
Reflections collected	27446	
Independent reflections	4206 [R(int) = 0.0214]	
Completeness to theta = 25.99°	99.9 %	
Absorption correction	Multi-scan	
Refinement method	Full-matrix least-squares on F^2	
Data / restraints / parameters	4206 / 0 / 229	
Goodness-of-fit on F^2	1.024	
Final R indices [I>2sigma(I)]	R1 = 0.0341	
R indices (all data)	wR2 = 0.0968	
Largest diff. peak and hole	0.300 and -0.279 e.$Å^{-3}$	

Crystal Data of [(Me)(I)(COD)Ir(μ-I)$_2$Ir(COD)(I)(Me)]

Empirical formula	$C_{17.90}H_{29.70}I_{3.90}Ir_2$
Formula weight	1124.22
Temperature	-93(2) °C [180(2) K]
Wavelength (Mo K_α)	0.71073 Å
Crystal system	monoclinic
Space group	$P2_1/c$ [No. 14]
Unit cell parameters	a = 9.0341(5) (Å) α = 90°
	b = 10.2653(6) (Å) β = 97.092(3)°
	c = 12.0991(7) (Å) γ = 90°
Volume	113.46(11) Å^3
Z	2
Density (calculated)	3.353 Mg/m^3
Absorption coefficient	17.346 mm^{-1}
F(000)	996
Crystal dimensions	0.198 × 0.175 × 0.108 mm^3
Theta range for data collection	2.610 to 25.672°.
Index ranges	$-11 \le h \le 11$, $-11 \le k \le 12$, $-14 \le l \le 14$
Reflections collected	8333
Independent reflections	2104 [R(int) = 0.0331]
Completeness to theta = 25.242°	99.5%
Absorption correction method	multi-scan
Max. and min transmission	0.4315 and 0.2080
Refinement method	Full-matrix least-squares on F^2
Data / restraints / parameters	2104 / 0 / 89
Goodness-of-fit on F^2	1.090
Final R indices	
R1 = $[\Sigma\|\|F_o\|-\|F_c\|\|]/[\Sigma\|F_o\|]$ for $[F_o^2 > 2\sigma(F_o^2)]$	0.0292
wR2 = $([\Sigma w(F_o^2-F_c^2)^2]/[\Sigma w(F_o^2)^2])^{1/2}$ [all data]	0.0704
Largest difference peak and hole	1.971 and -1.548 e.Å^{-3}

References

(1) Ramirez, F.; Levy, S. *The Journal of Organic Chemistry* **1956**, *21*, 488.
(2) Ramirez, F.; Dershowitz, S. *The Journal of Organic Chemistry* **1957**, *22*, 41.
(3) Ramirez, F.; Levy, S. *The Journal of Organic Chemistry* **1956**, *21*, 1333.
(4) Ramirez, F.; Levy, S. *Journal of the American Chemical Society* **1957**, *79*, 67.
(5) Ramirez, F.; Levy, S. *Journal of the American Chemical Society* **1957**, *79*, 6167.
(6) Ramirez, F.; Levy, S. *The Journal of Organic Chemistry* **1958**, *23*, 2036.
(7) Ramirez, F.; Levy, S. *The Journal of Organic Chemistry* **1958**, *23*, 2035.
(8) Ammon, H. L.; Wheeler, G. L.; Watts, P. H. *Journal of the American Chemical Society* **1973**, *95*, 6158.
(9) Daly, J. J.; Wheatley, P. J. *Journal of the Chemical Society A: Inorganic, Physical, Theoretical* **1966**, 1703.
(10) Vincent, A. T.; Wheatley, P. J. *Journal of the Chemical Society, Dalton Transactions* **1972**, 617.
(11) Bart, J. C. J. *Journal of the Chemical Society B: Physical Organic* **1969**, 350.
(12) Gray, G. A. *Journal of the American Chemical Society* **1973**, *95*, 7736.
(13) Brownie, J. H.; Baird, M. C. *Coordination Chemistry Reviews* **2008**, *252*, 1734.
(14) Yoshida, Z.-i.; Iwata, K.; Yoneda, S. *Tetrahedron Letters* **1971**, *12*, 1519.
(15) Freeman, B. H.; Lloyd, D.; Singer, M. I. C. *Tetrahedron* **1972**, *28*, 343.
(16) Lloyd, D.; Singer, M. I. C. *Journal of the Chemical Society C: Organic* **1971**, 2941.
(17) Freeman, B. H.; Lloyd, D. *Tetrahedron* **1974**, *30*, 2257.
(18) Freeman, B. H.; Lloyd, D.; Singer, M. I. C. *Tetrahedron* **1974**, *30*, 211.
(19) Mathey, F.; Lampin, J. P. *Tetrahedron* **1975**, *31*, 2685.
(20) Rudie, A. W.; Lichtenberg, D. W.; Katcher, M. L.; Davison, A. *Inorganic Chemistry* **1978**, *17*, 2859.
(21) Casey, C. P.; Bullock, R. M.; Fultz, W. C.; Rheingold, A. L. *Organometallics* **1982**, *1*, 1591.
(22) Brownie, J. H.; Baird, M. C.; Schmider, H. *Organometallics* **2007**, *26*, 1433.
(23) Lichtenberg, C.; Hillesheim, N. S.; Elfferding, M.; Oelkers, B.; Sundermeyer, J. *Organometallics* **2012**, *31*, 4259.
(24) Schröder, F. G.; Lichtenberg, C.; Elfferding, M.; Sundermeyer, J. *Organometallics* **2013**, *32*, 5082.
(25) Kübler, P.; Oelkers, B.; Sundermeyer, J. *Journal of Organometallic Chemistry* **2014**, *767*, 165.
(26) Holy, N. L.; Nalesnik, T. E.; Warfield, L. T. *Inorganic and Nuclear Chemistry Letters* **1977**, *13*, 569.
(27) Shin, J. H.; Bridgewater, B. M.; Parkin, G. *Organometallics* **2000**, *19*, 5155.
(28) Debaerdemaeker, T. In *Zeitschrift für Kristallographie* **1980**; Vol. 153, p 221.
(29) McEwen, W. E.; Sullivan, C. E.; Day, R. O. *Organometallics* **1983**, *2*, 420.
(30) Baenziger, N. C.; Flynn, R. M.; Holy, N. L. *Acta Crystallographica Section B* **1979**, *35*, 741.
(31) Holy, N. L.; Baenziger, N. C.; Flynn, R. M. *Angewandte Chemie International Edition in English* **1978**, *17*, 686.

(32) Bombieri, G.; Tresoldi, G.; Faraone, F.; Bruno, G.; Cavoli-Belluco, P. *Inorganica Chimica Acta* **1982**, *57*, 1.
(33) Pierpont, C. G.; Downs, H. H.; Itoh, K.; Nishiyama, J.; Ishii, Y. *Journal of Organometallic Chemistry* **1977**, *124*, 93.
(34) Abel, E. W.; Singh, A.; Wilkinson, G. *Chem. Ind. (London)* **1959**, 1067.
(35) Kotz, J. C.; Pedrotty, D. G. *Journal of Organometallic Chemistry* **1970**, *22*, 425.
(36) Cashman, D.; Lalor, F. J. *Journal of Organometallic Chemistry* **1970**, *24*, C29.
(37) Cashman, D.; Lalor, F. J. *Journal of Organometallic Chemistry* **1971**, *32*, 351.
(38) Setkina, V. N.; Zhakaeva, A. Z.; Panosyan, G. A.; Zdanovitch, V. I.; Petrovskii, P. V.; Kursanov, D. N. *Journal of Organometallic Chemistry* **1977**, *129*, 361.
(39) Brownie, J. H.; Baird, M. C.; Laws, D. R.; Geiger, W. E. *Organometallics* **2007**, *26*, 5890.
(40) McKinney, R. J. *Inorganic Chemistry* **1982**, *21*, 2051.
(41) Tresoldi, G.; Recca, A.; Finocchiaro, P.; Faraone, F. *Inorganic Chemistry* **1981**, *20*, 3103.
(42) Rerek, M. E.; Basolo, F. *Journal of the American Chemical Society* **1984**, *106*, 5908.
(43) Abdulla, K.; Booth, B. L.; Stacey, C. *Journal of Organometallic Chemistry* **1985**, *293*, 103.
(44) Pinck, L.; Hilbert, G. *Journal of the American Chemical Society* **1947**, *69*, 723.
(45) Johnson, A. W.; Lee, S. Y.; Swor, R. A.; Royer, L. D. *Journal of the American Chemical Society* **1966**, *88*, 1953.
(46) Holy, N.; Deschler, U.; Schmidbaur, H. *Chemische Berichte* **1982**, *115*, 1379.
(47) Schmidbaur, H.; Deschler, U. *Chemische Berichte* **1981**, *114*, 2491.
(48) Ito, Y.; Okano, O.; Oda, R. *Tetrahedron* **1966**, *22*, 2615.
(49) Crofts, P. C.; Williamson, M. P. *Journal of the Chemical Society C: Organic* **1967**, 1093.
(50) Rufanov, Konstantin A.; Ziemer, B.; Hummert, M.; Schutte, S. *European Journal of Inorganic Chemistry* **2004**, *2004*, 4759.
(51) Buu-Hoï, N. P. *Justus Liebigs Annalen der Chemie* **1944**, *556*, 1.
(52) Woell, J. B.; Boudjouk, P. *The Journal of Organic Chemistry* **1980**, *45*, 5213.
(53) Murphy, J. A.; Patterson, C. W. *Journal of the Chemical Society, Perkin Transactions 1* **1993**, 405.
(54) Fowler, K. G.; Littlefield, S. L.; Baird, M. C.; Budzelaar, P. H. M. *Organometallics* **2011**, *30*, 6098.
(55) Brownie, J. H.; Baird, M. C. *Journal of Organometallic Chemistry* **2008**, *693*, 2812.
(56) Fallis, K. A.; Anderson, G. K.; Rath, N. P. *Organometallics* **1992**, *11*, 885.
(57) Bochkarev, M. N. *Chemical Reviews* **2002**, *102*, 2089.
(58) Muetterties, E. L.; Bleeke, J. R.; Sievert, A. C. *Journal of Organometallic Chemistry* **1979**, *178*, 197.
(59) Muetterties, E. L.; Bleeke, J. R.; Wucherer, E. J.; Albright, T. *Chemical Reviews* **1982**, *82*, 499.
(60) Allen, A. D.; Tidwell, T. T. *Chemical Reviews* **2001**, *101*, 1333.
(61) Butenschön, H. *Chemical Reviews* **2000**, *100*, 1527.

(62) González-Gallardo, S.; Bollermann, T.; Fischer, R. A.; Murugavel, R. *Chemical Reviews* **2012**, *112*, 3136.
(63) Halterman, R. L. *Chemical Reviews* **1992**, *92*, 965.
(64) Jutzi, P.; Burford, N. *Chemical Reviews* **1999**, *99*, 969.
(65) Paley, R. S. *Chemical Reviews* **2002**, *102*, 1493.
(66) Poli, R. *Chemical Reviews* **1991**, *91*, 509.
(67) Slugovc, C.; Rüba, E.; Schmid, R.; Kirchner, K.; Mereiter, K. *Monatshefte fuer Chemie* **2000**, *131*, 1241.
(68) Trost, B. M.; Older, C. M. *Organometallics* **2002**, *21*, 2544.
(69) Solari, E.; Floriani, C.; Chiesi-Villa, A.; Guastini, C. *Journal of the Chemical Society, Chemical Communications* **1989**, 1747.
(70) Solari, E.; Floriani, C.; Schenk, K.; Chiesi-Villa, A.; Rizzoli, C.; Rosi, M.; Sgamellotti, A. *Inorganic Chemistry* **1994**, *33*, 2018.
(71) Calderazzo, F.; Pampaloni, G.; Vallieri, A. *Inorganica Chimica Acta* **1995**, *229*, 179.
(72) Calderazzo, F.; Ferri, I.; Pampaloni, G.; Troyanov, S. *Journal of Organometallic Chemistry* **1996**, *518*, 189.
(73) Solari, E.; Musso, F.; Ferguson, R.; Floriani, C.; Chiesi-Villa, A.; Rizzoli, C. *Angewandte Chemie International Edition in English* **1995**, *34*, 1510.
(74) Buttler, O.; Al-Fawaz, A.; Kays, D. L.; Day, J. K.; Ooi, L.-L.; Aldridge, S. *Zeitschrift für anorganische und allgemeine Chemie* **2006**, *632*, 2187.
(75) Marcazzan, P.; Ezhova, M. B.; Patrick, B. O.; James, B. R. *Comptes Rendus Chimie* **2002**, *5*, 373.
(76) Rifat, A.; Patmore, N. J.; Mahon, M. F.; Weller, A. S. *Organometallics* **2002**, *21*, 2856.
(77) Woolf, A.; Chaplin, A. B.; McGrady, J. E.; Alibadi, M. A. M.; Rees, N.; Draper, S.; Murphy, F.; Weller, A. S. *European Journal of Inorganic Chemistry* **2011**, *2011*, 1614.
(78) Eisen, V., Queen's University, 2011.
(79) Littlefield, S. L., Queen's University, 2010.
(80) Sonnenberg, J., Queen's University, 2010.
(81) Knowles, W. S. *Angewandte Chemie International Edition* **2002**, *41*, 1998.
(82) Knowles, W. S. *Advanced Synthesis & Catalysis* **2003**, *345*, 3.
(83) Noyori, R. *Angewandte Chemie International Edition* **2002**, *41*, 2008.
(84) Tang, W.; Zhang, X. *Chemical Reviews* **2003**, *103*, 3029.
(85) Church, T. L.; Andersson, P. G. *Coordination Chemistry Reviews* **2008**, *252*, 513.
(86) Baenziger, N. C.; Flynn, R. M.; Swenson, D. C.; Holy, N. L. *Acta Crystallographica Section B* **1978**, *34*, 2300.
(87) Holy, N. L.; Baenziger, N. C.; Flynn, R. M.; Swenson, D. C. *Journal of the American Chemical Society* **1976**, *98*, 7823.
(88) Booth, B. L.; Smith, K. G. *Journal of Organometallic Chemistry* **1981**, *220*, 229.
(89) Bruker AXS Crystal Structure Analysis Package, S. N. V., SAINT-Plus (Version 6.01), SHELXTL (Version 5.1); Bruker AXS Inc.: Madison, WI, 1999.
(90) Cromer, D. T.; Waber, J. T. *International Tables for X-ray Crystallography*; Kynoch Press: Birmingham, UK, 1974; Vol. 4.
(91) Coe, J. W.; Vetelino, M. G.; Kemp, D. S. *Tetrahedron Letters* **1994**, *35*, 6627.

(92) Erker, G.; Psiorz, C.; Fröhlich, R.; Grehl, M.; Krüger, C.; Noe, R.; Nolte, M. *Tetrahedron* **1995**, *51*, 4347.
(93) Curnow, O. J.; Fern, G. M.; Hamilton, M. L.; Jenkins, E. M. *Journal of Organometallic Chemistry* **2004**, *689*, 1897.
(94) Herde, J. L.; Lambert, J. C.; Senoff, C. V.; Cushing, M. A. In *Inorganic Syntheses*; John Wiley & Sons, Inc.: 1974; Vol. 15, p 18.
(95) Cotton, F. A.; Lahuerta, P.; Sanau, M.; Schwotzer, W. *Inorganica Chimica Acta* **1986**, *120*, 153.
(96) Crabtree, R. H.; Quirk, J. M.; Felkin, H.; Fillebeen-khan, T. *Synthesis and Reactivity in Inorganic and Metal-Organic Chemistry* **1982**, *12*, 407.
(97) Choudhury, J.; Podder, S.; Roy, S. *Journal of the American Chemical Society* **2005**, *127*, 6162.
(98) Nagata, M.; Tani, K.; Mashima, K.; Yamagata, T. *Acta Crystallographica Section E* **2007**, *63*, m1498.
(99) Osborn, J. A.; Jardine, F. H.; Young, J. F.; Wilkinson, G. *Journal of the Chemical Society A: Inorganic, Physical, Theoretical* **1966**, 1711.
(100) Manxzer, L. E.; Deaton, J.; Sharp, P.; Schrock, R. R. In *Inorganic Syntheses*; John Wiley & Sons, Inc.: 1982; Vol. 21, p 135.
(101) Wolczanski, P. T.; Bercaw, J. E. *Organometallics* **1982**, *1*, 793.
(102) Fernelius, W. C.; Blanch, J. E.; Bryant, B. E.; Terada, K.; Drago, R. S.; Stille, J. K. In *Inorganic Syntheses*; John Wiley & Sons, Inc.: 1957; Vol. 5, p 130.
(103) Fowler, K. G., Queen's University, 2014.
(104) Adriaensens, P. J.; Karssenberg, F. G.; Gelan, J. M.; Mathot, V. B. F. *Polymer* **2003**, *44*, 3483.
(105) Singh, G.; Kothari, A. V.; Gupta, V. K. *Polymer Testing* **2009**, *28*, 475.
(106) Gillis, D. J.; Tudoret, M. J.; Baird, M. C. *Journal of the American Chemical Society* **1993**, *115*, 2543.
(107) Gillis, D. J.; Quyoum, R.; Tudoret, M.-J.; Wang, Q.; Jeremic, D.; Roszak, A. W.; Baird, M. C. *Organometallics* **1996**, *15*, 3600.
(108) Baird, M. C. *Chemical Reviews* **2000**, *100*, 1471.
(109) Arae, S.; Ogasawara, M. *Tetrahedron Letters* **2015**, *56*, 1751.
(110) Hillard, E. A.; Jaouen, G. *Organometallics* **2011**, *30*, 20.
(111) Bauer, E. B. *Chemical Society Reviews* **2012**, *41*, 3153.
(112) Bolm, C.; Gladysz, J. A. *Chemical Reviews* **2003**, *103*, 2761.
(113) Malcolmson, S. J.; Meek, S. J.; Sattely, E. S.; Schrock, R. R.; Hoveyda, A. H. *Nature* **2008**, *456*, 933.